Coulomb gluons and the ordering variable

A thesis submitted to
The University of Manchester
for the degree of Doctor of Philosophy
in the Faculty of Engineering and Physical Sciences

2015

René Ángeles Martínez

School of Physics and Astronomy

Contents

1 QCD preliminaries **21**

1.1 Introduction . . . 21
1.2 Perturbative Quantum Chromodynamics . . . 22
1.3 Renormalisation and asymptotic freedom . . . 26
1.4 Observables in QCD: infrared safety and factorisation . . . 27
1.4.1 Parton model and factorisation theorems . . . 29
1.5 Factorisation and physics of non-inclusive observables . . . 32
1.6 Outline . . . 32

2 Soft gluons and the colour evolution picture **35**

2.1 Eikonal approximation . . . 35
2.2 Colour + spin state notation . . . 38
2.3 First soft corrections . . . 39
2.3.1 Real emission contribution . . . 40
2.3.2 One-loop contribuions . . . 40
2.3.3 Observables and infrared finiteness at order α_s . . . 44
2.4 Collinear factorisation (breaking) in QCD . . . 44
2.4.1 Collinear limit . . . 45
2.4.2 Tree-level . . . 45
2.4.3 All-orders collinear factorisation of QCD amplitudes . . . 46
2.4.4 One loop . . . 48
2.4.5 Two loops . . . 52
2.4.6 Beyond two loops . . . 53
2.5 On the structure of soft corrections to all orders . . . 55
2.5.1 Enter the game: Coulomb gluons . . . 58
2.6 Super-leading logarithms and the ordering problem . . . 60
2.6.1 Standing on firm ground: Bloch-Nordsieck cancellation of soft singularities . . . 63
2.7 Summary . . . 63

3 One-loop, one-emission soft corrections **65**
3.1 Coulomb gluons of Drell-Yan process with one emission 66
3.1.1 Physical picture 68
3.2 General hard process 69
3.2.1 Initial state eikonal cuts 70
3.2.2 Final state eikonal cuts 71
3.2.3 Re-scattering cuts 72
3.2.4 Re-scattering cuts graph-by-graph 74
3.3 Eikonal and Coulomb gluons in dimensional regularisation 75
3.4 On the colour evolution picture 78
3.4.1 Wide-angle and collinear limits 81
3.5 Summary 83

4 Structure of infrared cancellations at order α_s^2 **85**
4.1 Double real contributions 86
4.1.1 Leading two-parton corrections $\mathbf{K}^2_{\text{s.o.2}}$ 87
4.1.2 Leading three and four partons corrections $\mathbf{K}^2_{\text{s.o.3.4}}$ 88
4.1.3 Subleading terms involving one or two partons $\mathbf{K}^2_{\text{sub}}$ 91
4.2 Real-virtual contributions 92
4.3 Purely virtual contributions 95
4.3.1 Two-loop contributions 96
4.3.2 On the role of Coulomb gluons 98
4.4 Summary 99

5 One-loop, two-emission soft corrections **101**
5.1 Phase-space limits 101
5.2 Tree-level amplitude 103
5.3 Two emissions at one loop 105
5.4 Eikonal cuts 106
5.4.1 Physical picture 110
5.5 Soft gluon cuts 111
5.5.1 Physical picture 118
5.6 Physics of two collinear gluons 119
5.7 Summary 120

6 General hard processes **123**
6.1 Physical mechanisms for double emission 124
6.2 Exact results and cross-checks 125
6.3 Notation 126
6.4 Initial- and final-state eikonal cuts 128

6.5 Soft gluon cuts . . . 130
6.6 Re-scattering cuts . . . 131
6.6.1 Physical picture . . . 133
6.7 Conjecture for the case of many emissions . . . 134

7 Conclusions **139**

A Regularisation of one loop corrections **141**

B Gauge invariance and consistency with the Bloch-Nordsieck theorem **143**
B.1 Gauge invariance . . . 143
B.2 Bloch-Nordsieck cancellation of soft gluons . . . 144

C Choice of polarisation vectors **147**
C.1 Collinear limit of the tree-level single emission amplitude . . . 148

D Cutting rules **151**
D.1 Cutting rules to calculate the imaginary part . . . 151
D.2 Cutting rules to calculate the real part . . . 155
D.3 On the cancellation of "mixed cuts" . . . 156
D.4 On the cancellation of single cuts over eikonal lines . . . 157
D.5 Deduction of cutting rules for a particular graph . . . 159
D.5.1 Final remarks . . . 163

E Reductions of $\left|n_{+1}^{(1)}\right\rangle$ **165**

F Virtual and phase space integrals at order α_s^2 **169**
F.1 Imaginary parts of the one emission amplitude $\left|n_{+1}^{(1)}\right\rangle$ . . . 169
F.1.1 Eikonal cuts . . . 169
F.1.2 Re-scattering cuts . . . 170
F.2 Real parts of the integrals of $\left|n_{+1}^{(1)}\right\rangle$ . . . 171
F.3 $\mathrm{D}_{ij}^{1}(q)$ . . . 171
F.3.1 Catani and Grazzini's Integral . . . 173
F.4 $\mathrm{D}_{ij}^{2}(q)$ and $\mathrm{C}_{ij}^{3}(q)$ . . . 175
F.5 Phase space integrals for double emission . . . 175
F.5.1 Integrals for $\mathbf{K}_{\mathrm{s.o.2}}^{2}$ . . . 176
F.5.2 Integral for $\mathbf{K}_{\mathrm{sub}}^{2}$ . . . 177

G On the breaking of strict collinear factorisation **179**

H Reductions: from cut pentagons into boxes **181**

H.0.3 Master integrals for eikonal and re-scattering cuts 185

H.0.4 Master integrals for soft gluon cuts 185

This thesis contains 36375 words and 35 figures.

List of Figures

1.1 Feynman rules for $SU(N)$ non-abelian gauge theories in the Feynman gauge. Curly lines represent gluons, solid lines represent quarks and dashed lines represent ghosts. 25

2.1 Eikonal rules for the blue vertex and propagator due to soft gluon radiation off an incoming (left) or outgoing(right) hard parton (solid line) with momentum p_i. The imaginary prescription should be set to zero if there is not virtual momentum flowing through this line. The shaded blob denotes the non-relevant parts of the graph and crosses indicate that gluons can be re-attached anywhere or branch into many more emissions. 37

2.2 Soft gluon corrections to a hard wide-angle scattering. Henceforth, the white blob always denotes the hard scattering and solid lines represent hard partons 38

2.3 One loop and one real emission exchange between $\{i, j\}$. Only partons involved in the exchange are explicitly drawn. 41

2.4 Multiparton collinear limit of a general process $\mathcal{M}$ at tree-level. . . . 45

2.5 Schematic representation of collinear factorisation of an scattering amplitude at one-loop order, Eq. (2.37), for which splitting kernel is independent of the non-collinear partons. 48

2.6 Representation of the terms that break the strict collinear factorisation in Eq. (2.47), when the parent parton, $\widetilde{P}$, is incoming and Eq. (2.48) is satisfied. The red curly lines represent Coulomb gluons exchanged between collinear and non-collinear partons. 51

2.7 A particular graph that gives rise to super-leading logarithms in GBJ. The out of the gap real emission k_2 is nearly collinear with the incoming hard parton p_1. 62

3.1 Four cut graphs contributing to the amplitude for the emission of a gluon, with four-momentum q and colour c, off hard parton i. There are three further graphs obtained by swapping $(i \leftrightarrow j)$ in the first three graphs. 66
3.2 The two cuts corresponding to the two different physical mechanisms for single gluon emission. The hatched circular blob denotes the hard process with the emission emitted off one of the external partons. . . 68
3.3 Imaginary part of the one loop corrections to a general hard process organised in terms of the different physical mechanisms for gluon emission. Observe that the mechanisms label by $(\mathrm{A}_{ij}^{\mathrm{in}})$ and $(\mathrm{B}_{ij}^{\mathrm{in}})$ are the generalisation of graphs (A) and (B) in Fig. 3.2 70
3.4 On a graph by graph basis, the infrared operator associated with the eikonal cut on the initial state is the same as if the cut partons were in the final state. 72
3.5 On-shell scatterings between an emitted gluon and an outgoing hard parton l. 74
3.6 One loop corrections to a general hard process. The small blue blobs denotes self energy corrections. 76
3.7 The real part of the four point scalar function is equal to the sum of single cuts over the soft gluons lines. 78

4.1 Different topologies that contribute to the double emission amplitude of a general hard process. Hard partons legs not involved in the soft gluon emission are not shown. 86
4.2 Purely (first row) real and and purely virtual (second row) graphs involving three partons. 89

5.1 The case of two real emissions. There are four more graphs obtained by swapping $(i \leftrightarrow j)$. 103
5.2 Diagrammatic representation of how to group the graphs in order to write the final result as a product of single emission operators. There are three further structures, obtained by exchanging $i \leftrightarrow j$. 105
5.3 The three cuts corresponding to the three different physical mechanisms for double-gluon emission. Each of these cuts is gauge invariant. 106
5.4 Diagrammatic representation of how to group the graphs that give rise to the transverse momentum ordered expression (3.7). Two more structures are obtained by permuting $(i \leftrightarrow j)$. 107

5.5 Diagrammatic representation of how to group the graphs that give rise to the transverse momentum-ordered expression in the case of two emissions at one loop. There are 12 more structures to consider: 8 are obtained by permuting $(i \leftrightarrow j)$ and the other four are obtained by permuting $(1 \leftrightarrow 2)$ and $(i \leftrightarrow j, 1 \leftrightarrow 2)$ in groups 3 and 7. 108
5.6 Kinematically allowed soft gluon cuts. 112
5.7 Schematic representation of regions that give rise to infrared poles. Poles arise as a result of the vanishing of the red propagators. 112
5.8 Cancellation of collinear poles. The operator $\mathcal{P}$ projects out the appropriate colour structure. 113
5.9 The relevant $1/\epsilon$ poles arising from soft-gluon cuts correspond to Coulomb exchange between the two real emissions. 114
5.10 Leading graphs in limits 1–3. Their contributions are projected onto the two colour structures in the final column. 116

6.1 Imaginary part of the one-loop corrections to a general hard process organised in terms of the different physical mechanisms for double gluon emission. These graphs are the generalisation of Fig. 3.3. The second graph in the fourth row stands for the production of two ghosts that scatter into two gluons. 124
6.2 Explicit representation of the red oval of first graph in the fourth row of Fig. 6.1. 131
6.3 In the strongly ordered regime $q_1 \gg q_2$ the sum of these two gauge invariant physical mechanisms adds up to the simple transverse momentum expression given by Eq. (6.23). 132

D.1 The three types of one loop contribution. Only those hard parton legs that couple to the virtual exchange are drawn. 152
D.2 The two types of cut that contribute to the imaginary part of graphs with a virtual exchange between the incoming partons. 153
D.3 The two types of cut that contribute to the imaginary part of graphs with a virtual between an incoming parton. 154
D.4 A particular graph that we consider to illustrate the cancellation of single cuts over the eikonal lines. 158

F.1 Contour integration for the case $s = -t + i0$. The zig-zag line indicates the branch cut of the complex function (F.18) and the black dot denotes the only (simple) pole of the integrand. The blue contour is located at a infinitesimal distance κ from the negative real axis, and δ is a small radius of the orange semicircular contour. 174

Abstract

The University of Manchester

Abstract of thesis submitted by **René Ángeles Martínez** for the degree of Doctor of Philosophy and entitled **Coulomb gluons and the ordering variable**.

Month and Year of Submission: 27th December, 2015.

In this thesis, we study the soft gluon corrections to hard wide-angle scattering processes due to a virtual gluon exchange (one-loop order) and the emission of up to two gluons. Our primary aim is to determine the ordering condition that should be used to dress a hard scattering process with corrections due to gluon emissions and a Coulomb (Glauber) gluon exchange. We find that, due to an elegant cancellation of many Feynman diagrams, a specific ordering variable should be used to order the transverse momentum of the exchanged Coulomb gluon with respect to the real emissions. Furthermore, in the case of the scattering process accompanied with a single emission, we find that the radiative part of the loop correction satisfies the same ordering condition as the Coulomb gluon contribution. Based upon the assumption that the ordering condition continues at higher orders, we conjecture an expression for the soft corrections to a general hard scattering process due to one-loop and any number of gluon emissions.

Declaration

No portion of the work referred to in this thesis has been submitted in support of an application for another degree or qualification of this or any other university or other institute of learning.

Copyright and ownership of intellectual property rights

1. The author of this thesis (including any appendices and/or schedules to this thesis) owns certain copyright or related rights in it (the "Copyright") and s/he has given The University of Manchester certain rights to use such Copyright, including for administrative purposes.

2. Copies of this thesis, either in full or in extracts and whether in hard or electronic copy, may be made **only** in accordance with the Copyright, Designs and Patents Act 1988 (as amended) and regulations issued under it or, where appropriate, in accordance with licensing agreements which the University has from time to time. This page must form part of any such copies made.

3. The ownership of certain Copyright, patents, designs, trade marks and other intellectual property (the "Intellectual Property") and any reproductions of copyright works in the thesis, for example graphs and tables ("Reproductions"), which may be described in this thesis, may not be owned by the author and may be owned by third parties. Such Intellectual Property and Reproductions cannot and must not be made available for use without the prior written permission of the owner(s) of the relevant Intellectual Property and/or Reproductions.

4. Further information on the conditions under which disclosure, publication and commercialisation of this thesis, the Copyright and any Intellectual Property and/or Reproductions described in it may take place is available in the University IP Policy (see `http://documents.manchester.ac.uk/DocuInfo.aspx?DocID=487`), in any relevant Thesis restriction declarations deposited in the University Library, The University Library's regulations (see `http://www.manchester.ac.uk/library/aboutus/regulations`) and in The University's policy on Presentation of Theses.

List of publications

The following publication is based on material discussed on Section 3.1 of Chapter 3 and Chapter 5 of this thesis:

- René Ángeles-Martínez, Jeffrey R. Forshaw and Michael H. Seymour, *Coulomb gluons and the ordering variable*, JHEP 12 (2015) 091, arXiv:1510.07998

Acknowledgements

In the very first place I have to thank the public education system in Mexico and in particular to the National Council of Science and Technology (CONACyT) for sponsoring my PhD degree. Then, the most special thanks go to my family Paulita, Pali, René and Martita. Thanks for your infinite love and support that is always with me.

I specially like to thank to my supervisor, Jeff Forshaw, for all his guidance, for teaching me the foundations of this field and for the support and confidence in my work. I shall always remember that the best way to solve a complicated problem is by finding the few key pieces of the puzzle. Special thanks to my co-supervisor, Mike Seymour, whose insights were central in all stages of this project and who freely surrendered his time to give me many guidance sessions. Thanks to both for putting up with me. Also special acknowledgements to Mauro Napsuciale and Selim Gomez who taught me how to use relativity in all its different presentations, without your teachings I would have never got this work done. I gratefully acknowledge the help of Alessandro Fregoso in early stages of this project and of Jimmy, Benjamin, Graeme, Dan and specially to Jeff and Matthew for proofreading my sometimes nonsensical sentences. I also like to thank all the members of the theory office including Alex, Daniele and Sotirios and our special guest Andrzej, not only for the help with physics problems but for your friendship and always making the office such a fun place to work in. I would also like to thank the particle physics group at Manchester for their hospitality and help.

Being in Manchester these years has given the opportunity to strengthen some friendships and start a few more, I like to take this opportunity to thank: Benjamin and Erick, *you do not know how much I appreciate your simple courage of being* my friends; Jimmy, you are a caring friend and I hope we can keep climbing; Natalia, thanks for all your support in these last months; Fabiola we had lots of fun, thanks looking after me when I needed it; Cariño, Tania, Miguel, Lucia, Fred, Roxana, Raul and Alejandra, thank you for reminding me the meaning of the words freedom and justice; Zach, Mikey and Edson, you are amazing housemates and friends and Shanly, thank you for the serious amount of laughter we had together.

This document was typeset in LaTeX and used the INSPIRE `utphys` BibTeX style

file. The algebraic manipulations we carried out using `Wolfram Mathematica` with the `Feyncalc` package. All of the Figures were drawn using `TikZ` and the word count was generated by TEXcount.

Chapter 1

QCD preliminaries

> ...mathematicians may be completely repelled by the liberties taken here. The liberties are taken not because the mathematical problems are considered unimportant.... in the meantime, just as a poet often has license from the rules of grammar and pronunciation, we should like to ask for physicists' license from the rules of mathematics in order to express what we wish to say in as simple a manner as possible.
>
> R. P. Feynman.

1.1 Introduction

In the history of physics there has always been the pursuit of understanding nature in terms of simple principles. Nowadays, particle physics offers a mathematical description of nature in terms of a small number of fundamental particles (constituents), and only four interactions. The current theory of particle physics that best describes experimental observations is the Standard Model (SM).

This model is based on the principles of quantum mechanics and on the symmetries that we have observed in nature. Special relativity, the symmetry that dictates the equivalence of the laws of physics for inertial observers, implies that the fundamental particles have definite mass and spin (intrinsic angular momentum). The SM contains particles with three different spins: fermions which have spin 1/2, bosons

with spin-1 and one scalar particle. We currently understand that these particles experience electroweak and strong interactions and that their structure is dictated, to a great extent, by symmetry principles known as gauge invariance. Gravity is another interaction that all constituents in the universe are believed to experience. Although Einstein formulated a classical theory of gravity that has been widely corroborated, there is not at the moment a fundamental theory of gravity with predictions that have been tested.

There are two classes of fermion in the SM: leptons and quarks. Both experience electroweak interactions that are mediated by four spin 1 bosons: the photon γ that mediates electromagnetic interactions and three gauge bosons (W^+, W^-, Z) that mediate the weak interactions. Through the mechanism of spontaneous symmetry breaking of the electroweak interactions, the (W^+, W^-, Z) bosons and the quarks and charged leptons become massive particles through their interactions with a scalar particle known as known as the Higgs. In contrast, only the quarks known as up, down, strange, charm, bottom and top ($\{u, d, s, c, b, t\}$) are affected by the strong interactions mediated by a spin-1 boson known as gluon.

The LHC is now performing proton-proton collision experiments at ~ 13 TeV and, in order to be prepared to measure even the smallest deviations from the SM, the particle physics community has the challenge to increase the accuracy of theoretical predictions. This thesis is devoted to improving the understanding of 'soft gluon corrections' relevant in high-energy experiments. Ultimately, we hope these studies help to increase the accuracy of predictions for the LHC and future experiments. This chapter aims to provide a brief summation of the basis of perturbative QCD and to present the outline of the rest of the thesis.

1.2 Perturbative Quantum Chromodynamics

The mathematical framework of the SM is Quantum Field Theory (QFT). The standard procedure to construct a field theory is to assign a local function $\phi_l(x)$ to each particle l and to combine them into a local functional known as Lagrangian density $\mathcal{L}[\phi_l]$ from which the theory can be constructed. The success of this method relies on the fact that we have learned how to translate the symmetries of nature into symmetries of $\mathcal{L}[\phi_l]$, which are then inherited by the field theory. The field theory of the strong interactions is known as Quantum Chromodynamics (QCD), its Lagrangian density is:

$$\mathcal{L}_{QCD} = -\frac{1}{4}\mathcal{F}^a_{\mu\nu}\mathcal{F}^{a,\mu\nu} + \sum_{i=1}^{n_f} q^\dagger_{iA}\gamma^0(i\gamma_\mu D^\mu_{AC} - m_i\delta_{AC})q_{i,C}, \tag{1.1}$$

where

$$\begin{aligned} \mathcal{F}^a_{\mu\nu} &\equiv \partial_\mu \mathcal{A}^a_\nu - \partial_\nu \mathcal{A}^a_\mu - i g_s (t^a_{\rm ad})_{bc} \mathcal{A}^b_\mu \mathcal{A}^c_\nu \\ D^\mu_{AC} &\equiv \delta_{AC} \partial^\mu - i g_s \mathcal{A}^b (t^b_{\rm F})_{AC}, \end{aligned} \tag{1.2}$$

and where $q_{i,A}$ ($\{A, B, C\} \in \{1, \ldots N\}$, $N = 3$ for the strong interactions) is the Dirac field associated with a quark of flavour i and mass m_i; $\mathcal{A}^a_\mu$ ($\{a, b, c\} \in \{1, \ldots, N^2-1\}$) is the gluon vector field; the matrices γ^μ satisfy the Clifford algebra $\{\gamma^\nu, \gamma^\nu\} = 2g^{\mu\nu}$, where $g^{\mu\nu} = \mathrm{diag}(1, -1, -1, -1)$ is the Minkowski metric; $\{t^a_{\rm F}, t^a_{\rm ad}\}$ are matrices related to the symmetry group of the gauge interactions, see below, and g_s is the QCD coupling.

The symmetry group associated with special relativity is the Poincaré group, a general element of this group consist of a space-time translation y and Lorentz transformations $\Lambda^\mu_\nu = \delta^{\mu\nu} + \omega^{\mu\nu}$. The QCD Lagrangian $\mathcal{L}(x^\nu) \to \mathcal{L}(\Lambda^\nu_\mu x^\mu + y^\nu)$ transforms as a scalar when the quark and gluon fields transform under the following representations of this group:

$$\begin{aligned} q_{i,A}(x^\nu) &\to \exp\left(\frac{i}{4}[\gamma^\mu, \gamma^\nu]\omega_{\mu\nu}\right) q_{i,A}(\Lambda^\nu_\mu x^\mu + y^\nu), \\ \mathcal{A}^a_\mu(x^\nu) &\to (\Lambda^{-1})_\mu{}^\nu \mathcal{A}^a_\nu(\Lambda^\nu_\mu x^\mu + y^\nu). \end{aligned} \tag{1.3}$$

Due to their symmetry transformation, the gluon field is associated with spin 1 states and the quark fields with spin 1/2 states.

The QCD Lagrangian contains a further global symmetry corresponding to the SU(N) group: the set of all $N \times N$ unitary complex matrices with unit determinant. The Lagrangian exhibits this symmetry as it remains invariant when the quark and gluon fields transform under the so-called fundamental and adjoint representation of SU(N):

$$\begin{aligned} q_{i,A}(x) &\to \left(\mathrm{e}^{i\alpha_b t^b_{\rm F}}\right)_{AC} q_{i,C}(x), \\ t^a_F \mathcal{A}^a_\mu(x) &\to t^a_F \left(\mathrm{e}^{i\alpha_c t^c_{\rm ad}}\right)_{ab} \mathcal{A}^b_\mu(x) = \left(\mathrm{e}^{i\alpha_b t^b_{\rm F}}\right) t^a_F \mathcal{A}^a_\mu(x) \left(\mathrm{e}^{-i\alpha_c t^c_{\rm F}}\right), \end{aligned} \tag{1.4}$$

where α_a are real constants that parametrise the group elements and the matrices $t^b_{\rm F}$ and $t^b_{\rm ad}$ are the generators of the adjoint and fundamental representation that satisfy

$$[t^a_{\rm ad/F}, t^b_{\rm ad/F}] = i f^{abc} t^c_{\rm ad/F}, \tag{1.5}$$

where the structure constants f^{abc} form a completely antisymmetric arrangement of constants defined by the adjoint representation $if^{abc} \equiv (t^b_{\rm ad})_{ac}$. We will not present a particular basis for these generators as we never evaluate them explicitly. To compare with results in literature, we adopt the customary normalisation of the fundamental

representation:

$$\text{Trace}\left(t_{\rm F}^a t_{\rm F}^b\right) = \delta_{ab} T_{\rm F}, \qquad {\rm T_F} = 1/2. \tag{1.6}$$

With this normalisation the generators satisfy

$$\begin{aligned} (t_{\rm F}^a t_{\rm F}^a)_{CD} &= C_F \delta_{CD}, \qquad C_F = \frac{N^2-1}{2N}, \\ (t_{\rm ad}^a t_{\rm ad}^a)_{cd} &= C_A \delta_{cd}, \qquad C_A = N \ , \end{aligned} \tag{1.7}$$

where C_F and C_A are known respectively as the Casimir coefficients of the fundamental and adjoint representation.

Crucially, the QCD Lagrangian is not only invariant under the transformations in Eq. (1.4) for constant α_a but also under transformations with $\alpha_a = \alpha_a(x)$ being local functions of the space-time coordinates:

$$\begin{aligned} q_{i,A}(x) &\to \left({\rm e}^{i\alpha_b(x) t_{\rm F}^b}\right)_{AC} q_{i,C}(x), \\ t_F^a \mathcal{A}_\mu^a(x) &\to \left({\rm e}^{i\alpha_b(x) t_{\rm F}^b}\right) t_F^a \mathcal{A}_\mu^a(x) \left({\rm e}^{-i\alpha_c(x) t_{\rm F}^c}\right) + \frac{i}{g_s}\left(\partial_\mu {\rm e}^{i\alpha_b(x) t_{\rm F}^b}\right) {\rm e}^{-i\alpha_c(x) t_{\rm F}^c} \ . \end{aligned} \tag{1.8}$$

The invariance under this transformation is known as the non-abelian $SU(N)$ gauge symmetry of the theory. One can think of this symmetry as the principle that dictates the structure of the interactions of the quark and gluon fields in QCD.

Finally, there are standard procedures [1] to use $\mathcal{L}_{QCD}$ to construct the quantum theory that inherits these symmetries. As we will see in Section 1.3, during high-energy collision experiments there is a regime in which the QCD coupling decreases asymptotically to zero and one can think of the quarks and gluons as asymptotic free states. In this perturbative regime experiments can be related to the S matrix: the transition probability between incoming $|\alpha, \text{in}\rangle$ and outgoing $|\beta, \text{out}\rangle$ asymptotically free states:

$$S_{\alpha\beta} \equiv \langle \beta, \text{out} | \alpha, \text{in} \rangle = \delta_{\alpha\beta} + i\delta^4(p_\beta - p_\alpha)(2\pi)^4 \mathcal{M}_{\beta\alpha} \ , \tag{1.9}$$

where the probability amplitude $\mathcal{M}_{\beta\alpha}$ can be expanded as a perturbative series in the coupling constant g_s. In our work we will study particular amplitudes, $\mathcal{M}_{\beta\alpha}$, organising their contributions according to the technique of Feynman diagrams.

The quantisation of theories with non-abelian gauge symmetries like QCD was formalised by Faddeev and Popov [2] using the path integral approach to field theory. According to this, the redundancies introduced by the field configurations related by a gauge transformation can be controlled by choosing a gauge. Although the S matrix is invariant under the choice of gauge, we work in the Feynman gauge as it simplifies our calculations. In this gauge the complete Lagrangian we need to

consider is $\mathcal{L}_{\text{QCD}} + \mathcal{L}_{\text{Feynman}} + \mathcal{L}_{\text{Ghost}}$ with

$$\mathcal{L}_{\text{Feynman}} + \mathcal{L}_{\text{Ghost}} = -\frac{1}{2}\left(\partial^\mu A^a_\mu\right)\left(\partial^\nu A^a_\nu\right) - G^{*a}\partial^\mu(\delta^{ac}\partial_\mu - g_s f^{abc}\mathcal{A}^b))G^c, \tag{1.10}$$

here G^a is the (anti-commuting scalar) ghost field that is required in the Feynman gauge. It ensures that only the physical degrees of the gluon propagate. The Feynman rules are depicted in Figure 1.1, where we have used the following abbreviated

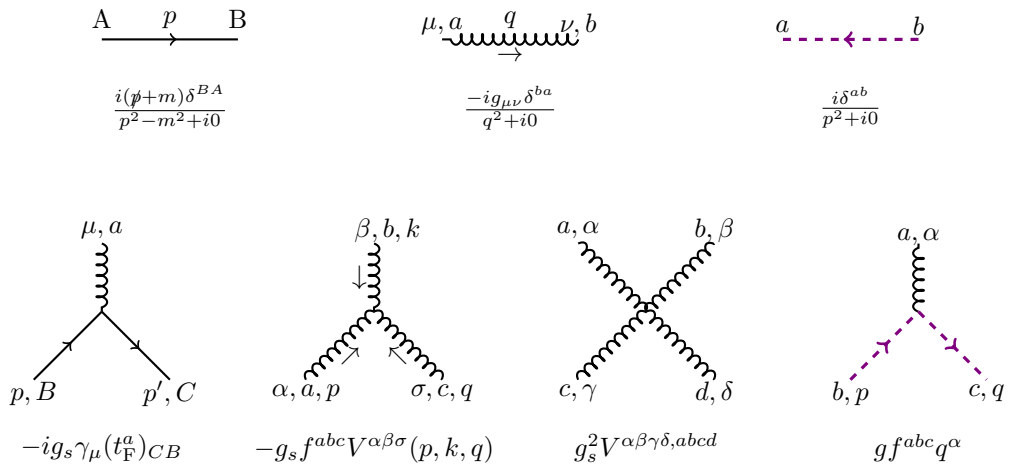

Figure 1.1: Feynman rules for $SU(N)$ non-abelian gauge theories in the Feynman gauge. Curly lines represent gluons, solid lines represent quarks and dashed lines represent ghosts.

notation

$$V^{\alpha\beta\sigma}(p,k,q) \equiv g^{\beta\alpha}(p-k)^\sigma + g^{\alpha\sigma}(q-p)^\beta + g^{\beta\sigma}(k-q)^\alpha, \tag{1.11}$$

$$V^{\alpha\beta\gamma\delta,abcd} \equiv -i\left[f^{eac}f^{ebd}(g^{\alpha\beta}g^{\gamma\delta} - g^{\beta\gamma}\gamma^{\alpha\delta}) + f^{eab}f^{ecd}(g^{\alpha\gamma}g^{\beta\delta} - g^{\alpha\delta}g^{\beta\gamma})\right.$$
$$\left. + f^{ead}f^{ebc}(g^{\alpha\beta}g^{\gamma\delta} - g^{\alpha\gamma}g^{\beta\delta})\right]. \tag{1.12}$$

In addition to these rules, external lines corresponding to quarks (antiquarks) in the incoming and outgoing state with spin σ have associated spinors $u(q,\sigma)$ and $\bar{u}(p,\sigma) = u^\dagger(p,\sigma)\gamma^0$ ($\bar{v}(p,\sigma)$ and $v(q,\sigma)$) that satisfy the Dirac equation $(\not{p} - m)u(p,\sigma) = (\not{p} - m)v(p,\sigma) = 0$ where $\not{p} \equiv \gamma_\mu p^\mu$. Finally, external lines associated to outgoing (incoming) gluons with helicity σ have associated a polarisation vector $\varepsilon(q,\sigma)$ ($\varepsilon^*(q,\sigma)$) that satisfies the constraint of the Feynman gauge $q\cdot\varepsilon(q,\sigma) = 0$.

In principle, the external quarks and antiquarks (gluons) have associated $A = \{1,\ldots,N\}$ ($a = \{1,\ldots,N^2-1\}$) different colour states. However, the experimental observation and lattice computations [3] suggests that none of these states exists in isolation. Instead, the experimental evidence suggests that strong interactions have the property of confinement [4]: all the physically observable states are colour-singlets. These observable states are collectively referred to as hadrons and it is

customary to refer to quarks and gluons collectively as partons.

1.3 Renormalisation and asymptotic freedom

Part of the remnant freedom left by the symmetries of the Lagrangian is expressed in terms of unfixed *bare* masses m_i the coupling g_s and the wave function constants (re-scaling of the fields). Before predictions can be made with a field theory it is necessary to re-express it in terms of physically measurable (observable) quantities. After this, the theory becomes predictive by relating observables to these parameters. This procedure is known as renormalisation and typically the measurable parameters are taken to be the renormalised masses and coupling(s) $\{g_{sR}, m_{iR}\}$.

The perturbative series of QCD amplitudes contains divergences due to arbitrarily high-energy (uv) momentum modes of the virtual particles. The first step in the renormalisation of QCD is to regularise such singularities. The standard regularisation procedure is to consider the same theory defined in $d = 4 - 2\epsilon$ space-time dimensions [5]. By doing this, the uv divergences in the theory, expressed in terms of the bare parameters, appear in the limit $\epsilon \to 0^+$ as poles ($1/\epsilon^n$ with $n = \{1, 2, \dots\}$) in the perturbative expansion. QCD is a very particular field theory in which the renormalisation procedure only requires a finite number of measurable parameters (one for the QCD coupling and one for each mass) to remove the uv divergences in the perturbative expansion [5] and, due to the property of asymptotic freedom [6, 7, 8] that we shall discuss below, predictions at high-energies can be made.

Within the context of perturbation theory, the regularisation of uv divergences introduces an arbitrary momentum scale μ known as the renormalisation scale. In dimensional regularisation this scale appears through the renormalised coupling and masses[1]: $\mu^\epsilon g_s(\mu)$ and $m_i(\mu)$. Physically, the arbitrariness of this scale can be interpreted as the arbitrariness in choosing a renormalisation scheme, i.e. the definition of renormalised parameters [9].

The independence of physical observables on μ implies a series of renormalisation group equations that govern how $g_s(\mu)$ and $m_i(\mu)$ change with different choices of μ. At first order in the perturbative expansion, the running coupling $g_s = \sqrt{4\pi\alpha_s}$ satisfies the following equation:

$$\frac{\mathrm{d}\alpha_s(\mu)}{\mathrm{d}\ln\mu} = -\beta_0 \frac{\alpha_s^2(\mu)}{4\pi^2} + \mathcal{O}(\alpha_s^3) \ . \tag{1.13}$$

Then, since the coefficient $\beta_0 = \frac{11}{6}C_A - \frac{4}{6}n_f T_\mathrm{F}$ is positive for $n_f < 17$ the coupling becomes smaller as μ increases. This behaviour of the coupling at high energies

[1] From now on we drop the R subindex of the renormalised parameters since we always refer to renormalised parameters.

is known as asymptotic freedom and is of crucial importance as it provides the foundation upon which perturbation theory can be applied to make predictions in high-energy collision experiments. In contrast, the coupling increases as we go to smaller energy scales and perturbation no longer holds. A rough estimate of when perturbation theory breaks down is $\Lambda_{\rm QCD} \approx 200$ MeV. This is obtained using the solution of Eq. (1.13) to estimate the scale at which the coupling becomes arbitrarily large [9].

A further property of theories with asymptotic freedom is that they become massless theories at high energies in the sense that [1]

$$\lim_{\mu\to\infty} \frac{m_i(\mu)}{\mu} \to 0 \ . \tag{1.14}$$

Since $\Lambda_{\rm QCD}$ is much larger than the masses of the $\{u, d, s\}$ quarks, QCD is essentially a theory of massless particles at the scales at which perturbative theory can be applied [10]. The heavier quarks $\{c, b, t\}$ require special treatment and are beyond the scope of this work. We will always take the masses of the quarks equal to zero, $m_i \to 0$. In particular, this assumption requires that the considered observables stay finite as $m_i \to 0$.

1.4 Observables in QCD: infrared safety and factorisation

We shall now discuss how the perturbative regime of QCD can be used to make predictions in high-energy collision experiments. For this propose, we consider the differential partonic cross section for a scattering that involves $\{\widetilde{p}_1, \ldots, \widetilde{p}_i\}$ ($i \leq 2$) incoming partons that scatter into a final state X consisting of n partons with momentum $\{p_1, \cdots, p_n\}$ and, additional, non-coloured particles (both incoming or outgoing) with total momentum Q^μ:

$$\begin{aligned} &\mathrm{d}\sigma(\widetilde{p}_1 + \ldots \widetilde{p}_i \to X; Q) = \frac{1}{\mathcal{F}S}\overline{\sum}|\mathcal{M}|^2 \ \ \mathrm{dLIPS}, \\ &\mathrm{dLIPS} \equiv \delta^d(Q + \widetilde{p}_1 + \cdots + \widetilde{p}_i - p_1 - \cdots - p_n) \prod_{i=m+1}^{n} \delta^+(p_i) \frac{\mathrm{d}^d p_i}{(2\pi)^{d-1}}, \end{aligned} \tag{1.15}$$

here $\mathcal{M}$ denotes the scattering amplitude, $\overline{\sum}$ denotes the sum (averaged) over the spin and colour states of the outgoing (incoming) particles[2], $\mathcal{F}$ is a flux factor, S denotes symmetry factors due to identical particles and the Lorentz invariant measure dLIPS enforces global momentum conservation and sets the integration of

[2]At the level of the squared amplitude we will always sum over polarisations.

the outgoing partons over their mass-shell. Throughout all this work we only ever consider corrections due to QCD interactions so $\mathcal{M}$ is a series in the QCD coupling only.

We shall now briefly discuss how observable quantities in high-energy collision experiments can be calculated by adding together the contributions from individual partonic cross sections like the one in (1.15), integrated over the phase space of the outgoing particles defined by specific observables. Due to the poor current understanding of non-perturbative strong interactions, these observables should be such that the sum of individual partonic cross sections is either insensitive to non-perturbative regime of QCD or such that the non-perturbative part can be factorised into universal (process independent) functions that can be measured in experiments and then used to make predictions. We shall now discuss this in more detail.

Apart from the *uv* divergences, which are removed by the process of renormalisation, individual contributions to observables contain "infrared" singularities due to kinematical configurations where propagators become arbitrarily small. In massless QCD (in fact, in any field theory with massless fields), this occurs when a group of (nearly) on-shell partons become collinear or when some partons are soft (their momentum components become arbitrarily small[3]). These are only necessary conditions and there exists a systematic classification of the kinematical regions that give rise to infrared divergences for important high-energy processes [11, 12, 13, 14, 15]. The presence of infrared singularities in partonic cross sections signals the presence of physics that is not well described by perturbation theory. The first step to dealing with these divergences is to regularise them. Henceforth, we adopt the method of dimensional regularisation [16, 10] to regularise virtual loop and phase space integrals. By doing this, infrared singularities appear as poles ($1/\epsilon^n$ with $n = \{1, 2, \dots\}$) in the limit $\epsilon \to 0^-$.

One of the first formal results that showed how to combine partonic cross sections to form measurable observables is the Kinoshita, Lee, Nauenberg (KLN) theorem [17, 18]. As presented in [4], this states that: in a theory with massless fields, transition rates are free from soft and collinear infrared divergences ($1/\epsilon$ poles in the limit $\epsilon \to 0^-$) if the summation over the initial and final degenerate states is carried out. Here, by "degenerate states" it should be understood states that differ by any number of collinear and soft partons.

In the particular case of an experiment without incoming hadrons, and thus $i = 0$, the KLN theorem guaranties that the total cross section is finite, e.g. the total cross section for the process $e^+e^- \to$ partons. This cross section is obtained by setting $i = 0$ in Eq. (1.15), taking Q^μ as the momentum of the incoming leptons

[3]Here we are including the case in which the momentum of a virtual parton is in the Glauber region, i.e. it corresponds to an on-shell (Coulomb gluon) scattering, see below.

and adding the individual cross sections for all possible partonic final states X. After the perturbative regime of QCD the final state partons group into hadrons due the confinement mechanism. However, provided the e^+e^- scattering occurs at high energies, a naïve use of quantum mechanics [9] can be used to argue that

$$\sigma_{e^+e^-\to\text{hadrons}} = \sigma_{e^+e^-\to\text{partons}} + \left(\frac{m_H}{Q}\right)^n , \tag{1.16}$$

where m_H is the typical mass of the hadrons produced with $n \geq 1$, and formal studies of the non-perturbative effects [19] show that $n = 4$ for this cross-section.

1.4.1 Parton model and factorisation theorems

For the case of experiments that involve one or two incoming hadrons it is not possible to use the KLN theorem to define observables in a straightforward manner. The obstacle is the lack of sum over all the possible degenerate configurations in the initial state; even if one fully integrates the partonic cross sections like in Eq. (1.15) for all possible final states X and then add them together infrared divergences would not cancel. The solution to this problem is a series of factorization theorems that we shall now discuss.

The naïve parton model by Feynman [20] of lepton-hadron high-energy collision experiments provided the key elements of these theorems. In this model, each incoming hadron is considered as an extended object composed of partons bound together by the non-perturbative effects of the strong interactions. At very high energies, relativity (in the center of mass frame [21]) dictates that the lepton probes a Lorentz contracted hadron whose internal interactions can be neglected due to the time dilation effect. In addition, provided the lepton is scattered at a wide angle and the momentum transfer is sufficiently high[4], the mediator boson (e.g. a photon) will scatter incoherently off a single parton inside the hadron. Then, the cross section for such collisions can be written in terms of the parton density $f_{a,A}(\xi)$, the probability of finding a parton of type a inside the hadron A with a longitudinal momentum fraction ξ, times the (Born level) probability of this parton to scatter with the lepton. The key property of the parton distribution functions (PDF's) $f_{a/A}(\xi)$ is their universality: they are independent of the type of particle, in this case a lepton, used to scatter (probe) the parton inside the hadron. With this reasoning, the naïve parton model provides a method to measure the PDF's and shows how they can be applied to make predictions for other experiments.

[4]This type of experiment is known as lepton-hadron deep inelastic scattering (DIS) and these kinematical conditions imply that the scattering will be mediated by a boson with high virtuality. Note that this process corresponds to setting $i = 1$ in Eq. (1.15) and with Q being the virtual photon.

An analogous heuristic argument can be applied to the case of hadron-hadron collisions [22]. The factorisation theorems in [21], for hadron-lepton and for hadron-hadron initiated processes, constitute the formal proof of how the (Born level) naïve parton model can be extended to all orders, see also [23, 24]. We shall now present a factorisation theorem for hadron-hadron collisions [25, 22, 26] that is relevant for the discussion in the next section. This states that the cross section for the process

$$A + B \to \mu^+\mu^- + X \tag{1.17}$$

consisting of a pair of hadrons $A + B$ (with momenta P_A and P_B and center of mass energy $\sqrt{s}$) to scatter into a pair of leptons[5] $\mu^+\mu^-$ (with momentum Q^μ and rapidity $y = \frac{1}{2}\ln\frac{Q\cdot P_A}{Q\cdot P_B}$) and anything else X is given by

$$\begin{aligned}\frac{\mathrm{d}\sigma_{AB}}{\mathrm{d}Q^2\mathrm{d}y} = \sum_{a,b}\int_{x_A}^1 \mathrm{d}\xi_A \int_{x_B}^1 \mathrm{d}\xi_B\, f_{a/A}(\xi_A,\mu_F)\; f_{b/B}(\xi_B,\mu_F)\times \\ H_{ab}\left(\frac{x_A}{\xi_A},\frac{x_B}{\xi_B},Q,\mu,\alpha_s(\mu),\mu_F;\epsilon\right) + \mathcal{O}\left(\frac{\Lambda^2_{\mathrm{QCD}}}{Q^2}\right)\end{aligned} \tag{1.18}$$

where $x_A \equiv e^y\sqrt{Q^2/s}$ and $x_B \equiv e^{-y}\sqrt{Q^2/s}$, the sum runs over the different parton species, $f_{a/A}(\xi_a,\mu_F)$ gives the distribution of parton a in hadron A with a longitudinal momentum fraction ξ_A, μ denotes the renormalisation scale and μ_F is the arbitrary factorisation scale, see below. Finally, H_{ab} is a consistent choice of the (infrared finite) hard part of the equivalent cross section for the partonic process

$$a + b \to \mu^+\mu^- + X. \tag{1.19}$$

There is a high degree of arbitrariness in how to apply this theorem as, at each order, one should choose a factorisation scheme: a definition of the finite parts of H_{ab} and accordingly of the parton distributions functions $f_{a/A}(\xi_A,\mu_F)$.

We shall now illustrate how a scheme is adopted at next to leading order. Firstly, we note that, at all orders in the perturbative expansion, the partonic cross section for the process in Eq. (1.19) can be written as

$$\begin{aligned}&\frac{\mathrm{d}\sigma_{ab}}{\mathrm{d}Q^2\mathrm{d}y}\,(x_a,x_b,Q,\mu,\alpha;\epsilon) \\ &= \sum_{c,d}\int_{x_a}^1 \mathrm{d}\xi_a \int_{x_b}^1 \mathrm{d}\xi_b f_{c/a}(\xi_a;\epsilon)\; \widetilde{H}_{ab}\left(\frac{x_a}{\xi_a},\frac{x_b}{\xi_b},Q,\mu,\alpha_s(\mu);\epsilon\right)\; f_{d/b}(\xi_b;\epsilon)\;.\end{aligned} \tag{1.20}$$

On the right hand side, $\widetilde{H}_{ab}(\frac{x_a}{\xi_a},\frac{x_b}{\xi_b},Q,\mu,\alpha_s;\epsilon)$ denotes the finite hard part of the scattering and $f_{d/b}(\xi_b;\epsilon)$ is a universal (independent of the hard scattering $\tilde{H}_{ab}$) and

[5] At lowest order in quantum electrodynamics but in principle to any order [21].

infrared divergent distribution of parton d in parton b. All the infrared divergences in $f_{d/b}(\xi_b;\epsilon)$ are of hard collinear origin because all the soft[6] contributions cancel when one sums inclusively over X in Eq. (1.19). Its explicit expression is given by[7]

$$f_{a/b}(x;\epsilon) = \delta_{ab}\delta(1-x) - \frac{1}{2\epsilon}\frac{\alpha_s}{\pi}P^{(1)}_{a/b}(x) + \mathcal{O}(\alpha_s^2), \tag{1.21}$$

where $P^{(1)}_{a/b}$ are the Altarelli-Parisi splitting functions [27].

Let us denote the perturbative expansions to hard part of the scattering H_{ab} and of the partonic cross section as

$$\begin{aligned} H_{ab} &= H^{(0)}_{ab} + \frac{\alpha_s}{2\pi}H^{(1)}_{ab} + \mathcal{O}(\alpha_s^2) \\ \frac{\mathrm{d}\sigma_{ab}}{\mathrm{d}Q^2\mathrm{d}y} &= \frac{\mathrm{d}\sigma^0_{ab}}{\mathrm{d}Q^2\mathrm{d}y} + \frac{\alpha_s}{2\pi}\frac{\mathrm{d}\sigma^{(1)}_{ab}}{\mathrm{d}Q^2\mathrm{d}y} + \mathcal{O}(\alpha_s^2) \end{aligned} \tag{1.22}$$

At Born level, one can choose the hard part of the scattering to be

$$H^{(0)}_{ab}\left(x_a, x_b, Q, \mu, \mu_F; \epsilon\right) = \frac{\mathrm{d}\sigma^{(0)}_{ab}}{\mathrm{d}Q^2\mathrm{d}y}\left(x_a, x_b, Q, \mu; \epsilon\right). \tag{1.23}$$

At order α_s with respect to this expression, one can choose the one-loop hard part of the scattering, $H^{(1)}_{ab}$, in the hadronic cross section to be [28]

$$\begin{aligned} &H^{(1)}_{ab}\left(x_a, x_b, Q, \mu_F; \epsilon\right) = \frac{\mathrm{d}\sigma^{(1)}_{ab}}{\mathrm{d}Q^2\mathrm{d}y}\left(x_a, x_b, Q, \mu; \epsilon\right) \\ &+ \frac{\alpha_s}{2\pi}\sum_c \int_{x_a}^1 \mathrm{d}\xi_a \frac{\mathrm{d}\sigma^{(0)}_{ab}}{\mathrm{d}Q^2\mathrm{d}y}\left(\frac{x_a}{\xi_a}, x_b, \mu, Q; \epsilon\right)\left[\frac{1}{\epsilon}\left(\frac{\mu}{\mu_F}\right)^{-\epsilon} P^{(1)}_{c/a}(\xi_a) + K^{ac}_{\mathrm{F.S}}(\xi_a)\right] \\ &+ \frac{\alpha_s}{2\pi}\sum_d \int_{x_b}^1 \mathrm{d}\xi_b \frac{\mathrm{d}\sigma^{(0)}_{ab}}{\mathrm{d}Q^2\mathrm{d}y}\left(x_a, \frac{x_b}{\xi_b}, Q, \mu; \epsilon\right)\left[\frac{1}{\epsilon}\left(\frac{\mu}{\mu_F}\right)^{-\epsilon} P^{(1)}_{d/b}(\xi_b) + K^{db}_{\mathrm{F.S}}(\xi_b)\right] \end{aligned} \tag{1.24}$$

where $K^{ac}_{\mathrm{F.S}}$ are arbitrary infrared finite functions and μ_F is the arbitrary factorisation scale[8]. Each choice of these functions defines a factorisation scheme. By inserting Eqs. (1.20) and (1.21) into Eq. (1.24) one can check that this expression is infrared finite as the second and third lines in (1.24) (counter-terms) exactly cancel the collinear divergences. Finally, it is important to remark that the arbitrary factorisation scale μ_F can be thought of as the scale up to which the transverse momentum of the nearly collinear partons is included in $f_{a/A}(\xi_A, \mu_F)$.

[6] Partons with momentum components much smaller than $\sqrt{Q^2}$.

[7] In the minimal subtraction renormalisation scheme [21].

[8] In order to suppress large logarithmic corrections in the perturbative expansion, it is convenient to choose μ_F to be of order Q, the large scale of the problem. However, the scale $\sqrt{\hat{s}} = \sqrt{s\xi_A\xi_B}$ should be avoided as this produces large corrections even if the hard cross section is calculated to high perturbative orders [21].

1.5 Factorisation and physics of non-inclusive observables

The factorisation of the collinear divergences that the partonic cross section in Eq. (1.20) exhibits is characteristic of "inclusive" observables. In the next chapter we will review the collinear limits, not at the level of inclusive partonic cross sections, but at the level of the amplitude and squared amplitude before phase-space integration. Recent developments [29, 30] have confirmed that in general, the collinear limit of (squared) amplitudes does not satisfy strict (process-independent) factorisation formulae. This lack of strict factorisation is specific to partonic amplitudes with two or more incoming partons, which are relevant for hadron-hadron collisions. These violations originate from a particular type of soft gluon correction associated with an on-shell scattering between the incoming or outgoing partons. In the literature, these gluon corrections are commonly referred to as Coulomb (Glauber) gluon contributions. In accordance with the factorisation theorems for inclusive observables, these contributions cancel when one integrates inclusively over all possible final partonic states.

In the calculation of non-inclusive observables this cancellation is incomplete; the partonic cross section for such observables does not necessarily obey the strict collinear factorisation that Eq. (1.20) exhibits, and the contributions from soft gluons (including Coulomb gluons contributions) do not necessarily cancel. In spite of this, it has been pointed out [30] that for non-inclusive observables the factorisation of collinear divergences (into universal functions) is expected to be possible up to a scale Q_0 below which the real radiation is summed up inclusively. Additionally, above Q_0 the miscancellation of real and virtual radiation (including Coulomb gluons) gives rise to perturbatively-calculable effects [31].

In recent years, there has been a growing interest in gaining an understanding of how the violations of strict factorisation affect non-inclusive observables [23, 32, 33, 34, 35]. This interest was partially motivated by a series of studies [31, 36] on the Coulomb gluon corrections to the 'gaps between jets' observable. In these references, the authors anticipated the violations of strict collinear factorisation, which have now been confirmed [29, 37]. Within the framework of [31, 36], these effects have been shown to contribute to various event shape observables for hadron-hadron initiated processes [38].

1.6 Outline

The series of works on the 'gaps between jets' observable [31, 36] are based on a k_T-ordered colour evolution algorithm. This algorithm constitutes a framework for the

calculation of soft gluon corrections to non-inclusive observables at all orders in perturbation theory. Its remarkable feature is that it accounts for the colour interference due to multiple soft gluon corrections, including Coulomb gluons contributions. The primary aim of this work is to provide formal analytical evidence of this framework.

Chapter 2 is an introduction to the problem of incorporating soft gluon corrections into non-inclusive observables. Firstly, we will introduce the eikonal approximation used throughout this thesis. We will see that, within this approximation, one-loop integrals have eikonal and Coulomb gluon contributions. The eikonal part is real and are produced when an exchanged virtual gluon is nearly on-shell. In contrast, the Coulomb part is purely imaginary and corresponds to on-shell scatterings between the incoming partons and between outgoing partons. After a brief introduction to the physics of these contributions, we will review the collinear limit of partonic scatterings. In particular, we shall review how the Coulomb gluon contributions are responsible for the lack of strict (process-independent) factorisation in this limit. Immediately after this, the k_T-ordered colour evolution algorithm is introduced as a framework that incorporates the salient physics.

An important prediction of this algorithm is the existence of super-leading logarithmic corrections for 'gaps between jets'. However, this prediction suffers from an ordering problem that we now briefly discuss. Although within the context of a Sudakov resummation different variables can be used to order the successive radiation added at each order [39, 35], the choice of ordering variable turns out to be critical when the colour evolution algorithm is applied to 'gaps between jets'; it has been exemplified that the coefficients of the super-leading logarithms change if one uses different ordering variables [40]. To determine which is the correct variable, in chapters 3–6 we will perform full diagrammatic calculations to determine the correct ordering variable that should be used to dress a hard wide-angle scattering with soft corrections. We will not do this to all orders but rather to the first two non-trivial orders. Specifically, we will perform the one-loop corrections to a general hard wide-angle scattering accompanied by emission of up to two gluons.

In Chapter 3, we start this program focusing in the first non-trivial case: we study the one-loop, one-emission corrections to the general hard scattering. Although this amplitude has been previously studied [41], we will revisit its calculation here to shed light on its structure which, in turn, will be the basis of many physical interpretations and computations in this thesis. By expressing the amplitude as a sum of terms with a single emission and one virtual exchange we will be able to identify the ordering condition that should be used to order the virtual correction with respect to the real emission. We find that the eikonal and Coulomb parts satisfy the same ordering condition. In fact, we will see they have the same colour and kinematic pre-factors; the only difference is that Coulomb gluons are only exchanged between incoming

and between outgoing partons while eikonal exchanges also occurs between incoming and outgoing partons. The ordering condition that we find is very simple: virtual exchanges should be ordered with respect to the transverse momentum (defined by the pair of partons that exchange the virtual gluon) of the real emission.

Before we study the ordering variable in a second non-trivial case, we will discuss the infrared cancellations of the cross section at order α_s^2 in Chapter 4. This is the first order at which the one-loop, one-emission scattering amplitude contributes. We shall study these cancellations using a series of approximations but we shall discuss them for a general wide-angle hard process. As far as we are aware, these have been studied in literature to a high-accuracy but only for particular processes [42, 43, 44, 45]. Our aim in this chapter is to provide useful guidelines for a future implementation of the colour evolution picture at this order. In particular, we shall discuss the contributions of Coulomb gluons.

In chapters 5 and 6, we extend our studies of the ordering variable to the case of the one-loop corrections to a general hard scattering accompanied by the emission of two gluons. In these chapters, we mainly focus only on the Coulomb part of the loop integrals. As the calculation is complicated, we will first discuss the particular case of a Drell-Yan hard process in Chapter 5 and we then consider a general hard process in Chapter 6. As far as we are aware, these corrections have not been previously computed except for particular processes, see [43, 46].

In these two chapters we demonstrate that the leading behaviour of the amplitude, in various kinematical regions of interest, can be expressed in terms of the same emission and Coulomb gluon operator definitions that appear in the one-emission case. Furthermore, an elegant cancellation of many Feynman diagrams imposes that the ordering variable that should be used to order the Coulomb gluon exchanges is the same that in the one-emission case. Finally, in Chapter 6, by assuming that this ordering structure continues in the presence of many more emissions, we present a conjecture for the one-loop amplitude of a general hard wide-angle scattering process accompanied by the emission of any number of gluons. In Chapter 7, we draw conclusions. The technical derivations through the thesis are organised into appendices A-H.

Chapter 2

Soft gluons and the colour evolution picture

This chapter is an introduction to the rich physics of soft gluon corrections to hard processes and the problem of including them to all orders. We start in Section 2.1 describing the perturbative corrections we consider throughout this work and in Section 2.2 we introduce some useful notation. The first order soft corrections to a cross-section are discussed in Section 2.3. This shall be our first encounter with the two types of soft gluon correction that we aim to describe: eikonal and Coulomb (also known as Glauber) gluon contributions. After this discussion, we will have the basis to review, in Section 2.4, how the interplay of these two types of correction is responsible for the breaking of collinear factorisation. Subsequently, in Section 2.5, we discuss the soft gluon insertion technique that accounts for the most divergent part of the eikonal gluons at all orders. We then use the physics from this and previous sections to motivate the colour evolution picture: an framework to calculate the all orders soft corrections that incorporates Coulomb gluons and hence collinear factorisation breaking effects. Finally, in Section 2.6, we discuss the ordering problem that motivates our studies in subsequent chapters.

2.1 Eikonal approximation

We are interested in amplitudes that correspond to a hard wide-angle scattering of on-shell partons, more precisely, a high energy scattering in which all partons have wide angles between them and have energies of roughly the same order. These requirements are equivalent to the condition that the parton sub-energy of each pair of particles in the scattering be of the same order, i.e. $(p_i + p_j)^2 = 2p_i \cdot p_j \sim Q^2$ and, by high energy scattering, we understand that the characteristic scale of the hard process Q be sufficiently large so that perturbation theory can be applied. In addition to QCD particles, the hard scatterings we consider could contain any

number of colourless particles, but they do not play an active role.

In general, large perturbative corrections arise due to the miscancellation between real and virtual radiation in soft and collinear configurations. In this work, we consider corrections to hard wide-angle scattering due to soft gluons in the eikonal approximation. More precisely, gluons whose momentum components are all much smaller than the characteristic scale, Q, of the hard subprocess. Henceforth, we refer to Q as the *hard scale* and to partons in the hard wide-angle scattering as *hard partons*.

Within the eikonal approximation, the Feynman rules for soft gluon radiation off the hard partons simplifies. In order to illustrate how this occurs, let us consider a lowest order scattering amplitude $\bar{u}(p_k)\mathcal{N}^{(0)}(p_1,\dots,p_n)$ containing an outgoing quark $\bar{u}(p_k)$, and let $\mathcal{N}^{(0)}_{+1}$ be the same amplitude but with an additional gluon of momentum q and colour a emitted off $\bar{u}(p_k)$. The exact QCD Feynman rules for this graph yield

$$\begin{aligned}(\mathcal{N}^{(0)}_{+1})^a &= \bar{u}(p_k)\left[\Big(-igt^a_F\gamma^\mu\epsilon_\mu(q)\Big)\frac{i(\not{p}_k+\not{q})}{(p_k+q)^2}\right]\mathcal{N}^{(0)}(p_k+q,\dots), \qquad (2.1)\\ &= \bar{u}(p_k)\left[\Big(-igt^a_{\rm F}\epsilon_\mu(q)\Big)\left\{\frac{i[2p_k^\mu+2q^\mu-\gamma^\mu\not{q}]}{2p_k\cdot q}\right\}\right]\mathcal{N}^{(0)}(p_k+q,\dots)\ ,\end{aligned}$$

where, to derive the second line, we used the Dirac equation $\bar{u}(p_k)\not{p}_k = 0$ and $\{\gamma^\mu,\gamma^\nu\} = 2g^{\mu\nu}$. We now consider the limit of this expression when the gluon momentum components are much smaller than the hard scale. This limit can be implemented by rescaling the gluon momentum as $q\to\lambda q$ and making an expansion for small λ. The leading term in this expansion is

$$(\mathcal{N}^{(0)}_{+1})^a = \frac{1}{\lambda}\bar{u}(p_k)\epsilon^*_\mu(q)\left[\frac{g\,t^a_{\rm F}\,2p_k^\mu}{2p_k\cdot q}\right]\mathcal{N}^{(0)}(p_k,\dots)+\mathcal{O}(\lambda^0), \qquad (2.2)$$

where we have used $\epsilon^*_\mu(\lambda q)=\epsilon^*_\mu(q)$, see Eq. (C.2). The term inside brackets can be thought of as an effective Feynman rule for the emission of a soft gluon $\{q,a\}$ off $\bar{u}(p_k)$. Observe that the numerator of this rule is identical[1] to the gluon emission vertex in a scalar version of QCD. In other words, the soft gluon, q, probes the colour of $\bar{u}(p_k k)$ but does not resolve its helicity. It is straightforward to show that the analogous result holds for the case of m successive gluon emissions $(q_1,\dots,q_m)$ off the same parton:

$$\begin{aligned}&\bar{u}(p_k)\left[\frac{gt^{a_m}_{\rm F}\gamma^{\mu_m}\not{p}_k}{(p_k+\lambda q_m)^2}\cdots\frac{gt^{a_1}_{\rm F}\gamma^{\mu_1}\not{p}_k}{(p_k+\lambda q_1+\cdots+\lambda q_m)^2}\right]\mathcal{N}^{(0)} \qquad (2.3)\\ &=\frac{1}{\lambda^m}\bar{u}(p_k)\left[\frac{gt^{a_m}_{\rm F}p_k^{\mu_m}}{p_k\cdot q_m}\cdots\frac{gt^{a_1}_{\rm F}p_k^{\mu_1}}{p_k\cdot(q_1+\cdots+q_m)}\right]\mathcal{N}^{(0)}+\mathcal{O}(\lambda^{m-1}).\end{aligned}$$

[1]Strictly speaking, this is only true after neglecting the recoil against the soft gluon.

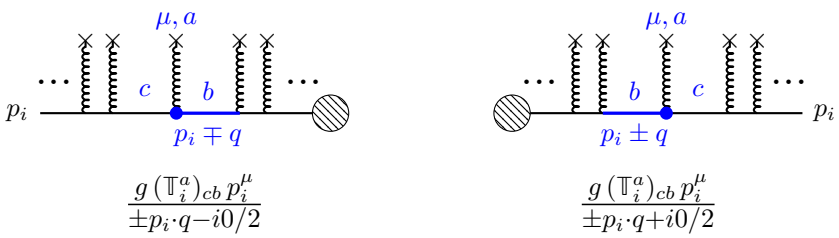

Figure 2.1: Eikonal rules for the blue vertex and propagator due to soft gluon radiation off an incoming (left) or outgoing(right) hard parton (solid line) with momentum p_i. The imaginary prescription should be set to zero if there is not virtual momentum flowing through this line. The shaded blob denotes the non-relevant parts of the graph and crosses indicate that gluons can be re-attached anywhere or branch into many more emissions.

Finally, entirely analogous simplifications are obtained when one considers soft gluon radiation, either real or virtual, off hard partons with other flavours[2]. In the same limit studied above, the propagators and vertices for gluon radiation off a hard parton with flavour i simplify as in Fig. 2.1, where the flavour dependent matrices $\mathbb{T}_i^a$ are equal to

$$(\mathbb{T}_i^a)_{dc} = \begin{cases} (t_{\rm F}^a)_{dc} & \text{if } i = \bar{u}, \text{ outgoing quark,} \\ (t_{\rm F}^a)_{dc} & \text{if } i = \bar{v}, \text{ incoming antiquark,} \\ (-t_{\rm F}^a)_{cd} & \text{if } i = u, \text{ incoming quark,} \\ (-t_{\rm F}^a)_{cd} & \text{if } i = v, \text{ outgoing antiquark,} \\ if^{dac} & \text{if } i = \varepsilon, \text{ outgoing gluon,} \\ -if^{cad} & \text{if } i = \varepsilon^*, \text{ incoming gluon.} \end{cases} \tag{2.4}$$

If we are considering Quantum Electrodynamics (QED), these matrices would be equal to the electric charges of the corresponding fermions. Analogously, in QCD it is customary to refer to $\mathbb{T}_i^a$ as the *colour charge* of parton i.

The eikonal rules are valid in physical gauges as well as in the Feynman gauge. The deduction of the eikonal rule, in the Feynman gauge, for a gluon radiated from other gluons can be found in Refs. [47, 48]. We have only inserted gluons on the external hard partons. However, internal insertions are subleading because the propagators are of the same order as the hard scale Q. Fig. 2.2 illustrates the corrections we consider in this work. It is worth noting that we do not make approximations for the shaded oval in this figure. More precisely, we *always* use the full triple-gluon and four-gluon vertices for soft gluon emissions off other soft gluons and the *exact* expressions for soft-gluon propagators, i.e. the eikonal approximation is only used

[2]Henceforth, as it is customary in the related literature, we refer to the different types of parton as parton flavours. We will always use the letters $\{i, j, k, l, m\}$ to label particular partons and letters $\{a, b, c, d, e, f, g\}$ to denote colour indices.

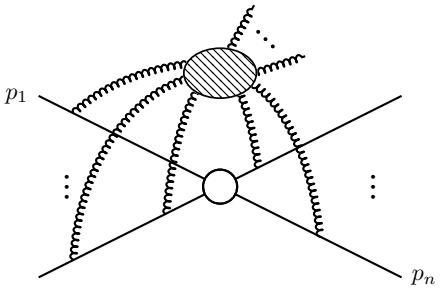

Figure 2.2: Soft gluon corrections to a hard wide-angle scattering. Henceforth, the white blob always denotes the hard scattering and solid lines represent hard partons

for the vertices and propagators over the hard parton lines.

2.2 Colour + spin state notation

It is useful to introduce a notation that makes manifest the universal structure of the eikonal rules [28, 49]. This can be done by noting that, in general, a physical amplitude, or a graph contributing to this, with n external partons can be written as $\mathcal{N}^{c_1,...,c_n;\sigma_1,...,\sigma_n}(p_1,...,p_n)$, where $\{c_i,\sigma_i,p_i\}$ denote the colour, spin and momentum of a parton with flavour i. Then, one can introduce an orthonormal basis in colour plus helicity space $\langle\sigma_1,...\sigma_n|\otimes\langle c_1,...,c_n|$ such that

$$\mathcal{N}^{\sigma_1,...,\sigma_n;c_n...,c_n}(p_1,...p_n)\equiv\left(\langle\sigma_1,\ldots,\sigma_n|\otimes\langle c_1\ldots,c_n|\right)|n(p_1,...,p_n)\rangle\,. \tag{2.5}$$

In this notation, the square of the amplitude summed over the colours and helicity states of the external partons reads

$$\sum_{\{c_i,\sigma_i\}}|\mathcal{N}|^2=\langle n(p_1,...,p_n)|n(p_1,...,p_n)\rangle\,. \tag{2.6}$$

It is also convenient to define colour operators $\mathbf{T}_i^a$ whose components are equal to the colour charges $\mathbb{T}_i^a$ for the emission of a gluon with colour a radiated from parton i:

$$\begin{aligned}\left\langle d_i\middle|\mathbf{T}_i^a\middle|c_i\right\rangle&\equiv(\mathbb{T}_i^a)_{d_ic_i},\\ \left\langle d_1,...d_n\middle|\mathbf{T}_i^a\middle|c_1,...c_n\right\rangle&=\delta_{d_1c_1}...(\mathbb{T}_i^a)_{d_ic_i}\delta_{d_nc_n}\ .\end{aligned} \tag{2.7}$$

In this notation, the eikonal rules in Fig. 2.1 simply read

$$\frac{\mathbf{T}_i^a p_i^\mu}{\pm p_i\cdot q+i\widetilde{\delta}_i 0/2}\ , \tag{2.8}$$

where $\widetilde{\delta}_i = \{1, -1\}$ if the propagator carries virtual momentum and is outgoing or incoming respectively and $\delta_i = 0$ otherwise. Using the above definitions and the fact that the matrices of the fundamental and the adjoint representations are hermitian, one can show that

$$\begin{gathered}\mathbf{T}_i \cdot \mathbf{T}_j \equiv \textstyle\sum_a (\mathbf{T}_i^a)^\dagger \cdot \mathbf{T}_j^a = \mathbf{T}_j^\dagger \cdot \mathbf{T}_i = \mathbf{T}_j \cdot \mathbf{T}_i = \mathbf{T}_j^\dagger \cdot \mathbf{T}_i^\dagger \quad , \\ \mathbf{T}_i \cdot \mathbf{T}_i = C_i \mathbb{1} \ ,\end{gathered} \tag{2.9}$$

where C_i is the Casimir coefficient associated with the colour representation of parton i, i.e. $C_i \equiv C_F$ when i is a quark or an antiquark, and $C_i \equiv C_A$ when i is a gluon. Given the definitions in Eq. (2.7) and the commutation relations of the adjoint and fundamental representation, one can prove that

$$[\mathbf{T}_i^a, \mathbf{T}_j^b] = \begin{cases} i f^{abc} \mathbf{T}_i^c & \text{if } i = j \ , \\ 0 & \text{if } i \neq j. \end{cases} \tag{2.10}$$

Below we collectively refer to these relations as the *colour algebra*.

The global colour symmetry of the QCD Lagrangian implies that physical amplitudes (each diagram that contributes to it) should be invariant under rotations in colour space. By making an infinitesimal colour rotation in Eq. (2.5), one can show that the colour charges are identical to the colour rotation matrices. Hence, if $|\tilde{n}\rangle$ denotes any physical amplitude with n external partons, or a graph that contributes to this, a colour rotation to these amplitudes reads

$$e^{i\alpha_a \sum_i^n \mathbf{T}_i^a} \left|\tilde{n}\right\rangle\!\!\right\rangle = \left|\tilde{n}\right\rangle\!\!\right\rangle \quad \Rightarrow \quad \left(\sum_{i=1}^{n} \mathbf{T}_i^a\right) \left|\tilde{n}\right\rangle\!\!\right\rangle = 0 \ . \tag{2.11}$$

It is customary to refer to the right-hand side of this expression as the *colour conservation* property. The notation described above works in any basis for the colour matrices and it is often referred to as the colour basis independent notation. Useful relations for the explicit evaluation of colour matrices can be found in [28, 50].

2.3 First soft corrections

In this section we compute the first soft corrections to the cross section, namely the corrections of order α_s. To familiarise ourselves with the notation and introduce useful definitions we study this simple case in some detail. In fact many of the central ideas that we will discuss in the proceeding chapters first appear at this order and, as we will see in Section 2.4, it is the exponentiation of these lowest order virtual corrections that gives rise to much of the physics we aim to describe.

2.3.1 Real emission contribution

Let $\left|n^{(0)}\right\rangle$ denote the lowest order amplitude of a hard process with n on-shell partons with momenta $\{p_1, ..., p_n\}$. The amplitude $\left|n^{(0)}_{+1}\right\rangle$ of this same scattering with a soft gluon of momentum q is obtained by inserting the extra gluon on each of the external hard partons:

$$\left|n^{(0)}_{+1}\right\rangle = \mathbf{J}^a_{n+1}(q)\left|n^{(0)}\right\rangle, \qquad \mathbf{J}^a_{n+1} \equiv g\mu^\epsilon \sum_{i=1}^{n} \mathbf{T}^a_i \frac{p_i\cdot\varepsilon}{p_i\cdot q}, \tag{2.12}$$

where $\varepsilon(q,\sigma)$ denotes the polarisation vector[3] and $\mathbf{J}_{n+1}(q)$ is commonly referred to as the soft-gluon current. Due to colour conservation, the one emission amplitude $\left|n^{(0)}_{+1}\right\rangle$ is gauge invariant in the following sense:

$$\mathbf{J}^a_{n+1}(q)\Big|_{\varepsilon\to q}\left|n^{(0)}\right\rangle = \sum_{i=1}^{n} \mathbf{T}^a_i \left|n^{(0)}\right\rangle = 0. \tag{2.13}$$

Finally, the contribution to a given observable ϕ from this correction yields[4]

$$\int^Q d[q]\left\langle n^{(0)}_{+1}\middle|n^{(0)}_{+1}\right\rangle\phi(q) = -\int^Q d[q]\left\langle n^{(0)}\middle|\mathbf{J}_{n+1}(q)\cdot\mathbf{J}_{n+1}(q)\middle|n^{(0)}\right\rangle\phi(q), \tag{2.14}$$

where $\mathrm{d}[q] = \mathrm{d}^d q(2\pi)^{1-d}\delta^+(q), \delta^+(q) \equiv \delta(q^2)\theta(q^0)$ denotes the differential measure for an on-shell emission, ϕ is a function of the phase space that defines the observable by weighting the phase space, e.g. $\phi(q) = 1$ for a completely inclusive case, and the hard scale Q in the upper integration limit indicates that momentum components above this scale should be cut off. It is worth noting that we have neglected the recoil against the gluon, i.e. we are not enforcing global momentum conservation. Also we are not including flux and symmetry factors in Eq. (2.14).

2.3.2 One-loop contribuions

Within the eikonal approximation, the one-loop corrected amplitude receives contributions from two graph topologies: self energy graphs, which do not give rise to soft enhancements in the Feynman gauge, and a virtual exchange between two different partons, the latter is illustrated in Fig. 2.3. The sum of the exchanges between

[3]Observe that our convention is to denote by ε the polarisation vector corresponding to an emission instead of ε^*.

[4]Here and whenever we consider squared matrix elements we will always consider unpolarised squared amplitudes summed over the colour states of the external partons.

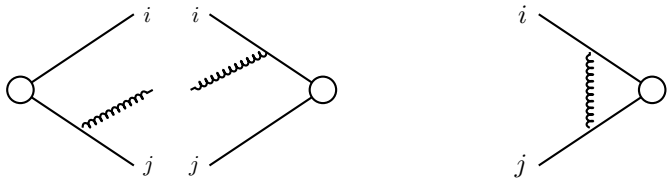

Figure 2.3: One loop and one real emission exchange between $\{i, j\}$. Only partons involved in the exchange are explicitly drawn.

different partons adds up to

$$\left|n^{(1)}\right\rangle \equiv \mathbf{I}_n^{(1)}\left|n^{(0)}\right\rangle = \sum_{i<j}^{n}\int^{Q}\frac{\mathrm{d}^d k}{(2\pi)^d}\left[\frac{g\mu^\epsilon \mathbf{T}_i^a p_i^\mu}{p_i\cdot k+\delta_i\frac{i0}{2}}\right]\left[\frac{g\mu^\epsilon \mathbf{T}_j^a p_{j\mu}}{-p_j\cdot k+\delta_j\frac{i0}{2}}\right]\left[\frac{-i}{k^2+i0}\right]\left|n^{(0)}\right\rangle. \tag{2.15}$$

For later use, we have introduced the colour operator $\mathbf{I}_n^{(1)}$ that, acting on the hard process amplitude, "inserts" the one-loop corrections.

In general, for every pair of partons $\{i, j\}$, the above integral contains a radiative and, in specific cases, an absorptive part. The integrals corresponding to these two types of contribution are respectively real and imaginary and can be isolated by putting, or cutting, specific propagators on-shell, see below. We postpone the deduction of these and more general cutting rules to isolate the real and imaginary parts for the next chapter, in the meantime we shall discuss the physics associated with them. For each pair $\{i, j\}$, there is a radiative contribution that can be isolated by setting on-shell the propagator of the exchanged gluon $(k^2+i0)^{-1} \to -2\pi i\delta^+(k)$. After doing this in Eq. (2.15) one gets

$$\sum_{i<j}^{n}\mathbf{T}_i\cdot\mathbf{T}_j\int^{Q}\mathrm{d}[k]\frac{g^2\mu^{2\epsilon}p_i\cdot p_j}{(p_j\cdot k)(p_i\cdot k)} = \frac{1}{2}\int^{Q}\mathrm{d}[k]\mathbf{J}_{n+1}^{\dagger}(k)\cdot\mathbf{J}_{n+1}(k)\ . \tag{2.16}$$

The right-hand side shows that the radiative part of the virtual integral behaves like minus the real emission correction, see below. One can show that Eq. (2.16) diverges logarithmically when its momentum becomes arbitrarily soft $k \to 0$ or when it is collinear with a hard parton, i.e. $p_i\cdot k \to 0$ or $p_j\cdot k \to 0$, see also [10].

In addition to the radiative part, the integrals in Eq. (2.15) contain an absorptive part for every pair $\{i, j\}$ of incoming and for every pair of outgoing partons. In each of these cases, the imaginary prescriptions of the two propagators in the eikonal approximation trap, or pinch, the contour integration over the loop momentum rendering an imaginary contribution. This part of the loop integral can be isolated by

setting these propagators on-shell in Eq. (2.15), i.e.

$$\mathbf{C}^{ij}(0,Q) \equiv -i\mathbf{T}_i\cdot\mathbf{T}_j \int^{Q} \frac{\mathrm{d}^d k}{(2\pi)^d} \frac{g_s^2\mu^{2\epsilon} p_i\cdot p_j}{k^2} \left[\frac{[-2\pi i\delta(p_i\cdot k)[[-2\pi i\delta(-p_j\cdot k)]}{2}\right] \ . \quad (2.17)$$

Observe that this expression contains an additional imaginary factor, $(-i)$, with respect to the radiative contribution. Subsequently, we refer to the imaginary part of one-loop integrals as being due to a Coulomb gluon exchange. After integrating out the delta functions, the expression for each exchanged Coulomb gluon becomes

$$\mathbf{C}^{ij}(0,Q) = -i\pi\frac{\alpha_s}{2\pi} c_\epsilon \mathbf{T}_i\cdot\mathbf{T}_j \int_0^{Q^2} \frac{\mathrm{d}k_T^2}{k_T^{6-d}} \ , \quad (2.18)$$

where k_T denotes the $d-2$ components of the virtual momentum that are transverse to the hard partons $p_i\cdot k_T = p_j\cdot k_T = 0$ and $c_\epsilon = (4\pi)^\epsilon/\Gamma[1-\epsilon]$ is a typical volume factor that we will often encounter in $d = 4-2\epsilon$ dimensions. The physics of each Coulomb exchange corresponds to an on-shell scattering. To be precise, we observe that Coulomb gluon contributions can be written as the product of two physical, i.e. on-shell, amplitudes:

$$\frac{1}{2i}\int \mathrm{dLIPS}_2\, \mathbf{A}^\dagger_{(2\to 2)}(p_i,p_j,p_i+k,p_j+k') \Big| n^{(0)}(k+p_i,k'+p_j,\dots)\Big\rangle \ , \quad (2.19)$$

where $\mathbf{A}^\dagger_{(2\to 2)}$ denotes the amplitude of the two-to-two scattering $p_i+p_j\to(p_i+k)+(p_j+k')$ and the differential Lorentz invariant phase space is

$$\mathrm{dLIPS}_2 \equiv \frac{\mathrm{d}^d k}{(2\pi)^d}\frac{\mathrm{d}^d k'}{(2\pi)^d}(2\pi)^d\delta^d(-k-k')(-i\delta^+(p_i+k))(-i\delta^+(p_j+k')) \ . \quad (2.20)$$

To identify Eq. (2.18) with the expression for the Coulomb gluon in Eq. (2.17), we need to use that, within the eikonal approximation,

$$\begin{aligned} \Big|n^{(0)}(k+p_i,k'+p_j,\dots)\Big\rangle &\approx \Big|n^{(0)}(p_i,p_j,\dots)\Big\rangle \ , \\ \mathbf{A}^\dagger_{(2\to 2)}(p_i,p_j,p_i+k,p_j+k') &\approx (-i)^\dagger (g\mu^\epsilon)^2 \left[\frac{-i}{k^2}\right](-2i\mathbf{T}_j^a p_{j\mu})(-2i\mathbf{T}_i^a p_i^\mu) \ , \\ \delta^+(k+p_i) &\approx 2\pi\delta(2p_i\cdot k) \ , \qquad \delta^+(p_j-k)\approx 2\pi\delta(-2p_j\cdot k) \ . \end{aligned} \quad (2.21)$$

Thus, Coulomb gluons correspond to on-shell scattering between incoming or outgoing partons.

Recall that we regularise the IR divergences of loop and phase-space integrals by working in $d = 4-2\epsilon > 0$ space-time dimensions. The radiative contributions and the phase-space integrals at this order have IR divergences associated with configurations in which the emitted gluon has arbitrarily small energy or is collinear

with a hard parton. The Coulomb gluon contributions have divergences associated to configurations with arbitrarily small $k_\perp$. We detail the integration at this order in Appendix A, the resulting expression for the radiative (Eq. (2.16)) and Coulomb (Eq. (2.17)) parts yield

$$\frac{1}{2}\int^{Q} \mathrm{d}[k]\mathbf{J}_{n+1}\cdot\mathbf{J}_{n+1} = \sum_{i<j}^{n} \mathbf{T}_i\cdot\mathbf{T}_j \frac{\alpha_s}{2\pi}\frac{c_\epsilon}{\epsilon^2}\left[\frac{2p_i\cdot p_j}{\mu^2}\right]^{-\epsilon} \tag{2.22}$$

$$\mathbf{C}^{ij}\left(0, 2p_i\cdot p_j\right) = -i\pi\mathbf{T}_i\cdot\mathbf{T}_j \frac{\alpha_s}{2\pi}\frac{c_\epsilon}{-\epsilon}\left[\frac{2p_i\cdot p_j}{\mu^2}\right]^{-\epsilon}. \tag{2.23}$$

Observe that the radiative and Coulomb parts are hermitian and anti-hermitian operators in colour space respectively, i.e.

$$\begin{aligned}(\mathbf{J}_{n+1}\cdot\mathbf{J}_{n+1})^\dagger &= \mathbf{J}_{n+1}\cdot\mathbf{J}_{n+1}\\ \left(\mathbf{C}^{ij}(0, 2p_i\cdot p_j)\right)^\dagger &= -\mathbf{C}^{ij}(0, 2p_i\cdot p_j)\,.\end{aligned} \tag{2.24}$$

The total contribution of the absorptive and radiative parts combine into the following compact form

$$\begin{aligned}\mathbf{I}_n^{(1)} &= \frac{1}{2}\int^{Q} \mathrm{d}[k]\mathbf{J}_{n+1}\cdot\mathbf{J}_{n+1} + \sum_{i<j}^{n}\widetilde{\delta}_{ij}\mathbf{C}^{ij}\left(0, 2p_i\cdot p_j\right)\ ,\\ &= \sum_{i<j}^{n}\frac{\alpha_s}{2\pi}c_\epsilon\mathbf{T}_i\cdot\mathbf{T}_j\left[1 + i\pi\epsilon\widetilde{\delta}_{ij}\right]\frac{1}{\epsilon^2}\left[\frac{2p_i\cdot p_j}{\mu^2}\right]^{-\epsilon}\ ,\end{aligned} \tag{2.25}$$

where $\widetilde{\delta}_{ij} = 1$ if $\{i, j\}$ are both incoming or outgoing and $\widetilde{\delta}_{ij} = 0$ otherwise. Due to colour conservation, the infrared ϵ poles of this equation can be written as

$$\mathbf{I}_n^{(1)} = \frac{\alpha_s c_\epsilon}{2\pi}\frac{1}{2}\left[-\frac{1}{\epsilon^2}\sum_{i=1}^{n} C_i - \frac{1}{\epsilon}\sum_{j\neq i}^{n}\mathbf{T}_i\cdot\mathbf{T}_j\left(\ln\left(\frac{2p_i\cdot p_j}{\mu^2}\right) - i\pi\widetilde{\delta}_{ij}\right)\right] + \mathcal{O}(\epsilon^0). \tag{2.26}$$

The double pole $1/\epsilon^2$ corresponds to the region of integration of an on-shell virtual gluon which is both soft and collinear. It is noteworthy mentioning that this part is diagonal in colour space whilst the $1/\epsilon$ poles remain as non-trivial colour operators.

2.3.3 Observables and infrared finiteness at order α_s

We now have all of the amplitudes necessary to assemble the corrections of order α_s to a given observable ϕ, i.e.

$$\begin{aligned}&\left\langle n^{(1)}\middle|n^{(0)}\right\rangle + \left\langle n^{(0)}\middle|n^{(1)}\right\rangle + \int^{Q} d[q]\left\langle n^{(0)}_{+1}\middle|n^{(0)}_{+1}\right\rangle \phi(q)\\ &= \int^{Q} d[q]\left\langle n^{(0)}\middle|\mathbf{J}_1(q)\cdot\mathbf{J}_1(q)\middle|n^{(0)}\right\rangle[\phi(q)-1]\ .\end{aligned} \tag{2.27}$$

This expression shows that for an observable to be finite, the source function $\phi(q)$ should assign unit weight to configurations in which the gluon emission has arbitrarily small momentum or is collinear with one of the hard partons. In particular, the corrections to the total cross-section, i.e. $\phi(q) = 1$, identically cancel. It is worth noting that although at this order Coulomb gluons identically cancel, the mechanism of cancellation is completely different from the radiative part. While the radiative gluons behave exactly like minus the one real emission part, Coulomb gluons cancel because of their imaginary character, i.e. it cancels with its hermitian conjugate contribution $\mathbf{C}^{ij} + (\mathbf{C}^{ij})^{\dagger} = 0$. Since this occurs similarly at higher orders, we refer to real gluons and to the radiative part of the virtual soft gluons collectively as eikonal gluons.

2.4 Collinear factorisation (breaking) in QCD

Broadly speaking, the singular part of the amplitude associated with soft and collinear partons factorises from the hard process. The corresponding factorisation formulae always exhibit a high degree of universality in the sense that the factors associated with soft and collinear modes do not depend on the details of the particular hard process and often are strictly independent of it. In [29], Catani, de Florian and Rodrigo (CdFR) proved that in the most general case, factorisation formulae for QCD amplitudes in collinear kinematical configurations cannot be written in a strict process-independent way. As we will see, this occurs due to the non-trivial colour structure of soft gluon corrections. Specifically, to the interplay between eikonal and Coulomb gluon contributions.

In a series of papers [31, 36] on the 'gaps between jets' (GBJ) observable Forshaw, Kyrieleis and Seymour (FKS) anticipated violations of strict factorisation and showed that they can give rise to interesting phenomenological implications. This observable is defined as the cross-section for the production of two high transverse momentum jets (Q) with the condition that any additional central jet should have smaller transverse momentum than a given scale $Q_0 \ll Q$. Surprisingly, the authors found that while corrections due to eikonal gluons behave as $\alpha_s^n \ln^n (Q^2/Q_0^2)$, the

interplay between eikonal and Coulomb gluons, responsible for the breaking of strict factorisations, give rise to larger logarithmic corrections of the form $\alpha_s^4 \ln^5 (Q^2/Q_0^2)$ with respect to the Born term, and more generally is expected [51] to give rise to contributions of the form $\alpha_s^m \ln^{2m-3} (Q^2/Q_0^2)$ for $m \geq 4$. This discovery showed that the perturbative corrections to observables that are sensitive to the breaking of strict factorisation require careful analysis. In this section, we review the behaviour of QCD amplitudes in collinear limits with the purpose of showing some of the necessary elements that a general framework encompassing such physics should have. Our presentation closely follows the original Refs. [29, 30], where additional details can be found.

2.4.1 Collinear limit

CdFR considered a general scattering process[5] $\mathcal{M}$ with n external on-shell partons in kinematical configurations where a subset C with m of the n partons become simultaneously collinear ($m \geq 2$). More precisely, the limit in which the parton sub-energies of the collinear (massless) partons $\sqrt{2p_i \cdot p_j},\ i,j \in \mathrm{C}$ are all of the same order $\sqrt{2p_i \cdot p_j} \sim \lambda$ and vanish simultaneously as $\lambda \to 0$. Only the dominant singular behaviour in this limit was considered[6], which behaves as $\mathcal{M} \sim \lambda^{-m-1}$. Here and throughout this section, the momenta of the n external partons (either incoming and outgoing) have positive energies[7].

2.4.2 Tree-level

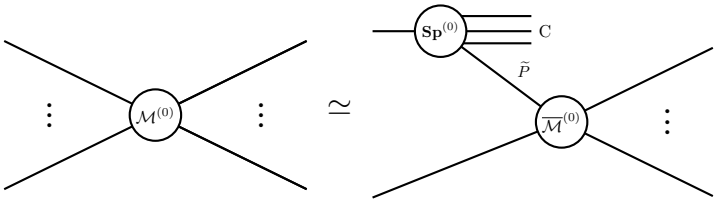

Figure 2.4: Multiparton collinear limit of a general process $\mathcal{M}$ at tree-level.

At tree-level, the multiparton collinear limit of a general process satisfies the

[5] In this section, we use italic capital letters to denote scattering amplitudes, e.g. $|\mathcal{N}\rangle$ instead of $|n\rangle$. We do this in order to emphasise that the results in this section hold for more general scattering of on-shell processes, and not only for hard wide-angle scatterings with soft corrections that we consider in the rest of this work.

[6] Strictly speaking, the collinear limit of QCD amplitudes is gauge dependent. CdFR worked in a light-like axial gauge where the dominant behaviour of the squared amplitude is equal to the square of the dominant behaviour of the amplitude.

[7] A different convention is used in [29, 30] where all the external partons are outgoing and can have positive or negative energy.

following factorisation formula:

$$\left|\mathcal{M}^{(0)}\right\rangle \simeq \mathbf{Sp}^{(0)}(p_1,\ldots,p_m;\widetilde{P})\left|\overline{\mathcal{M}}^{(0)}\right\rangle . \tag{2.28}$$

Here and in the rest of this section, the symbol $\simeq$ denotes the dominant contribution in the collinear limit. On the right-hand side, $\left|\overline{\mathcal{M}}^{(0)}\right\rangle$ is a tree level *reduced amplitude* with $n-m+1$ partons obtained from $\left|\mathcal{M}^{(0)}\right\rangle$ by replacing the m collinear partons with a single *parent parton* whose flavour and momentum are inherited from the collinear partons from conservation rules, in particular, its momentum can be written as

$$\widetilde{P} = \sum_{i\in \mathrm{C}} p_i - \frac{\left(\sum_{i\in \mathrm{C}} p_i\right)^2}{2\left(\sum_{i\in \mathrm{C}} p_i\right)\cdot n} n^\mu, \tag{2.29}$$

where n^μ is an auxiliary light-like vector[8]. Finally, the tree level splitting $\mathbf{Sp}^{(0)}$ is an operator (in spin and colour space) that describes the splitting of the collinear partons into the parent parton $\{p_1,\ldots,p_m\}\to\widetilde{P}$. The factorisation formula (2.28) is illustrated in Fig. 2.4.

Explicit representations of the splitting operator $\mathbf{Sp}^{(0)}$ can be found in [29] and references therein. However, for the sake of clarity we illustrate a particular case. The splitting operator for the case of a double collinear splitting ($m=2$) is of the form

$$\mathbf{Sp}(p_1,p_2;\widetilde{P}) \propto (\textbf{color matrix}) \times \mathrm{Split}^{(0)} , \tag{2.30}$$

where $\mathrm{Split}^{(0)}$ is a matrix in helicity space. For instance, if p_1,p_2 are respectively a $q,\bar{q}$ pair of outgoing partons, then, kinematics and flavour conservation determine that the parent parton, $\widetilde{P}$, is an outgoing gluon and it is straightforward to show that

$$\left\langle \sigma_1\sigma_2;c_1c_2\middle|\mathbf{Sp}^{(0)}(p_1,p_2,\widetilde{P})\middle|\bar{c};\bar{\sigma}\right\rangle = (t)^{\bar{c}}_{c_1,c_2} \times \frac{\mu^\epsilon g_s}{2p_1\cdot p_2}\bar{u}(p_1,\sigma_1)\gamma^\mu\varepsilon_\mu(\widetilde{P},\bar{\sigma})v(p_2,\sigma_2). \tag{2.31}$$

2.4.3 All-orders collinear factorisation of QCD amplitudes

CdFR demonstrated that, in general, the structure of tree-level factorisation for the multiparton collinear limit generalises to all orders:

$$\left|\mathcal{M}\right\rangle \simeq \mathbf{Sp}\left(\{m\},\{n-m\};\widetilde{P}\right)\left|\overline{\mathcal{M}}\right\rangle . \tag{2.32}$$

[8]This way of writing the momentum of the parent parton makes manifest its identification with a massless state.

Again, $\left|\overline{\mathcal{M}}\right\rangle$ is the all orders reduced amplitude of the physical process obtained by replacing the m collinear partons with $\widetilde{P}$, however, this time the all orders splitting operator $\mathbf{Sp}$ is process dependent, i.e. it depends on the quantum numbers of the external non-collinear partons $\{n-m\}$. CdFR showed that strict collinear factorisation, the property of the splitting operator of being independent of the non-collinear partons (i.e. $\mathbf{Sp} = \mathbf{Sp}\big(\{m\};\widetilde{P}\big)$), is only a feature of particular cases that we shall discuss in this section. We already illustrated this factorisation in Fig. 2.4 where a parton in the initial state branches into many emissions and $\widetilde{P}$ is in the initial state.

Here and throughout this thesis we organise the perturbative series of a physical process $\mathcal{N}$ (equal to $\mathcal{M}$ or $\overline{\mathcal{M}}$) as

$$\left|\mathcal{N}\right\rangle = \left|\mathcal{N}^{(0)}\right\rangle + \left|\mathcal{N}^{(1)}\right\rangle + \left|\mathcal{N}^{(2)}\right\rangle + \dots \tag{2.33}$$

where $\left|\mathcal{N}^{(0)}\right\rangle$ denotes the lowest order amplitude at which $\mathcal{N}$ can occur, and $\left|\mathcal{N}^{(l)}\right\rangle$ denotes the same amplitude dressed with l additional loops, i.e. $\mathcal{N}^l/\mathcal{N}^0 \propto \alpha_s^l$. Similarly, the perturbative expansion of the splitting operator can be expanded as

$$\mathbf{Sp} \equiv \mathbf{Sp}^{(0)} + \mathbf{Sp}^{(1)} + \mathbf{Sp}^{(2)} + \dots \tag{2.34}$$

with $Sp^{(l)}/Sp^{(0)} \propto \alpha_s^l$. Order by order, the CdFR factorisation formula (2.32) is the same expressed in terms of the unrenormalised splitting operator and amplitudes $\{\mathbf{Sp}, |\mathcal{M}\rangle, \left|\overline{\mathcal{M}}\right\rangle\}$ as of the renormalised ones $\{\mathbf{Sp}^R, |\mathcal{M}\rangle^R, \left|\overline{\mathcal{M}}\right\rangle^R\}$, i.e perturbative renormalisation *commutes* with the collinear limit [29]. In what follows we work with the renormalised amplitudes and adopt the $\overline{\text{MS}}$ scheme, as in the original reference[9].

The generalised collinear factorisation formula (2.32) at the level of squared amplitude reads

$$\langle\mathcal{M}\Big|\mathcal{M}\Big\rangle \simeq \Big\langle\overline{\mathcal{M}}\Big|\mathbf{P}\Big|\overline{\mathcal{M}}\Big\rangle, \qquad \mathbf{P} \simeq \mathbf{Sp}^\dagger\mathbf{Sp}. \tag{2.35}$$

Clearly, whenever $\mathbf{Sp}$ obeys strict factorisation so does kernel $\mathbf{P}$. There are cases, already at one loop order, in which the splitting $\mathbf{Sp}^{(l)}$ does not strictly factorise but the terms that break strict factorisation cancel at the level of the squared amplitude, see below. In view of this, it is convenient to consider the perturbative expansion of the kernel:

$$\mathbf{P} = \mathbf{P}^{(0)} + \mathbf{P}^{(1)} + \mathbf{P}^{(2)} + \dots \tag{2.36}$$

where $\mathbf{P}^{(0)} = \mathbf{Sp}^{(0)\dagger}\mathbf{Sp}^{(0)}$ is the squared tree-level splitting and $\mathbf{P}^{(l)}$ is the contribution of order α_s^l with respect to this.

[9]In this scheme the renormalisation scale in the QCD coupling $\alpha_s(\mu_R)$ is set equal to the dimensional regularisation scale μ. We will also drop the superscript R that distinguish bare from unrenormalised quantities.

2.4.4 One loop

Using the above series expansions, the collinear factorisation formula (2.32) at one loop order reads

$$\left|\mathcal{M}^{(1)}\right\rangle \simeq \mathbf{Sp}^{(1)}\left|\overline{\mathcal{M}}^{(0)}\right\rangle + \mathbf{Sp}^{(0)}\left|\overline{\mathcal{M}}^{(1)}\right\rangle. \tag{2.37}$$

Below we will discuss this expression for a general scattering $\mathcal{M}$. By way of illustration, we schematically represent this equation in Fig. 2.5 in a case in which the one-loop splitting kernel, $\mathbf{Sp}^{(1)}$, obeys strict collinear factorisation. In specific scatterings, the one-loop splitting has terms that do not obey strict collinear factorisation. In particular, the infrared divergent terms that correlate collinear and non-collinear for a more general scattering are schematically depicted in Fig. 2.6.

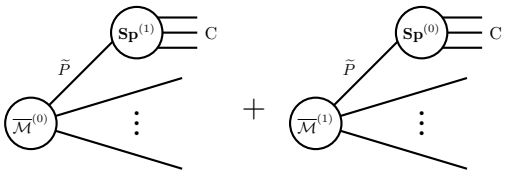

Figure 2.5: Schematic representation of collinear factorisation of an scattering amplitude at one-loop order, Eq. (2.37), for which splitting kernel is independent of the non-collinear partons.

In the particular case of the double collinear limit $m = 2$, CdFR computed the right-hand side in exactly $d = 4 - 2\epsilon$ dimensions, i.e. to all orders in the ϵ expansion. Nevertheless, here we will be mostly interested in studying singular infrared behaviour ($1/\epsilon$ poles) of this operator. To study the singular part, one can invoke that the (renormalised) one-loop QCD corrections to any physical process $\mathcal{N}$ with n external partons (in $d = 4 - 2\epsilon$ dimensions) can be written as [28]

$$\left|\mathcal{N}^{(1)}\right\rangle = \mathbf{I}^{(1)}_{\mathcal{N}}(\epsilon)\left|\mathcal{N}^{(0)}\right\rangle + \left|\mathcal{N}^{(1)}\right\rangle_{\text{fin}}, \tag{2.38}$$

where $\left|\mathcal{N}^{(1)}\right\rangle_{\text{fin}}$ is a renormalisation scheme dependent part that is finite as $\epsilon \to 0$ and, therefore, the operator $\mathbf{I}^{(1)}_{\mathcal{N}}$ embodies the universal[10] singular behaviour (soft and collinear):

$$\mathbf{I}^{(1)}_{\mathcal{N}}(\epsilon) \equiv \frac{\alpha_s}{2\pi}\frac{1}{2}\left[-\sum_i^n \left[\frac{1}{\epsilon^2}C_i + \frac{1}{\epsilon}\gamma_i\right] - \frac{1}{\epsilon}\sum_{i\neq j}^n \mathbf{T}_i\cdot\mathbf{T}_j\left[\ln\left(\frac{2p_i\cdot p_j}{\mu^2}\right) - i\pi\widetilde{\delta}_{ij}\right]\right]. \tag{2.39}$$

By comparing with Eq. (2.26) we can easily identify the ϵ poles corresponding to eikonal and Coulomb gluons. The single poles with the flavour dependent colour

[10] In the sense that its structure is the same for any scattering amplitude.

coefficients, γ_i, are given by

$$\gamma_q = \gamma_{\bar{q}} = 3/2C_F,\ \gamma_g = \frac{11}{6}C_A - \frac{2}{3}\mathrm{T_F}n_f, \tag{2.40}$$

and correspond to hard on-shell virtual fluctuations collinear with parton i. These hard collinear poles are included only in this section, before Section 2.5. In the rest of this work, we work within the approximation described in Section 2.1.

The universal formula (2.38) can be applied to the complete, $\left|\mathcal{M}^{(1)}\right\rangle$, and reduced, $\left|\overline{\mathcal{M}}^{(1)}\right\rangle$, one-loop amplitudes to write the one loop splitting operator in Eq. (2.37) as

$$\mathbf{Sp}^{(1)}\left|\overline{\mathcal{M}}^{(0)}\right\rangle \simeq \left(\mathbf{I}^{(1)}_{\mathcal{M}}\mathbf{Sp}^{(0)} - \mathbf{Sp}^{(0)}\mathbf{I}^{(1)}_{\overline{\mathcal{M}}} + \mathbf{Sp}^{(1)}_{\mathrm{fin}}\right)\left|\overline{\mathcal{M}}^{(0)}\right\rangle, \tag{2.41}$$

where $\mathbf{Sp}^{(1)}_{\mathrm{fin}}$ is the finite part of the splitting as $\epsilon \to 0$ and where

$$\mathbf{I}^{(1)}_{\mathcal{M}} \simeq (\mathrm{C}) + (\mathrm{NC}) + \frac{\alpha_s}{2\pi}\frac{1}{2}\left[-\frac{2}{\epsilon}\sum_{\substack{i\in C\\ j\in NC}}^{n}\mathbf{T}_i\cdot\mathbf{T}_j\left[\ln\left(\frac{z_i 2\widetilde{P}\cdot p_j}{\mu^2}\right) - i\pi\delta_{ij}\right]\right], \tag{2.42a}$$

$$\mathbf{I}^{(1)}_{\overline{\mathcal{M}}} = (\mathrm{NC}) + \frac{\alpha_s}{2\pi}\frac{1}{2}\left[-\frac{1}{\epsilon^2}C_{\mathcal{P}} - \frac{1}{\epsilon}\gamma_{\mathcal{P}} - \frac{2}{\epsilon}\sum_{j\in NC}\mathbf{T}_{\widetilde{P}}\cdot\mathbf{T}_j\left[\ln\left(\frac{2\widetilde{P}\cdot p_j}{\mu^2}\right) - i\pi\widetilde{\delta}_{\widetilde{P}j}\right]\right], \tag{2.42b}$$

where the symbols (C) and (NC) stand for terms that depend only on the collinear and only non-collinear partons respectively[11]. Also, in Eq. (2.42a) we used that for $i \in \mathrm{C}$ and $j \in \mathrm{NC}$ the following identity holds $p_i\cdot p_j \simeq z_i\widetilde{P}\cdot p_j$ where $z_i \equiv p_i\cdot n/\widetilde{P}\cdot n$ is the momentum fraction of parton i in the direction of the parent parton. The colour charge of the parent parton, $\mathbf{T}_{\widetilde{P}}$, is fixed by colour conservation:

$$\mathbf{T}_{\widetilde{P}}\left|\overline{\mathcal{M}}\right\rangle = -\sum_{i\in NC}\mathbf{T}_i\left|\overline{\mathcal{M}}\right\rangle. \tag{2.43}$$

Then, since $\mathbf{Sp}^{(0)}$ is independent of the non-collinear partons it commutes with the $\mathbf{T}_{\widetilde{P}}$ and we can write

$$\mathbf{Sp}^{(0)}\mathbf{T}_{\widetilde{P}}\left|\overline{\mathcal{M}}^{(0)}\right\rangle = \left(-\sum_{i\in\mathrm{NC}}\mathbf{T}_i\right)\mathbf{Sp}^{(0)}\left|\overline{\mathcal{M}}^{(0)}\right\rangle = \left(\sum_{i\in\mathrm{C}}\mathbf{T}_i\right)\mathbf{Sp}^{(0)}\left|\overline{\mathcal{M}}^{(0)}\right\rangle, \tag{2.44}$$

[11] Their explicit form can be deduced by applying Eq. (2.39) to $\mathcal{M}$ and $\overline{\mathcal{M}}$. More details of their deduction can be found in Section. 5.3 of Ref. [29]

where in the second identity we have exploited that $\mathbf{Sp}^{(0)}\left|\overline{\mathcal{M}}^{(0)}\right\rangle$ is a colour singlet. We now have all the necessary ingredients to study under which circumstances the singular part of one loop splitting operator strictly factorises. After applying this identity to Eq. (2.41), we observe that $\mathbf{Sp}^{(1)}$ can be written as

$$\mathbf{Sp}^{(1)} = \left(\mathbf{I}^{(1)}_{\mathcal{M}} - \mathbf{I}^{(1)}_{\overline{\mathcal{M}}}\right)\mathbf{Sp}^{(0)} + \mathbf{Sp}^{(1)}_{\text{fin}}. \tag{2.45}$$

By means of colour conservation, the term inside parenthesis in this expression yields

$$\begin{aligned}\mathbf{I}_C(\epsilon) \equiv \mathbf{I}^{(1)}_{\mathcal{M}} - \mathbf{I}^{(1)}_{\overline{\mathcal{M}}} = \frac{\alpha_s}{4\pi}\Bigg\{ &\frac{1}{\epsilon^2}\left[C_{\widetilde{P}} - \sum_{i\in C} C_i\right] - \frac{1}{\epsilon}\sum_{\substack{i\neq j\\ i,j\in \mathrm{C}}} \mathbf{T}_i\cdot\mathbf{T}_j \ln\frac{2p_i\cdot p_j}{z_i z_j \mu^2} \\ &+ \frac{1}{\epsilon}\left[\gamma_{\widetilde{P}} - i\pi\left[C_{\widetilde{P}} + \sum_{i\in C} C_i\right] + \sum_{i\in C}\left[2C_i \ln z_i - \gamma_i - C_i\right]\right]\Bigg\} + \widetilde{\mathbf{\Delta}}^{(1)}_C,\end{aligned} \tag{2.46}$$

where $\widetilde{\mathbf{\Delta}}^{(1)}_C(\epsilon)$ is an operator in colour space that contains only Coulomb gluons. It is defined as:

$$\widetilde{\mathbf{\Delta}}^{(1)}_C = \begin{cases} \frac{\alpha_s}{4\pi}\left(\frac{4i\pi}{\epsilon}\mathbf{T}_{\mathrm{NC}\cap\mathrm{in}}\cdot\left\{\mathbf{T}_{\mathrm{C}\cap\mathrm{in}} - \mathbf{T}_{\widetilde{P}}\right\} + \frac{2\pi i}{\epsilon}\mathbf{T}^2_{\mathrm{C}\cap\mathrm{in}}\right) & \text{if } \widetilde{P} \text{ is incoming ,} \\ \frac{\alpha_s}{4\pi}\left(\frac{4i\pi}{\epsilon}\mathbf{T}_{\mathrm{NC}\cap\mathrm{out}}\cdot\left\{\mathbf{T}_{\mathrm{C}\cap\mathrm{out}} - \mathbf{T}_{\widetilde{P}}\right\} + \frac{2\pi i}{\epsilon}\mathbf{T}^2_{\mathrm{C}\cap\mathrm{out}}\right) & \text{if } \widetilde{P} \text{ is outgoing .}\end{cases} \tag{2.47}$$

The colour charges $\mathbf{T}_{\mathrm{C}\cap\mathrm{in}}, \mathbf{T}_{\mathrm{C}\cap\mathrm{out}}, \mathbf{T}_{\mathrm{NC}\cap\mathrm{in}}, \mathbf{T}_{\mathrm{C}\cap\mathrm{out}}$ denote the total charge of the incoming-collinear, outgoing-collinear, incoming-non-collinear and outgoing-non-collinear partons respectively, e.g.

$$\mathbf{T}_{\mathrm{C}\cap\mathrm{in}} = \sum_{i\in\mathrm{C}\cap\mathrm{in}} \mathbf{T}_i.$$

Observe that the only terms dependent upon the collinear and non-collinear partons in Eq. (2.46) are contained in $\widetilde{\mathbf{\Delta}}^{(1)}_C$. Hence, strict factorisation is only satisfied when this operator can be expressed in terms of the collinear partons only. There are only six cases in which this can be done:

1. All the collinear partons are in the final state (as in e^+e^- annihilation into partons). Proof: $\widetilde{P}$ must be outgoing and equal to $\mathbf{T}_{\widetilde{P}} = \mathbf{T}_{\mathrm{C}\cap\mathrm{out}}$ and hence $\widetilde{\mathbf{\Delta}}_C$ depends only on the collinear partons.

2. All the collinear partons are in the initial state. The proof is similar to the previous case.

3. All the non-collinear partons are in the initial state. This implies that $\mathbf{T}_{\mathrm{NC}\cap\mathrm{out}} = 0$ and $\mathbf{T}_{\mathrm{NC}\cap\mathrm{in}} = -\mathbf{T}_{\widetilde{P}} = -\mathbf{T}_{\mathrm{C}\cap\mathrm{in}} - \mathbf{T}_{\mathrm{C}\cap\mathrm{out}}$ and hence $\widetilde{\mathbf{\Delta}}_C$ depends only on the collinear partons.

4. All the non-collinear partons are in the final state. The proof is similar to the previous case.

5. The process $\mathcal{M}$ has only one parton in the initial state (as in Lepton-Hadron DIS). Proof: Because of the first point we can assume that the incoming parton is collinear. In this case we have $\mathbf{T}_{\mathrm{NC}\cap\mathrm{in}} = 0$. Then, if $\widetilde{P}$ is incoming, $\widetilde{\mathbf{\Delta}}_C$ depends only on the collinear partons and, if $\widetilde{P}$ is outgoing, we have $\mathbf{T}_{\mathrm{NC}\cap\mathrm{out}} = -\mathbf{T}_{\widetilde{P}} = -\mathbf{T}_{\mathrm{C}\cap\mathrm{in}} - \mathbf{T}_{\mathrm{C}\cap\mathrm{out}}$ and again $\widetilde{\mathbf{\Delta}}_C$ can be re-expressed in terms of the collinear partons only.

6. $\mathcal{M}$ has only one outgoing parton. The proof is similar to the previous case.

To show that there are no other cases in which the amplitude strictly factorises, we note that the only cases not included in the above list require:

$$\mathbf{T}_{\mathrm{NC}\cap\mathrm{in}}, \mathbf{T}_{\mathrm{NC}\cap\mathrm{out}}, \mathbf{T}_{\mathrm{C}\cap\mathrm{in}}, \mathbf{T}_{\mathrm{C}\cap\mathrm{out}} \neq 0 \ . \tag{2.48}$$

In such cases[12], colour conservation cannot be used to express the total incoming (or outgoing) non-collinear colour charge in terms of the colour charge of the collinear partons only. It follows that Eq. (2.47) can no longer be solely expressed in terms of the collinear partons. The terms that break collinear factorisation in Eq. (2.47) when $\widetilde{P}$ is incoming are schematically illustrated as in Fig. 2.6.

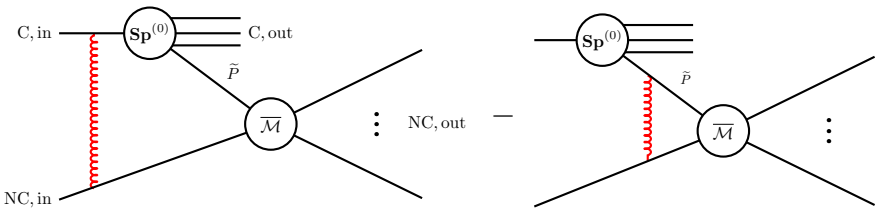

Figure 2.6: Representation of the terms that break the strict collinear factorisation in Eq. (2.47), when the parent parton, $\widetilde{P}$, is incoming and Eq. (2.48) is satisfied. The red curly lines represent Coulomb gluons exchanged between collinear and non-collinear partons.

CdFR showed that in the first two cases, which they referred to as time-like kinematics, the amplitude strictly factorises to all orders but, for more general kinematics, the amplitude does not obey strict collinear factorisation beyond one loop order. A special exception is fifth case in the aforementioned list. It is worth noting that, in the last four cases in this list, strict factorisation is effectively restored by colour conservation.

[12] i.e. for an scattering involving incoming and outgoing collinear partons, and also incoming and outgoing non-collinear partons.

Finally, by squaring Eq. (2.45) we get the following expression for the kernel $\mathbf{P}$

$$\mathbf{P}^{(1)} = \mathbf{Sp}^{(0)} \left[\mathbf{I}_C + \mathbf{I}_C^\dagger\right] \mathbf{Sp}^{(0)} + \left\{\mathbf{Sp}^{(0)\dagger}\mathbf{Sp}^{(1)}_{\text{fin}} + \text{h.c.}\right\} \ . \tag{2.49}$$

Due to their anti-hermitian nature, the Coulomb gluons in the first term cancel and hence the only possible violations of strict factorisation at this order are due to the finite terms inside braces. In the next chapter, we will show these finite contributions for the case of the double collinear limit $m = 2$ (within the eikonal approximation). We anticipate that they obey exactly the same factorisation formulae as the IR contributions, see Eq. (G.3) of Appendix G.

2.4.5 Two loops

Within the framework of dimensional regularisation, the structure of the IR divergences of the two-loop QCD corrections to a general scattering process $\mathcal{N}$ was first reported in [52]. After renormalisation in the $\overline{MS}$ scheme these can be expressed as

$$\left|\mathcal{N}^{(2)}\right\rangle = \mathbf{I}_N^{(1)}(\epsilon)\left|\mathcal{N}^{(1)}\right\rangle + \mathbf{I}_{\mathcal{N}}^{(2)}(\epsilon)\left|\mathcal{N}^{(0)}\right\rangle + \left|\mathcal{N}^{(2)}\right\rangle_{\text{fin}} \tag{2.50}$$

where $\left|\mathcal{N}^{(1)}\right\rangle$ is the same as in Eq. (2.38), $\left|\mathcal{N}^{(2)}\right\rangle_{\text{fin}}$ denotes (scheme dependent) finite contributions, and $\mathbf{I}_{\mathcal{N}}^{(2)}$ is a colour operator given by

$$\begin{aligned}\mathbf{I}_{\mathcal{N}}^{(2)}(\epsilon) = &-\frac{1}{2}\left[\mathbf{I}_{\mathcal{N}}^{(1)}(\epsilon)\right]^2 + \frac{\alpha_s}{2\pi}\frac{b_0}{\epsilon}\left[\mathbf{I}_{\mathcal{N}}^{(1)}(2\epsilon) - \mathbf{I}_{\mathcal{N}}^{(1)}(\epsilon)\right] \\ &+ \frac{\alpha_s K}{2\pi}\mathbf{I}_{\mathcal{N}}^{(1)}(2\epsilon) + \left(\frac{\alpha_s}{2\pi}\right)^2 \sum_{i=1}^{n} \frac{1}{\epsilon} H_i\end{aligned} \tag{2.51}$$

where $K = \left[\frac{67}{18} - \frac{\pi^2}{6}\right] - \frac{10}{9}T_R N_F$ and the flavour coefficients H_i are real constants that can be found in CdFR. As in the one-loop case, the universal formula (2.50) can be applied on the complete, $\left|\mathcal{M}^{(1)}\right\rangle$, and reduced, $\left|\overline{\mathcal{M}}^{(1)}\right\rangle$, two-loop amplitude to write down expressions for the two-loop splitting, $\mathbf{Sp}^{(2)}$, and kernel, $\mathbf{P}^{(2)}$. These expressions can be found in [30]. In general, the two-loop kernel no longer satisfies strict factorisation. The possible violations of factorisation are all of the form

$$\begin{aligned}\mathbf{P}^{(2)}_{\text{n.f.}} =& \frac{1}{2}\mathbf{Sp}^{(0)\dagger}\left[\left\{\mathbf{I}^{(1)}_{\overline{\mathcal{M}}} + \mathbf{I}^{(1)\dagger}_{\overline{\mathcal{M}}} + \mathbf{I}^{(1)}_{C} + \mathbf{I}^{(1)\dagger}_{C}\right\}, \widetilde{\mathbf{\Delta}}^{(1)}\right]\mathbf{Sp}^{(0)} \\ &+ \left(\mathbf{Sp}^{(0)\dagger}\mathbf{I}^{(1)}_{C\mathcal{M}}\mathbf{Sp}^{(1)}_{\text{fin}} + \mathbf{Sp}^{(0)\dagger}\left[\mathbf{I}^{(1)}_{\overline{\mathcal{M}}}, \mathbf{Sp}^{(1)}_{\text{fin}}\right] + \text{h.c.}\right) \\ &+ \mathbf{Sp}^{(1)\dagger}_{\text{fin}}\mathbf{Sp}^{(1)}_{\text{fin}} + \mathbf{Sp}^{(2)\dagger}_{\text{fin}}\mathbf{Sp}^{(0)} + \mathbf{Sp}^{(0)\dagger}\mathbf{Sp}^{(2)}_{\text{fin}},\end{aligned} \tag{2.52}$$

where $\mathbf{Sp}^{(2)}_{\text{fin}}$ is the finite part of the splitting at two-loop order. The violations of strict factorisation in the first line are equal to the commutator between the

eikonal terms inside curly braces, and the Coulomb gluons in $\widetilde{\mathbf{\Delta}}^{(1)}$. Since, due to colour conservation, the eikonal gluons in $\mathbf{I}^{(1)}_{\overline{\mathcal{M}}} + \mathbf{I}^{(1)\dagger}_{\overline{\mathcal{M}}}$ and in $\mathbf{I}^{(1)}_{C\mathcal{M}} + \mathbf{I}^{(1)\dagger}_{C\mathcal{M}}$ can be expressed in terms of the collinear partons only, it follows that the first line obeys strict factorisation if $\widetilde{\mathbf{\Delta}}^{(1)}$ can be expressed in terms of the colour charges of the collinear partons only. This implies that the first line also obeys strict factorisation in of all the six cases described at one loop order.

In a strict sense, the operator in first line is not vanishing, however, its contribution to a pure QCD process exactly cancels. This was first shown in [36] by noting that, for a pure QCD processes $\mathcal{M}$, there is a colour basis [53] in which $\left|\mathcal{M}^{(0)}\right\rangle \left\langle\mathcal{M}^{(0)}\right|$ and the product of any two colour charges, $\mathbf{T}_i\cdot\mathbf{T}_j$, are real symmetric matrices. In this basis, each term in the first line of Eq. (2.52) identically vanishes because it reduces to the trace of a symmetric times an antisymmetric matrix:

$$\mathrm{Tr}\left[\left|\overline{M}\right\rangle\left\langle\overline{M}\right|[\mathbf{T}_i\cdot\mathbf{T}_j, \mathbf{T}_l\cdot\mathbf{T}_m]\right] = 0\ , \tag{2.53}$$

where the trace is over the colour of the external partons.

2.4.6 Beyond two loops

We shall now describe the all-orders factorisation formula in Eq. (2.32). Following CdFR, we organise the IR divergences of every (renormalised) scattering amplitude $\mathcal{N}$ as follows:

$$\begin{gathered}\left|\mathcal{N}\right\rangle = \widetilde{\mathbf{V}}_{\mathcal{N}}(\epsilon)\left|\mathcal{N}\right\rangle_{\mathrm{fin}},\\ \widetilde{\mathbf{V}}^{-1}_{\mathcal{N}}(\epsilon) = 1 - \mathbf{I}_{\mathcal{N}}, \quad \mathbf{I}_{\mathcal{N}} = \mathbf{I}^{(1)}_{\mathcal{N}} + \mathbf{I}^{(2)}_{\mathcal{N}} + \mathbf{I}^{(3)}_{\mathcal{N}} + \dots .\end{gathered} \tag{2.54}$$

where the IR operators $\mathbf{I}^{(1)}_{\mathcal{N}}$ and $\mathbf{I}^{(2)}_{\mathcal{N}}$ are the same as above, and, in general, their divergent behaviour goes as $\mathbf{I}^{(l)}_{\mathcal{N}} \sim \alpha_s^l/\epsilon^{2l}$. Additionally, the amplitude $|\mathcal{N}\rangle_{\mathrm{fin}}$ denotes the finite part (as $\epsilon \to 0$) of the amplitude after renormalisation and hence the operator $\widetilde{\mathbf{V}}_{\mathcal{N}}(\epsilon)$, embodies all the IR poles of the amplitude. It has been pointed out that this operator exponentiates [54, 55, 56, 57, 58, 59, 59, 60], i.e. it can be written as

$$\widetilde{\mathbf{V}}_{\mathcal{N}}(\epsilon) = \exp\left(\mathbf{I}_{\mathcal{N},\mathrm{cor}}\right), \tag{2.55}$$

where the operator $\mathbf{I}_{\mathcal{N},\mathrm{cor}}$ can be expressed as a power series in the coupling

$$\mathbf{I}_{\mathcal{N},\mathrm{cor}} = \mathbf{I}^{(1)}_{\mathcal{N},\mathrm{cor}} + \mathbf{I}^{(2)}_{\mathcal{N},\mathrm{cor}} + \dots \tag{2.56}$$

and where the infrared behaviour of this operator at each order goes as $\mathbf{I}^{(l)}_{\mathcal{N},\mathrm{cor}} \sim \alpha_s^l/\epsilon^{l+1}$. Clearly, the first term in the expansion should satisfy $\mathbf{I}^{(1)}_{\mathcal{N},\mathrm{cor}} = \mathbf{I}^{(1)}_{\mathcal{N}}$. The

exponentiation given by Eqs. (2.55) and (2.56) exhibits the fact that the dominant singular IR behaviour at high orders in the coupling is captured by the exponentiation of the lower terms in the perturbative expansion[13] [29].

By organising the infrared divergences of $\mathcal{M}$ and $\overline{\mathcal{M}}$ as in (2.54), CdFR deduced the following all orders factorisation formula for the splitting operator in Eq. (2.28)

$$\Big|\mathcal{M}\Big\rangle \simeq \mathbf{Sp}\Big|\overline{\mathcal{M}}\Big\rangle = \widetilde{\mathbf{V}}_{\mathcal{M}}(\epsilon)\ \mathbf{Sp}_{\text{fin}}\ \widetilde{\mathbf{V}}^{-1}_{\overline{\mathcal{M}}}(\epsilon)\Big|_{\mathbf{T}_{\tilde{P}}=-\mathbf{T}_{\text{NC}}}\Big|\overline{\mathcal{M}}\Big\rangle, \tag{2.57}$$

where the operator $\mathbf{V}_{\mathcal{M}}(\epsilon)$ is understood to be evaluated in the respective collinear limit[14], and the finite part of the splitting $\mathbf{Sp}_{\text{fin}}$ can be expanded as a perturbative series

$$\mathbf{Sp}_{\text{fin}} \equiv \mathbf{Sp}^{(0)} + \mathbf{Sp}^{(1)}_{\text{fin}} + \mathbf{Sp}^{(2)}_{\text{fin}} + \dots \tag{2.58}$$

with $Sp^{(l)}_{\text{fin}}/Sp^{(0)} \propto \alpha_s^l$. We are not interested in evaluating Eq. (2.57) to higher orders but there is a lesson that can be learned from it [30]. By approximating the infrared operators $\{\mathbf{V}_{\mathcal{M}}, \mathbf{V}_{\overline{\mathcal{M}}}\}$ as the exponentiation of the universal infrared part of the one-loop effects, i.e.

$$\widetilde{\mathbf{V}}_{\mathcal{M}}(\epsilon) \to \exp\left(\mathbf{I}^{(1)}_{\mathcal{M}}\right) \qquad \text{and} \qquad \widetilde{\mathbf{V}}_{\overline{\mathcal{M}}}(\epsilon) \to \exp\left(\mathbf{I}^{(1)}_{\overline{\mathcal{M}}}\right), \tag{2.59}$$

in Eq. (2.28) and expanding to order α_s^2 one can deduce the two-loop violations of strict factorisation in Eq. (2.52). This means that, at order α_s^2, the violations of strict factorisation are only due to the exponentiation of the soft (eikonal and Coulomb) one-loop corrections. In [30], this was noticed and used to infer the violations of strict factorisation that should appear at three-loop order. This time, the violations no longer vanish for pure QCD processes. Furthermore, the terms that break factorisation at this order have the same structure[15] as the terms responsible for the appearance of super-leading contributions in GBJ, and this confirms that the physics of super-leading logarithms is related to the violations of strict collinear factorisation [30].

It is important to remark that the violations of strict factorisation, at amplitude and squared amplitude level, do not contradict well established theorems [26, 22, 25] on the collinear factorisation for inclusive observables involving hadron–lepton or hadron–hadron initiated processes. As we discussed in Section 1.4.1, for such cases the contributions that break strict collinear factorisation cancel once a sufficiently

[13] The study of the perturbative expansion of (2.56), and more generally the infrared behaviour of multi-parton scattering amplitudes and its organisation in terms of webs [61] is a very active area of research, see [37, 62, 63, 64] and references therein.

[14] More precisely, the collinear momenta should be evaluated at $p_i \simeq z_i \tilde{P}$ in all the terms that are not singular in this limit.

[15] Double commutators of two Coulomb and one eikonal gluon.

inclusive sum over the final states is carried out [22].

As we discussed in Section 1.5, for non-inclusive observables the factorisation of collinear divergences is expected [30] to be possible up to the scale Q_0 below which the real radiation is summed up inclusively[16]. In addition, above Q_0 the miscancellation of real and virtual (including Coulomb) contributions is expected [30] to give rise to perturbatively-calculable effects with contributions that cannot be written in a strict process independent manner. This could be a general prescription to calculate the perturbative corrections to non-inclusive observables. It was first studied in the calculation of the GBJ in Refs. [31, 36]. However, it is important to point out that it is not yet clear which observables are non-inclusive in this sense and what a general definition of Q_0 might be. There is still work to be done in elucidating these issues.

We close this section by reiterating the main conclusion we will use in the forthcoming sections: the exponentiation of the eikonal and Coulomb one-loop virtual corrections seeds the violations of strict collinear factorisation and any framework that aims to describe this physics should incorporate them.

2.5 On the structure of soft corrections to all orders

The series of papers on the super-leading logarithms by FKS are based on an algorithm for the inclusion of eikonal and Coulomb gluons to all orders in the perturbative expansion [31, 36]. Starting from the next chapter, we will provide formal evidence of its correctness in particular cases. In this section we shall motivate its structure at amplitude level and illustrate some of its properties.

In Section 2.1 we presented the eikonal rules for the soft gluon corrections to a hard wide-angle scattering. A heuristic construction of the dominant contributions at each order is known as the soft gluon insertion technique [65, 49, 66, 67], for a first introduction see [68]. We emphasise that, although this construction includes the colour interference between different partons, it ignores the contributions of Coulomb gluons.

To be concrete, let us consider the hard wide-angle scattering $\left|n^{(0)}(p_1,\ldots,p_n)\right\rangle$ of n on-shell partons. The contribution of the matrix element with $\{l_1,\ldots,l_m\}$ gluons, either real or virtual, can be constructed following simples rules [67]:

- Firstly, it is assumed that the leading contribution of a matrix element with m gluons comes from kinematical regions in which their energies are strongly ordered, i.e.

$$l_m^0 \ll l_{m-1}^0 \ll \cdots \ll l_1^0 \ll Q \ , \tag{2.60}$$

[16] To some degree, all observables have an inclusivity scale.

Q is the characteristic scale of the hard scattering. This applies to both real and virtual gluons because the latter are assumed to be nearly on-shell.

- Secondly, the leading graphs in this region are obtained by inserting first the hardest of the soft gluons l_1 on each of the external partons of the hard scattering subprocess, then l_2 on each of the external legs of the relatively harder partons (including l_1), and so on.

- Finally, the eikonal rules are used to approximate the radiation of any soft gluon off relatively harder partons.

These rules can be systematically implemented through soft-gluon current operators $\mathbf{J}^{\mu}_{m}(q_m)$ defined as the operation of inserting an eikonal gluon q_m on each of the external legs of a matrix element with n hard partons and with $m-1$ additional gluons, i.e.

$$\mathbf{J}^{\mu}_{n+m}(q_m) \equiv g_s\mu^{\epsilon}\sum_{i=1}^{n}\mathbf{T}_l\frac{p_i\cdot\varepsilon_m}{p_i\cdot q_m} + g_s\mu^{\epsilon}\sum_{i=n+1}^{m-1}\mathbf{T}_i\frac{q_i\cdot\varepsilon_m}{q_i\cdot q_m}\ . \tag{2.61}$$

Then, according to the soft gluon insertion technique, the complete lowest order amplitude with m real emissions $q_m^0 \ll \cdots \ll q_1^0 \ll Q$ is

$$\left|n^{(0)}_{+m}\right\rangle = \mathbf{J}_{n+m}(q_m)\ldots\mathbf{J}_{n+1}(q_1)\left|n^{(0)}\right\rangle\ . \tag{2.62}$$

Virtual corrections are often introduced indirectly [67, 49, 65] by invoking the cancellation of soft singularities in the total cross section (Bloch-Nordsieck theorem [69]) that we discuss below. Instead of this approach, we directly include the virtual radiation using the soft insertion technique. To do this, we first note that the sum of any number of virtual insertions with energies in the interval $\left(q_l^0, q_{l-1}^0\right)$ exponentiate, i.e.

$$\begin{aligned}
&1 + \frac{1}{2}\int_{q_l^0}^{q_{l-1}^0}\mathrm{d}[k_1]\mathbf{J}^2_{n+l}(k_1) + \left(\frac{1}{2}\int_{q_{l-1}^0}^{q_l^0}\mathrm{d}[k_1]\mathbf{J}^2_{n+l}(k_1)\right)\left(\frac{1}{2}\int_{q_l^0}^{k_1^0}\mathrm{d}[k_2]\mathbf{J}^2_{n+l}(k_2)\right) + \ldots \\
&= \exp\left(\frac{1}{2}\int_{q_l^0}^{q_{l-1}^0}\mathrm{d}[k_1]\mathbf{J}^2_{n+l}(k_1)\right)\ .
\end{aligned} \tag{2.63}$$

where $\mathrm{d}[k]$ is defined below Eq. (2.14) and we have used the shorthand $\mathbf{J}^2_{n+l} \equiv \mathbf{J}^{\mu}_{n+m}\cdot\mathbf{J}_{n+1\mu}$. To deduce the right-hand side one needs to order the energy limits using Eq. (B.8) and then use that

$$\left[\int \mathrm{d}[k]\mathbf{J}^2(k), \int \mathrm{d}[k']\mathbf{J}^2(k')\right] = 0. \tag{2.64}$$

This identity (Eq. (2.63)) allows us to introduce the virtual corrections between each of the emissions in the tree level amplitude (2.62). After this, the all orders m emission amplitude $\left|n_{+m}\right\rangle$ reads

$$\left|n_{+m}\right\rangle \equiv \mathbf{V}_{n+m}^{(0,q_m^0)}\mathbf{J}_{n+m}(q_m)\mathbf{V}_{n+m-1}^{(q_m^0,q_{m-1}^0)}\dots\mathbf{J}_{n+1}^{\mu}(q_1)\mathbf{V}_{n}^{(q_1^0,Q)}\left|n^{(0)}\right\rangle\,, \tag{2.65}$$

where the virtual gluon corrections are encoded in the Sudakov operator:

$$\mathbf{V}_{n+r}^{(\beta,\alpha)} \equiv \exp\left[\frac{1}{2}\int \mathrm{d}[k]\mathbf{J}_{n+r+1}(k)\cdot\mathbf{J}_{n+r+1}(k)\,\Theta(\alpha<k_0<\beta)\right]. \tag{2.66}$$

Equation (2.65) is expressed as a product of energy ordered real emissions with Sudakov operators expressing the non-emission factors at intermediate scales. These matrix elements satisfy the following properties:

1. Gauge invariance. The amplitude $\left|n_{+m}\right\rangle$ identically vanishes under the substitution $\varepsilon(q_i)\to q_i$.

2. Bloch-Nordsieck cancellation of soft gluons. The contributions of the real and virtual gluons cancel when they are integrated inclusively in d dimensions, i.e

$$\begin{aligned}\langle n|n\rangle + \int \mathrm{d}[q_1]\,\langle n_{+1}|n_{+1}\rangle + \int_{q_2^0<q_1^0}\mathrm{d}[q_1]\mathrm{d}[q_2]\,\langle n_{+2}|n_{+2}\rangle + \dots \\ = \left\langle n^{(0)}\middle|n^{(0)}\right\rangle\,.\end{aligned} \tag{2.67}$$

   Furthermore, in the calculation of an observable ϕ that is fully inclusive below a given scale[17] Q_0, we can set this scale as the lower integration limit of all the real and virtual contributions, i.e.

$$\langle n|n\rangle + \int_{Q_0}\mathrm{d}[q_1]\,\langle n_{+1}|n_{+1}\rangle\,\phi_1 + \int_{Q_0<q_2^0<q_1^0}\mathrm{d}[q_1]\mathrm{d}[q_2]\,\langle n_{+2}|n_{+2}\rangle\,\phi_2 + \dots \tag{2.68}$$

   here ϕ_i $(i=\{1,,2\dots\})$

3. Coherence. Let $\{l,k\}$ be two real or virtual gluons that become collinear. In this limit, each soft-gluon current corresponding to radiation of a softer gluon q, either real or virtual, that has wide angles with $\{l,k\}$ becomes

$$\begin{aligned}\mathbf{J}_{n+m}^{\mu}(q) &= g\mu^{2\epsilon}\left[\mathbf{T}_k\frac{p_k^{\mu}}{p_k\cdot q}+\mathbf{T}_l\frac{p_l^{\mu}}{p_l\cdot q}+\sum_{i\neq\{k,l\}}\mathbf{T}_i\frac{p_i^{\mu}}{p_i\cdot q}\right] \\ &\simeq g\mu^{2\epsilon}\left[(\mathbf{T}_k+\mathbf{T}_l)\,\frac{(p_k+p_l)^{\mu}}{(p_k+p_l)\cdot q}+\sum_{i\neq\{k,l\}}\mathbf{T}_i\frac{p_i^{\mu}}{p_i\cdot q}\right]\,.\end{aligned} \tag{2.69}$$

[17] For instance, this would be the veto scale in the calculation of 'gaps between jets'.

where we have used that, for the kinematics considered, $p_k^\mu/p_k \cdot q \simeq p_l^\mu/p_l \cdot q = p^\mu/p \cdot q$ where p is any light-like vector with positive energy oriented in the collinear direction. Hence, given two collinear $\{k, l\}$ partons, the relatively soft wide-angle radiation only probes the total charge and momentum of the pair $\{l, k\}$. This property is commonly referred to as the coherence of wide-angle radiation.

It is worth mentioning that, within the context of a Sudakov resummation at double logarithmic accuracy there are now studies [39, 40] that shows that different ordering variables can be used (transverse momentum, angle, virtuality, among other variables), and that the coherence property of QCD radiation [35] is understood to be responsible for this freedom. A review of different ordering variables for the radiative part of the soft corrections is beyond the scope of this work, instead, we are mainly interested in including the contribution of Coulomb gluons.

2.5.1 Enter the game: Coulomb gluons

For the purpose of studying factorisation breaking effects, the soft gluon insertion technique described above is insufficient because it does not include Coulomb gluons. In order to motivate how to include them into the soft insertion technique we turn our attention to the two following properties of scattering amplitudes:

- The eikonal virtual corrections to general hard wide-angle scattering exponentiate [70, 71, 72, 73, 74, 75, 76, 77]. More precisely, given a hard wide-angle process, the loop corrections can be written as the exponential of a power series in strong coupling:

$$\Big|n\Big\rangle = \exp\left(\mathbf{I}_n\right)\Big|n^{(0)}\Big\rangle, \qquad \mathbf{I}_n = \mathbf{I}_n^{(1)} + \mathbf{I}_n^{(2)} + \dots \tag{2.70}$$

  where $\mathbf{I}_n^{(l)}$ denote terms of order α_s^l. In particular, $\mathbf{I}_n^{(1)}$ is exactly equal to Eq. (2.15).

- The S-matrix is expected to be an analytic function of its Lorentz invariants[18] (regarded as complex variables), with only those singularities required by unitarity [78].

With an eye on the structure of the one loop corrections, these two properties suggest that Coulomb gluons may be introduced into the soft gluon insertion matrix elements,

[18] Strictly speaking, the transverse momentum and not the energy is a Lorentz invariant, see below.

Eq. (2.65), simply by modifying the virtual operators as follows:

$$\begin{aligned}
\Big|n_{+m}\Big\rangle &\equiv \mathbf{V}_{n+m}^{(0,q_m^0)}\mathbf{J}_{n+m}(q_m)\mathbf{V}_{n+m-1}^{(q_m^0,q_{m-1}^0)}\dots\mathbf{J}_{n+1}^{\mu}(q_1)\mathbf{V}_{n}^{(q_1^0,Q)}\Big|n^{(0)}\Big\rangle \ , \\
\mathbf{V}_{n+r}^{(\beta,\alpha)} &\equiv \exp\left[\frac{1}{2}\int \mathrm{d}[k]\mathbf{J}_{r+1}(k)\cdot\mathbf{J}_{r+1}(k)\,\Theta(\alpha<k_0<\beta)+\sum_{i<j}^{n+r}\widetilde{\delta}_{ij}\mathbf{C}^{ij}(\beta,\alpha)\right] \ , \\
\mathbf{C}_{ij}^{(\beta,\alpha)} &= -i\pi\frac{\alpha_s}{2\pi}c_\epsilon\mathbf{T}_i\cdot\mathbf{T}_j\int_{\alpha^2}^{\beta^2}\frac{\mathrm{d}k_T^2}{k_T^{d-2}} \ .
\end{aligned} \tag{2.71}$$

As we show in Appendix B, this modified picture is again gauge invariant, satisfies the Bloch-Nordsieck theorem and even the perfect cancellation below the inclusivity scale. This time, however, the violations of strict factorisation (due to the exponentiation of the one loop corrections) are included and, in addition, there is a drastic change [36]: the coherence property of soft wide-angle radiation, illustrated by Eq. (2.69), is not respected by the Coulomb gluons. More precisely, given two partons $\{l,k\}$ that are incoming and outgoing respectively, the Coulomb gluons in the virtual operator, $\mathbf{V}_{n+r}$, (2.71) have the following dependence on the colour charges of these two gluons

$$\begin{aligned}
&\sim \sum_{i\neq\{k,l\}}\widetilde{\delta}_{ki}\mathbf{T}_k\cdot\mathbf{T}_i+\sum_{i\neq\{k,l\}}\widetilde{\delta}_{li}\mathbf{T}_l\cdot\mathbf{T}_i+\widetilde{\delta}_{lk}\mathbf{T}_l\cdot\mathbf{T}_i \ , \\
&= \mathbf{T}_k\cdot\sum_{\substack{i\in\mathrm{Out}\\ i\neq k}}\mathbf{T}_i+\mathbf{T}_l\cdot\sum_{\substack{i\in\mathrm{In}\\ i\neq l}}\mathbf{T}_i \ .
\end{aligned} \tag{2.72}$$

where $\widetilde{\delta}_{ij}$ is defined below Eq. (2.25). The right-hand side of this expression clearly shows that, in general, Coulomb gluons depend separately on $\mathbf{T}_k$ and $\mathbf{T}_l$, and one can check that this persists even when $\{l,k\}$ are collinear.

One can give a simple physical interpretation to the colour evolution picture described by Eqs. (2.71), which is often used within the context of parton showers [35]. The main feature of this picture is that the radiated gluons, either real or virtual, are ordered with respect to the size of their momentum components, with radiation with greater components acting closer to the hard process. A naïve use of quantum uncertainty suggests that we can associate a time scale to the radiation as the inverse of the magnitude of its momentum components. In accordance with this, the colour evolution picture is time-ordered.

2.6 Super-leading logarithms and the ordering problem

In the original Refs. [31, 36], where FKS introduced the colour evolution picture, the variable that orders the radiation is the transverse momentum and not the energy. The motivations behind this choice were previous studies of the soft anomalous dimension matrix [79] and the observation that in general Coulomb gluon corrections, see Eq. (2.17), can be expressed as transverse momentum integrals. In this section, we study how this algorithm gives rise to super-leading logarithms.

For the sake of clarity, we shall present the k_T colour evolution algorithm in the notation of [31, 36]. The algorithm for a general observable, is built from the set of cross sections corresponding to exclusive m gluon emission, $\{\mathrm{d}\sigma_m\}$:

$$\begin{aligned}
\mathrm{d}\sigma_0 &= \left\langle n^{(0)}\right| \mathbf{V}_{0,Q}^{\dagger}\mathbf{V}_{0,Q} \left|n^{(0)}\right\rangle \,\mathrm{d}\Pi_0 \\
\mathrm{d}\sigma_1 &= \left\langle n^{(0)}\right| \mathbf{V}_{q_{1T},Q}^{\dagger}\mathbf{D}_{1\mu}^{\dagger}\mathbf{V}_{0,q_{1T}}^{\dagger}\mathbf{V}_{0,q_{1T}}\mathbf{D}_{1}^{\mu}\mathbf{V}_{q_{1T},Q} \left|n^{(0)}\right\rangle \,\mathrm{d}\Pi_0\mathrm{d}\Pi_1 \\
\mathrm{d}\sigma_2 &= \left\langle n^{(0)}\right| \mathbf{V}_{q_{1T},Q}^{\dagger}\mathbf{D}_{1\mu}^{\dagger}\mathbf{V}_{q_{2T},q_{1T}}^{\dagger}\mathbf{D}_{2\nu}^{\dagger}\mathbf{V}_{0,q_{2T}}^{\dagger}\mathbf{V}_{0,q_{2T}}\mathbf{D}_{2}^{\nu}\mathbf{V}_{q_{2T},q_{1T}}\mathbf{D}_{1}^{\mu}\mathbf{V}_{q_{1T},Q} \left|n^{(0)}\right\rangle \,\mathrm{d}\Pi_0\mathrm{d}\Pi_1\mathrm{d}\Pi_2 \\
&\text{etc.}
\end{aligned} \tag{2.73}$$

We now explain this condensed notation. The fixed-order matrix element is represented by a vector in colour and spin $\left|M^{(0)}\right\rangle$, and $\mathrm{d}\Pi_0$ is the corresponding phase-space. The crucial difference with the energy ordered picture in Eq. (2.71) is that the successive radiation, and in particular the Sudakov operators $\mathbf{V}_{q_{2T},q_{1T}}$, are ordered with respect to the transverse momentum of the real gluon emissions:

$$\mathbf{V}_{a,b} = \exp\left[-\frac{2\alpha_s}{\pi}\int_a^b \frac{\mathrm{d}k_T}{k_T}\sum_{i<j}(-\mathbf{T}_i\cdot\mathbf{T}_j)\frac{1}{2}\left\{\int\frac{\mathrm{d}y\,\mathrm{d}\phi}{2\pi}\omega_{ij} - i\pi\,\widetilde{\delta}_{ij}\right\}\right] \,, \tag{2.74}$$

where

$$\omega_{ij} = \frac{1}{2}k_T^2\frac{p_i\cdot p_j}{(p_i\cdot k)(p_j\cdot k)} \tag{2.75}$$

and k_T, y and ϕ are the transverse momentum, rapidity and azimuth of the virtual gluon with momentum k that is exchanged between partons i and j. The operator $\mathbf{D}_i^{\mu}$, corresponds to the real emission of a gluon with transverse momentum q_{Ti} and the associated phase-space element (including a factor α_s for convenience) is $\mathrm{d}\Pi_i$:

$$\begin{aligned}
\mathbf{D}_i^{\mu} &= \sum_j \mathbf{T}_j\,\frac{1}{2}q_{Ti}\frac{p_j^{\mu}}{p_j\cdot q_i} \,, \\
\mathrm{d}\Pi_i &= -\frac{2\alpha_s}{\pi}\frac{\mathrm{d}q_{Ti}}{q_{Ti}}\frac{\mathrm{d}y_i\mathrm{d}\phi_i}{2\pi} \,.
\end{aligned} \tag{2.76}$$

Observe that $\mathbf{J}(q_i)\mathrm{d}[q_i] \propto \mathbf{D}_i\,\mathrm{d}\Pi_i$. A general cross section can then be written

$$\sigma = \sum_{m=0}^{\infty} \int \mathrm{d}\sigma_m\,\phi_m \ , \tag{2.77}$$

where $\{\phi_m\}$ are functions of the phase-space that define the observable.

We recall that the GBJ observable is the cross-section for the production of two high transverse momentum jets with the condition that any additional central jet should have smaller transverse momentum than a given scale Q_0. This is a particular case of the so-called non-global observables that are characterised for only being sensitive to the (real) radiation in a limited region of phase space. In [80, 81], these observables were shown to contain a series of single (non-global) logarithmic corrections, $\propto (\alpha_s \ln^n(Q^2/Q_0^2)$, associated with the miscancellation of the virtual radiation that dresses real emissions. Specifically, this miscancellation occurs because while such virtual radiation is unrestricted the real emissions, that otherwise would cancel it, are constrained to lie in a restricted region of the phase-space.

This is a good moment to point out that FKS envisioned the algorithm in (2.73) as a framework to compute soft corrections that accounts for the non-trivial colour structure of Coulomb gluons. In particular, a complete calculation of non-global observables requires the inclusion of such contributions. In the so-called large N approximation[19], that was previously used to study the non-global logarithms, the colour evolution in (2.73) becomes diagonal and Coulomb gluons become phases that trivially cancel. This is the reason why super-leading contributions were not previously observed.

In the GBJ case, the non-global logarithms originate due to fact that emissions outside of the gap (away from the central region) are forbidden from radiating back into central region with $k_T > Q_0$, but the virtual corrections that dress such emissions do not have to obey this constraint. Thus motivated, FKS formulated Eq. (2.73) to calculate the cross-section for events consisting of one real or virtual gluon radiated 'outside of the gap' dressed with any number of Coulomb and eikonal virtual gluons with $k_T > Q_0$. Surprisingly, they found that while miscancellations between eikonal gluons give rise to single logarithmic corrections (including non-global logarithms), the miscancellation between eikonal and Coulomb gluons gives rise to super-leading logarithms of the form $\propto \alpha_s^m \ln(Q/Q_0)^{m+1}$ $m \geq 4$. It is worth to remark that these are the uncancelled logarithmic contributions, discussed at the end of Section 2.4.6, that arise above the inclusivity scale Q_0.

Within the context of a Sudakov resummation different ordering variables can be used [39, 35]. However, the choice of ordering variable turns out to be critical when applying Eq. (2.73) to calculate the out of the gap cross-section. This was first

[19] where powers of $1/N$ are neglected

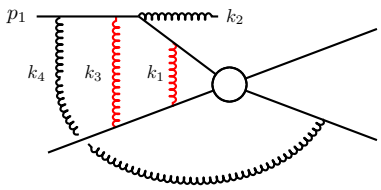

Figure 2.7: A particular graph that gives rise to super-leading logarithms in GBJ. The out of the gap real emission k_2 is nearly collinear with the incoming hard parton p_1.

exemplified in [38], where the authors explicitly considered terms in which the out of the gap emission (nearly collinear with a jet) k_2 is accompanied with a central[20] (either real or virtual) eikonal gluon k_4 and two Coulomb gluons k_{1T} and k_{3T}. Let us consider first the case in which the ordering takes place with respect the transverse momentum as in as Eq. (2.73). Following [38], we consider the contribution in which $k_{1T} \gg k_{2T} \gg k_{3T} \gg k_{4T}$. Figure 2.7 illustrates a graph that contributes in this ordered region. The relevant kinematical part of the cross-section in this region yields a super-leading logarithm:

$$\alpha_s^4 \int_{Q_0}^{Q} \frac{\mathrm{d}k_{1T}}{k_{1T}} \left[\int_{Q_0}^{k_{1T}} \frac{\mathrm{d}k_{2T}}{k_{2T}} \int_{k_{2T}/Q}^{1} \frac{\mathrm{d}\theta_2}{\theta_2} \right] \int_{Q_0}^{k_{2T}} \frac{\mathrm{d}k_{3T}}{k_{3T}} \int_{Q_0}^{k_{3T}} \frac{\mathrm{d}k_{4T}}{k_{4T}} = \alpha_s^4 \frac{1}{5!} \ln^5 \frac{Q}{Q_0} \tag{2.78}$$

where k_{2T}/Q is the smallest kinematically allowed angle for the out of the gap gluon. In stark contrast, if radiation is ordered with respect to the energy, the ordering condition reads $k_{1T} \gg E_2 = k_{2T}/\theta_2 \gg k_{3T} \gg k_{4T}$ and the equivalent contribution to expression (2.78) renders

$$\alpha_s^4 \int_{Q_0}^{Q} \frac{\mathrm{d}k_{1T}}{k_{1T}} \left[\int_{Q_0}^{k_{1T}} \frac{\mathrm{d}E_2}{E_2} \int_{0}^{1} \frac{\mathrm{d}\theta_2}{\theta_2} \right] \int_{Q_0}^{E_2} \frac{\mathrm{d}k_{3T}}{k_{3T}} \int_{Q_0}^{k_{3T}} \frac{\mathrm{d}k_{4T}}{k_{4T}} = \infty. \tag{2.79}$$

In addition, if the ordering takes place with respect to virtuality, the ordering condition reads $k_{1T} \gg t_2 = k_{2T}\theta_2 \gg k_{3T} \gg k_{4T}$ and the equivalent contribution to Eq. (2.78) is doubled, i.e.

$$\alpha_s^4 \int_{Q_0}^{Q} \frac{\mathrm{d}k_{1T}}{k_{1T}} \left[\int_{Q_0}^{k_{1T}} \frac{\mathrm{d}t_2}{t_2} \int_{\sqrt{t_2/Q}}^{1} \frac{\mathrm{d}\theta_2}{\theta_2} \right] \int_{Q_0}^{t_2} \frac{\mathrm{d}k_{3T}}{k_{3T}} \int_{Q_0}^{k_{3T}} \frac{\mathrm{d}k_{4T}}{k_{4T}} = 2 \times \alpha_s^4 \frac{1}{5!} \ln^5 \frac{Q}{Q_0} \ . \tag{2.80}$$

Let us recall that, as we illustrated in Eq. (2.72), the introduction of Coulomb

[20] Central radiation can be characterised by having $k_{iT} \sim E_i$

gluons necessarily implies the loss of the coherence property of wide-angle radiation. In view of the loss of this property, the variations exemplified in [38] were not completly unexpected [31]. In order to solve this problem there is no option but to check directly the colour evolution by explicitly calculating the matrix elements, as we do in the subsequent chapters.

2.6.1 Standing on firm ground: Bloch-Nordsieck cancellation of soft singularities

Before we venture into the enterprise of including Coulomb gluons, we remark that the possibility of obtaining IR finite results when these are included is guaranteed by the QCD Bloch-Nordsieck theorem [22, 23, 82, 83, 84]. This states that the inclusive (full) sum over the real and virtual (both eikonal or Coulomb) soft gluon corrections to a general hard wide-angle process cancels at leading twist[21]. The inclusivity condition includes the sum (average) over the colour states of the outgoing (incoming) hard partons. This theorem was originally demonstrated for photons in QED [69] and its extension to non-abelian gauge theories is not straightforward because of the charged nature of gluons.

2.7 Summary

In general, partonic amplitudes do not obey strict (process independent) factorisation in collinear limits involving incoming and outgoing partons if, in addition, the scattering contains also non-collinear incoming and outgoing partons. Thus, this physics is relevant for hadron-hadron initiated processes. The violations of strict factorisation are first triggered by the exponentiation of the one-loop virtual corrections. For inclusive observables these violations exactly cancel. For non-inclusive observables, the factorisation of collinear divergences is expected to be possible up to the scale, Q_0, below which real radiation is summed up inclusively and above this scale there should be perturbatively-calculable effects that in general cannot be written in a process independent way.

The colour evolution picture is an algorithm that incorporates this physics by including the leading soft gluon corrections of a general hard process. In principle, this can be used to calculate the perturbative corrections to non-inclusive observables above the inclusivity scale Q_0. This algorithm implies the loss of the coherence property for wide-angle radiation. In addition, previous studies have shown that the colour evolution picture suffers from an ordering problem as it renders different results for different ordering variables.

[21] i.e. up to corrections suppressed by the characteristic scale of the hard process Q.

With the aim of determining which is the correct ordering variable, we will perform full diagrammatic calculations of the soft correction to a hard process within the eikonal approximation. Specifically, we will study the corrections at one-loop to a general scattering accompanied by the emission of up to two gluons. We will find an elegant cancellation of graphs that imposes a precise ordering on the momentum of the virtual exchanges.

Chapter 3

One-loop, one-emission soft corrections

Motivated by the ordering problem, in this chapter we will study the soft corrections to a general hard scattering due to one virtual gluon and one emission, $\left|n^{(1)}_{+1}\right\rangle$. Our aim is to test, in this first non-trivial case, which is the correct ordering variable in the colour evolution picture given by Eq. (2.71). By combining the different contributions, we will find that the amplitude can be written in terms of eikonal emissions ($\propto \mathbf{T}_i p_i\cdot\varepsilon/p_i\cdot q$) and virtual exchanges ($\propto \mathbf{T}_i\cdot\mathbf{T}_j$) with the following structure:

$$\left(\mathbf{T}_i\cdot\mathbf{T}_j\int_0^{q_{T(ij)}}\right)\left(\mathbf{T}_i\frac{p_i\cdot\varepsilon}{p_i\cdot q}\right)+\left(\mathbf{T}_i\frac{p_i\cdot\varepsilon}{p_i\cdot q}\right)\left(\mathbf{T}_i\cdot\mathbf{T}_j\int_{q_{T(ij)}}^{Q}\right)\ . \tag{3.1}$$

Crucially, the integration limits of the virtual exchanges appear ordered with respect to $q_{T(ij)}$, the transverse momentum components of the gluon emission with respect to hard partons $\{i,j\}$ involved in the exchange. The non-Abelian nature of QCD plays a central role in engineering this ordering condition.

The one-loop, one emission amplitude amplitude $\left|n^{(1)}_{+1}\right\rangle$ has been previously studied in [54]. We will revisit it here to introduce novel methods of calculation that shed light on its physics and generalise to higher orders. We start by considering first the imaginary, or Coulomb, part in sections 3.1 and 3.2. Then we include the real, or eikonal, part of the virtual corrections in Section 3.3. Finally, in Section 3.4 we will relate the amplitude to the colour evolution picture and to shed light on its structure we shall study its behaviour in collinear and wide-angle limits. We present technical details in appendices D–F and discuss the relation with the breaking of collinear factorisation in Appendix G.

3.1 Coulomb gluons of Drell-Yan process with one emission

The first non-trivial case in which the colour evolution can be tested is in the case of a Drell-Yan hard process $\left|2^{(1)}_{+1}\right\rangle$. More precisely, a process with two incoming partons that annihilate into any number of colourless particles with one loop and one real emission. In this section we will focus on the imaginary part. Our presentation is based on [85].

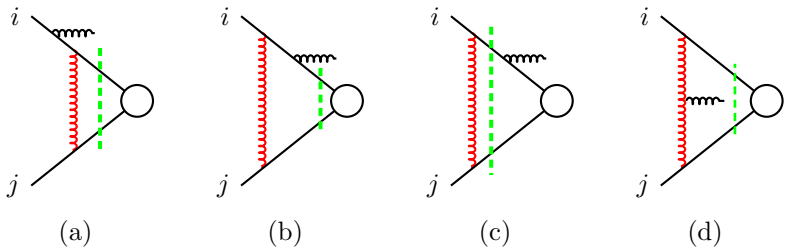

Figure 3.1: Four cut graphs contributing to the amplitude for the emission of a gluon, with four-momentum q and colour c, off hard parton i. There are three further graphs obtained by swapping $(i \leftrightarrow j)$ in the first three graphs.

The imaginary and real parts of the one-loop integrals can be separated by studying the contour of the loop integrals. In particular, the imaginary part can be obtained from the "cut graphs" illustrated in Fig. 3.1. The dashed line in each graph indicates that the crossed lines should be set on-shell. To illustrate this, let us consider graph (d) of Fig. 3.1. Before applying the cut, the eikonal rules for this graph yield

$$\int \frac{\mathrm{d}^d k}{(2\pi)^d} \left[\frac{\mathbf{T}_j^b p_{j\beta}}{-p_j\cdot k - \frac{i0}{2}}\right] \left[\frac{(g\mu^\epsilon)^3 i f^{bca} V^{\beta\mu\alpha}\varepsilon_{1\mu}}{[k^2+i0][(k+q)^2+i0]}\right] \left[\frac{\mathbf{T}_i^a p_{i\alpha}}{p_i\cdot(k+q) - \frac{i0}{2}}\right] \left|2^{(0)}\right\rangle, \tag{3.2}$$

where $V^{\beta\mu\alpha} = V^{\beta\mu\alpha}(-k,-q,k+q)$ is the exact triple gluon vertex and $\left|2^{(0)}\right\rangle$ denotes the lowest order amplitude for the hard subprocess. In Fig. 3.1, the dashed line cuts the two hard partons indicating that their corresponding propagators should be set on-shell, i.e.

$$\frac{1}{-p_j\cdot k - \frac{i0}{2}} \frac{1}{p_i\cdot(k+q) - \frac{i0}{2}} \to \frac{[-2\pi i\delta(-p_j\cdot k)][-2\pi i\delta(p_i\cdot(k+q))]}{2}. \tag{3.3}$$

Henceforth, we refer to cuts that pass through two hard parton lines as "eikonal cuts". We present the derivation of these cutting rules in Appendix D. There, we consider the more general case of one-loop graphs with any number of real emissions and derive cutting rules to calculate their imaginary part. In addition, we also present

a method to calculate the real part. Although the cutting rules are crucial to our work, their derivation is rather technical and, as we will see, we can understand its physics without having to look at those technical details.

By integrating out the delta functions associated to cuts, each graph in Fig. 3.1 can be reduced to an integral over the transverse momentum components, k_T, relative to the incoming partons, i.e. $p_i \cdot k_T = p_j \cdot k_T = 0$. After this, the contribution to the amplitude from graphs (a)–(c) in Fig. 3.1 yields[1]

$$-\frac{i\pi}{8\pi^2}\frac{p_i\cdot\varepsilon_1}{p_i\cdot q_1}\left[\mathbf{T}_i^{c_1}(\mathbf{T}_i\cdot\mathbf{T}_j)-(\mathbf{T}_i\cdot\mathbf{T}_j)\mathbf{T}_i^{c_1}+(\mathbf{T}_i\cdot\mathbf{T}_j)\mathbf{T}_i^{c_1}\right]\int_0^{Q^2}\frac{\mathrm{d}k_T^2}{k_T^2}\Big|2^{(0)}\Big\rangle. \tag{3.4}$$

Although the contributions from graphs (b) and (c) cancel, it is more instructive to keep them apart. The integral of the Coulomb gluon momentum, k_T, is over the full range from 0 up to the characteristic scale of the hard process, $Q \sim 2p_i \cdot p_j$. Graph (d) is responsible for triggering the k_T ordering. This is the only cut graph involving the triple-gluon vertex and it gives rise to the contribution:

$$-\frac{i\pi}{8\pi^2}\frac{p_i\cdot\varepsilon}{p_i\cdot q}\left[(\mathbf{T}_i\cdot\mathbf{T}_j)\mathbf{T}_i^{c}-\mathbf{T}_i^{c}(\mathbf{T}_i\cdot\mathbf{T}_j)\right]\int_0^{Q^2}\frac{\mathrm{d}k_T^2}{k_T^2}\frac{q_T^2}{k_T^2+q_T^2}\Big|2^{(0)}\Big\rangle. \tag{3.5}$$

Crucially, the loop integral of graph (d) acts as a switch. It is zero (i.e. sub-leading) if $k_T > q_T$ and when it is active it has the effect of exactly cancelling the contribution from graphs (a) and (b). The result is that for $k_T > q_T$ only graph (a) survives whilst for $k_T < q_T$ only graph (c) survives, i.e. the final result is

$$-\frac{i\pi}{8\pi^2}\frac{p_i\cdot\varepsilon}{p_i\cdot q}\left[\mathbf{T}_i^{c_1}(\mathbf{T}_i\cdot\mathbf{T}_j)\int_{q_T^2}^{Q^2}\frac{\mathrm{d}k_T^2}{k_T^2}+(\mathbf{T}_i\cdot\mathbf{T}_j)\mathbf{T}_i^{c_1}\int_0^{q_T^2}\frac{\mathrm{d}k_T^2}{k_T^2}\right]\Big|2^{(0)}\Big\rangle. \tag{3.6}$$

These contributions, with the Coulomb gluon k_T restricted by the q_T of the real emission are in exact accordance with the colour evolution picture ordered in k_T; after adding the contribution obtained after swapping $i \leftrightarrow j$ we get

$$\Big[\mathbf{J}_{2+1}(q)\,\mathbf{C}^{ij}(q_T,Q)+\mathbf{C}^{ij}(0,q_T)\,\mathbf{J}_{2+1}(q)\Big]\Big|2^{(0)}\Big\rangle, \tag{3.7}$$

where $\mathbf{J}_{2+1}(q)$ is the tree level current due to the incoming hard partons:

$$\mathbf{J}_{2+1}(q) \equiv \mathbf{T}_i\frac{p_i\cdot\varepsilon}{p_i\cdot q}+\mathbf{T}_j\frac{p_j\cdot\varepsilon}{p_j\cdot q}, \tag{3.8}$$

[1] In dimensional regularisation, we write $\mathrm{d}k_T^2(k_T^2)^{-1} \to \mathrm{d}k_T^2(k_T^2)^{-1-\epsilon}g(\epsilon)\mu^{2\epsilon}$ with $g(\epsilon) = 1+\mathcal{O}(\epsilon)$. In this section and the next, we drop the explicit regularisation and the coupling constant to simplify our expressions.

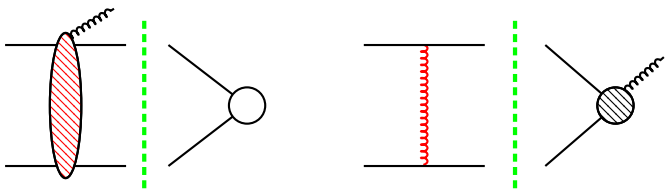

Figure 3.2: The two cuts corresponding to the two different physical mechanisms for single gluon emission. The hatched circular blob denotes the hard process with the emission emitted off one of the external partons.

and the Coulomb exchange operator is defined as:

$$\mathbf{C}^{ij}(a,b) \equiv -\frac{i\pi}{8\pi^2}\mathbf{T}_i\cdot\mathbf{T}_j\int_{a^2}^{b^2}\frac{\mathrm{d}k_T^2}{k_T^2}. \tag{3.9}$$

Of particular note is the way that the unwanted cut of graph (b) always cancels, either against graph (c) or graph (d). Such a contribution would be problematic for any local evolution picture, since it corresponds to a Coulomb exchange retrospectively putting on-shell a pair of hard partons earlier in the k_T evolution chain.

3.1.1 Physical picture

There is another way to think about this physics. The Coulomb exchange corresponds to on-shell scattering of the incoming partons, before the hard subprocess, and the real emission can occur either as part of this initial-state scattering or as part of the hard scattering. These two possibilities are illustrated in Fig. 3.2.

Graphs (a), (b) and (d) of Fig. 3.1 are all included into the set of graphs (A) of Fig. 3.2 and, in the domain where (d) is active, it cancels the other graphs. This means that the k_T of the Coulomb gluon must be greater than that of the real emission, i.e. it is as if the real emission is occurring off a hard partonic subprocess mediated by the Coulomb gluon. The total expression for graphs of type (A) illustrated in Fig. 3.2 is

$$-\frac{i\pi}{8\pi^2}\mathbf{T}_j^b if^{bac}\mathbf{T}_i^a\left[\frac{p_j\cdot\varepsilon}{p_j\cdot q}-\frac{p_i\cdot\varepsilon}{p_i\cdot q}\right]\int_{q_T^2}^{Q^2}\frac{\mathrm{d}k_T^2}{k_T^2}\Big|2^{(0)}\Big\rangle\ . \tag{3.10}$$

By using the colour algebra, this expression can also be written as

$$-\frac{i\pi}{8\pi^2}\Big[\mathbf{T}_j\cdot\mathbf{T}_i\,\mathbf{J}_{2+1}(q)-\mathbf{J}_{2+1}(q)\,\mathbf{T}_j\cdot\mathbf{T}_i\Big]\int_{q_T^2}^{Q^2}\frac{dk_T^2}{k_T^2}\Big|2^{(0)}\Big\rangle. \tag{3.11}$$

This shows that, up to the integral factor, Eq. (3.10) can be obtained directly by considering the coherent insertion of q off the lowest order Coulomb exchange between

$\{i, j\}$. Graph (c) and the graph obtained after swapping $(i \leftrightarrow j)$ are the only graphs of type (B). In this case, the gluon emission occurs much later than the Coulomb exchange, which therefore knows nothing of the emission and so its k_T can take any value, i.e.

$$\mathbf{C}^{ij}_{(0,Q)}\ \mathbf{J}_{2+1}(q)\Big|2^{(0)}\Big\rangle\ . \tag{3.12}$$

Observe that the total expression for (A) is manifestly gauge invariant, i.e. it identically vanishes under the substitution $\varepsilon \to q$. The contributions of type (B) also form a gauge invariant set of graphs. In this case, the invariance is inherited from the colour conservation of the hard subprocess, i.e. $[\mathbf{T}_i + \mathbf{T}_j]\left|2^{(0)}\right\rangle = 0$. The fact that these two sets of graphs are separately invariant is not an accident. Indeed, exactly as we did with the Coulomb gluons in previous chapter, see Eq. (2.21), the cuts of type (A) and (B) can be written as the product of on-shell scattering amplitudes. To illustrate this point, we observe that the sum of graphs of type (B) can be written as

$$\frac{1}{2i}\int \mathrm{dLIPS}_2\ \mathbf{A}^{\dagger}_{(2\to 2)}\mathbf{A}^{c}_{(2\to 3)}(p_i + k, p_j + k'; p_i + k, p_j + k', q_1), \tag{3.13}$$

where the amplitude $\mathbf{A}^{\dagger}_{(2\to 2)}$ and the integration measure dLIPS are the same as in Eqs. (2.19) and (2.21) and $\mathbf{A}_{(2\to 3)}$ is the one emission scattering amplitude that, within the eikonal approximation, can be approximated as

$$\mathbf{A}^{c}_{(2\to 3)}(p_i + k, p_j + k', p_i + k, p_j + k', q) \approx \left[\frac{g\mu^{\epsilon}\mathbf{T}^{c}_{i} p_i\cdot\varepsilon_1}{p_i\cdot(q_1 + k)} + \frac{g\mu^{\epsilon}\mathbf{T}^{c}_{j} p_j\cdot\varepsilon_1}{p_j\cdot(q_1 + k')}\right]\Big|2^{(0)}\Big\rangle\ .$$

We close this section by remarking that Fig. 3.1 does not have contributions arising from cuts that pass through a hard parton and a soft gluon. Such cuts would not correspond to physical mechanisms and their cancellation occurs more generally, as we demonstrate in Appendix D.

3.2 General hard process

We will now generalise the previous section from the Drell-Yan case to a completely general hard process. More precisely, the scattering of any number of (incoming and outgoing) hard partons and one soft gluon emission at one-loop order. Exactly as we saw in the Drell-Yan case, the imaginary part of the amplitude can be organised into gauge invariant sets of graphs, each of which corresponds to a physical mechanism for gluon production. This time, there are five different possibilities; these are illustrated in Fig. 3.3. Each oval in this figure represents exactly the same graphs that it did in Fig. 3.2. However, in Fig. 3.3, we have further abbreviated the graphs by only showing the lines that are cut and the emitted gluon. Furthermore, we recall that

the gluon radiated from the black hatched blob should be understood to be emitted from any parton in the hard subprocess, e.g. the graphs in the fourth line of this figure abbreviate the graphs depicted in Fig. 3.5.

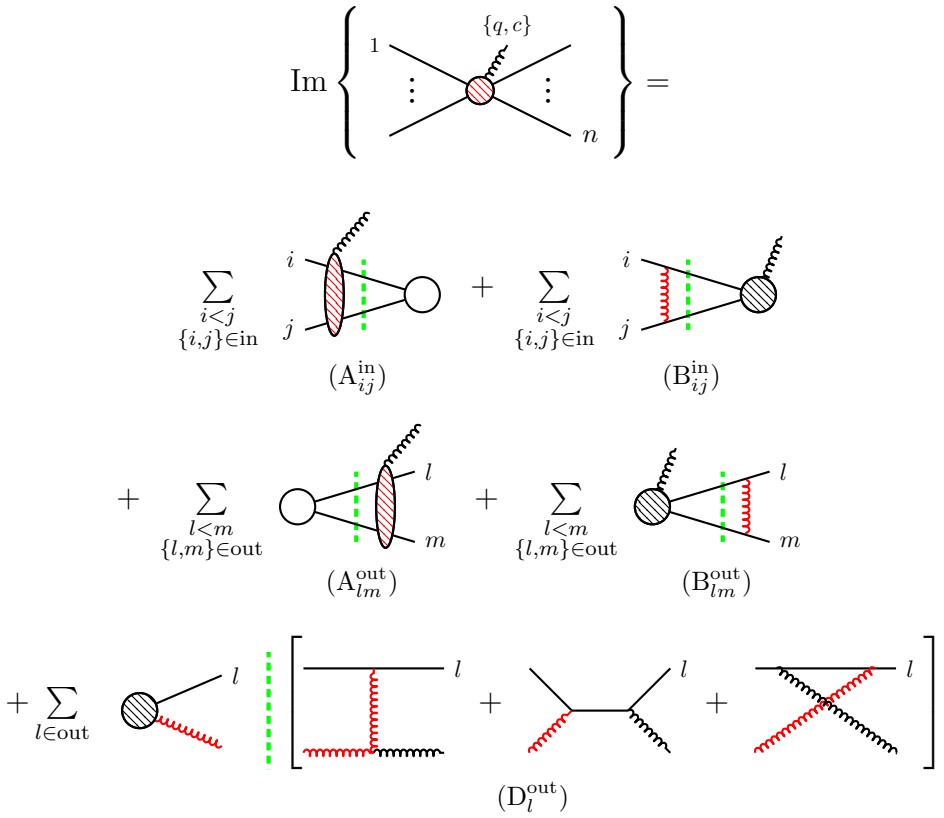

Figure 3.3: Imaginary part of the one loop corrections to a general hard process organised in terms of the different physical mechanisms for gluon emission. Observe that the mechanisms label by (A$^{\text{in}}_{ij}$) and (B$^{\text{in}}_{ij}$) are the generalisation of graphs (A) and (B) in Fig. 3.2

3.2.1 Initial state eikonal cuts

As this will simplify the notation, it is convenient to define a notation for the transverse momentum of any l to a pair of non-collinear light-like vectors $\{p_i, p_j\}$. These components are defined through the following Sudakov decomposition:

$$l^\mu = \frac{p_j\cdot l}{p_i\cdot p_j}p_i^\mu + \frac{p_i\cdot l}{p_i\cdot p_j}p_j^\mu + l^\mu_{T(ij)}, \tag{3.14}$$

with $l_{T(ij)}\cdot p_l = l_{T(ij)}\cdot p_m = 0$. From this definition it follows that the transverse momentum components of the massless vector $q^2 = 0$ satisfies

$$q^2_{T(ij)} \equiv \frac{2\,p_i\cdot q\,p_j\cdot q}{p_i\cdot p_j}\,. \tag{3.15}$$

For each pair of outgoing partons $\{i,j\}$, we now consider the physical mechanisms $(A_{ij}^{\rm in})$ and $(B_{ij}^{\rm in})$ illustrated in Fig. 3.3. Here the Coulomb exchange corresponds to an on-shell scattering between two eikonal lines in the initial state and the real emission can occur either as part of this initial-state scattering or as part of the hard scattering.

The graphs of type $({\rm A}_{ij}^{\rm in})$ are exactly the same as those on the left of Fig. 3.2 and, then, they add up to

$$-\frac{i\pi}{8\pi^2}\mathbf{T}_i^d if^{dce}\mathbf{T}_j^e\left[\frac{p_i\cdot\varepsilon}{p_i\cdot q}-\frac{p_j\cdot\varepsilon}{p_j\cdot q}\right]\int_0^{Q^2}\left[\frac{{\rm d}k_{T(ij)}^2}{k_{T(ij)}^2}-\frac{{\rm d}k_{T(ij)}^2}{k_{T(ij)}^2}\frac{q_{T(ij)}^2}{k_{T(ij)}^2+q_{T(ij)}^2}\right]\Big|n^{(0)}\Big\rangle, \quad (3.16)$$

where $\{k_{T(ij)},q_{T(ij)}\}$ are the transverse components to $\{p_i,p_j\}$. The rightmost integral in Eq. (3.16) is the contribution of the triple gluon vertex and, as in the previous case, it acts as a switch that cancels the contributions of the unbounded integral when $k_{T(ij)}<q_{T(ij)}$.

Similarly, for each pair of incoming partons $\{i,j\}$, the graphs in $({\rm B}_{ij}^{\rm in})$, contain the same cuts in set (B) of Fig. 3.2 but, in addition, $({\rm B}_{ij}^{\rm in})$ has also graphs in which the gluon is emitted off partons different than the ones involved in the virtual exchange. In these graphs the emission and virtual exchange are independent events as their colour factors commute and the integral of the virtual exchange is completely unrestricted. It follows that we can write the sum over all contribution in $({\rm B}_{ij}^{\rm in})$ as

$$\mathbf{C}^{ij}(0,Q)\;\mathbf{J}_{n+1}(q)\Big|n^{(0)}\Big\rangle\;. \quad (3.17)$$

All the physical interpretations that we discussed in Section 3.1 also apply to $({\rm A}_{ij}^{\rm in})$ and $({\rm B}_{ij}^{\rm in})$. Finally, their sum can also be expressed as a chain of Coulomb and emission operators ordered with respect to $q_{T(ij)}$, the transverse momentum with respect to the partons involved in the exchange, i.e. by using the colour algebra, the sum of the cuts in $({\rm A}_{ij}^{\rm in})$ and $({\rm B}_{ij}^{\rm in})$ yields

$$\Big[\mathbf{J}_{n+1}(q)\mathbf{C}^{ij}\left(q_{T(ij)},Q\right)+\mathbf{C}^{ij}(0,q_{Tij})\,\mathbf{J}_{n+1}(q)\Big]\Big|n^{(0)}\Big\rangle\;. \quad (3.18)$$

3.2.2 Final state eikonal cuts

For each pair of outgoing partons $\{l,m\}$, we now consider the physical mechanisms $(A_{lm}^{\rm out})$ and $(B_{lm}^{\rm out})$ illustrated in Fig. 3.3. These two mechanisms correspond to an on-shell scattering of two eikonal lines in the final state and the real emission can occur either as part of the hard scattering or of the final-state scattering.

The physics of these two possibilities is equivalent to that of $(A_{ij}^{\rm in})$ and $(B_{ij}^{\rm in})$. In fact, this observation holds on a graph by graph basis because the operator (acting on the hard subprocess) associated with an eikonal cut in the initial state is exactly

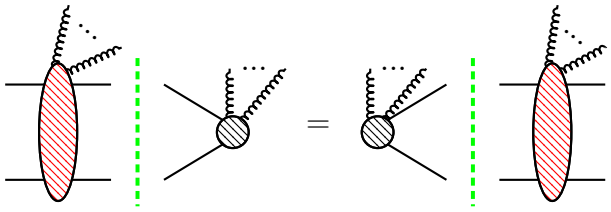

Figure 3.4: On a graph by graph basis, the infrared operator associated with the eikonal cut on the initial state is the same as if the cut partons were in the final state.

the same when the cut lines are in the final state[2]. This identity holds not only in the present case but when there are any number of emissions, as we illustrate in Fig. 3.4. According to these identities the expressions for $(A_{lm}^{\rm out})$, $(B_{lm}^{\rm out})$ and their sum gives:

$$\begin{aligned} &-\frac{i\alpha_s}{2\pi}\mathbf{T}_l^d i f^{dce}\mathbf{T}_m^e\left[\frac{p_l\cdot\varepsilon}{p_l\cdot q}-\frac{p_m\cdot\varepsilon}{p_m\cdot q}\right]\int_{q^2_{T(lm)}}^{Q^2}\frac{\mathrm{d}k^2_{Tlm}}{k^2_{Tlm}}\Big|n^{(0)}\Big\rangle, \\ &\qquad\mathbf{C}^{lm}(0,Q,)\ \mathbf{J}_{n+1}(q)\Big|n^{(0)}\Big\rangle, \\ &\Big[\mathbf{J}_{n+1}(q)\,\mathbf{C}^{lm}\left(q_{T(lm)},Q\right)+\mathbf{C}^{lm}\big(0,q_{T(lm)}\big)\,\mathbf{J}_{n+1}(q)\Big]\Big|n^{(0)}\Big\rangle. \end{aligned} \tag{3.19}$$

Clearly, analogous physical interpretations to the ones discussed in Section 3.1.1 apply to the first two equations.

3.2.3 Re-scattering cuts

Whenever there are final state hard partons, there are more imaginary contributions to consider. For each outgoing parton l in the hard subprocess, there is a physical mechanism $\mathrm{D}_l^{\rm out}$, that is illustrated by the bottom line of Fig. 3.3. This corresponds to the re-scattering between the on-shell gluon emission and l. The total amplitude can be written as

$$\begin{aligned} &\frac{1}{2i}\int \mathrm{dLIPS}_2\, i\mathcal{B}_l^\mu\left[\sum_\sigma \varepsilon^*_{\mu'}\varepsilon_{\nu'}\right]\ i\mathbf{J}^\nu_{n+1}(q')\Big|2^{(0)}\Big\rangle, \\ &\mathrm{dLIPS}_2=\frac{\mathrm{d}^d p_l'}{(2\pi)^d}\frac{\mathrm{d}^d q'}{(2\pi)^d}(2\pi)^d\delta^d(p_l+q-p_l'-q')2\pi\delta^+(p_l')2\pi\delta^+(q') \end{aligned} \tag{3.20}$$

where $\mathcal{B}_l^\mu$ is the amplitude for the gluon to scatter with parton l and, within the eikonal approximation, $\delta^+(p_l')\approx\delta(2p_i(q-q'))$. We will show the individual contributions from the re-scattering cuts $(\mathrm{D}_l^{\rm out})$ in a subsequent section, see Fig. 3.5, in the meantime, we are interested in its total expression. For each outgoing parton l

[2]No change of signs in any momenta is required.

in the hard subprocess, the cut graphs in $\mathrm{D}_l^{\mathrm{out}}$ sum up to

$$-\frac{i\pi}{8\pi^2}\mathbf{T}_l^d if^{dce}\sum_{j\neq\{l\}}^{n}\mathbf{T}_j^e\left[\frac{p_l\cdot\varepsilon}{p_l\cdot q}-\frac{p_j\cdot\varepsilon}{p_j\cdot q}\right]\int_0^{Q^2}\left[\frac{\mathrm{d}k^2_{T(lj)}}{k^2_{T(lj)}}\frac{q^2_{T(lj)}}{k^2_{T(lj)}+q^2_{T(lj)}}\right]\left|n^{(0)}\right\rangle\,. \tag{3.21}$$

Observe that this time there are only switch-like contributions, one for each parton $j\neq\{i\}$ in the hard subprocess which is active in the domain $k_{T(lj)}<q_{T(lj)}$.

In the domain where the switches are active, Eq. (3.21) can be written as

$$\begin{aligned}&\sum_{j\neq\{l\}}^{n}\left\{-\frac{i\pi}{8\pi^2}\mathbf{T}_l\cdot(\mathbf{T}_q)_{ce}\int_0^{q^2_{T(lj)}}\frac{\mathrm{d}k^2_{T(lj)}}{k^2_{T(lj)}}\right\}\mathbf{T}_j^e\left[\frac{p_j\cdot\varepsilon}{p_j\cdot q}-\frac{p_l\cdot\varepsilon}{p_l\cdot q}\right]\left|n^{(0)}\right\rangle\\&=\left\langle c\right|\sum_{j\neq\{l\}}^{n}\left\{\mathbf{C}^{lq}\big(0,q_{T(jl)}\big)\right\}\mathbf{T}_j\left[\frac{p_j\cdot\varepsilon}{p_j\cdot q}-\frac{p_l\cdot\varepsilon}{p_l\cdot q}\right]\left|n^{(0)}\right\rangle,\end{aligned} \tag{3.22}$$

where in the first line we noticed that $(\mathbf{T}_q^b)_{ce}\equiv if^{cbe}$ is the colour charge of the emitted gluon[3]. Finally, to write the second line, we noted that the term inside braces is exactly equal to a Coulomb gluon exchange between partons l and q bounded by $q^2_{T(lj)}$. The term inside square brackets would be equal to the tree level emission current $\mathbf{J}_{n+1}(q)$ if the sum symbol could be commuted to the right of the Coulomb operator so that one could write $-\sum_{j\neq\{i\}}\mathbf{T}_j^d\frac{p_i\cdot\varepsilon}{p_i\cdot q}=\mathbf{T}_l\frac{p_l\cdot\varepsilon}{p_l\cdot q}$. However, this is not possible because the Coulomb gluon has a "memory" of the origin of the partons from where q was emitted. To be precise, the k_T of each Coulomb exchange is limited by the transverse momentum of the emitted gluon with respect to l and j (i.e. $k_T\leq q_{T(lj)}=2p_l\cdot q\,p_j\cdot q/p_i\cdot p_l$), which are the partons that radiate q. It is this memory and the requirement of gauge invariant that forces the emission to have the dipole structure appearing in Eq. (3.22).

Although for general kinematics the re-scattering cuts cannot be written in terms of a Coulomb operator and tree-level emissions, this is again a feature of the leading behaviour of the amplitude in wide-angle and collinear configurations. Let us first show this in the kinematical configuration when q becomes collinear with p_m. This kinematical regime is precisely defined as:

$$\begin{aligned}&q^\mu=\frac{r\cdot q}{r\cdot p_m}p_m^\mu+\frac{q^2_{T(mr)}}{2r\cdot q}r^\mu+q^\mu_{T(mr)},\\&q^2_{T(mr)}=\frac{2p_m\cdot qr\cdot q}{p_m\cdot r}\,,\\&q_{T(mr)}\to 0,\end{aligned} \tag{3.23}$$

where the light-like vector r specifies the direction in which the collinear limit is

[3]To be precise, $(\mathbf{T}_q^b)_{cd}\mathbf{T}_j^d$ are the colour factors for the emission of a gluon with colour b off a gluon, with colour c, previously radiated off parton j.

approached through the conditions $p_l \cdot q_{T(lr)} = r \cdot q_{T(lr)} = 0$. The leading behaviour of Eq. (3.22) in this limit is

$$\mathbf{C}^{ql}(0, q_{T(mr)}) \frac{\mathbf{T}_m p_m \cdot \varepsilon}{p_m \cdot q} \Big| n^{(0)} \Big\rangle \ . \tag{3.24}$$

We shall now consider the kinematical region in which the gluon is emitted at a wide angle. This corresponds to the regime in which $\hat{q} \cdot \hat{p}_m \approx 0$ for every parton m in the hard subprocess. When this approximation holds, Eq. (3.22) simplifies to

$$\approx \mathbf{C}^{lq}\big(0, q^0\big)\, \mathbf{J}_{n+1} \Big| n^{(0)} \Big\rangle \ . \tag{3.25}$$

where q^0 is the energy of the gluon emission. Therefore, we conclude that although the exact expression for the re-scattering cuts cannot be written as an ordered chain of emissions and Coulomb gluons, its leading behaviour in wide-angle and collinear limits has again this property. We will come back to discuss collinear and wide angle limits once we have added the eikonal part of the loop corrections.

3.2.4 Re-scattering cuts graph-by-graph

We shall now show the individual contributions to $(\mathrm{D}_l^{\mathrm{out}})$, see Fig. 3.3. For each outgoing hard parton l, the different topologies contributing to $(\mathrm{D}_l^{\mathrm{out}})$ are depicted in Fig. 3.5. The contributions of graphs (a),(b) and (c) in this figure are respectively

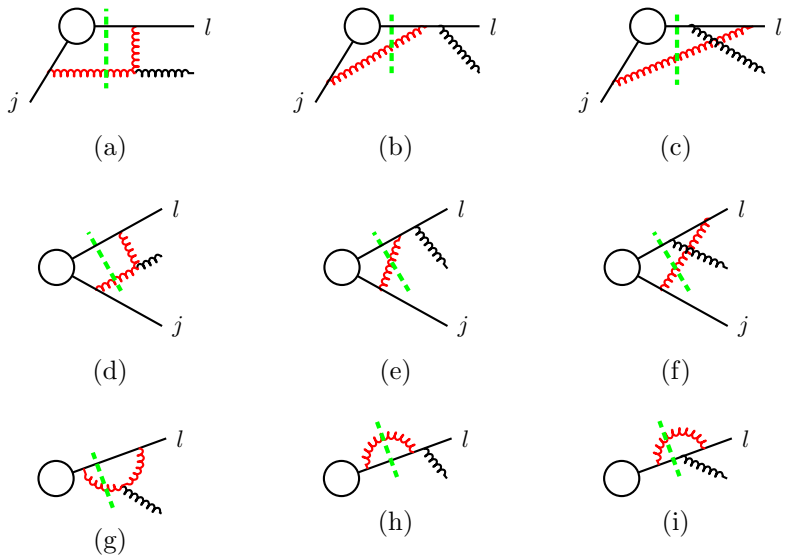

Figure 3.5: On-shell scatterings between an emitted gluon and an outgoing hard parton l.

identical to the contributions of graphs (d),(e) and (f), and they yield respectively

$$\begin{aligned}
&-\frac{i\pi}{8\pi^2}\,\mathbf{T}_l^d i f^{dce}\mathbf{T}_j^e\left[\left[\frac{p_l\cdot\varepsilon}{p_l\cdot q}-\frac{p_j\cdot\varepsilon}{p_j\cdot q}\right]\mathcal{S}\left(q^2_{T(lj)}\right)+\frac{1}{2}\frac{p_l\cdot\varepsilon}{p_l\cdot q}\,\mathcal{I}_{lj}\right]\Big|n^{(0)}\Big\rangle,\\
&\frac{i\pi}{8\pi^2}\,\mathbf{T}_l^c\,\mathbf{T}_l\cdot\mathbf{T}_j\,\frac{p_l\cdot\varepsilon}{p_l\cdot q}\,\mathcal{I}_{lj}\Big|n^{(0)}\Big\rangle,\\
&-\frac{i\pi}{8\pi^2}\,\mathbf{T}_l\cdot\mathbf{T}_j\,\mathbf{T}_l^c\,\frac{p_l\cdot\varepsilon}{p_l\cdot q}\,\mathcal{I}_{lj}\Big|n^{(0)}\Big\rangle,
\end{aligned}\tag{3.26}$$

where the scalar integrals $\mathcal{I}_{lj}$ and $\mathcal{S}\big(q^2_{T(lj)}\big)$ are defined by:

$$\begin{aligned}
\mathcal{I}_{lj}&=\int_0^{p_l\cdot q}\frac{\mathrm{d}k^2_{T(lj)}}{k^2_{T(lj)}},\\
\mathcal{S}_{lj}\left(q^2_{T(lj)}\right)&=\int\frac{\mathrm{d}k^2_{T(lj)}}{k^2_{T(lj)}}\frac{q^2_{T(lj)}}{k^2_{T(lj)}+q^2_{T(lj)}}\ .
\end{aligned}\tag{3.27}$$

Observe that the contributions proportional to $\mathcal{S}_{jl}\left(q^2_{T(lj)}\right)$ are the switches in Eq. (3.21). The contributions of (h) and (i) identically vanish in the Feynman gauge, and the contributions from (g) yields

$$\frac{i\pi}{8\pi^2}\mathbf{T}_l^d i f^{dce}\mathbf{T}_l^e\,\frac{1}{2}\frac{p_l\cdot\varepsilon}{p_l\cdot r}\,\mathcal{I}_{lr}\Big|n^{(0)}\Big\rangle,\tag{3.28}$$

where the vector r is any light-like momentum not collinear to l. By means of colour conservation all terms containing the scalar integrals $\{\mathcal{I}_{lj},\mathcal{I}_{lr}\}$ add up to zero and, after this, one is left with Eq. (3.21).

3.3 Eikonal and Coulomb gluons in dimensional regularisation

In this section we will complete our calculation of the one loop corrections by adding the real, or eikonal, parts of the loop integrals. This time we will carry out the integration in dimensional regularisation and we will write our expressions in this section in the form as they were originally presented in [41]. The agreement of our results with this reference constitutes a non-trivial cross-check of the cutting rules derived in Appendix D.

In the Feynman gauge, the different topologies that contribute to this amplitude are illustrated in Fig. 3.6. In Appendix E, we show that the sum over these graphs can be reduced to the following expression

$$\Big|n^{(1)}_{+1}\Big\rangle\equiv\mathbf{J}_{n+1}(q)\left(\mathbf{I}_n^{(1)}+\widetilde{K}_{uv}\right)\Big|n^{(0)}\Big\rangle+\mathbf{J}^{(1)}_{n+1}(q)\Big|n^{(0)}\Big\rangle,\tag{3.29}$$

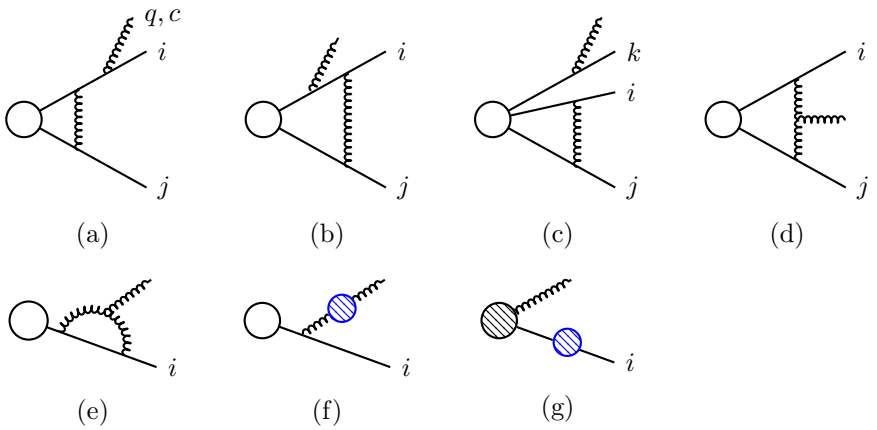

Figure 3.6: One loop corrections to a general hard process. The small blue blobs denotes self energy corrections.

where $\mathbf{I}_n^{(1)}$ denotes the operator that accounts for the one-loop corrections to the hard process, i.e. Eq. (2.15). We will show the expressions for the operator $\mathbf{J}_{n+1}^{(1)}(q)$ and for factor $\widetilde{K}_{uv}$ below.

The contribution from the operator $\mathbf{J}_{n+1}^{(1)}(q)$, known as the one-loop soft-gluon current [41], is given by

$$\begin{aligned} \mathbf{J}_{n+1}^{(1)}(q) &= (g_s\mu^\epsilon)^3 \sum_{i<j}^{n} \mathbf{T}_q{\cdot}\mathbf{T}_i\,\mathbf{T}_j \left[p_j{\cdot}\varepsilon p_i{\cdot}q - p_i{\cdot}\varepsilon p_j{\cdot}q\right] \mathrm{D}_{ij}^1(q), \\ \mathrm{D}_{ij}^1(q) &\equiv \int_l \frac{-i}{\left[k^2+i0\right]\left[(k+q)^2+i0\right]\left[p_i{\cdot}(k+q)+\delta_i\frac{i0}{2}\right]\left[-p_j{\cdot}k+\delta_j\frac{i0}{2}\right]} \,. \end{aligned} \tag{3.30}$$

Observe that $\mathrm{D}_{ij}^1(q)$ is the four point scalar integral corresponding to graph (d) of Fig. 3.6.

The term with the $\tilde{K}_{uv}$ factor accounts for the self energy corrections, i.e. graphs (f) and (g), and the part of graph (e) proportional to a two point function[4]. By using colour conservation, the sum of these contributions can be written as

$$\widetilde{K}_{uv} \equiv \int \frac{\mathrm{d}^d k}{(2\pi)^d} \left[\frac{-iC_A}{[k^2+i0][(k+q)^2+i0]}\right] + \pi(q^2) + \sum_i^n \Sigma_i(p_i^2) \,. \tag{3.31}$$

The rules to calculate the imaginary contributions derived in Appendix D can be applied to both individual graphs or, as in the present case, to their associated scalar integrals if tensorial reductions are performed first. In particular, the imaginary part of $\mathrm{D}_{ij}^1(q)$ can be obtained by applying the cuts discussed in sections 3.1 and 3.2. The calculation of the resulting scalar integrals in dimensional regularisation are carried

[4]Precisely speaking, all the graphs with this same topology.

out in Section F.1 of Appendix F, they yield

$$\mathrm{Im}\{D^1_{ij}(q)\} = -i\sin(\pi\epsilon)(\widetilde{\delta}_{ij} - \widetilde{\delta}_{iq} - \widetilde{\delta}_{qj})\frac{c_\Gamma\left(q^2_{T(ij)}\right)^{-\epsilon}}{8\pi^2 p_i{\cdot}q\ p{\cdot}q\,\epsilon^2}$$

where $\widetilde{\delta}_{ab} = 1$ if $\{a,b\}$ are both incoming or outgoing and $\widetilde{\delta}_{ab} = 0$ otherwise and c_Γ is a typical volume factor:

$$c_\Gamma \equiv \frac{(4\pi)^\epsilon\Gamma^2[1+\epsilon]\Gamma^3[1-\epsilon]}{\Gamma[1-2\epsilon]} = c_\epsilon + \mathcal{O}(\epsilon^2)\ .$$

A by-product of our derivations in Appendix D is a method to calculate the real part of one-loop integrals in the eikonal approximation. According to this method, see Eq. (D.7b), the real (eikonal) part of $\mathrm{D}^1_{ij}(q)$ is equal to the sum of the single cuts over gluon lines illustrated in Fig. 3.7 with the principal value prescription (defined in Eq. (D.13)) applied on the propagators that are not cut. The details on the integration of these single cuts is presented in Appendix F. These two single cut contributions add up to

$$\begin{aligned}\mathrm{Re}\{D^1_{ij}(q)\} &= \frac{(g_s\mu^\epsilon)^3 c_\Gamma\cos(\epsilon\pi)\left(q^2_{T(ij)}\right)^{-\epsilon}}{8\pi^2 p_i{\cdot}q\ p{\cdot}q\,\epsilon^2},\\ &= (g_s\mu^\epsilon)^3\cos^2(\pi\epsilon)\int \mathrm{d}[k]\frac{1}{[p_j{\cdot}(k+q)]\,[p_i{\cdot}k]\,[k{\cdot}q]}\ .\end{aligned} \tag{3.32}$$

The first equality in Eq. (3.32) shows us that the logarithmic enhancements depend only on $q_{T(ij)}$ whereas the second equality exhibits the fact that up to subleading terms, i.e. $\cos^2(\pi\epsilon) = 1 + \mathcal{O}(\epsilon^2)$, this is equal to a phase space integral. Using this latter form, the total real part of the one-loop emission current can be expressed as

$$\mathrm{Re}\left\{\mathbf{J}^{(1)}_{n+1}\right\} = (g_s^3\mu^{3\epsilon})\cos^2(\pi\epsilon)\sum_{i<j}^{n}\int \mathrm{d}[k]\left\{\frac{\mathbf{T}_i{\cdot}\mathbf{T}_q\, p_i{\cdot}q}{(p_i{\cdot}k)(k{\cdot}q)}\left[\frac{\mathbf{T}_j\, p_j{\cdot}\varepsilon}{p_j{\cdot}(k+q)}\right] + (i\leftrightarrow j)\right\}.$$

Written in this form, the virtual scattering can be interpreted as a real emission process: from right to left, j emits an off-shell gluon with momentum $q+k$ and, subsequently, the emitted gluon exchanges an on-shell gluon k with parton i. By combining the real and imaginary contributions we obtain the conventional form of the one loop soft current [41]:

$$\mathbf{J}^{(1)c}_{n+1}(q) = \frac{\alpha_s g_s\mu^\epsilon}{2\pi}\frac{c_\Gamma}{\epsilon^2}\sum_{i<j}^{n}\mathbf{T}_q{\cdot}\mathbf{T}_i\,\mathbf{T}_j\left[\frac{p_j{\cdot}\varepsilon}{p_j{\cdot}q} - \frac{p_i{\cdot}\varepsilon}{p_i{\cdot}q}\right]\left(\frac{q^2_{T(ij)}}{\mu^2}\frac{e^{-\widetilde{\delta}_{iq}i\pi}e^{-\widetilde{\delta}_{jq}i\pi}}{e^{-\widetilde{\delta}_{ij}i\pi}}\right)^{-\epsilon}\ . \tag{3.33}$$

Finally, the scalar integrals in $\widetilde{K}_{uv}$ are purely real and only have divergences

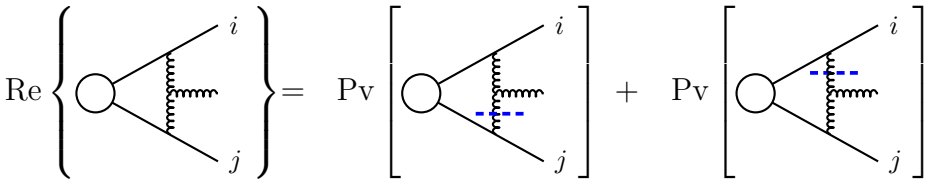

Figure 3.7: The real part of the four point scalar function is equal to the sum of single cuts over the soft gluons lines.

of collinear and ultraviolet origin. To properly include these virtual corrections we would have to perform a renormalisation of the theory; we will ignore that here as we are only interested in the soft enhancements[5].

3.4 On the colour evolution picture

Now that we have completed the calculation of the one-loop, one-emission amplitude in dimensional regularisation, we close this chapter by relating the complete amplitude to the colour evolution picture discussed in the previous chapter, in sections 2.5.1 and 2.6.

Let us start by writing the complete amplitude in a convenient form for comparison with the colour evolution picture. To do this, we insert the integrated expression for the one loop insertion operator

$$\mathbf{I}_n^{(1)} = \sum_{i<j}^{n} \frac{\alpha_s}{2\pi} c_\epsilon \mathbf{T}_i \cdot \mathbf{T}_j \left[1 + i\pi\epsilon\widetilde{\delta}_{ij}\right] \frac{1}{\epsilon^2} \left[\frac{2p_i\cdot p_j}{\mu^2}\right]^{-\epsilon} \tag{3.35}$$

[5]Nevertheless, the collinear pole in $\tilde{K}_{uv}$ can be anticipated in view of the following considerations. Firstly, we invoke that the uv poles of the bare QCD matrix elements that are proportional to the mth power of the coupling are given by [28]

$$\text{UV part}\left\{\left\langle n_{+1}^{(1)}\middle|n_{+1}^{(1)}\right\rangle_{\text{(1-loop)}}\right\} = m\frac{\alpha_s}{2\pi}\left[\frac{\beta_0}{\epsilon_{uv}}\right]\left\langle n_{+1}^{(0)}\middle|n_{+1}^{(0)}\right\rangle$$

where $\beta_0 = (11C_A - 4T_{\rm F}n_f)/6$. In the Feynman gauge, the term proportional to C_F arises from the fermion loop in the vacuum polarisation. Secondly, we invoke that after tensorial reductions, the one-loop uv divergences arises from two point functions and, within the context of dimensional regularisation of massless gauge theories [86, 4], the uv pole in this integral is accompanied by a collinear divergence, which is equal and opposite. Thus, we can anticipate that the collinear pole in $\tilde{K}_{uv}$ should be equal to

$$\text{Collinear pole}\left\{\tilde{K}_{uv}\right\} = -\frac{1}{2}\frac{\alpha_s}{2\pi}\left[\frac{\beta_0}{\epsilon}\right] \ . \tag{3.34}$$

This is of course a preliminary analysis that needs to be formalised. From now on we will drop the contributions proportional to $\tilde{K}_{uv}$ as they do not contain soft enhancements.

into the amplitude Eq. (3.29) and use the colour algebra to write it as:

$$\begin{aligned}\left|n^{(1)}_{+1}\right\rangle = \frac{\alpha_s}{2\pi}\frac{c_\epsilon}{\epsilon^2}\Bigg[&\mathbf{J}_{n+1}\sum_{i<j}^{n}\left\{\mathbf{T}_i\cdot\mathbf{T}_j\left[1+\widetilde{\delta}_{ij}i\pi\epsilon\right]\left[\left(\frac{2p_i\cdot p_j}{\mu^2}\right)^{-\epsilon}-\left(\frac{q^2_{T(ij)}}{\mu^2}\right)^{-\epsilon}\right]\right\}\\
&+\sum_{i<j}^{n}\left\{\mathbf{T}_i\cdot\mathbf{T}_j\left[1+\widetilde{\delta}_{ij}i\pi\epsilon\right]\left(\frac{q^2_{T(ij)}}{\mu^2}\right)^{-\epsilon}\right\}\mathbf{J}_{n+1}\\
&+\sum_{\substack{i=1\\ j\neq\{i\}}}^{n}\left\{\mathbf{T}_i\cdot\mathbf{T}_q\left[1+\widetilde{\delta}_{iq}i\pi\epsilon\right]\left(\frac{q^2_{T(ij)}}{\mu^2}\right)^{-\epsilon}\right\}\mathbf{T}_j\left[\frac{p_j\cdot\varepsilon}{p_j\cdot q}-\frac{p_i\cdot\varepsilon}{p_i\cdot q}\right]\Bigg]\left|n^{(0)}\right\rangle\\
&+\mathcal{O}(\epsilon^0\times\mathrm{Re}).\end{aligned} \tag{3.36}$$

Here, $\mathcal{O}(\epsilon^0\times\mathrm{Re})$ denotes real constant terms of order ϵ^0 plus higher order contributions and in the rest of this section we neglect these terms for the sake of studying the leading infrared behaviour of this amplitude. Note that in the third line the argument of the logarithmic enhancements is not $q^2_{Tqi}/\mu^2=0$. The relation between this way of writing the amplitude and the colour evolution picture becomes clearer when we consider its limiting behaviour in wide-angle and collinear configurations. Before studying these limits we shall describe its exact structure. Firstly, observe that each term in the above sums appears accompanied by a factor $[1+i\pi\widetilde{\delta}_{lm}\epsilon]$, this means that the real and the imaginary parts have exactly the same kinematic and colour pre-factors. The only difference between them is that imaginary parts only occur between incoming or between outgoing partons. Secondly, observe that the argument of all of the logarithms are either the transverse momentum (with respect to a pair of hard partons) or the hard scale of the process. This is remarkable as there are other possibilities allowed by Lorentz invariance and dimensional analysis[6].

Let us focus our attention on the imaginary part of Eq. (3.36) as this will help us to relate this amplitude with our studies in Secs. 3.1 and 3.2. Using the following definition of the Coulomb operator in dimensional regularisation:

$$\mathbf{C}^{ij}(\alpha,\beta)\equiv -i\pi\mathbf{T}_i\cdot\mathbf{T}_j\frac{\alpha_s c_\epsilon\mu^{2\epsilon}}{2\pi}\int_{\alpha^2}^{\beta^2}\frac{\mathrm{d}k^2_{Tij}}{(k^2_{Tij})^{1+\epsilon}}, \tag{3.37}$$

[6]In fact, other enhancements appear in intermediate steps, see Eqs. (F.21) and (F.22) in Appendix F, but they all cancel as we show in Appendix E.

the imaginary part of (3.36) can be expressed as

$$\begin{aligned}\mathrm{Im}\left\{\left|n^{(1)}\right\rangle\right\} = &\sum_{i<j}^{n}\widetilde{\delta}_{ij}\left[\mathbf{J}_{n+1}(q)\,\mathbf{C}^{ij}\big(q_{T(ij)},2p_i{\cdot}p_j\big)+\mathbf{C}^{ij}\big(0,q_{T(ij)}\big)\;\mathbf{J}_{n+1}(q)\right]\left|n^{(0)}\right\rangle\\ &+\sum_{i=1}^{n}\widetilde{\delta}_{iq}\sum_{j\neq\{i\}}^{n}\mathbf{C}^{iq}\big(0,q_{T(ji)}\big)\,\mathbf{T}_j\left[\frac{p_j{\cdot}\varepsilon}{p_j{\cdot}q}-\frac{p_i{\cdot}\varepsilon}{p_i{\cdot}q}\right]\left|n^{(0)}\right\rangle\,.\end{aligned} \tag{3.38}$$

The first line in Eq. (3.38) accounts for the eikonal cuts in the initial and final state (see Eqs. (3.18) and (3.19)) while the second line contains the re-scattering cuts (see Eq. (3.22)). We shall now study these type of cuts (two lines) separately.

The first line of Eq. (3.38) shows us that the sum of eikonal cuts through a pair of hard partons $\{i,j\}$ can be always expressed in terms of Coulomb exchanges between them. Crucially, they appear ordered specifically with respect to $q_{T(ij)}$, the transverse momentum of the emissions with respect to $\{p_i,p_j\}$. Finally, we recall that the invariant mass of every pair of hard partons should be thought of as the scale of the hard subprocess, i.e. $2p_i{\cdot}p_j\sim Q^2$.

As we discussed in Section 3.2.3, the operator associated with the gluon emission in the re-scattering cuts cannot be written as a single emission current $\mathbf{J}_{n+1}(q)$. The reason is the dipole structure of the re-scattering cuts that we shall now describe in detail. In this case, and also in the forthcoming chapters, gluons that will subsequently exchange a virtual (in this case Coulomb) gluon always appear emitted via this same dipole structure. Anticipating this, we introduce the operator:

$$\mathbf{d}_{n+1(ji)}(q)\equiv g_s\mu^{\epsilon}\,\mathbf{T}_j\left[\frac{p_j\cdot\varepsilon}{p_j\cdot q}-\frac{p_i\cdot\varepsilon}{p_i\cdot q}\right], \tag{3.39}$$

associated with the emission of gluon q from the dipole formed by i (the other parton involved in the exchange) and each of the hard partons $j\neq\{i\}$. In terms of this definition, the re-scattering cuts in the second line of Eq. (3.38) adopt a compact form:

$$\sum_{i=1}^{n}\widetilde{\delta}_{iq}\sum_{j\neq\{i\}}^{n}\mathbf{C}^{iq}\big(0,q_{T(ji)}\big)\,\mathbf{d}_{n+1(ji)}(q)\left|n^{(0)}\right\rangle\,. \tag{3.40}$$

Observe that the transverse momentum, k_T, of the Coulomb gluons is always bounded by the dipole momentum: $k_T<q_{T(ji)}$. Since this is the first Coulomb exchange that the emitted gluons experience, we can think of this upper limit as an effective hard scale that each dipole emission imposes on the transverse momentum of the subsequent Coulomb exchange.

Note that the sum over the different dipoles is exactly equal to the soft gluon

current

$$\sum_{j\neq\{i\}}^{n} \mathbf{d}_{n+1(ji)}(q)\Big|n^{(0)}\Big\rangle = \mathbf{J}_{n+1}(q)\ . \tag{3.41}$$

However, the sum over dipoles in Eq. (3.40) cannot be commuted past the Coulomb gluons as these depend upon a dipole momentum, $q_{T(ji)}$. It is this dependence and the requirement of gauge invariance that forces the soft emission to be emitted from a dipole instead of a soft-gluon current. The expressions that we found in this section might look very different from colour evolution picture that we described in Chapter 2. To clarify this identification we shall now consider the behaviour in the wide angle and collinear limits.

3.4.1 Wide-angle and collinear limits

Let us first show this structure in the kinematical configuration where q becomes collinear with a hard parton l, i.e. the same limit as in Eqs. (3.23) with $m = l$. The leading behaviour of Eq. (3.38) in this limit yields

$$\begin{aligned}
\mathrm{Im}\left\{\Big|n^{(1)}\Big\rangle\right\} = {}& \widetilde{\mathbf{Sp}}^{(0)}\left[\sum_{i\neq\{l\}}^{n}\widetilde{\delta}_{li}\mathbf{C}^{il}\big(q_{T(lr)},2p_i\cdot p_l\big)\right]\Big|n^{(0)}\Big\rangle \\
&+\left[\sum_{i\neq\{l\}}^{n}\widetilde{\delta}_{il}\mathbf{C}^{il}\left(0,q_{T(lr)}\right)+\sum_{i=1}^{n}\widetilde{\delta}_{iq}\mathbf{C}^{iq}\left(0,q_{T(lr)}\right)\right]\widetilde{\mathbf{Sp}}^{(0)} \\
&+\sum_{\substack{i<j\\ i,j\neq\{l,q\}}}^{n}\left[\mathbf{C}^{ij}\left(0,\alpha\right)\widetilde{\mathbf{Sp}}^{(0)}+\widetilde{\mathbf{Sp}}^{(0)}\mathbf{C}^{ij}\left(\alpha,2p_i\cdot p_j\right)\right]\Big|n^{(0)}\Big\rangle
\end{aligned} \tag{3.42}$$

where $\widetilde{\mathbf{Sp}}^{(0)}$ denotes the operator associated splitting of the two collinear partons $\{q,l\}$, with our choice of polarisation in Appendix C this yields

$$\widetilde{\mathbf{Sp}}^{(0)}(q,l) \equiv g_s\mu^{\epsilon}\mathbf{T}_l\frac{p_l\cdot\varepsilon}{p_l\cdot q} = -g_s\mu^{\epsilon}\mathbf{T}_l\frac{2}{q_{T(lr)}}\ , \tag{3.43}$$

and α is any variable with dimension of mass; we shall discuss its origin below.

Observe that Eq. (3.42) has now perfectly factorised into the product of Coulomb gluons and simple tree level emissions as in the colour evolution picture. The Coulomb gluon operators in the first two lines involve at least one of the two collinear partons $\{q,l\}$. They are all ordered with respect to $q_{T(lr)}$ which is the transverse momentum that defines the collinear limit. The third line accounts for Coulomb exchanges between partons other than $\{q,l\}$; they can be ordered with respect to any variable α because the colour charges of the exchange and emission involving

different partons commute:

$$[\mathbf{T}_l, \mathbf{T}_i \cdot \mathbf{T}_j] = 0 \text{ for } i,j \neq \{l\} \ . \tag{3.44}$$

Hence, in this collinear limit the transverse momentum that defines the collinear limit $q_{T(lr)}$ can be used to order the subsequent radiation.

Let us now consider the leading behaviour of Eq. (3.38) when q is emitted at a wide angle: $\hat{p}_i \cdot \hat{q} \approx 0$ for all of the hard partons. In this limit

$$\mathrm{Im}\left\{\left|n^{(1)}\right\rangle\right\} \approx \mathbf{J}_{n+1}(q) \sum_{i<j}^{n} \widetilde{\delta}_{ij} \mathbf{C}^{ij}(q_0, 2p_i \cdot p_j) \left|n^{(0)}\right\rangle + \sum_{i<j}^{n+1} \widetilde{\delta}_{ij} \mathbf{C}^{ij}(0, q_0)\, \mathbf{J}_{n+1}(q) \left|n^{(0)}\right\rangle,$$

where it should be understood that the $(n+1)$th parton in the sum corresponds to the gluon emission.

As we already mentioned, the eikonal and Coulomb parts of the virtual contributions have the same structure. Thus, it is straightforward to generalise wide-angle and collinear limits in the presence of eikonal gluons. In particular, the collinear limit of the complete amplitude, Eq. (3.36), yields

$$\begin{aligned}
\left|n^{(1)}_{+1}\right\rangle = \frac{\alpha}{2\pi}\frac{c_\epsilon}{\epsilon^2}\Bigg\{ & \widetilde{\mathbf{Sp}}^{(0)} \sum_{j,j\neq\{l\}}^{n} \mathbf{T}_j \cdot \mathbf{T}_l \left[1 + \widetilde{\delta}_{lj} i\pi\epsilon\right] \left[\left(\frac{2p_i\cdot p_j}{\mu^2}\right)^{-\epsilon} - \left(\frac{q^2_{T(lr)}}{\mu^2}\right)^{-\epsilon}\right] \\
& + \left[\sum_{j\neq\{l\}}^{n} \mathbf{T}_l \cdot \mathbf{T}_j \left[1 + \widetilde{\delta}_{lj} i\pi\epsilon\right] + \sum_{j=1}^{n} \mathbf{T}_j \cdot \mathbf{T}_q \left[1 + i\widetilde{\delta}_{qj}\pi\epsilon\right]\right] \left(\frac{q^2_{T(lr)}}{\mu^2}\right)^{-\epsilon} \widetilde{\mathbf{Sp}}^{(0)} \\
& + \widetilde{\mathbf{Sp}}^{(0)} \sum_{\substack{i<j \\ i,j\neq\{l,q\}}}^{n} \left[\left[1 + \widetilde{\delta}_{ij} i\pi\epsilon\right] \mathbf{T}_i \cdot \mathbf{T}_j \left[\left(\frac{2p_i\cdot p_j}{\mu^2}\right)^{-\epsilon} - \left(\frac{\alpha^2}{\mu^2}\right)^{-\epsilon}\right]\right] \\
& + \sum_{\substack{i<j \\ i,j\neq\{l,q\}}}^{n} \left[\left[1 + \widetilde{\delta}_{ij} i\pi\epsilon\right] \mathbf{T}_i \cdot \mathbf{T}_j \left(\frac{\alpha^2}{\mu^2}\right)^{-\epsilon}\right] \widetilde{\mathbf{Sp}}^{(0)} \Bigg\} \left|n^{(0)}\right\rangle \ ,
\end{aligned} \tag{3.45}$$

Again, the exchanges in the first two lines involve at least one of the two collinear partons; they always appear ordered with respect to $q_{T(lr)}$. The third and fourth lines contain all the exchanges between partons other than $\{q, l\}$ and can be ordered with respect to any variable α. Finally, in the wide-angle region, the leading behaviour of the complete amplitude, Eq. (3.36), is

$$\begin{aligned}
\left|n^{(1)}_{+1}\right\rangle = \frac{\alpha_s}{2\pi}\frac{c_\epsilon}{\epsilon^2}\Bigg[& \mathbf{J}_{n+1} \sum_{i<j}^{n} \left\{\left[1 + \widetilde{\delta}_{ij} i\pi\epsilon\right] \mathbf{T}_i \cdot \mathbf{T}_j \left[\left(\frac{2p_i\cdot p_j}{\mu^2}\right)^{-\epsilon} - \left(\frac{q_0^2}{\mu^2}\right)^{-\epsilon}\right]\right\} \\
& + \sum_{i<j}^{n+1} \left\{\left[1 + \widetilde{\delta}_{ij} i\pi\epsilon\right] \mathbf{T}_i \cdot \mathbf{T}_j \left(\frac{q_0^2}{\mu^2}\right)^{-\epsilon}\right\} \mathbf{J}_{n+1}\Bigg] \left|n^{(0)}\right\rangle \ .
\end{aligned} \tag{3.46}$$

This expression is precisely what is obtained, at this order, in the colour evolution ordered in energy as presented in Section 2.5.1. However, this is only a good approximation in the wide-angle regime.

3.5 Summary

The form in which the amplitude $\left|n_{+1}^{(1)}\right\rangle$ is written in Eq. (3.36) is of course one of many possibilities. There are two reasons why we presented the amplitude in this way. Firstly, it exhibits the structure of the colour evolution picture that we described in the previous chapter; it shows us which is the correct ordering variable that orders the virtual operator with respect to the real emissions. Secondly, in chapters 5 and 6 we will show that the ordering condition that we found at this order generalises for the case of two emissions and we think it is likely that it generalises for any number of gluon emissions.

The ordering condition in Eq. (3.36) can be summarised in a very simple form. The virtual exchange between two hard partons $\{i, j\}$ should be alternated with a real emission, $\mathbf{J}_{n+1}(q)$, and should be ordered with respect to $q_{T(ij)}$. In addition, the emitted gluon that subsequently exchanges a virtual gluon is radiated from a dipole $\mathbf{d}_{n+1(ji)}$ and each dipole sets an effective hard scale $q_{T(ji)}$ that limits the virtual momentum of the exchange.

The form in which we presented the amplitude, Eq. (3.36), shows that the eikonal and Coulomb parts of the loop integral have the same colour and kinematic prefactors, the only difference is that Coulomb gluons are only exchanged between incoming and between outgoing partons while eikonal gluons are also exchanged between incoming and outgoing partons. To be precise about this statement, we point out that the complete amplitude, Eq. (3.36), can be obtained from its imaginary part, Eq. (3.42), simply by replacing the Coulomb operators as:

$$\begin{aligned}\widetilde{\delta}_{ij}\mathbf{C}^{ij}(\alpha,\beta) &= i\pi\tilde{\delta}_{ij}\mathbf{T}_i\cdot\mathbf{T}_j\frac{\alpha_s c_\epsilon}{\epsilon}\left[\left(\frac{\beta^2}{\mu^2}\right)^{-\epsilon}-\left(\frac{\alpha^2}{\mu^2}\right)^{-\epsilon}\right]\\ &\to [1+i\pi\tilde{\delta}_{ij}\epsilon]\mathbf{T}_i\cdot\mathbf{T}_j\frac{\alpha_s c_\epsilon}{\epsilon^2}\left[\left(\frac{\beta^2}{\mu^2}\right)^{-\epsilon}-\left(\frac{\alpha^2}{\mu^2}\right)^{-\epsilon}\right]\ .\end{aligned} \tag{3.47}$$

The expression for the integrated amplitude Eq. (3.36) has the virtue of showing the simplicity of the ordering conditions. However, in order to compare with parton shower formalism it is also interesting to write the eikonal part of amplitude in terms

of phase-space integrals, i.e.

$$\begin{aligned}\mathrm{Re}\left\{\left|n^{(1)}\right\rangle\right\} = g^2\mu^{2\epsilon}\Bigg[&\mathbf{J}_{n+1}\sum_{i<j}^{n}\mathbf{T}_i\cdot\mathbf{T}_j\int \mathrm{d}[k]\frac{p_i\cdot p_j\Big[\theta_{ij}(k)-\theta_{ij}(q>k)\Big]}{p_i\cdot k p_j\cdot k}\\ &+\sum_{i<j}^{n}\left\{\int \mathrm{d}[k]\frac{\mathbf{T}_i\cdot\mathbf{T}_j p_i\cdot p_j\theta_{ij}(q>k)}{p_i\cdot k p_j\cdot k}\right\}\mathbf{J}_{n+1}\\ &+\sum_{\substack{i=1\\ j\neq\{i\}}}^{n}\left\{\mathbf{T}_i\cdot\mathbf{T}_{n+1}\mathbf{T}_j\int \mathrm{d}[k]\frac{g\mu^{\epsilon}\, p_i\cdot q\; p_j\cdot\varepsilon}{[p_i\cdot k]\,[k\cdot q]\,[p_j\cdot(k+q)]}\right\}\\ &-\sum_{\substack{i=1\\ j\neq\{i\}}}^{n}\left\{\mathbf{T}_i\cdot\mathbf{T}_{n+1}\mathbf{T}_j\int \mathrm{d}[k]\frac{g\mu^{\epsilon}\, p_j\cdot q\; p_i\cdot\varepsilon}{[p_j\cdot k]\,[k\cdot q]\,[p_i\cdot(k+q)]}\right\}\Bigg]\left|n^{(0)}\right\rangle\,,\end{aligned} \tag{3.48}$$

where we have used the definitions $\theta_{ij}(q>k)\equiv\theta(p_i\cdot(q-k))\theta(p_j\cdot(q-k))$ and $\theta_{ij}(k)\equiv\theta(p_i\cdot(p_j-k))\theta(p_j\cdot(p_i-k))$. In particular, $\theta_{ij}(q>k)$ allows us to write

$$\frac{c_\epsilon\alpha_s}{2\pi\epsilon^2}\left(\frac{q_{T(ij)}}{\mu^2}\right)^{-\epsilon}=\int \mathrm{d}[k]\frac{(g\mu^{\epsilon})^2 p_i\cdot p_j\;\theta_{ij}(q>k)}{p_i\cdot k p_j\cdot k}\,.$$

It would be interesting to investigate further the connection between the above expression and the dipole parton showers where the $q_{T(ij)}$ are used to order emissions [87, 88, 89, 90, 91, 92, 93].

Finally, to further show the relation between Eq. (3.48) and the colour evolution picture as it was introduced in the previous chapter, we point out that in the wide-angle regime this expression should reduce to Eq. (3.46), which can be written as

$$\begin{aligned}&\Bigg[\mathbf{J}_{n+1}(q)\left(\frac{1}{2}h(\epsilon)\int \mathrm{d}[k]\mathbf{J}^2_{n+1}(k)\,\Theta(Q>k_0>q_0)\right)\\ &+\left(\frac{1}{2}h(\epsilon)\int \mathrm{d}[k]\mathbf{J}^2_{n+2}(k)\,\Theta(q_0>k_0)\right)\mathbf{J}_{n+1}(q)\Bigg]\left|n^{(0)}\right\rangle,\end{aligned} \tag{3.49}$$

where $h(\epsilon)=\frac{(4\pi^2)^\epsilon\Gamma^2[1-\epsilon]}{\Gamma[1-2\epsilon]}=1+\mathcal{O}(\epsilon)$. Up to subleading contributions, this expression corresponds to the energy-ordered colour evolution picture, Eq. (2.71). In chapter 6, when we generalise the results in this chapter for the case of two emissions, we will see that again energy ordering is a good approximation in the wide-angle regime but we must emphasise that the expression that reproduces correctly the collinear limits is Eq. (3.36).

Chapter 4

Structure of infrared cancellations at order α_s^2

The one-loop, one-emission corrections that we studied in Chapter 3 first contribute to cross-sections at order α_s^2 (relative to the order of the hard-scattering), when they are multiplied by the tree level one-emission amplitude. The complete list of matrix elements that contribute to an observable at this order is:

$$\int \frac{\mathrm{d}[q_1]\mathrm{d}[q_2]}{2!} \left\langle n^{(0)}_{+2} \middle| n^{(0)}_{+2} \right\rangle \phi_2 + \int \mathrm{d}[q] \left[\left\langle n^{(0)}_{+1} \middle| n^{(1)}_{+1} \right\rangle + \mathrm{h.c.} \right] \phi_1 + \left\langle n^{(1)} \middle| n^{(1)} \right\rangle + \left\langle n^{(0)} \middle| n^{(2)} \right\rangle + \left\langle n^{(2)} \middle| n^{(0)} \right\rangle, \tag{4.1}$$

where ϕ_1, ϕ_2 are functions of the phase space that define the observable. According to the Bloch-Nordsieck theorem, the inclusive integration over the soft gluon emissions, i.e. $\phi_a = 1$ for $a = \{1, \dots\}$, should cancel; this chapter is dedicated to the study of these cancellations.

Our approach to the integration of these matrix elements uses a series of approximations, however it suffices to reveal some of the structure of the infrared cancellations for a completely general wide-angle hard process. The primary aim of this chapter is to provide some guidelines for the implementation of the colour evolution picture at this order. In addition, these calculations will show us the order at which the corrections to the colour evolution picture enter. For instance, we will study the corrections due to the emission of a soft gluon that branches into a fermion pair. Furthermore, this is the first order (α^2 with respect to the Born term) at which Coulomb gluon contributions can contribute to particular observables and we will pay close attention to such contributions.

The approximation consists of performing the phase space integrals neglecting the recoil effects against the gluon emissions. Precisely speaking, soft gluon emissions are integrated over their mass-shell without enforcing global momentum conservation. We regularise infrared divergences performing the integrals in $d = 4 - 2\epsilon$ dimensions

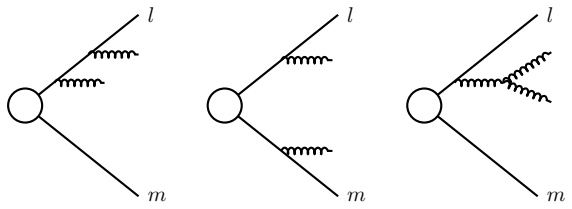

Figure 4.1: Different topologies that contribute to the double emission amplitude of a general hard process. Hard partons legs not involved in the soft gluon emission are not shown. .

and cut off the high-energy momentum modes that are divergent due to the absence of global momentum conservation. In order to focus on physics only, the reader is referred to Section F.5 of Appendix F where we present the details of the integration.

We will study the different contributions of the double emission matrix elements to the total cross-section in Section 4.1. Subsequently, in Section 4.2, we will study the inclusive integration of the one-loop, one-emission matrix elements and will pay attention to role of the Coulomb gluons at this order. Finally, in Section 4.3.1, we shall study the Bloch-Nordsieck theorem to deduce the form of the two-loop corrections necessary to cancel the above matrix elements. We will compare the resulting expression with Catani's formula for the singular infrared behaviour of the two-loop corrections for a general scattering process, Eqs. (2.50) and (2.51).

4.1 Double real contributions

The lowest order amplitude of a general process with two soft emissions $\left|n^{(0)}_{+2}\right\rangle$ can be expressed [54] in terms of an operator $\mathbf{K}_{n+2}(q_1,q_2)$ that acts on the hard process to insert two real emissions:

$$\left|n^{(0)}_{+2}\right\rangle = g_s^2\mu^{2\epsilon}\mathbf{K}_{n+2}(q_1,q_2)\left|n^{(0)}\right\rangle \,. \tag{4.2}$$

The different topologies that contribute to this operator are depicted in Fig. 4.1. In the Feynman gauge their explicit contributions add up to

$$\begin{aligned}\mathbf{K}^{a_1a_2}_{n+2}(q_1,q_2) \equiv &\sum_{l=1}^{n}\left[\frac{\mathbf{T}^{a_1}_l\, p_l\cdot\varepsilon_1}{p_l\cdot q_1}\frac{\mathbf{T}^{a_2}_l\, p_l\cdot\varepsilon_2}{p_l\cdot(q_1+q_2)} + (1\leftrightarrow 2)\right] + \\ &\sum_{l\neq m}^{n}\frac{\mathbf{T}^{a_1}_l\, p_l\cdot\varepsilon_1}{p_l\cdot q_1}\frac{\mathbf{T}^{a_2}_m p_m\cdot\varepsilon_2}{p_m\cdot q_2} + \\ &\sum_{l=1}^{n}\frac{\mathbf{T}^{c}_l\, p_{l\,\mu}}{p_l\cdot(q_1+q_2)}\frac{if^{ca_1a_2}\widetilde{V}^{\mu\nu_1\nu_2}(q_1+q_2,-q_1,-q_2)\varepsilon_{\nu_1}(q_1)\varepsilon_{\nu_2}(q_2)}{2q_1\cdot q_2}\,,\end{aligned} \tag{4.3}$$

where

$$\widetilde{V}^{\mu\nu_1\nu_2}(q_1+q_2,-q_1,-q_2) \equiv 2q_1^{\nu_2}g^{\mu\nu_1} + (q_2-q_1)^{\mu}g^{\nu_1\nu_2} - 2q_2^{\nu_2}g^{\mu\nu_1} \tag{4.4}$$

is the triple gluon vertex contribution but with unphysical terms, $\varepsilon_1 \cdot q_1 = 0$ and $\varepsilon_2 \cdot q_1 = 0$, removed. The double emission tensor $\mathbf{K}_{n+2}(q_1, q_2)$ has the same expression in the Axial gauge [54]. Indeed, this amplitude is gauge invariant as its action on the hard subprocess vanishes when one of the polarisation vectors is substituted by its respective momentum. We will study the factorisation properties of the double emission tensor $\mathbf{K}_{n+2}(q_1, q_2)$ in the next chapter, here we are interested in its contributions to the total cross section. For this propose it is convenient to organise its contributions into three groups:

$$\left\langle n^{(0)}\middle|\mathbf{K}_{n+2}^{\dagger}\cdot\mathbf{K}_{n+2}\middle|n^{(0)}\right\rangle = \left\langle n^{(0)}\middle|\left[\mathbf{K}^2_{\text{s.o.2}} + \mathbf{K}^2_{\text{s.o.3.4}} + \mathbf{K}^2_{\text{sub}}\right]\middle|n^{(0)}\right\rangle, \tag{4.5}$$

The contributions in $\mathbf{K}^2_{\text{s.o.2.}}$ and $\mathbf{K}^2_{\text{s.o.3,4}}$ contain only terms that are leading in the strongly ordered regime, i.e. terms such that when the momentum of one of the gluons, say q_1, is re-scaled as $q_1 \to \lambda q_1$, the dominant term in the small λ expansion behaves as λ^{-2}. , whereas $\mathbf{K}^2_{\text{sub}}$ contains the terms that are subleading in the same regime. Each term in $\mathbf{K}^2_{\text{s.o.2.}}$ and $\mathbf{K}^2_{\text{sub}}$ depends at most on the colour and kinematics of two hard partons whilst each term in $\mathbf{K}^2_{\text{s.o.3,4}}$ depends on three or four different hard partons.

4.1.1 Leading two-parton corrections $\mathbf{K}^2_{\text{s.o.2}}$

As terms in $\mathbf{K}^2_{\text{s.o.2}}$ depend on two hard partons, we can write

$$\mathbf{K}^2_{\text{s.o.2}} = \sum_{i<j}^{n} \widetilde{\mathbf{K}}^2_{\text{s.o.}}(i,j) \tag{4.6}$$

where

$$\begin{aligned}
\widetilde{\mathbf{K}}^2_{\text{s.o.}}(i,j) \equiv{}& 4\left[\mathbf{T}_i\cdot\mathbf{T}_j\frac{p_i\cdot p_j}{p_i\cdot q_1\; p_j\cdot q_1}\right]\left[\mathbf{T}_i\cdot\mathbf{T}_j\frac{p_i\cdot p_j}{p_i\cdot q_2\; p_j\cdot q_2}\right] \\
&+ \left[\mathbf{T}_i^a\,\mathbf{T}_i\cdot\mathbf{T}_j\,\mathbf{T}_j^a - (\mathbf{T}_i\cdot\mathbf{T}_j)^2\right]\left[\frac{2(p_i\cdot p_j)^2}{p_i\cdot q_1\; p_j\cdot q_1\; p_i\cdot(q_1+q_2)\; p_j\cdot(q_1+q_2)} + (1\leftrightarrow 2)\right] \\
&+ \mathbf{T}_i^a\mathbf{T}_i^b i f^{abd}\mathbf{T}_j^d\left\{\left[\frac{3p_i\cdot p_j}{p_i\cdot q_1\; q_2\cdot q_1\; p_j\cdot(q_1+q_2)} + (1\leftrightarrow 2)\right] + (i\leftrightarrow j)\right\} \\
&+ \mathbf{T}_i^a\mathbf{T}_j^b i f^{abd}\mathbf{T}_j^d\left\{\left[\frac{p_i\cdot p_j\; p_i\cdot q_2}{p_j\cdot q_2\; q_2\cdot q_1\; p_i\cdot(q_1+q_2)\; p_i\cdot q_1} + (1\leftrightarrow 2)\right] + (i\leftrightarrow j)\right\} \\
&- \mathbf{T}_i^a\mathbf{T}_j^b i f^{abd}\mathbf{T}_j^d\left\{\left[\frac{(p_i\cdot p_j)^2}{p_j\cdot q_2\; p_j\cdot q_1\; p_i\cdot(q_1+q_2)\; p_i\cdot q_1} + (1\leftrightarrow 2)\right] + (i\leftrightarrow j)\right\}\,.
\end{aligned} \tag{4.7}$$

Each term in this expression is leading in the strongly ordered regime.

Within our approximated methods of integration, the inclusive integration of the fourth line of Eq. (4.7) exactly cancels the fifth one. In fact, this occurs immediately after the integration over the phase space of one of the emissions (see Eqs. (F.25) (F.26)):

$$\int \mathrm{d}[q_1] \frac{p_i\cdot p_j \; p_i\cdot q_2}{p_j\cdot q_2 \; q_2\cdot q_1 \; p_i\cdot(q_1+q_2) \; p_i\cdot q_1} = \int \mathrm{d}[q_1] \frac{(p_i\cdot p_j)^2}{p_j\cdot q_2 \; p_j\cdot q_1 \; p_i\cdot(q_1+q_2) \; p_i\cdot q_1}$$
$$= \frac{(4\pi)^\epsilon \Gamma[1+\epsilon]}{8\pi^2} \frac{p_i\cdot p_j}{p_i\cdot q_2 \; p_j\cdot q_2} \frac{(2p_i\cdot q_2)^{-\epsilon}}{\epsilon^2} \; . \tag{4.8}$$

Hence, when one calculates the total cross-section only the first three lines in Eq. (4.7) contribute.

The terms in the first line of Eq. (4.7) are just the product of tree level single gluon real exchanges. The contributions in the second and third line of Eq. (4.7) have the interesting property that the integration over one of the gluon momenta renders an expression which only depends of the transverse components of the other momentum:

$$\int \mathrm{d}[q_1] \frac{(p_i\cdot p_j)^2}{p_i\cdot q_1 \; p_j\cdot q_1 \; p_i\cdot(q_1+q_2) \; p_j\cdot(q_1+q_2)} = \int \mathrm{d}[q_1] \frac{p_i\cdot p_j}{p_i\cdot q_1 \; q_1\cdot q_2 \; p_j\cdot(q_1+q_2)}$$
$$= \frac{c_\epsilon}{8\pi^2} \frac{p_i\cdot p_j}{p_i\cdot q_2 \; p_j\cdot q_2} \frac{(q^2_{2T(ij)})^{-\epsilon}}{\epsilon^2} f(\epsilon) \tag{4.9}$$

where $f(\epsilon)$ denotes constant terms such that $f(\epsilon) = 1 + \mathcal{O}(\epsilon^2)$. Finally, using the scalar integrals in Section F.5 we arrive at the following expression for the contribution of $\widetilde{\mathbf{K}}^2_{\text{s.o.2}}(i,j)$ to the total cross-section

$$(g_s\mu^\epsilon)^4 \int \frac{\mathrm{d}[q_1]\mathrm{d}[q_2]}{2!} \mathbf{K}^2_{\text{s.o.2}}(i,j) \equiv \left[2(\mathbf{T}_i\cdot\mathbf{T}_j)^2 + \frac{C_A}{4}\mathbf{T}_i\cdot\mathbf{T}_j\right] \left[\frac{c_\epsilon\alpha_s}{2\pi}\frac{1}{\epsilon^2}\left[\frac{2p_i\cdot p_j}{\mu^2}\right]^{-\epsilon}\right]^2$$
$$- \frac{3C_A}{4}\mathbf{T}_i\cdot\mathbf{T}_j \Gamma[1+2\epsilon]\Gamma[1+\epsilon]\Gamma^3[1-\epsilon] \left[\frac{c_\epsilon\alpha_s}{2\pi}\frac{1}{\epsilon^2}\left[\frac{2p_i\cdot p_j}{\mu^2}\right]^{-\epsilon}\right]^2 ,$$
$$= \left[2(\mathbf{T}_i\cdot\mathbf{T}_j)^2 - \frac{C_A}{2}\mathbf{T}_i\cdot\mathbf{T}_j\right] \left[\frac{c_\epsilon\alpha_s}{2\pi}\frac{1}{\epsilon^2}\left[\frac{2p_i\cdot p_j}{\mu^2}\right]^{-\epsilon}\right]^2$$
$$- \frac{\alpha_s}{2\pi}\left[2\pi^2 + \mathcal{O}(\epsilon)\right] C_A \left[\mathbf{T}_i\cdot\mathbf{T}_j \frac{c_{2\epsilon}\alpha_s}{2\pi}\frac{1}{(2\epsilon)^2}\left[\frac{2p_i\cdot p_j}{\mu^2}\right]^{-2\epsilon}\right] \; . \tag{4.10}$$

4.1.2 Leading three and four partons corrections $\mathbf{K}^2_{\text{s.o.3.4}}$

We recall that terms $\mathbf{K}^2_{\text{s.o.3.4}}$ are leading in the strongly ordered regime. Below we will demonstrate that their contribution to the cross-section perfectly factorises into

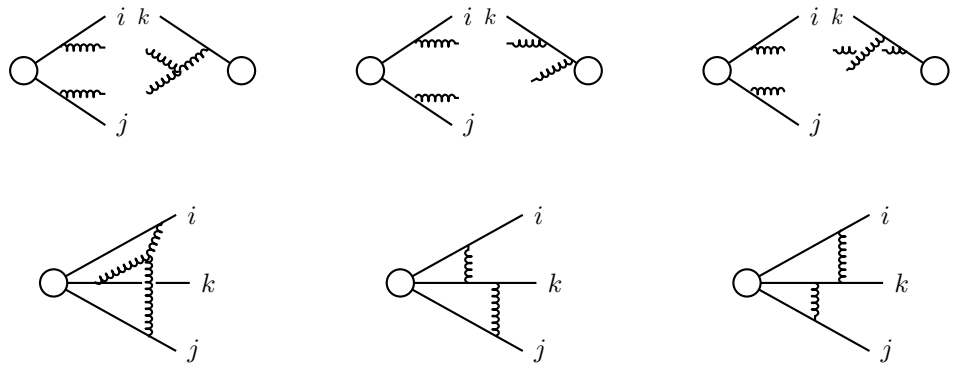

Figure 4.2: Purely (first row) real and and purely virtual (second row) graphs involving three partons.

the product of two single real gluon exchanges.

Let us consider the graphs in the first line of Fig. 4.2. Each of these graphs involves three different partons $\{i, j, k\}$. The first graph in this figure illustrates the contribution with a triple gluon vertex. Its unpolarised contribution to the cross-section is given by

$$\left\langle \left| [\mathbf{T}_i \cdot \mathbf{T}_k, \mathbf{T}_j \cdot \mathbf{T}_k] \right| \right\rangle \int \mathrm{d}[q_1]\mathrm{d}[q_2] \frac{p_i^{\mu_1}}{p_i \cdot q_1} \frac{p_j^{\mu_2}}{p_j \cdot q_2} \frac{\widetilde{V}_{\mu\mu_1\mu_2}(q_1+q_2,-q_1,-q_2)\; p_k^{\mu}}{p_k \cdot (q_1+q_2)(q_1+q_2)^2} \;, \quad (4.11)$$

here, and the rest of this chapter we abbreviate the hard process amplitude as $|\rangle \equiv \left|n^{(0)}\right\rangle$. Observe that the colour operator corresponding to this graph is anti-hermitian, i.e. $[\mathbf{T}_i \cdot \mathbf{T}_k, \mathbf{T}_j \cdot \mathbf{T}_k]^\dagger = -[\mathbf{T}_i \cdot \mathbf{T}_k, \mathbf{T}_j \cdot \mathbf{T}_k]$. Thus, the sum of this, Eq. (4.11), and its hermitian conjugate contribution exactly cancels. Nevertheless, it is interesting to note that the inclusive integration of Eq. (4.11) also vanishes. To see this, it is convenient to express the gluon momentum in light-cone coordinates[1] where $p_i = (p_i^+, 0, 0_T), p_i = (0, p_j^-, 0_T)$. The following change of variables

$$\begin{aligned} (q_1^-, q_1^+, q_{1T}) &\to \left(\frac{p_k^-}{p_k^+} q_2^+, \frac{p_k^+}{p_k^-} q_2^-, q_{2T} \right), \\ (q_2^-, q_2^+, q_{2T}) &\to \left(\frac{p_k^-}{p_k^+} q_1^+, \frac{p_k^+}{p_k^-} q_1^-, q_{1T} \right), \end{aligned} \quad (4.12)$$

has a unit Jacobian. In addition, it changes the sign of the numerator, i.e.

$$p_i^{\mu_1} p_j^{\mu_2} p_k^{\mu} \widetilde{V}_{\mu\mu_1\mu_2}(q_1+q_2,-q_1,-q_2) \to -p_i^{\mu_1} p_j^{\mu_2} p_k^{\mu} \widetilde{V}_{\mu\mu_1\mu_2}(q_1+q_2,-q_1,-q_2), \quad (4.13)$$

and leaves the rest of the integrand invariant. Thus, this integral exactly vanishes it whenever is integrated over a domain invariant under the transformation in Eq. (4.12). Next we consider the second and third graphs in the first line of

[1] $l^\pm = (l_0 \pm l_1)/\sqrt{2}$.

Fig. 4.2. The sum of their contributions can be written as

$$\begin{aligned}
&\Big\langle\Big|\int \mathrm{d}[q_1]\mathrm{d}[q_2]\frac{\mathbf{T}_i^{c_1}p_i^{\mu_1}}{p_i\cdot q_1}\frac{\mathbf{T}_j^{c_2}p_j^{\mu_2}}{p_j\cdot q_2}\left[\frac{\mathbf{T}_k^{c_1}p_k^{\mu_1}}{p_k\cdot q_1}\frac{\mathbf{T}_k^{c_2}p_k^{\mu_2}}{p_k\cdot(q_1+q_2)}+\frac{\mathbf{T}_k^{c_2}p_k^{\mu_2}}{p_k\cdot q_2}\frac{\mathbf{T}_k^{c_1}p_k^{\mu_1}}{p_k\cdot(q_1+q_2)}\right]\Big|\Big\rangle \\
&\quad=\Big\langle\Big|\frac{1}{2}\left\{\int \mathrm{d}[q_1]\frac{\mathbf{T}_i\cdot\mathbf{T}_k p_i\cdot p_k}{p_i\cdot q_1\ p_k\cdot q_1},\int \mathrm{d}[q_2]\frac{\mathbf{T}_i\cdot\mathbf{T}_k p_j\cdot p_k}{p_j\cdot q_2\ p_k\cdot q_2}\right\}\Big|\Big\rangle+ \\
&\quad\Big\langle\Big|\frac{[\mathbf{T}_i\cdot\mathbf{T}_k,\mathbf{T}_j\cdot\mathbf{T}_k]}{2}\Big|\Big\rangle\int \mathrm{d}[q_1]\mathrm{d}[q_2]\frac{p_i\cdot p_k\ p_j\cdot p_k}{p_i\cdot q_1\ p_j\cdot q_2\ p_k\cdot(q_1+q_2)}\left[\frac{1}{p_k\cdot q_1}-\frac{1}{p_k\cdot q_2}\right]\ .
\end{aligned}\tag{4.14}$$

The right-hand side follows from expressing the product of colour charges associated with parton k as the sum of its symmetric and its anti-symmetric part and then using the identity (E.4) over the symmetric part to combine its propagators.

The term on the second line of (4.14) is just the product of (uncorrelated) single real exchanges. The colour part of the third line is the same as in (4.11) and therefore the contribution of this expression is also exactly cancelled by its hermitian conjugate part even before integration. However, it is again worth remarking that the inclusive integration of the the third line vanishes, as it changes sign under the transformation in Eq. (4.12). Hence, we have shown that the contributions in $\mathbf{K}^2_{\text{s.o.3.4}}$ that involve three partons either vanish or can be expressed as the product of two uncorrelated single-gluon exchanges.

We shall now consider the contributions in $\mathbf{K}^2_{\text{s.o.3.4}}$ that involve four-partons. These are obtained by the multiplication of two graphs with the second topology in Fig. 4.1 but involving four different partons. Because they involve four different colour charges they can be expressed exactly as the product of two single-gluon exchanges. Thus, we have shown that the contributions involving three or four hard partons perfectly factorises into a product of single-gluon exchanges, i.e.

$$\int\frac{\mathrm{d}[q_1]\mathrm{d}[q_2]}{2}\Big\langle n^{(0)}\Big|\mathbf{K}^2_{\text{s.o.3.4}}\Big|n^{(0)}\Big\rangle=2\Big\langle n^{(0)}\Big|\left[\left(\sum_{i<j}^{n}\widetilde{\mathbf{I}}^{ij}(\epsilon)\right)^2-\sum_{i<j}^{n}\left(\widetilde{\mathbf{I}}^{ij}(\epsilon)\right)^2\right]\Big|n^{(0)}\Big\rangle\ .\tag{4.15}$$

where $\widetilde{\mathbf{I}}^{ij}$ is the operator corresponding to inclusive integration of an eikonal exchange between $\{i,j\}$:

$$\widetilde{\mathbf{I}}^{ij}(\epsilon)\equiv g_s\mu^{2\epsilon}\mathbf{T}_i\cdot\mathbf{T}_j\int \mathrm{d}[q]\frac{p_i\cdot p_j}{p_i\cdot q\ p\cdot q}=\mathbf{T}_i\cdot\mathbf{T}_j\frac{\alpha_s c_\epsilon}{2\pi}\frac{1}{\epsilon^2}\left[\frac{2p_i\cdot p_j}{\mu^2}\right]^{-\epsilon}\ .\tag{4.16}$$

The change of variables in Eq. (4.12) was also used in [94] to show that these same conclusions hold for the two-loop corrections involving three or four hard partons, i.e. the same conclusions that we obtained for the graphs in the first row Fig. 4.2 hold for the graphs in the second row of this same figure.

4.1.3 Subleading terms involving one or two partons $\mathbf{K}^2_{\mathbf{sub}}$

We shall now complete our calculation of the double emission matrix elements by considering the contributions in $\mathbf{K}^2_{\rm sub}$. These contribution are subleading with respect to $\mathbf{K}^2_{\rm s.o.2}$ and $\mathbf{K}^2_{\rm s.o.3.4}$ in the strongly ordered regime. More precisely, when one of the gluon momenta is re-scaled as $q_i \to \lambda q_i$, the dominant term in the small λ expansion behaves as λ^{-1}. Their exact expression is given by

$$\begin{aligned}
\mathbf{K}^2_{\rm sub} &\equiv \sum_{i<j} \mathbf{K}^2_{\rm sub}(i,j) \ , \\
\mathbf{K}^2_{\rm sub}(i,j) &= \frac{C_A \mathbf{T}_i\cdot\mathbf{T}_j}{2}\left[8(2-d)\left[\frac{p_i\cdot q_2\ p_j\cdot q_1 - p_i\cdot q_1\ p_j\cdot q_2}{(2q_1\cdot q_2)\ p_i\cdot(q_1+q_2)\ p_j\cdot(q_1+q_2)}\right]^2\right. \\
&\qquad \left. + \frac{16 p_i\cdot p_j}{q_1\cdot q_2\ p_i\cdot(q_1+q_2)\ p_j\cdot(q_1+q_2)}\right] .
\end{aligned} \tag{4.17}$$

The emission of a soft fermion by a hard parton is subleading with respect to soft gluon emission, this is the reason why we did not include them in Section 2.1. Nevertheless, the emission of a $\{q\bar{q}\}$ soft pair via a gluon is of the same order as the matrix elements in $\mathbf{K}^2_{\rm sub}$. To see this, we note that their total expression can be written as the sum of terms involving two hard partons:

$$\begin{aligned}
\mathbf{K}^2_{\rm fer} &\equiv \sum_{i<j} \mathbf{K}^2_{\rm fer}(i,j) \ , \\
\mathbf{K}^2_{\rm fer}(i,j) &= \mathbf{T}_i\cdot\mathbf{T}_j \mathrm{n}_f \mathrm{T_F}\left[\left[\frac{p_i\cdot q_2\ p_j\cdot q_1 - p_i\cdot q_1\ p_j\cdot q_2}{(2q_1\cdot q_2)\ p_i\cdot(q_1+q_2)\ p_j\cdot(q_1+q_2)}\right]^2\right. \\
&\qquad \left. - \frac{2 p_i\cdot p_j}{q_1\cdot q_2\ p_i\cdot(q_1+q_2)\ p_j\cdot(q_1+q_2)}\right] .
\end{aligned} \tag{4.18}$$

Then, by comparing this with Eq. (4.17) we see that they involve the same integrals with different pre-factors. To understand the physics of these contributions we will now integrate inclusively over one of the two emissions. After tensorial decompositions, the integration can be reduced to the integral in Eq. (F.30) of Appendix F, and yields

$$\begin{aligned}
&\int \frac{\mathrm{d}[q_1]\mathrm{d}[q_2]}{2!}\mathbf{K}^2_{\rm sub}(ij) + \int \mathrm{d}[q_1]\mathrm{d}[q_2]\mathbf{K}^2_{\rm fer}(ij) \\
&= \left[\frac{2}{-\epsilon}\gamma_g\frac{\alpha_s}{2\pi}\right]\int \mathrm{d}[q_1]\frac{\mathbf{T}_i\cdot\mathbf{T}_j p_i\cdot p_j}{p_i\cdot q_1\ p_j\cdot q_1}\left[\frac{q^2_{1T(ij)}}{\mu^2}\right]^{-\epsilon} f(\epsilon) \ ,
\end{aligned} \tag{4.19}$$

here $f(\epsilon)$ denotes a constant such that $f(\epsilon) = 1 + \mathcal{O}(\epsilon)$ and we recall that $\beta_0 = \gamma_g = \frac{11}{6}C_A - \frac{2}{3}n_f \mathrm{T_F}$ is the coefficient that accompanies the single $1/\epsilon$ hard pole in the one loop insertion operator, see Eqs. (2.39) and (2.40). This pole corresponds to the

branching of a gluon into a pair of gluons or into a $\{q,\bar{q}\}$ pair. Indeed, one can track the origin of this pole back to the region of integration where q_2 becomes collinear with q_1. Observe that the remaining integral over q_1 corresponds to a single emission but with an extra enhancement factor whose argument is the transverse momentum $q_{1T(ij)}$. Finally, the integral over q_1 yields

$$\begin{aligned}
&\left\langle\right| \left[\int \frac{\mathrm{d}[q_1]\mathrm{d}[q_2]}{2!}\mathbf{K}^2_{\mathrm{sub}}(ij) + \int \mathrm{d}[q_1]\mathrm{d}[q_2]\mathbf{K}^2_{\mathrm{fer}}(ij)\right] \left|\right\rangle \\
&= \frac{\alpha_s c_\epsilon}{2\pi(-\epsilon)}\left\langle\right|\widetilde{\mathbf{I}}^{ij}(2\epsilon)\left|\right\rangle \left[\left[\frac{11-7\epsilon}{3-2\epsilon}\right] C_A - \left[\frac{4-4\epsilon}{3-2\epsilon}\right] n_f \mathrm{T_F}\right] \frac{\Gamma^2[1+\epsilon]\Gamma[1-2\epsilon]}{(1+2\epsilon)} \\
&= \frac{\alpha_s}{2\pi} 2\left[\frac{\gamma_g}{-\epsilon} + \left[\frac{65}{18}C_A - \frac{14}{9}n_f \mathrm{T_F}\right] + \mathcal{O}(\epsilon^1)\right]\left\langle\right|\widetilde{\mathbf{I}}^{ij}(2\epsilon)\left|\right\rangle ,
\end{aligned} \tag{4.20}$$

Note that the highest infrared pole in this expression goes as $1/\epsilon^3$ which is subleading with respect to the $1/\epsilon^4$ poles that appear in the calculation of the terms which are leading in the strongly ordered regime. The above expression shows that, up to the collinear pole γ_g/ϵ, the contribution of $\mathbf{K}^2_{\mathrm{fer}}(ij)$ to the inclusive cross-section resembles a single gluon exchange between $\{i,j\}$, but because this in fact represents two collinear partons, the argument of $\widetilde{\mathbf{I}}^{ij}(2\epsilon)$ appears doubled. We have now completed the inclusive integration of the double emission matrix elements.

4.2 Real-virtual contributions

We shall now consider the inclusive integration of the one-loop, one-emission matrix elements of the previous chapter:

$$\int \mathrm{d}[q]\left[\left\langle n^{(0)}_{+1}\middle| n^{(1)}_{+1}\right\rangle + \mathrm{h.c.}\right] = -\int \mathrm{d}[q]\left\langle n^{(0)}\right| \left[\mathbf{J}^2_{n+1}\mathbf{I}^{(1)}_n + \mathbf{J}_{n+1}\cdot\mathbf{J}^{(1)}_{n+1} + \mathrm{h.c.}\right]\left|n^{(0)}\right\rangle . \tag{4.21}$$

This is first order at which, in general, Coulomb gluons interaction can have a non-zero contribution. Let us consider first the contributions from the one-loop soft-gluon current $\mathbf{J}^{(1)}_{n+1}$. This can be written as a sum over terms that depend on two hard partons,

$$\begin{aligned}
\mathbf{J}^{(1)}_{n+1} &\equiv \sum_{i<j}^{n} \mathbf{J}^{(1)}_{ij} , \\
\mathbf{J}^{(1)}_{ij} &\equiv \frac{\alpha_s g_s \mu^\epsilon}{2\pi}\frac{c_\Gamma}{\epsilon^2}\mathbf{T}^b_j i f^{bca}\mathbf{T}^a_i \left[\frac{p_j\cdot\varepsilon}{p_j\cdot q} - \frac{p_i\cdot\varepsilon}{p_i\cdot q}\right]\left(\frac{q^2_{Tij}}{\mu^2}\frac{e^{-\widetilde{\delta}_{iq}i\pi}e^{-\widetilde{\delta}_{jq}i\pi}}{e^{-\widetilde{\delta}_{ij}i\pi}}\right)^{-\epsilon} .
\end{aligned} \tag{4.22}$$

Again, it is convenient to consider the contributions that involve only two hard partons and three hard partons separately. The part involving two hard partons

sums up to

$$\sum_{i<j}^{n}\Big\langle\Big|\left[-\left(\frac{\mathbf{T}_i^c p_{i\mu}}{p_i\cdot q}+\frac{\mathbf{T}_j^c p_{j\mu}}{p_j\cdot q}\right)\cdot\mathbf{J}_{ij}^{(1)c\mu}+\text{h.c.}\right]\Big|\Big\rangle\,. \tag{4.23}$$

Using the colour algebra, each term inside brackets can be written as

$$\begin{aligned}
&-\left\langle\right|\left[\frac{\mathbf{T}_i^c p_i^\mu}{p_i\cdot q}+\frac{\mathbf{T}_j^c p_j^\mu}{p_j\cdot q}\right]\mathbf{J}_{ij,\mu}^{(1),c}\left|\right\rangle+\text{h.c}\\
&=\left\langle\right|\left[\frac{\alpha_s g_s\mu^\epsilon}{2\pi}\frac{c_\Gamma}{\epsilon^2}\frac{C_A}{2}\mathbf{T}_i\cdot\mathbf{T}_j\frac{2p_i\cdot p_j}{p_i\cdot q\;p\cdot q}\left(\frac{q_{Tij}^2}{\mu^2}\frac{e^{-\widetilde{\delta}_{iq}i\pi}e^{-\widetilde{\delta}_{jq}i\pi}}{e^{-\widetilde{\delta}_{ij}i\pi}}\right)^{-\epsilon}\right]\left|\right\rangle+\text{h.c.}
\end{aligned} \tag{4.24}$$

Observe that the colour part of these contributions is hermitian. Hence, even before the integration, the contribution from the Coulomb gluons exactly cancels when the hermitian conjugate expression is added. Hence, contributions involving only two hard partons are only due to eikonal gluons. They can be integrated using (F.29), and give

$$\begin{aligned}
&-g_s\mu^{2\epsilon}\int d[q]\left(\frac{\mathbf{T}_i^c p_i^\mu}{p_i\cdot q}+\frac{\mathbf{T}_j^c p_j^\mu}{p_j\cdot q}\right)\mathbf{J}_{ij,\mu}^{(1),c}+\text{h.c.}\,,\\
&=\frac{C_A}{2}\mathbf{T}_i\cdot\mathbf{T}_j\frac{\Gamma^2[1+\epsilon]\Gamma^4[1-\epsilon]}{\Gamma[1-2\epsilon]}\left[\frac{\alpha_s c_\epsilon}{2\pi}\frac{(2p_i\cdot p_j)^{-\epsilon}}{\epsilon^2}\right]^2\,,\\
&=\frac{C_A}{2}\mathbf{T}_i\cdot\mathbf{T}_j\left[\frac{\alpha_s c_\epsilon}{2\pi}\frac{1}{\epsilon^2}\left(\frac{p_i\cdot p_j}{\mu^2}\right)^{-\epsilon}\right]^2+\frac{\alpha_s}{2\pi}C_A\left[-\frac{2\pi^2}{3}+\mathcal{O}(\epsilon)\right]\widetilde{\mathbf{I}}^{ij}(2\epsilon)\,,
\end{aligned} \tag{4.25}$$

where $\widetilde{\mathbf{I}}^{ij}$ is given in Eq. (4.16).

We shall now consider the contributions involving three hard partons. They amount to

$$\begin{aligned}
&-\left\langle\right|\sum_{i<j}^{n}\sum_{k\neq\{i,j\}}^{n}\frac{\mathbf{T}_k^c p_k^\mu\mathbf{J}_{ij,\mu}^{(1),c}}{p_k\cdot q}\left|\right\rangle+\text{h.c.}=\sum_{i<j}^{n}\sum_{k\neq\{i,j\}}^{n}\langle|\left[\mathbf{T}_j\cdot\mathbf{T}_k,\mathbf{T}_i\cdot\mathbf{T}_k\right]|\rangle\times\\
&\left[\frac{p_k\cdot p_j}{p_k\cdot q p_j\cdot q}-\frac{p_k\cdot p_i}{p_k\cdot q p_i\cdot q}\right]\left[\frac{q_{T(ij)}^2}{\mu^2}\frac{e^{-\widetilde{\delta}_{iq}i\pi}e^{-\widetilde{\delta}_{jq}i\pi}}{e^{-\widetilde{\delta}_{ij}i\pi}}\right]^{-\epsilon}\frac{\alpha_s g_s\mu^\epsilon}{2\pi}\frac{c_\Gamma}{\epsilon^2}+\text{h.c.}
\end{aligned} \tag{4.26}$$

When the hard process contains only three hard partons, $\{i,j,k\}$, one can use colour conservation to write $\mathbf{T}_k=-\mathbf{T}_i-\mathbf{T}_j$ and the colour part of this expression vanishes because $(\mathbf{T}_i^c+\mathbf{T}_j^c)\mathbf{T}_j^b if^{bca}\mathbf{T}_i^a=0$. More generally, when there are at least four hard partons this expression no longer vanishes. In this case, the colour part of each term in Eq. (4.26) is anti-hermitian. Hence, the situation is now reversed; the real (or eikonal) part of the loop integral vanishes when one adds its hermitian conjugate counterpart whereas the Coulomb gluon contribution doubles when the hermitian

conjugate is added. Hence, the above expression reduces to

$$\begin{aligned}
&-\left\langle\Big|\sum_{i<j}^{n}\sum_{k\neq\{i,j\}}^{n}\frac{\mathbf{T}_k p_k^\mu\cdot\mathbf{J}^{(1)}_{ij,\mu}}{p_k\cdot q}\Big|\right\rangle+\text{h.c.}=\\
&\sum_{i<j}^{n}\sum_{k\neq\{i,j\}}^{n}\left\langle\Big|[\mathbf{T}_j\cdot\mathbf{T}_k,\mathbf{T}_i\cdot\mathbf{T}_k]\Big|\right\rangle\left[\frac{p_k\cdot p_j}{p_k\cdot q p_j\cdot q}-\frac{p_k\cdot p_i}{p_k\cdot q p_i\cdot q}\right]\times\\
&2i(\widetilde{\delta}_{iq}+\widetilde{\delta}_{jq}-\widetilde{\delta}_{ij})\sin(\pi\epsilon)\frac{\alpha_s g_s\mu^\epsilon}{2\pi}\frac{c_\Gamma}{\epsilon^2}\left[\frac{q^2_{T(ij)}}{\mu^2}\right]^{-\epsilon}.
\end{aligned}\tag{4.27}$$

For pure QCD processes, the contribution of this operator to the cross-section identically cancels for the same reason that Eq. (2.53) does. However, for more general processes, it can contribute to observables, but it gives a vanishing contribution to the total cross-section. To see this, we note that the integrals involving three partons are all of the form

$$\int \mathrm{d}^d q\,\delta^+(q)\left(\frac{p_k\cdot p_j}{p_k\cdot q p_j\cdot q}-\frac{p_k\cdot p_i}{p_k\cdot q p_i\cdot q}\right)g(q_{T(ij)}).\tag{4.28}$$

By expressing q in light-cone coordinates, one can check that the following change of variables

$$(q^-,q^+)\to\left(\frac{p_k^-}{p_k^+}q^+,\frac{p_k^+}{p_k^-}q^-\right),\tag{4.29}$$

has unit Jacobian. Additionally, it leaves the kinematical variable, $q_{\perp,ik}$, and the on-shell conditions, $\delta^+(q)$, invariant but it changes the sign of the term inside parenthesis in Eq. (4.28). Therefore, integrals of the form of Eq. (4.28) vanish if they are integrated over a domain which is invariant under the transformation in Eq. (4.29). Finally, we can now write the contribution to the total cross-section as:

$$\begin{aligned}
&-\left\langle\Big|\int\mathrm{d}[q]\mathbf{J}_{n+1}\cdot\mathbf{J}^{(1)}_{n+1}\Big|\right\rangle+\text{h.c.}=\\
&\sum_{i<j}^{n}\left\langle\Big|\left[\frac{C_A}{2}\mathbf{T}_i\cdot\mathbf{T}_j\left[\frac{\alpha_s c_\epsilon}{2\pi}\frac{(p_i\cdot p_j)^{-\epsilon}}{\epsilon^2}\right]^2+\frac{\alpha}{2\pi}C_A\left[-\frac{2\pi^2}{3}+\mathcal{O}(\epsilon)\right]\widetilde{\mathbf{I}}^{ij}(2\epsilon)\right]\Big|\right\rangle.
\end{aligned}\tag{4.30}$$

We shall now study the remaining part of the one-loop, one-emission amplitude that contributes at this order (see Eq. (4.21)):

$$-\left\langle n^{(0)}\Big|\mathbf{J}^2_{n+1}\mathbf{I}^{(1)}_n\Big|n^{(0)}\right\rangle+\text{h.c.}\tag{4.31}$$

It is straightforward to show that the contributions containing the eikonal part of

the virtual radiation are just the product of single real exchanges, i.e.

$$-\Big\langle\Big|\int \mathrm{d}[q]\mathbf{J}^2_{n+1}(q)\int d[k]\frac{\mathbf{J}^2_{n+1}(k)}{2}\Big|\Big\rangle + \text{h.c.} = -4\Big\langle\Big|\left[\sum_{i<j}^{n}\widetilde{\mathbf{I}}^{ij}(\epsilon)\right]^2\Big|\Big\rangle\,. \tag{4.32}$$

Next we consider the Coulomb gluons in Eq. (4.31). Once again, it is convenient to discuss the terms that depend on two, three and four hard partons separately. As we will see, none of them contribute to the total cross-section, but terms involving three partons contribute to non-inclusive observables.

Terms involving two and four hard partons exactly cancel before integration, as their hermitian conjugates are equal and opposite. On the other hand, the terms involving three hard partons add up to

$$\begin{aligned}\Big\langle\Big|\left[-\sum_{\substack{i<j\\k\neq\{i,j\}}}^{n}2\left[\frac{\mathbf{T}_i\cdot\mathbf{T}_k p_i\cdot p_k}{p_i\cdot q\; p\cdot q}+\frac{\mathbf{T}_j\cdot\mathbf{T}_k p_j\cdot p_k}{p_j\cdot q\; p\cdot q}\right]\widetilde{\delta}_{ij}\mathbf{C}^{ij}(0,2p_i\cdot p_j)+\text{h.c.}\right]\Big|\Big\rangle =\\ -\sum_{\substack{i<j\\k\neq\{i,j\}}}^{n}2\Big\langle\Big|[\mathbf{T}_j\cdot\mathbf{T}_k,\mathbf{T}_i\cdot\mathbf{T}_k]\Big|\Big\rangle\left[\frac{p_j\cdot p_k}{p_j\cdot q\; p\cdot q}-\frac{p_i\cdot p_j}{p_i\cdot q\; p\cdot q}\right]\widetilde{\delta}_{ij}\frac{i\pi\alpha_s c_\epsilon}{-\epsilon}\left[\frac{2p_i\cdot p_j}{\mu^2}\right]^{-\epsilon}\,.\end{aligned} \tag{4.33}$$

The right-hand side of this expression is obtained by combining each term in the sum with its hermitian conjugate. Indeed, each term in the sum is of the same form as (4.28) and hence the change of variables in Eq. (4.29) shows that their inclusive contribution cancels.

To summarise, if we neglect recoil effects, the contributions of this matrix element to the total cross section yield:

$$\begin{aligned}\int \mathrm{d}[q]\left[\Big\langle n^{(0)}_{+1}\Big|n^{(1)}_{+1}\Big\rangle+\text{h.c.}\right] = -4\Big\langle\Big|\left[\sum_{i<j}^{n}\widetilde{\mathbf{I}}^{ij}(\epsilon)\right]^2\Big|\Big\rangle+\\ \sum_{i<j}^{n}\Big\langle\Big|\left[\frac{C_A}{2}\mathbf{T}_i\cdot\mathbf{T}_j\left[\frac{\alpha_s c_\epsilon}{2\pi}\frac{(p_i\cdot p_j)^{-\epsilon}}{\epsilon^2}\right]^2+\frac{\alpha}{2\pi}C_A\left[-\frac{2\pi^2}{3}+\mathcal{O}(\epsilon)\right]\widetilde{\mathbf{I}}^{ij}(2\epsilon)\right]\Big|\Big\rangle\,.\end{aligned} \tag{4.34}$$

Remarkably, there are no terms that correlate three or four hard partons.

4.3 Purely virtual contributions

In the previous sections we have calculated all of the contributions to the total cross-section except the purely virtual contributions:

$$\Big\langle n^{(1)}\Big|n^{(1)}\Big\rangle+\Big\langle n^{(0)}\Big|n^{(2)}\Big\rangle+\Big\langle n^{(2)}\Big|n^{(0)}\Big\rangle\,, \tag{4.35}$$

which we shall now discuss. As they have a similar structure to one-loop, one-emission corrections in (4.31), we shall consider first the contribution from the one-loop matrix element squared:

$$\left\langle n^{(1)}\middle|n^{(1)}\right\rangle = \left\langle n^{(0)}\middle|\mathbf{I}_n^{(1)\,\dagger}\mathbf{I}_n^{(1)}\middle|n^{(0)}\right\rangle . \tag{4.36}$$

The product of the two one-loop insertion operators has almost the same structure as the one loop corrections in Eq. (4.31). Using exactly the same decompositions as we did for those contributions, their total expression can be written as

$$\begin{aligned}\mathbf{I}_n^{(1)\,\dagger}\mathbf{I}_n^{(1)} = &\left[\sum_{i<j}\widetilde{\mathbf{I}}^{ij}(\epsilon)\right]^2 - \left[\sum_{i<j}\widetilde{\delta}_{ij}\mathbf{C}^{ij}(0,2p_i\cdot p_j)\right]^2 + \\ &\sum_{\substack{i<j\\k\neq\{i,j\}}}^{n}[\mathbf{T}_j\cdot\mathbf{T}_k,\mathbf{T}_i\cdot\mathbf{T}_k]\int d[k]\left[\frac{p_j\cdot p_k}{p_j\cdot k p_k\cdot k}-\frac{p_i\cdot p_j}{p_i\cdot k p_k\cdot k}\right]\widetilde{\delta}_{ij}\frac{i\pi\alpha_s c_\epsilon}{-\epsilon}\left[\frac{2p_i\cdot p_j}{\mu^2}\right]^{-\epsilon} .\end{aligned} \tag{4.37}$$

In the second line, we have contributions that arise from combining the contributions with one eikonal and one Coulomb gluon. They have exactly the same structure as Eq. (4.28); thus they integrate to zero. Finally, as we will see, the Coulomb gluons in the second line are exactly cancelled by pure two-loop virtual contributions.

4.3.1 Two-loop contributions

Anticipating the exponentiation of the soft (purely) virtual corrections, see Eq. (2.70), the two-loop matrix elements can be expressed as

$$\left|n^{(2)}\right\rangle = \left(\frac{[\mathbf{I}_n^{(1)}(\epsilon)]^2}{2!}+\mathbf{I}_n^{(2)}(\epsilon)\right)\left|n^{(0)}\right\rangle, \tag{4.38}$$

where $\mathbf{I}_n^{(2)}(\epsilon)$ is an operator of order α_s^2 that gives the first correction to the exponentiation of the one loop corrections.

We shall now use the Bloch-Nordsieck theorem to deduce the explicit expression of this operator. According to this theorem, the sum over the soft corrections should exactly cancel, i.e.

$$\begin{aligned}&\left\langle n^{(0)}\middle|n^{(2)}\right\rangle + \left\langle n^{(2)}\middle|n^{(0)}\right\rangle = -\int \mathrm{d}[q]\left[\left\langle n_1^{(0)}\middle|n_1^{(1)}\right\rangle + \left\langle n_1^{(1)}\middle|n_1^{(0)}\right\rangle\right]\\ &-\left\langle n^{(1)}\middle|n^{(1)}\right\rangle - \int \mathrm{d}[q_1]\mathrm{d}[q_2]\left[\frac{1}{2}\left\langle n_{+2}^{(0)}\middle|n_{+2}^{(0)}\right\rangle + \left\langle n_{\text{pair }q\bar{q}}^{(0)}\middle|n_{\text{pair }q\bar{q}}^{(0)}\right\rangle\right]\\ &=\left[\sum_{i<j}^{n}\widetilde{\mathbf{I}}^{ij}(\epsilon)\right]^2 + \left[\sum_{i<j}^{n}\mathbf{C}^{ij}_{(0,2p_ip_j)}\right]^2 + 2\frac{\alpha_s}{2\pi}\left[\frac{\gamma_g}{\epsilon}+\widetilde{K}+\mathcal{O}(\epsilon)\right]\left[\sum_{i<j}^{n}\widetilde{\mathbf{I}}^{ij}(2\epsilon)\right]\end{aligned} \tag{4.39}$$

where we used the definition $\widetilde{K} = \left[-\frac{65}{18} + \frac{4\pi^2}{3}\right] C_A + \frac{14}{9} n_f \mathrm{T_F}$. To obtain the latter identity we introduced the integrated expressions from the previous sections, i.e. Eq. (4.10), (4.15), (4.20), (4.30) and (4.37). By inserting this expression into Eq. (4.38) we can solve $\mathbf{I}_n^{(2)}(\epsilon)$, this yields

$$\left\langle n^{(0)} \right| \left[\mathbf{I}_n^{(2)} + \mathbf{I}_n^{(2)\dagger}\right] \left| n^{(0)} \right\rangle = \frac{\alpha_s}{2\pi} \left[\frac{\gamma_g}{\epsilon} + \widetilde{K} + \mathcal{O}(\epsilon)\right] \mathbf{I}_n^{(1)}(2\epsilon) + \text{h.c.} \tag{4.40}$$

It is interesting to compare this expression with the singular behaviour of the two-loop corrections to a general process $\mathcal{N}$. According to this (see Eqs. (2.51))

$$\begin{aligned}
&\langle \mathcal{N}^{(0)} | \mathcal{N}^{(2)} \rangle + \langle \mathcal{N}^{(2)} | \mathcal{N}^{(0)} \rangle - \left\langle \mathcal{N}^{(0)} \right| \left[\frac{1}{2!} \left[\mathbf{I}_{\mathcal{N}}^{(1)}(\epsilon)\right]^2 + \text{h.c.}\right] \left| \mathcal{N}^{(0)} \right\rangle \\
&= \left\langle \mathcal{N}^{(0)} \right| \frac{\alpha_s}{2\pi} \frac{\gamma_g}{\epsilon} \left[\mathbf{I}_{\mathcal{N}}^{(1)}(2\epsilon) - \mathbf{I}_{\mathcal{N}}^{(1)}(\epsilon)\right] \left| \mathcal{N}^{(0)} \right\rangle \\
&+ \left\langle \mathcal{N}^{(0)} \right| \left[\frac{\alpha_s}{2\pi} K\, \mathbf{I}_{\mathcal{N}}^{(1)}(2\epsilon) + \left(\frac{\alpha_s}{2\pi}\right)^2 \sum_{i=1}^{n} \frac{1}{\epsilon} H_i\right] \left| \mathcal{N}^{(0)} \right\rangle \\
&+ \left\langle \mathcal{N}^{(0)} \right| \mathbf{I}_n^{(1)}(\epsilon) \left| \mathcal{N}^{(1)} \right\rangle_{\text{fin}} + \text{h.c.} + \mathrm{O}(\epsilon^0),
\end{aligned} \tag{4.41}$$

where

$$K = \left[\frac{67}{18} - \frac{\pi^2}{6}\right] C_A - \frac{10}{9} \mathrm{T_F} n_f, \tag{4.42}$$

and H_i denote flavour dependent coefficients and we used $\gamma_g = \beta_0$. The comparison between our calculation in the eikonal approximation (4.40) and the exact expression (4.41) shows that, in both cases, the poles of order $1/\epsilon^4, 1/\epsilon^3, 1/\epsilon^2$ are controlled by constant coefficients and the one-loop insertion operator. However, Catani's formula, Eq. (4.41), has two terms proportional to γ_g (see second line in Eq. (4.41)). Within our approximation we only recover the first. Nevertheless, we remind the reader that there is a contribution to the one emission amplitude $\left|n_{+1}^{(1)}\right\rangle$ that still has not been included into our calculation, see Eq. (3.29) and the last paragraph of that Section 3.3. Its contribution to the cross-section is equal to

$$-\int d[q] \left\langle n^{(0)} \right| \mathbf{J}_{n+1}^2 \left| n^{(0)} \right\rangle \widetilde{K}_{uv} + \text{h.c.} = -\left\langle n^{(0)} \right| \mathbf{I}_n^{(1)}(\epsilon) \left| n^{(0)} \right\rangle \widetilde{K}_{uv} + \text{h.c.}\ . \tag{4.43}$$

The coefficient $\widetilde{K}_{uv} = \widetilde{K}_{uv}(\epsilon)$ has a single collinear and single uv pole and we expect it accounts for the missing contribution. To close this section, we recall that in this chapter we neglected the recoil effect against gluon emissions, i.e. global

momentum conservation[2]. By including the recoil effects one shall get the correct[3] K factor in Eq. (4.42). We leave this improvement as a pending task that might be relevant to incorporate the effects of the running coupling; it is well known that in the resummation of a wide class of observables at next-to-leading logarithmic (NLL) accuracy, terms proportional to K can be absorbed into the running coupling [40] in the so-called CMW scheme [95, 96].

4.3.2 On the role of Coulomb gluons

We close this section summarising the role of the Coulomb gluon from the one-loop, one-emission amplitude to the cross-section[4]. Terms that involve two hard partons exactly cancel with their hermitian conjugate. Thus, only terms that correlate three hard partons, say $\{i, j, k\}$, can contribute and, up to irrelevant factors, these (Eqs.(4.27) and (4.33)) have the following structure:

$$\left\langle n^{(0)}\right| \frac{\mathbf{T}_k^c p_k^\mu}{p_k\cdot q} \times (-i\pi)\mathbf{T}_j^b i f^{bca}\mathbf{T}_i \left[\frac{p_{j\mu}}{p_j\cdot q} - \frac{p_{i\mu}}{p_i\cdot q}\right] g(q_{T(ij)}) \left|n^{(0)}\right\rangle \,. \tag{4.44}$$

where $g = g(q_{T(ij)})$ is a function of $q_{T(ij)}$ only. When there are no more hard partons than $\{i, j, k\}$ in the hard subprocess this operator identically vanishes. When there is at least one more hard parton in the scattering, the operator enclosed between the hard subprocess amplitude ($\left|n^{(0)}\right\rangle$) is strictly speaking non-vanishing. However, its contribution to a pure QCD process vanishes for the same reason Eq. (2.53) does[5]. For a more general observable, these Coulomb gluons can actually contribute but they give a vanishing contribution to the total cross-section. This cancellation occurs more generally when the domain of integration is invariant under the transformation in (4.29). Since, we are dealing with wide-angle scatterings, we can assume that $p_k^+/p_k^- = \mathcal{O}(1)$, then this change of variables is nothing but the symmetry along the directions defined by p_i and p_j, invariance under $(q^+ \leftrightarrow q^-)$. We think this is an

[2]Because of this, gluon emissions are integrated over their complete mass-shell (emissions can have arbitrarily large energy) and one needs to regularise the resulting *uv* divergences. One can show that different *uv* regularisation procedures changes the coefficients at order $1/\epsilon^{-2}$. To see this it is sufficient to choose different cut-off scales in the integrals of Appendix F.5. Then, to reproduce the correct K constant one should perform the phase-space integrals of Appendix F.5 without neglecting global momentum conservation as in Section 2.21 of [40]. The *uv* regularisation procedure used throughout this chapter is discussed in Section F.5. Although unrelated to this chapter, it is worth pointing out that the conclusions of chapters 3, 5 and 6 are equivalent for different *uv* regularisation procedures, this is explained in detail in Section 6.2.

[3]In accordance with the calculation of the two-loop matrix elements within the eikonal approximation [94]. In this reference the authors also show that the two-loop soft anomalous dimension can be written as the product of the one-loop anomalous dimension and the K constant.

[4]The Coulomb gluons from the one-loop purely virtual contributions, Eq. (4.37), exactly cancel with Coulomb gluons in the two-loop purely virtual contribution in Eq. (4.39).

[5]Succinctly, the trace over colour space that appears at cross-section level can be reduced to the trace of a symmetric matrix times an anti-symmetric matrix, which is identically zero.

interesting result, as the corrections at higher orders also exhibit the following dipole structure:

$$(-i\pi)\mathbf{T}_j^b if^{bca}\mathbf{T}_i^a \left[\frac{p_{j\mu}}{p_j\cdot q} - \frac{p_{i\mu}}{p_i\cdot q}\right] g(q_{T(ij)}) \ . \tag{4.45}$$

Perhaps this kind of symmetry is responsible for the cancellation of Coulomb gluons in the total cross-section at higher orders.

4.4 Summary

We have integrated the double real and the real-virtual soft corrections neglecting the recoil against gluon emissions. By exploiting the Bloch-Nordsieck theorem we deduced the expression for the pure two-loop virtual correction. The resulting operator is consistent with the exponentiation of virtual corrections in Eq. (4.38) and has the structure of Catani's two-loop infrared operator. The calculations in this chapter are sufficient to reveal some of the structure of the infrared cancellations for a general hard process. For instance, one can track down the contributions that cancel the exponentiation of the one loop corrections (first term in Eq. (4.38)).

In addition, we paid close attention to the contribution of Coulomb gluons at this order. It is worth pointing out that in the subsequent chapters, when we study the corrections due to one Coulomb gluon and two real emissions in chapters 5 and 6, we will find again emissions with a "dipole structure" whenever an emitted gluon subsequently exchanges a Coulomb gluon, see for instance Eq. (5.39). We expect that the change of variables that we studied in this chapter (Eq. (4.29)) will help to understand the infrared cancellation of terms involving dipole emissions more generally.

Chapter 5

One-loop, two-emission soft corrections

In Section 3.1 of Chapter 3, we studied the imaginary part of the one-loop, one-emission to a Drell-Yan hard process. After combining the different cut graphs that contribute at this order (see Fig. 3.1) we found that the amplitude can be expressed as[1]

$$\mathrm{Im}\left\{\left|2^{(1)}\right\rangle\right\} = \left[\mathbf{J}_{2+1}(q)\,\mathbf{C}^{ij}(q_T,Q) + \mathbf{C}^{ij}(0,q_T)\;\mathbf{J}_{2+1}(q)\right]\left|2^{(0)}\right\rangle\,. \tag{5.1}$$

In this chapter we will study the generalisation of this expression for the case of two-real gluon emissions. In this case, the transverse momentum ordering property of Eq. (5.1) is not an exact result anymore. Instead, it is a property of the amplitude in certain regions of the phase-space of the emitted gluons. We will discuss these regions in the next Section 5.1, after which we will proceed to study the behaviour of the amplitude at tree level in Section 5.2. This will provide the foundation for the calculation, which appears in sections 5.3–5.5, of the two-gluon emission amplitude with a Coulomb exchange. Finally, in Section 5.6 we study one more (subleading) kinematical region which can be also understood in terms of Coulomb gluon exchanges.

5.1 Phase-space limits

In the first part of this chapter we will focus upon the following three limits. All of them correspond to a strong ordering in the transverse momenta of the real emissions, i.e. $q_{1T} \gg q_{2T}$. In terms of light-cone variables, the three limits are:

[1]Here and through all this chapter, to avoid cluttered notation, we will denote the transverse components of any vector l with respect to the incoming partons p_i, p_j simply as $l_{T(ij)} \equiv l_T$ and we will omit the strong coupling g_s. Also light-cone variables are always defined with respect to these vectors, i.e. $p_i = (p_i^+, 0, 0_T)$ and $p_j = (0, p_j^-, 0_T)$.

- Limit 1: Both emissions are at wide angle but one gluon is much softer than the other, i.e. $(q_1^{\pm} \sim q_{1T}) \gg (q_2^{\pm} \sim q_{2T})$. Specifically, we take $q_2 \to \lambda q_2$ and keep the leading term for small λ.

- Limit 2: One emission (q_2) collinear with p_i by virtue of its small transverse momentum and the other (q_1) at a wide angle, i.e. $q_2^+ \gg q_{2T}$ and $q_1^+ \sim q_{1T} \gg q_{2T}$. Specifically, we take $q_2 \to (q_2^+, \lambda^2 q_{2T}^2/(2q_2^+), \lambda \mathbf{q}_{2T})$ and keep the leading term for small λ.

- Limit 3: One emission (q_1) collinear with p_i by virtue of its high energy and the other (q_2) at a wide angle, i.e. $q_1^+ \gg q_{1T}$ and $q_{1T} \gg q_{2T} \sim q_2^+$. Specifically, we take[2] $q_1 \to (q_1^+/\lambda, \lambda q_{1T}^2/(2q_1^+), \mathbf{q}_{1T})$ and $q_2 \to \lambda q_2$, and keep the leading term for small λ.

When we consider the leading behaviour of the amplitude, either at tree or one-loop level, we will make an expansion for small λ, keeping only the leading terms. We work with the following choice of polarisation vectors for the emitted gluons:

$$\begin{aligned} \varepsilon^{\mu}(q,\perp) &= \frac{i\epsilon^{\mu\nu\alpha\beta} q_\nu p_{i\alpha} p_{j\beta}}{\sqrt{2p_i\cdot p_j\, p_i\cdot q\, p_j\cdot q}}\,, \\ \varepsilon^{\mu}(q,\parallel) &= \frac{q\cdot p_j\, p_i^\mu - q\cdot p_i\, p_j^\mu - p_i\cdot p_j\, q^\mu}{\sqrt{2p_i\cdot p_j\, p_i\cdot q\, p_j\cdot q}}\,. \end{aligned} \tag{5.2}$$

In limits 2 and 3, only $\varepsilon^-(q,\parallel)$ of the collinear gluon, gives rise to a leading contribution, see Appendix C for more details.

Limit 3 is of particular interest because it is the limit that gives rise to the super-leading logarithms[3] [31, 36]. It is worth noting that although $q_{1T} \gg q_{2T}$ in all three limits, we may have $q_1^+ \sim q_2^+$ in limit 2 and $q_1^- \sim q_2^-$ in limit 3. This means that limits 2 and 3 are not sub-limits of limit 1. We will see that different Feynman diagrams contribute differently in the different limits. It is therefore remarkable that the final result is identical in all three limits. Although we have not yet proven it, we suspect that the final results may well hold in the more general case in which only $q_{1T} \gg q_{2T}$.

[2]We use the eikonal approximation for the emitted gluons, in which the hard partons define light-like directions whose energies can be taken to be arbitrarily high. So even in the limit $\lambda \to 0$, we assume $q_1^+/\lambda \ll p_i^+$.

[3]Here we are thinking of gluon 2 as the central emission and gluon 1 as the out of the gap emission. It is worth mentioning that the super-leading logarithms found in GBJ [31, 36, 51] arise at one order higher in the perturbation expansion ($\mathrm{N^4LO}$). Their existence is based on the k_T-ordering property that is proven in this chapter. For completeness, we point out that these super-leading logarithms in GBJ have subleading colour factors. To be precise, they have subleading colour coefficients in the large N_c expansion with respect to terms that only involve eikonal gluons. Finally, it is worth mentioning that the results of [97] (see Eq. 15 of this reference) can be used to show that the Coulomb gluons contributions of the k_T colour evolution picture given by Eq. (2.73), only give rise to subleading colour contributions in this same sense.

5.2 Tree-level amplitude

The tree-level amplitude with two soft gluon emissions is given by

$$\left|2^{(0)}_{+2}\right\rangle = \mathbf{K}_{2+2}(q_1,q_2)\left|2^{(0)}\right\rangle \,. \tag{5.3}$$

where $\mathbf{K}_{2+2}(q_1,q_2$ is defined in Eq. (4.3). In the case of only two incoming hard partons $\{i,j\}$, the double emission tensor $\mathbf{K}_{2+2}$ receives contributions from the four graphs in Fig. 5.1 plus four further graphs corresponding to the interchange $i \leftrightarrow j$. As we will now show, $\mathbf{K}_{2+2}$ simplifies in each of the limits 1–3 to a product of two single emission operators.

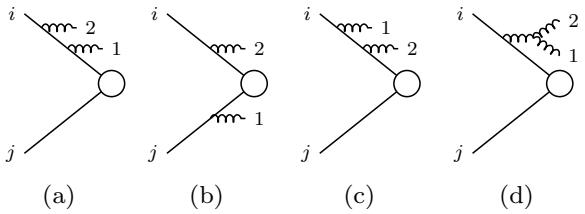

Figure 5.1: The case of two real emissions. There are four more graphs obtained by swapping $(i \leftrightarrow j)$.

Let us consider first the leading behaviour in limit 1. In this region only graphs (a), (b) and (d) in Fig. 5.1 are leading. They give

$$\begin{aligned}\mathbf{K}^{c_1c_2}_{2+2}(q_1,q_2) = &\left[\frac{\mathbf{T}_i^{c_2}p_i\cdot\varepsilon_2}{p_i\cdot q_2}\frac{\mathbf{T}_i^{c_1}p_i\cdot\varepsilon_1}{p_i\cdot q_1}\right] + \left[\frac{\mathbf{T}_i^{c_2}p_i\cdot\varepsilon_2}{p_i\cdot q_2}\frac{\mathbf{T}_j^{c_1}p_j\cdot\varepsilon_1}{p_j\cdot q_1}\right] \\ &+ \left[\frac{if^{c_1c_2a}q_1\cdot\varepsilon_2}{q_1\cdot q_2}\frac{\mathbf{T}_i^{a}p_i\cdot\varepsilon_1}{p_i\cdot q_1} - \frac{if^{c_1c_2a}\mathbf{T}_i^{a}\varepsilon_1\cdot\varepsilon_2}{2q_1\cdot q_2}\right] + (i\leftrightarrow j)\,.\end{aligned} \tag{5.4}$$

The $\varepsilon_1\cdot\varepsilon_2$ term vanishes when it acts upon $\left|2^{(0)}\right\rangle$ due to colour conservation. The leading behaviour can thus be written

$$\left\langle c_1c_2\middle|n^{(0)}_2\right\rangle = \mathbf{J}^{c_2c_1a}_{2+2}(q_2)\mathbf{J}^{a}_{2+1}(q_1)\left|n^{(0)}\right\rangle\,, \tag{5.5a}$$

$$\mathbf{J}^{c_2c_1a_1}_{2+2}(q_2) \equiv \mathbf{J}^{c_2}_{2+1}(q_2)\delta^{c_1a_1} + \frac{if^{c_1c_2a_1}\,q_1\cdot\varepsilon_2}{q_1\cdot q_2}, \tag{5.5b}$$

where $\mathbf{J}^{c_2c_1a_1}_{2+2}(q_2)$ is the current operator that adds a second soft gluon (q_2) acting on $\left|2^{(0)}_{+1}\right\rangle = \mathbf{J}_{2+1}(q_1)\left|2^{(0)}\right\rangle$.

In limit 2 only the first two graphs in Fig. 5.1 are leading and they can be written

$$\left\langle c_1c_2\middle|2^{(0)}_{+2}\right\rangle = \left[\frac{\mathbf{T}_i^{c_2}p_i\cdot\varepsilon_2}{p_i\cdot q_2}\right]\mathbf{J}^{c_1}_1(q_1)\left|2^{(0)}\right\rangle\,. \tag{5.6}$$

This is exactly what is obtained by taking the collinear limit $q_2 \parallel p_i$ in the expression

for limit 1, Eq. (5.5a).

We now turn our attention to limit 3. The leading contributions are graphs (a), (c) and (d), and the $(i \leftrightarrow j)$ permutation of graph (b) in Fig. 5.1. These four contributions (in order) sum to

$$\begin{aligned}\mathbf{K}_{2+2}^{c_1,c_2}(q_1,q_2) = &\left[\frac{\mathbf{T}_i^{c_2}\varepsilon_2^-}{q_2^-}\frac{\mathbf{T}_i^{c_1}\varepsilon_1^-}{q_1^- + q_2^-}\right] + \left[\frac{\mathbf{T}_i^{c_1}\varepsilon_1^-}{q_1^-}\frac{\mathbf{T}_i^{c_2}\varepsilon_2^-}{q_1^- + q_2^-}\right] \\ &+ \left[\frac{if^{c_1c_2a}\,\varepsilon_2^-}{q_2^-}\frac{\mathbf{T}_i^a\varepsilon_1^-}{q_1^- + q_2^-}\right] + \left[\frac{\mathbf{T}_j^{c_2}\varepsilon_2^+}{q_2^+}\frac{\mathbf{T}_i^{c_1}\varepsilon_1^-}{q_1^-}\right] . \end{aligned} \tag{5.7}$$

At first glance it seems like an interpretation in terms of a product of single emission operators is not possible any more. However, using $\mathbf{T}_i^{c_1}\mathbf{T}_i^{c_2} = \mathbf{T}_i^{c_2}\mathbf{T}_i^{c_1} + if^{c_1c_2a}\mathbf{T}_i^a$, the contribution of graph (c) can be written

$$\frac{\mathbf{T}_i^{c_1}\varepsilon_1^-}{q_1^-}\frac{\mathbf{T}_i^{c_2}\varepsilon_2^-}{q_1^- + q_2^-} = \left[\frac{\mathbf{T}_i^{c_2}\varepsilon_2^-}{q_1^-}\frac{\mathbf{T}_i^{c_1}\varepsilon_1^-}{q_1^- + q_2^-}\right] + \left[\frac{if^{c_1c_2a}\varepsilon_2^-}{q_1^-}\frac{\mathbf{T}_i^a\varepsilon_1^-}{q_1^- + q_2^-}\right] . \tag{5.8}$$

The light cone variables make clear the fact that the two terms on the right-hand side have the same dependence on colour and spin as the first term on each line of Eq. (5.7). Their momentum dependence can be combined using the identity

$$\frac{1}{q_1^-}\frac{1}{q_1^- + q_2^-} + \frac{1}{q_2^-}\frac{1}{q_1^- + q_2^-} = \frac{1}{q_1^-}\frac{1}{q_2^-} , \tag{5.9}$$

to give

$$\left\langle c_1c_2\middle|2_{+2}^{(0)}\right\rangle = \mathbf{J}_{3+1}^{c_1c_2a}(q_2)\left(\frac{\mathbf{T}_i^a p_i\cdot\varepsilon_1}{p_i\cdot q_1}\right)\left|2^{(0)}\right\rangle . \tag{5.10}$$

As in the case of limit 2, this can be obtained by taking the collinear limit $q_1 \parallel p_i$ in Eq. (5.5a). Remarkably, we will have the same property at one-loop order, i.e. the leading expressions in limits 2 and 3 can be reached by taking the relevant collinear limit of the leading expression in limit 1. This is particularly non-trivial in limit 3, because the leading graphs are not a subset of those in limit 1.

Figure 5.2 shows how the graphs in Fig. 5.1 can be projected onto three spin and colour structures. These particular structures are special because the net projection onto each can be represented in terms of a product of two single emission operators. Each grouping of graphs is associated with a specific spin and colour structure, which can be read off from the graph at the end of each row. These are

$$\left\{\frac{\mathbf{T}_i^{c_2}p_i\cdot\varepsilon_2}{p_i\cdot q_2}\frac{\mathbf{T}_i^{c_1}p_i\cdot\varepsilon_1}{p_i\cdot q_1}, \frac{if^{c_1c_2a}\,q_1\cdot\varepsilon_2}{q_1\cdot q_2}\frac{\mathbf{T}_i^a p_i\cdot\varepsilon_1}{p_i\cdot q_1}, \frac{\mathbf{T}_i^{c_2}p_i\cdot\varepsilon_2}{p_i\cdot q_2}\frac{\mathbf{T}_j^{c_1}p_j\cdot\varepsilon_1}{p_j\cdot q_1}\right\} + \{(i\leftrightarrow j)\} . \tag{5.11}$$

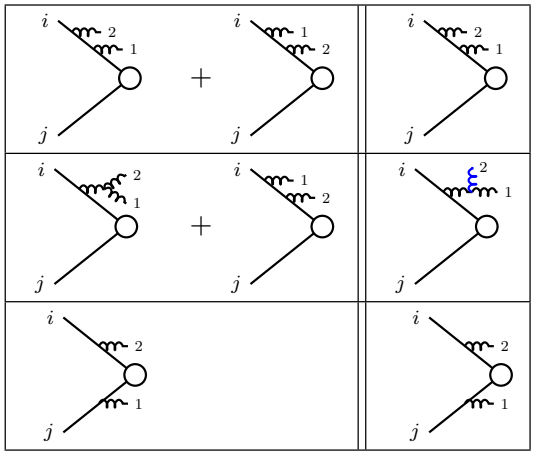

Figure 5.2: Diagrammatic representation of how to group the graphs in order to write the final result as a product of single emission operators. There are three further structures, obtained by exchanging $i \leftrightarrow j$.

In limit 3, the two diagrams on each of the first two lines of Fig. 5.2 combine to give each effective diagram on the right, interpreted *as if* the two emissions were independent. Equivalently, they conspire to act *as if* q_1^- and q_2^- were strongly ordered, even though they are not. It is this fact that allows the limit 3 result to be obtained from the limit 1 result (in which they are strongly ordered).

5.3 Two emissions at one loop

We now consider the one-loop amplitude for a hard process with two incoming partons and two soft emissions. The imaginary parts of these graphs correspond to eikonal cuts through the incoming partons and, in contrast to the single real emission case, we must now consider graphs with cuts through two soft gluon lines, i.e. corresponding to a Coulomb exchange between the two outgoing soft gluons. The derivation of the cutting rules corresponding to this amplitude are presented in Appendix D, see Eq. (D.2). We have calculated the exact infrared poles and the logarithmic enhancements of these imaginary contributions within the eikonal approximation. The necessary methods are discussed in Appendix H and these were implemented in `Wolfram Mathematica` with the `Feyncalc` package. We recall that we are only using the Eikonal approximation for the emission off the hard parton lines. This is the only approximation we make and, in particular, we use the full triple-gluon and four-gluon vertices for soft gluon emissions off other soft gluons and we use the exact expressions for soft-gluon propagators. This means that we make no assumptions about the relative sizes of the momenta of real and virtual soft radiation.

5.4 Eikonal cuts

Figure 5.3 illustrates the three gauge-invariant classes of cut graph, where the cut is through the two hard partons. As before, we refer to these as eikonal cuts. The corresponding amplitudes can be reduced to transverse momentum integrals. In order to regulate the diagrams that do not involve any emissions off the virtual gluon, we introduce an *uv* cutoff Q^2. In all cases we regularize the infrared divergences by analytically continuing the dimension of the transverse momentum integral $\mathrm{d}^2k_T \to \mathrm{d}^{d-2}k_T$. We start by simply stating the bottom line. The remainder of this section

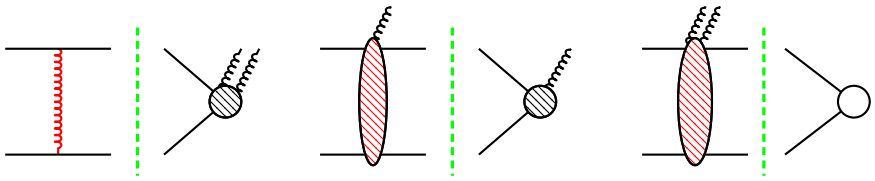

Figure 5.3: The three cuts corresponding to the three different physical mechanisms for double-gluon emission. Each of these cuts is gauge invariant.

will be devoted to examining how these results arise. The complete calculation involves explicitly computing the diagrams Fig. 5.5.

The leading behaviour arising from eikonal cuts in limit 1 is

$$\Big[\mathbf{C}^{ij}(0,q_{2T})\,\mathbf{J}^{c_2c_1a}_{2+2}(q_2)\mathbf{J}^{a}_{1}(q_1) + \mathbf{J}^{c_2c_1a}_{2+2}(q_2)\mathbf{C}^{ij}(q_{2T},q_{1T})\,\mathbf{J}^{a}_{2+1}(q_1) + \mathbf{J}^{c_2c_1a}_{2+2}(q_2)\mathbf{J}^{a}_{2+1}(q_1)\mathbf{C}^{ij}(q_{1T},Q)\Big]\Big|2^{(0)}\Big\rangle\,, \tag{5.12}$$

where the current $\mathbf{J}^{c_2c_1a}_{2+2}(q_2)$ is defined in Eq. (5.5b). This expression is the expected generalization of the one-emission case (3.7) and the key point is that the k_T of the Coulomb exchange is ordered with respect to the real-emission transverse momenta. For the first two terms, the vector $\mathbf{J}^{a}_{2+1}(q_1)\Big|2^{(0)}\Big\rangle$ acts as a hard subprocess for the second gluon emission, i.e. as in Eq. (3.7) with q_{1T} playing the role of Q.

Similarly, in limit 2 the sum over eikonal cuts gives

$$\left[\mathbf{C}^{ij}(0,q_{2T})\left[\frac{\mathbf{T}_i^{c_2}\;p_i\cdot\varepsilon_2}{p_i\cdot q_2}\right]\mathbf{J}^{c_1}_{2+1}(q_1) + \left[\frac{\mathbf{T}_i^{c_2}\;p_i\cdot\varepsilon_2}{p_i\cdot q_2}\right]\mathbf{C}^{ij}(q_{2T},q_{1T})\,\mathbf{J}^{c_1}_{2+1}(q_1) + \left[\frac{\mathbf{T}_i^{c_2}\;p_i\cdot\varepsilon_2}{p_i\cdot q_2}\right]\mathbf{J}^{c_1}_{2+1}(q_1)\,\mathbf{C}^{ij}(q_{1T},Q)\right]\Big|2^{(0)}\Big\rangle\,, \tag{5.13}$$

whilst in limit 3 the result is

$$\left[\mathbf{C}^{ij}(0,q_{2T})\,\mathbf{J}^{c_2c_1a}_{2+2}(q_2)\left[\frac{\mathbf{T}^a_i\;p_i\cdot\varepsilon_1}{p_i\cdot q_1}\right]+\mathbf{J}^{c_2c_1a}_{2+2}(q_2)\,\mathbf{C}^{ij}(q_{2T},q_{1T})\left[\frac{\mathbf{T}^a_i\;p_i\cdot\varepsilon_1}{p_i\cdot q_1}\right]\right.$$
$$\left.+\,\mathbf{J}^{c_2c_1a}_{2+2}(q_2)\left[\frac{\mathbf{T}^a_i\;p_i\cdot\varepsilon_1}{p_i\cdot q_1}\right]\mathbf{C}^{ij}(q_{1T},Q)\right]\left|2^{(0)}\right\rangle\,. \tag{5.14}$$

As in the tree-level case, the leading behaviour in limits 2 and 3 coincides with the expressions that result from taking the relevant collinear limit of the leading expression in limit 1. These results showed that the eikonal cuts exactly behave as as chain of emissions and Coulomb gluons ordered with respect to the transverse momentum of the real emissions, although, as we will shortly see, the way that the k_T ordering establishes itself is rather involved.

In order to see our way to Eqs. (5.12)–(5.14) we must understand how to deal with the graphs involving the triple-gluon vertex. In the simpler case of only one real emission, this is illustrated in Fig. 5.4, which illustrates how the Feynman gauge graphs are to be grouped together and projected onto the relevant spin and colour tensors. The corresponding amplitudes are

$$\left\{\frac{\mathbf{T}_i\;p_i\cdot\varepsilon}{p_i\cdot q_1}\;\frac{-i\pi\;\mathbf{T}_j\cdot\mathbf{T}_i}{8\pi^2},\frac{-i\pi\;\mathbf{T}_j\cdot\mathbf{T}_i}{8\pi^2}\;\frac{\mathbf{T}_i\;p_i\cdot\varepsilon}{p_i\cdot q_1}\right\}+\{(i\leftrightarrow j)\}\,. \tag{5.15}$$

The single graph involving the triple gluon vertex is thus shared out between all four contributing tensors.

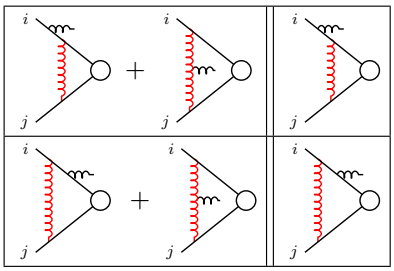

Figure 5.4: Diagrammatic representation of how to group the graphs that give rise to the transverse momentum ordered expression (3.7). Two more structures are obtained by permuting $(i\leftrightarrow j)$.

Figure 5.5 is the generalization of Fig. 5.2 and Fig. 5.4. By way of illustration, the graphs in the first row have all contributions to the tensor structure of the rightmost graph, this tensor reads

$$\frac{\mathbf{T}^{c_2}_i\;p_i\cdot\varepsilon_2}{p_i\cdot q_2}\;\frac{\mathbf{T}^{c_1}_i\;p_i\cdot\varepsilon_1}{p_i\cdot q_1}\;\frac{-i\pi\;\mathbf{T}_i\cdot\mathbf{T}_j}{8\pi^2}. \tag{5.16}$$

In limits 1–3, every row in Fig. 5.5 contribute to the respective tensor, shown in the rightmost column, and either adds up to a subleading expression or to one of

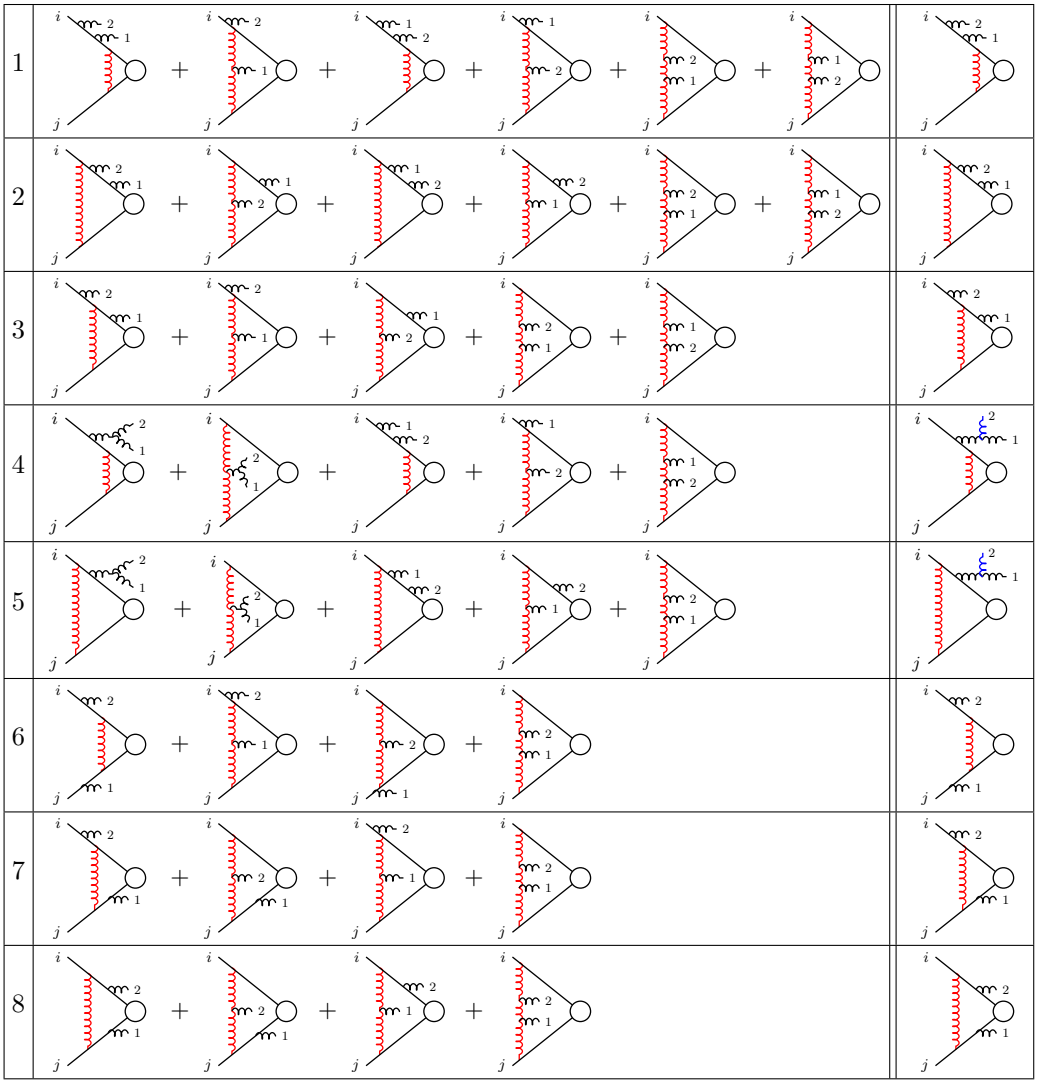

Figure 5.5: Diagrammatic representation of how to group the graphs that give rise to the transverse momentum-ordered expression in the case of two emissions at one loop. There are 12 more structures to consider: 8 are obtained by permuting $(i \leftrightarrow j)$ and the other four are obtained by permuting $(1 \leftrightarrow 2)$ and $(i \leftrightarrow j, 1 \leftrightarrow 2)$ in groups 3 and 7.

the terms in Eqs. (5.12)–(5.14). This figure contains all of the leading contributions arising from the 36 different graphs with eikonal cuts.

In order to illustrate how the transverse momentum ordered integrals arise, we will consider two examples in some detail. We will omit the respective tensor and will focus on the kinematical integral that accompanies it. We start by taking a closer look at the first row of six graphs in Fig. 5.5. All of these graphs have only a single cut, corresponding to production mechanism (C) in Fig. 5.3. The first graph

of the six gives rise to a factor of[4]

$$G_{11} = \frac{q_1^-}{(q_2^- + q_1^-)} \int_0^{Q^2} \frac{\mathrm{d}k_T^2}{k_T^2} \ . \tag{5.17}$$

The factor multiplying the integral simplifies to unity in the case of limits 1 and 2 but not in limit 3, where q_1^- and q_2^- could be of the same order. The projection of the third graph gives

$$G_{13} = \frac{q_2^-}{(q_1^- + q_2^-)} \int_0^{Q^2} \frac{\mathrm{d}k_T^2}{k_T^2} \tag{5.18}$$

and this is only leading in the case of limit 3. Obviously these Abelian-like contributions place no restriction on the k_T of the Coulomb exchange. Note that

$$G_{11} + G_{13} = \int_0^{Q^2} \frac{\mathrm{d}k_T^2}{k_T^2}. \tag{5.19}$$

The second graph is the first involving the triple gluon vertex. It gives

$$G_{12} = -\left[\int_0^{2q_1^- q_2^+} \frac{\mathrm{d}k_T^2}{k_T^2} + \frac{q_2^- - q_1^-}{q_2^- + q_1^-} \int_0^{2(q_1^+ + q_2^-)^2 q_2^+ / q_1^-} \frac{\mathrm{d}k_T^2}{k_T^2} \right] \ . \tag{5.20}$$

We note that the Coulomb integral cannot be written purely in terms of transverse momenta. However, the fourth graph is obtained from the second by interchanging q_1 and q_2. Thus the sum of graphs 2 and 4 is

$$G_{12} + G_{14} = -\frac{1}{(q_1^- + q_2^-)} \left[q_2^- \int_0^{q_{2T}^2} \frac{\mathrm{d}k_T^2}{k_T^2} + q_1^- \int_0^{q_{1T}^2} \frac{\mathrm{d}k_T^2}{k_T^2} \right] \ . \tag{5.21}$$

Graphs 5 and 6 also combine to produce a reasonably compact result involving the azimuthal angle between q_{1T} and q_{2T}. It is sub-leading in limits 1 and 2, and in limit 3 it simplifies to

$$G_{15} + G_{16} \approx -\frac{q_2^-}{(q_1^- + q_2^-)} \int_{q_{2T}^2}^{q_{1T}^2} \frac{\mathrm{d}k_T^2}{k_T^2} \ . \tag{5.22}$$

Now we can combine the graphs. In limits 1 and 2 only G_{11} and G_{14} contribute, with the latter contributing only for $k_T < q_{1T}$, exactly as in the one emission case. The two combine to give

$$\int_{q_{1T}^2}^{Q^2} \frac{\mathrm{d}k_T^2}{k_T^2} \ , \tag{5.23}$$

which is exactly as expected. Limit 3 is more subtle and involves the interplay of all

[4]In dimensional regularization, we write $\mathrm{d}k_T^2 (k_T^2)^{-1} \to \mu^{2\epsilon} \mathrm{d}k_T^2 (k_T^2)^{-1-\epsilon} g(\epsilon)$, where $g(\epsilon) = 1 + \mathcal{O}(\epsilon)$.

6 graphs. Remarkably, the sum of these is also exactly equal to (5.23). The key is the way graphs 5 and 6 serve to extend the upper limit in the first of the two terms in Eq. (5.21) from q_{2T}^2 to q_{1T}^2, so that the net effect of all four graphs involving the triple-gluon vertex is merely to cut out the region with $k_T < q_{1T}$.

It is also instructive to look at the graphs in the third row of Fig. 5.5. These involve cuts of type (B) and (C) in Fig. 5.3. We will just state the results (the subscripts B and C refer to the cut):

$$G_{31B} = \int_0^{Q^2} \frac{\mathrm{d}k_T^2}{k_T^2} = -G_{31C} \ , \tag{5.24}$$

$$G_{32} + G_{33C} = \frac{1}{(q_1^- + q_2^-)} \left[q_2^- \int_0^{q_{2T}^2} \frac{\mathrm{d}k_T^2}{k_T^2} + q_1^- \int_0^{q_{1T}^2} \frac{\mathrm{d}k_T^2}{k_T^2} \right], \tag{5.25}$$

$$G_{33B} = -\int_0^{q_{2T}^2} \frac{\mathrm{d}k_T^2}{k_T^2} \ , \tag{5.26}$$

so that

$$G_{32} + G_{33} = \frac{q_1^-}{(q_1^- + q_2^-)} \int_{q_{2T}^2}^{q_{1T}^2} \frac{\mathrm{d}k_T^2}{k_T^2} \ . \tag{5.27}$$

Once again the graphs where both gluons are emitted off the Coulomb exchange are sub-leading in limits 1 and 2 and in limit 3 we find

$$G_{34} + G_{35} \approx \frac{q_2^-}{(q_1^- + q_2^-)} \int_{q_{2T}^2}^{q_{1T}^2} \frac{\mathrm{d}k_T^2}{k_T^2} \ . \tag{5.28}$$

On summing the graphs we obtain the expected result:

$$\int_{q_{2T}^2}^{q_{1T}^2} \frac{\mathrm{d}k_T^2}{k_T^2}. \tag{5.29}$$

Notice how the sum of type (B) cuts is exactly as expected from the single-gluon emission case, i.e. the Coulomb exchange satisfies $k_T > q_{2T}$.

5.4.1 Physical picture

As we did for the one-emission amplitude, it is interesting to group together the cut graphs into gauge-invariant sets. In this case, that means according to the cuts shown in Fig. 5.3. Cuts (A) and (B) are quite straightforward because they can be deduced directly from the one real-emission case. In (A), the Coulomb exchange occurs long before the double-emission and its k_T is unbounded (see Eq. (3.12)); the

result (which is exact in the eikonal approximation) is

$$\mathbf{C}^{ij}(0,Q)\,\mathbf{K}^{c_1c_2}_{2+2}(q_1,q_2)\Big|2^{(0)}\Big\rangle\,. \tag{5.30}$$

The gauge invariance of this expression is inherited from the gauge invariance of the tree-level double emission amplitude, $\mathbf{K}_{2+2}(q_1,q_2)|2^{(0)}\rangle$.

In the case of cut (B), one of the emissions occurs together with the Coulomb exchange, before the hard scatter, and the other during the hard scatter. These could be $q_{1,2}$ either way round. In the case that it is q_1 that is emitted with the Coulomb exchange, just like the case of cut (A) in Fig. 3.2, its k_T must be larger than that of the real emission, $k_T > q_{1T}$ (see Eq. (3.10)):

$$\left[-\frac{i\pi}{8\pi^2}\mathbf{T}_j^b if^{bc_1a}\mathbf{T}_i^a\left[\frac{p_j\cdot\varepsilon_1}{p_j\cdot q_1}-\frac{p_i\cdot\varepsilon_1}{p_i\cdot q_1}\right]\int_{q_{1T}^2}^{Q^2}\frac{\mathrm{d}k_T^2}{k_T^2}\right]\mathbf{J}^{c_2}_{2+1}(q_2)\Big|2^{(0)}\Big\rangle\,, \tag{5.31}$$

which is manifestly gauge invariant.

Cut (C) involves physics that cannot be inferred from the one-emission amplitude. In view of Eq. (3.10), one might anticipate that this contribution is also infrared finite and this is indeed the case. The proof of this involves the graph containing the four-gluon vertex. The leading expression in limit 1 is

$$\begin{aligned}-\frac{i\pi}{8\pi^2}\left[\frac{p_j\cdot\varepsilon_1}{p_j\cdot q_1}-\frac{p_i\cdot\varepsilon_1}{p_i\cdot q_1}\right]\Bigg\{&\left[\frac{p_j\cdot\varepsilon_2}{p_j\cdot q_2}-\frac{q_1\cdot\varepsilon_2}{q_1\cdot q_2}\right]\left[\mathbf{T}_j^d if^{dc_2b}if^{bc_1a}\mathbf{T}_i^a\right]\\&+\left[\frac{q_1\cdot\varepsilon_2}{q_1\cdot q_2}-\frac{p_i\cdot\varepsilon_2}{p_i\cdot q_2}\right]\left[\mathbf{T}_j^d if^{dc_1b}if^{bc_2a}\mathbf{T}_i^a\right]\Bigg\}\int_{q_{1T}^2}^{Q^2}\frac{\mathrm{d}k_T^2}{k_T^2}\Big|2^{(0)}\Big\rangle\,.\end{aligned} \tag{5.32}$$

This is manifestly gauge invariant and, as anticipated, the result is cut off from below by the larger of the two emitted transverse momenta. As was the case at tree level, the leading behaviour of the expressions in limits 2 and 3 can be deduced by taking the respective collinear limits of this expression. By using the algebra of the generators one can show that the sum of Eq. (5.30), Eq. (5.31) and its permutation $(1 \leftrightarrow 2)$ and Eq. (5.32) is equal to (5.12), (5.13) and (5.14) in limits 1–3 respectively.

5.5 Soft gluon cuts

To complete the calculation of the imaginary contribution, we turn our attention to the "soft gluon cuts" illustrated in Fig. 5.6. We will show that the leading behaviour in limits 1–3 of this operator can be understood in terms of the re-scattering cuts that we encountered when studied the one-emission, one-loop amplitude.

Before presenting the full result, it is useful to focus first only on the $1/\epsilon$ poles. In general the integrals of these cut graphs contain more than one region in which

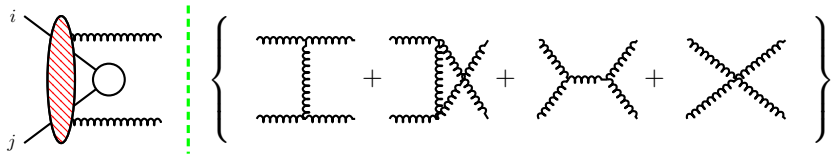

Figure 5.6: Kinematically allowed soft gluon cuts.

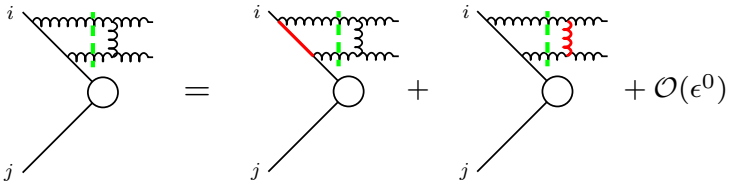

Figure 5.7: Schematic representation of regions that give rise to infrared poles. Poles arise as a result of the vanishing of the red propagators.

the propagators vanish and, in dimensional regularization, each region gives rise to a $1/\epsilon$ pole. To illustrate the point, we consider the first cut graph in Fig. 5.7, which gives

$$\frac{1}{2}\mathbf{T}_i^a if^{ac_2b} if^{bc_1d}\mathbf{T}_i^d \int \frac{\mathrm{d}^d l}{(2\pi)^d} \frac{if(l,p_i,q_1,q_2)\,(2\pi)\delta^+(l)\,(2\pi)\delta^+(q_1+q_2-l)}{(p_i\cdot l)(l\cdot q_1)}\,, \tag{5.33}$$

where f is a scalar function whose precise form is not important and $\delta^+(l) = \theta(l_0)\delta(l^2)$. In the reference frame in which the time-like vector q_1+q_2 is at rest, one can integrate over the energy l_0 and the magnitude of the $(d-1)$-momentum $|\vec{l}|$ to give

$$\frac{1}{2}\mathbf{T}_i^a if^{ac_2b} if^{bc_1d}\mathbf{T}_i^d \frac{((q_1^0+q_2^0)/2)^{d-6}}{8(2\pi)^{d-2}p_i^0 q_1^0} \int \mathrm{d}\Omega_{d-2} \frac{if(l)}{[1-\hat{p}_i\cdot\hat{l}][1-\hat{q}_1\cdot\hat{l}]}\,, \tag{5.34}$$

where $\mathrm{d}\Omega_{d-2}$ is the solid angle element of the unit $(d-2)$-sphere. Clearly the denominator of the integrand only vanishes when the virtual light-like momentum is either collinear with p_i or q_1, which cannot occur simultaneously[5]. It follows that the pole part of this expression can be computed as

$$\begin{aligned}\int \mathrm{d}\Omega_{d-2} \frac{f(l)}{[1-\hat{p}_i\cdot\hat{l}][1-\hat{q}_1\cdot\hat{l}]} &= \frac{f(l)|_{\hat{l}=\hat{p}_i}}{1-\hat{p}_i\cdot\hat{q}_1}\int \frac{\mathrm{d}\Omega_{d-2}}{[1-\hat{p}_i\cdot\hat{l}]} \\ &+ \frac{f(l)|_{\hat{l}=\hat{q}_1}}{1-\hat{p}_i\cdot\hat{q}_1}\int \frac{\mathrm{d}\Omega_{d-2}}{[1-\hat{q}_1\cdot\hat{l}]} + \mathcal{O}(\epsilon^0).\end{aligned} \tag{5.35}$$

The remaining angular integration can be performed by standard methods, after

[5]Unless these two vectors are exactly collinear, but we are excluding this case.

which, Eq. (5.33) can be written

$$\mathbf{T}_i^a if^{ac_2b} if^{bc_1d} \mathbf{T}_i^d \frac{-i\pi}{8\pi^2} \frac{1}{(-p_i\cdot q_1)(q_1+q_2)^2} \left[-\frac{f(l)}{\epsilon}\bigg|_{l=\frac{q_1\cdot q_2}{p_i\cdot(q_1+q_2)}p_i} - \frac{f(l)}{\epsilon}\bigg|_{l=q_1} \right] + \mathcal{O}(\epsilon^0). \tag{5.36}$$

This expression indicates that the pole part of this cut graph arises from the region in which the virtual emission is collinear to the hard momentum $l^\mu \to \frac{q_1\cdot q_2}{p_i\cdot(q_1+q_2)}p_i^\mu$ and from the region $l^\mu \to q_1^\mu$. The latter corresponds to an infinitely soft virtual exchange between the two real emissions. These two contributions are represented on the right-hand side of Fig. 5.7.

Exactly the same type of analysis can be carried out to compute the pole parts of each of the cut graphs in Fig. 5.6. In all cases, the $1/\epsilon$ poles arise either from the region in which one of the eikonal propagators vanishes (collinear singularities) or from the region in which the two real emissions exchange a soft gluon between them. We note that included in Fig. 5.6 are cut self-energy graphs and the corresponding ghost graphs should be added to these. However, neither of them gives rise to infrared poles (or their associated logarithms).

The colour operator associated with each leading graph in Fig. 5.6 can be written as a linear combination of the colour structure on the left-hand side of Fig. 5.8 and its permutation ($1 \leftrightarrow 2$). For example, the colour operator corresponding to the graph in Fig. 5.7 can be rewritten as

$$\mathbf{T}_i^a if^{ac_2b} if^{bc_1d} \mathbf{T}_i^d \Big| 2^{(0)} \Big\rangle = -\mathbf{T}_j^d if^{dc_1b} if^{bc_2a} \mathbf{T}_i^a \Big| 2^{(0)} \Big\rangle \,. \tag{5.37}$$

After expressing all of the colour structures in this way, one can confirm that the poles corresponding to collinear singularities cancel. This cancellation gives rise to the zero on the right-hand side of Fig. 5.8. It follows that the only $1/\epsilon$ poles of the

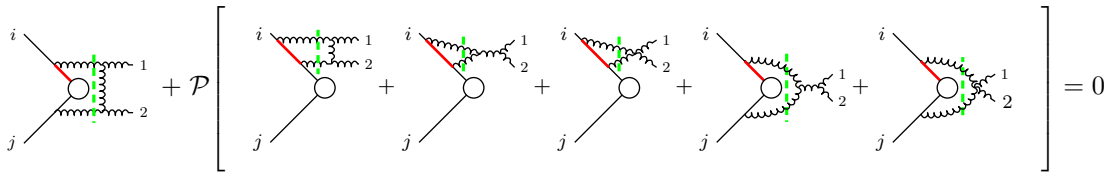

Figure 5.8: Cancellation of collinear poles. The operator $\mathcal{P}$ projects out the appropriate colour structure.

cut graphs in Fig. 5.6 arise from a Coulomb exchange between the two real emissions. These are represented in Fig. 5.9. Explicitly, the pole part of the amplitude arising

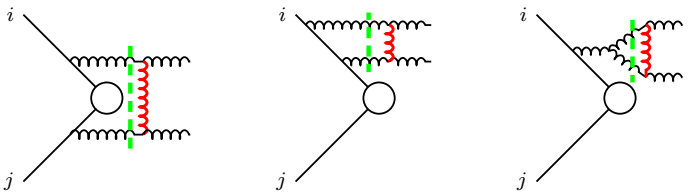

Figure 5.9: The relevant $1/\epsilon$ poles arising from soft-gluon cuts correspond to Coulomb exchange between the two real emissions.

from the sum over all soft gluon cuts can written

$$-\frac{1}{\epsilon}\left[\frac{-i\pi}{8\pi^2} if^{c_2ea_2} if^{c_1ea_1}\right] \mathbf{K}^{a_2a_1}_{2+2}(q_1,q_2)\Big|2^{(0)}\Big\rangle, \tag{5.38}$$

where $\mathbf{K}_{2+2}(q_1,q_2)$ is the two-gluon emission tensor. This expression can be combined with the pole part of Eq. (5.30) to determine the leading $1/\epsilon$ pole of the imaginary part of the double-emission amplitude.

We will now go beyond the calculation of the leading ϵ poles and compute the corresponding leading logarithmic contribution arising from the soft gluon cuts. As before we computed all of the contributing Feynman graphs exactly in dimensional regularisation and within the eikonal approximation, and then extract the leading behaviour in limits 1–3.

In limit 1 the amplitude is

$$\sum_{l=\{i,j\}} \frac{-i}{8\pi^2}\left\{ if^{c_1da_1} if^{c_2db_2} \int_0^{q^2_{2T(l1)}} \frac{\mathrm{d}k_T^2}{k_T^2}\right\} \mathbf{T}_l^{b_2}\left[\frac{p_l\cdot\varepsilon_2}{p_l\cdot q_2} - \frac{q_1\cdot\varepsilon_2}{q_1\cdot q_2}\right] \mathbf{J}^{a_1}_{2+1}(q_1)\Big|2^{(0)}\Big\rangle. \tag{5.39}$$

We recall that $q^2_{2T(1i)} \equiv \frac{2p_i\cdot q_2\, q_1\cdot q_2}{p_i\cdot q_1}$ is the transverse momentum of gluon q_2 oriented with respect to the $\{p_i, q_1\}$. It is important to remark that the colour charge of the term inside braces corresponds to the product of the colour charges associated with the soft gluons, i.e $if^{c_2db_2} if^{c_1da_1} \equiv (\mathbf{T}_{q_2})^{c_2b_2}\cdot(\mathbf{T}_{q_1})^{c_2a_1}$. In view of this observation, the comparison of the soft gluon cuts with Eq. (3.22) shows us that the soft gluon cuts in limit 1 are nothing but the re-scattering cuts where $\mathbf{J}_{2+1}(q_1)\,\big|2^{(0)}\big\rangle$, the Drell-Yan subprocess with the harder gluon q_1, plays the role of the hard subprocess (3.22). Observe that the term inside brackets would be exactly equal to the current $\mathbf{J}_{2+2}(q_2)$ if we could use colour conservation to write $-\sum_{l\neq\{q_1\}}\mathbf{T}_l\frac{q_1\cdot\varepsilon_2}{q_1\cdot q_2} = \mathbf{T}_{q_1}\frac{q_1\cdot\varepsilon_2}{q_1\cdot q_2}$. However, this is not possible as the Coulomb gluon is limited by the dipole momentum $q^2_{2T(1l)}$.

Let us recall that the plus and minus components in the $\{p_i, p_j\}$ frame are defined as

$$q_1^{\pm} = q_{1T}e^{\pm y_i}/\sqrt{2} \;\text{ and }\; q_i^{\pm} = q_{2T}e^{\pm y_i}/\sqrt{2}\,. \tag{5.40}$$

The logarithms are then

$$\begin{aligned}\ln\left(\frac{2q_2\cdot q_1\, p_i\cdot q_2}{q_1\cdot p_i\mu^2}\right) &= \ln\left(\frac{q_{2T(i1)}^2}{\mu^2}\right) = \ln\left(\frac{q_{2T}^2}{\mu^2}\right) + \ln\left(\frac{2q_1\cdot q_2}{q_{1T}q_{2T}}\right) + y_1 - y_2,\\ \ln\left(\frac{2q_2\cdot q_1\, p_j\cdot q_2}{q_1\cdot p_j\mu^2}\right) &= \ln\left(\frac{q_{2T(j1)}^2}{\mu^2}\right) = \ln\left(\frac{q_{2T}^2}{\mu^2}\right) + \ln\left(\frac{2q_1\cdot q_2}{q_{1T}q_{2T}}\right) + y_2 - y_1.\end{aligned} \tag{5.41}$$

In the calculation of observables where the terms $\propto y_i$ are formally subleading, Eq. (5.39) can therefore be simplified to

$$\left\{-\frac{i\pi}{8\pi^2} if^{c_1da_1} if^{c_2db_2}\left[-\frac{1}{\epsilon} + \ln\left(\frac{q_{2T}^2}{\mu^2}\right) + \ln\left(\frac{2q_1\cdot q_2}{q_{1T}q_{2T}}\right)\right]\right\}\ \mathbf{J}_{2+2}(q_2)\mathbf{J}_{2+1}(q_1)\Big|2^{(0)}\Big\rangle\ . \tag{5.42}$$

The operator enclosed in curly brackets has the colour structure of a Coulomb exchange between the two emissions, and its pole part agrees with Eq. (5.38). The first logarithm can be written as

$$-\frac{1}{\epsilon} + \ln\left(\frac{q_{2T}^2}{\mu^2}\right) + \mathcal{O}(\epsilon) = \int_0^{q_{2T}^2}\frac{\mu^{2\epsilon}\,\mathrm{d}k_T^2}{(k_T^2)^{1+\epsilon}}. \tag{5.43}$$

Then, since the second logarithm is sub-leading, the gluon cuts in limit 1 reduce to a simple product of emissions and Coulomb gluons that are ordered with respect to the transverse momentum with respect to the incoming partons.

In limits 2 and 3, the sum over soft gluon cuts yields respectively

$$\left\{-\frac{i\pi}{8\pi^2} if^{c_2db_2} if^{c_1da_1}\int_0^{q_{2T}^2}\frac{\mu^{2\epsilon}\,\mathrm{d}k_T^2}{(k_T^2)^{1+\epsilon}}\right\}\ \left[\mathbf{T}_i^{b_2}\frac{p_i\cdot\varepsilon_2}{p_i\cdot q_2}\right]\mathbf{J}_{2+1}^{a_1}(q_1)\Big|2^{(0)}\Big\rangle\ , \tag{5.44}$$

$$\left\{-\frac{i\pi}{8\pi^2} if^{c_2db_2} if^{c_1da_1}\int_0^{q_{2T}^2}\frac{\mu^{2\epsilon}\,\mathrm{d}k_T^2}{(k_T^2)^{1+\epsilon}}\right\}\ \mathbf{J}_{2+2}^{b_2}(q_2)\left[\mathbf{T}_i^{a_1}\frac{p_i\cdot\varepsilon_1}{p_i\cdot q_1}\right]\Big|2^{(0)}\Big\rangle\ . \tag{5.45}$$

Again, the result in limits 2 and 3 can be deduced by taking the corresponding collinear limit of the leading expression in limit 1, Eq. (5.39). It is worth remarking that Eqs. (5.44) and (5.45) contain the exact logarithmic contributions. In particular, in deducing these expressions we did not neglect any factors that we did to derive Eq. (5.43), which is only approximation in limit 1.

Soft gluon cuts graph-by-graph

We recall that the colour part of all of the graphs in Fig. 5.6 can be written as a linear combination of the colour structure of the graph on the left-hand side of Fig. 5.8 and its permutation ($1 \leftrightarrow 2$). Written in terms of these two colour tensors,

in limit 1, the amplitude is

$$\frac{-i\pi}{8\pi^2}\left[\frac{p_j\cdot\varepsilon_1}{p_j\cdot q_1}-\frac{p_i\cdot\varepsilon_1}{p_i\cdot q_1}\right]\left\{\left[\frac{p_j\cdot\varepsilon_2}{p_j\cdot q_2}-\frac{q_1\cdot\varepsilon_2}{q_1\cdot q_2}\right]\left[-\frac{1}{\epsilon}+\ln\left[\frac{q^2_{2T(1j)}}{\mu^2}\right]\right]\mathbf{T}^d_j i f^{dc_2b} i f^{bc_1a}\mathbf{T}^a_i\right.$$
$$\left.\left[\frac{p_i\cdot\varepsilon_2}{p_i\cdot q_2}-\frac{q_1\cdot\varepsilon_2}{q_1\cdot q_2}\right]\left[-\frac{1}{\epsilon}+\ln\left[\frac{q^2_{2T(1i)}}{\mu^2}\right]\right]\mathbf{T}^d_j i f^{dc_1b} i f^{bc_2a}\mathbf{T}^a_i\right\}\left|2^{(0)}\right\rangle\,. \tag{5.46}$$

The leading cuts in limits 1–3 are presented in Fig. 5.10 and can be expressed in terms of the two colour tensors in Eq. (5.46), which are illustrated in the final column of the figure. There are additional graphs, other than the ones shown, that involve the four-gluon vertex but, along with the ghost graphs, these are sub-leading. In

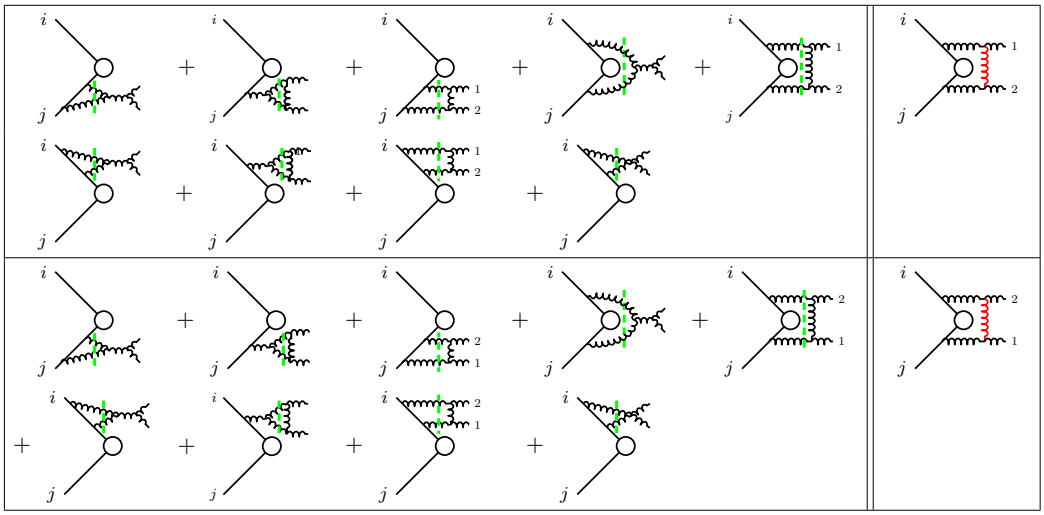

Figure 5.10: Leading graphs in limits 1–3. Their contributions are projected onto the two colour structures in the final column.

limit 1 all cuts in this figure are leading except that with a four-gluon vertex. The non-trivial way in which these graphs combine to deliver Eq. (5.46) is illustrated by considering, as an example, the graphs that give rise to the term with Lorentz structure

$$-\frac{i\pi}{8\pi^2}\frac{p_j\cdot\varepsilon_1}{p_j\cdot q_1}\frac{q_1\cdot\varepsilon_2}{q_1\cdot q_2} \tag{5.47}$$

in the first line of Eq. (5.46). The first five graphs of each colour structure are all leading. In the case of the first colour structure (the top half of Fig. 5.10) we label these $\{G_{1a}, G_{1b}, G_{1c}, G_{1d}, G_{1e}\}$. The first two of these cancel exactly, whilst the others give

$$G_{1c} \;=\; -\frac{3}{2}\int_{p_j\cdot q_1}^{p_j\cdot q_2}\frac{\mathrm{d}k_T^2}{k_T^2}-\frac{3}{2}\int_0^{2q_1\cdot q_2}\frac{\mathrm{d}k_T^2}{k_T^2}, \tag{5.48}$$

$$G_{1d} = \frac{3}{2}\int_0^{2q_1\cdot q_2}\frac{\mathrm{d}k_T^2}{k_T^2}, \tag{5.49}$$

$$G_{1e} = -\int_0^{2q_1\cdot q_2}\frac{\mathrm{d}k_T^2}{k_T^2}+\frac{1}{2}\int_{p_j\cdot q_1}^{p_j\cdot q_2}\frac{\mathrm{d}k_T^2}{k_T^2}. \tag{5.50}$$

In stark contrast, for the second colour structure the first two graphs again cancel exactly but the others now give

$$G_{2c} = \frac{3}{4}\int_0^{2q_1\cdot q_2}\frac{\mathrm{d}k_T^2}{k_T^2}, \tag{5.51}$$

$$G_{2d} = -\frac{3}{2}\int_0^{2q_1\cdot q_2}\frac{\mathrm{d}k_T^2}{k_T^2}, \tag{5.52}$$

$$G_{2e} = \frac{7}{4}\int_0^{2q_1\cdot q_2}\frac{\mathrm{d}k_T^2}{k_T^2}+\int_{p_i\cdot q_1}^{p_i\cdot q_2}\frac{\mathrm{d}k_T^2}{k_T^2}. \tag{5.53}$$

In both cases, these terms sum up to give the corresponding terms in Eq. (5.46).

Limit 2 is particularly simple since from all the graphs in Figure 5.10 only graphs G_{2e} and G_{2h} are leading and they give rise to the two terms

$$-\frac{i\pi}{8\pi^2}\frac{1}{2}\frac{p_i\cdot\varepsilon_2}{p_i\cdot q_2}\frac{p_i\cdot\varepsilon_1}{p_i\cdot q_1}\int_0^{q_{2T}^2}\frac{\mathrm{d}k_T^2}{k_T^2} \tag{5.54}$$

and

$$-\frac{i\pi}{8\pi^2}\left[\frac{1}{2}\frac{p_i\cdot\varepsilon_2}{p_i\cdot q_2}\frac{p_i\cdot\varepsilon_1}{p_i\cdot q_1}-\frac{p_i\cdot\varepsilon_2}{p_i\cdot q_2}\frac{p_j\cdot\varepsilon_1}{p_j\cdot q_1}\right]\int_0^{q_{2T}^2}\frac{\mathrm{d}k_T^2}{k_T^2}\ , \tag{5.55}$$

which add up to the corresponding collinear limit of Eq. (5.46).

Finally we study the leading cuts in limit 3. There are leading contributions to the second colour structure but they cancel. The first colour structure receives leading contributions to the following two Lorentz structures:

$$-\frac{i\pi}{8\pi^2}\left\{\frac{\varepsilon_1^-}{q_1^-}\frac{\varepsilon_2^+}{q_2^+},\frac{\varepsilon_1^-}{q_1^-}\frac{\varepsilon_2^-}{q_2^-}\right\}\ . \tag{5.56}$$

Only graph G_{1e} contributes to the first and it gives

$$-\int_0^{q_{2T}^2}\frac{\mathrm{d}l_T^2}{k_T^2}. \tag{5.57}$$

Graphs $\{G_{1a},G_{1b},G_{1c},G_{1d},G_{1e},G_{1i}\}$ contribute to the second Lorentz structure in (5.56). The contributions of graphs G_{1a},G_{1b} cancel whilst

$$G_{1c} = \left[\frac{3(q_1^-)^2+3q_1^-q_2^-+2(q_2^-)^2}{4(q_1^-+q_2^-)^2}\right]\int_0^{q_1^+q_2^-}\frac{\mathrm{d}k_T^2}{k_T^2}-\frac{1}{2}\int_{p_i\cdot q_1}^{p_i\cdot(q_1+q_2)}\frac{\mathrm{d}k_T^2}{k_T^2}, \tag{5.58}$$

$$G_{1d} = -\frac{3q_1^- + 2q_2^-}{2(q_1^- + q_2^-)} \int_0^{q_1^+ q_2^-} \frac{\mathrm{d}k_T^2}{k_T^2} + \int_{p_i \cdot q_1}^{p_i \cdot (q_1+q_2)} \frac{\mathrm{d}k_T^2}{k_T^2}, \tag{5.59}$$

$$G_{1e} = \frac{7q_1^- + 6q_2^-}{4(q_1^- + q_2^-)} \int_0^{q_1^+ q_2^-} \frac{\mathrm{d}k_T^2}{k_T^2} - \frac{1}{2} \int_{p_i \cdot q_1}^{p_i \cdot (q_1+q_2)} \frac{\mathrm{d}k_T^2}{k_T^2} - \int_{p_j \cdot q_2}^{p_j \cdot q_1} \frac{\mathrm{d}k_T^2}{k_T^2}. \tag{5.60}$$

The sum of these three contributions is

$$\int_0^{q_{2T}^2} \frac{\mathrm{d}k_T^2}{k_T^2} - \frac{q_1^- q_2^-}{2(q_1^- + q_2^-)^2} \int_0^{q_1^+ q_2^-} \frac{\mathrm{d}k_T^2}{k_T^2} \ . \tag{5.61}$$

Finally, the four-gluon vertex graph G_{1i} exactly cancels the second term of this expression and so the sum of leading graphs in limit 3 reduces to

$$-\frac{i\pi}{8\pi^2} \frac{\varepsilon_1^-}{q_1^-} \left[\frac{\varepsilon_2^-}{q_2^-} - \frac{\varepsilon_2^+}{q_2^+} \right] \int_0^{q_{2T}^2} \frac{\mathrm{d}k_T^2}{k_T^2} \mathbf{T}_j^d i f^{dc_2 b} i f^{bc_1 a} \mathbf{T}_i^a. \tag{5.62}$$

This expression is identical to the corresponding collinear limit of Eq. (5.46).

It is clear that while the sum of diagrams reproduces k_T ordering in all three limits, the contributions of individual diagrams are very different in each region. In particular, the emergence of k_T ordering in limit 3, of most importance for the understanding of super-leading logarithms and factorization breaking, involves a very non-trivial interplay of many different orderings in many different individual diagrams (in Feynman gauge at least) including diagrams involving the four-gluon vertex. Another derivation of the leading behaviour of the sum of the soft gluon cuts in limits 1-3 can be found in [85].

5.5.1 Physical picture

We close our study of the soft gluon cuts by relating them to physical amplitudes, just as we related the Coulomb gluons at previous orders. To do this, we first point out that the sum of cut graphs illustrated in Fig. 5.6 can be written as

$$\frac{1}{2i} \int \mathrm{dLIPS}_2 (i\mathcal{B}^{\mu\nu})[-g_{\mu\beta}][-g_{\nu\lambda}](i\mathcal{A}^{\beta\lambda}) \ , \tag{5.63}$$

where $\mathcal{A}$ is the amplitude to produce a pair of gluons with momenta q_1' and q_2', $\mathcal{B}$ is the amplitude for that same pair of gluons to scatter into the two final state gluons with momenta (q_1) and (q_2) and

$$\mathrm{dLIPS}_2 \equiv \frac{\mathrm{d}^d q_{1'}}{(2\pi)^d} \frac{\mathrm{d}^d q_{2'}}{(2\pi)^d} \delta^d(q_1 + q_2 - q_{1'} - q_{2'})(-2\pi i \delta^+(q_{1'}))(-2\pi i \delta^+(q_{2'})). \tag{5.64}$$

As we already mentioned, ghost graphs also have imaginary contributions, however we neglected them before this section because they do not give poles or logarithmic

enhancements. This occurs because the cut condition together with their numerator factors of ghost graphs effectively suppress their in the regions where propagators become small. Nevertheless, they allow one to substitute the metric tensors in the above expression by sums over physical polarisation, i.e.

$$\frac{1}{2i}\int \mathrm{dLIPS}_2(i\mathcal{B}^{\mu\nu})\left[\sum_{\sigma_{1'}}\varepsilon_{1'\mu}\varepsilon^*_{1'\beta}\sum_{\sigma_{2'}}\varepsilon_{2'\nu}\varepsilon^*_{2'\lambda}\right](i\mathcal{A}^{\beta\lambda})\ . \tag{5.65}$$

5.6 Physics of two collinear gluons

In addition to limits 2 and 3 there is one more collinear limit that we now address. Limit 4: the two gluons are nearly collinear, have wide-angle with respect to the incoming partons and their momentum components are of the same order ($q_1^\pm \sim q_{1T} \sim q_2^\pm \sim q_{2T}$). This kinematical configuration can be defined as

$$\begin{aligned} q_{1\mu} &= zq_\mu - \frac{q_T^2}{2z\tilde{q}\cdot r}r_\mu + \widetilde{q}_{\perp\mu}\ , \\ q_{2\mu} &= (1-z)q_\mu - \frac{q_T^2}{2(1-z)\tilde{q}\cdot r}r_\mu - \widetilde{q}_{\perp\mu}\ , \\ 2q_1\cdot q_2 &= \frac{q_T^2}{z(1-z)}\ , \qquad \widetilde{q}_T \to 0, \end{aligned} \tag{5.66}$$

where q is the vector that denotes the collinear direction and the vector r specifies the directions in which the collinear limit is approached ($\widetilde{q}_\perp \cdot q = \widetilde{q}_\perp \cdot r = 0$). At tree-level order, all the divergent terms in this limit are given by

$$\left|2^{(0)}_{+2}\right\rangle = \frac{4\pi\alpha_s\mu^{2\epsilon}}{\sqrt{q_1\cdot q_2}}\mathbf{S}^{(0)\mu}[-g_{\mu\mu}]\mathbf{J}^\nu_{2+1}(q_1+q_2)\left|2^{(0)}\right\rangle \tag{5.67}$$

here $\mathbf{J}^\nu_{2+1}(q)$ denotes soft-gluon current and $\mathbf{S}^{(0)\dagger\mu}(q_1+q_2)$ is the splitting operator that describes the splitting of the collinear gluons, its explicit expression yields

$$\left\langle c_1\, c_2\middle|\mathbf{S}^{(0)}(q_1,q_2)\middle|c\right\rangle \equiv \frac{if^{c_1c_2d}}{2\sqrt{q_1\cdot q_2}}\varepsilon_{2\mu1}\varepsilon_{2\mu_2}V^{\mu_1\mu_2\mu}(-q_1,-q_2,q_1+q_2)\ , \tag{5.68}$$

since we have $\varepsilon_{1\mu1}\varepsilon_{2\mu_2}V^{\mu_1\mu_2\mu}(-q_1,-q_2,q_1+q_2)(q_1+q_2)_\mu = 0$, we can re-write the above expression as

$$\begin{aligned} &\left|2^{(0)}_{+2}\right\rangle = \mathbf{S}^{(0)\mu}[-g_{\perp\mu\nu}(q_1+q_2)]\mathbf{J}^\nu_{2+1}(q)\left|2^{(0)}\right\rangle, \\ &g_{\perp\mu\nu}(q_1+q_2) \equiv g_{\mu\nu} + \frac{r_\mu(q_1+q_2)_\nu + r_\nu(q_1+q_2)_\mu}{r\cdot(q_1+q_2)}\ . \end{aligned} \tag{5.69}$$

Using the polarisation vectors in Eq. (5.2) with $p_j \to r$ one can show that the splitting operator is related to the Altarelli-Parisi gluon-gluon splitting function $P_{gg\alpha\nu}(z,q_T)$

[27] via

$$
\begin{aligned}
P_{gg\alpha\nu}(z,q_T)\delta^{c'c} &= \sum_{\sigma_1,\sigma_2}^{2} g_{\perp\alpha\beta}(q_1+q_2)\Big\langle c'\Big|\mathbf{S}^{(0)\dagger\beta}\mathbf{S}^{(0)\mu}\Big|c\Big\rangle g_{\perp\mu\nu}(q_1+q_2) \\
&= C_A\delta^{c'c}\left[-g_{\alpha\nu}\left(\frac{z}{1-z}+\frac{1-z}{z}\right)-4z(1-z)\frac{q_{\perp\alpha}q_{\perp\nu}}{q_T^2}\right] .
\end{aligned}
\tag{5.70}
$$

We now proceed to study the collinear limits of the one loop amplitude. In limit 4, the eikonal cuts adds up to

$$
\begin{aligned}
&\frac{4\pi\alpha_s\mu^{2\epsilon}}{\sqrt{q_1\cdot q_2}}\mathbf{S}^{(0)\mu}[-g_{\mu\mu}(q_1+q_2)]\left[\mathbf{J}^{\nu}_{2+1}(q_1+q_2)\mathbf{C}^{ij}\big(q_{T(ij)},Q\big)\right. \\
&\left.+\mathbf{C}^{ij}\big(0,q_{T(ij)}\big)\,\mathbf{J}^{\nu}_{2+1}(q_1+q_2)\right]\Big|2^{(0)}\Big\rangle .
\end{aligned}
\tag{5.71}
$$

This expression shows that the physics of the eikonal cuts in the double emission case can be understood in terms of the physics of the one-emission case, see Eq. (5.1). On the other hand, in limit 4 the soft gluon cuts adds up to

$$
\frac{4\pi\alpha_s\mu^{2\epsilon}}{\sqrt{q_1\cdot q_2}}\mathbf{C}^{q_1q_2}(0,\widetilde{q}_\perp)\,\mathbf{S}^{(0)\mu}[-g_{\perp\mu\nu}]\mathbf{J}^{\nu}_{2+1}(q_1+q_2)\Big|2^{(0)}\Big\rangle . \tag{5.72}
$$

Hence, the amplitude reduces to a single Coulomb gluon operator acting on the collinear emissions and the k_T of the Coulomb gluon is limited by $\tilde{q}_\perp$, the transverse momentum that defines the collinear limit in Eq. (5.66).

We close this section with two remarks. Firstly, we mention that, although in this section we deduced the divergent terms in limit 4 at amplitude level, there is a missing step necessary to deduce the squared amplitude in this same limit. Due to our poor choice of polarisation vectors in this section, the tree-level (one-loop) amplitude has terms that behave as $\widetilde{q}_\perp^{-1}$ and as $\widetilde{q}_\perp^{-2}$. We expect that, as at tree-level, the one-loop contribution to the squared amplitude in limit 4 will be equal to the product of the tree-level amplitude (Eq. (5.72)) and the one-loop amplitude (the sum Eqs. (5.71) and (5.72)) in this limit. However, to prove this one needs to check that the interference between terms of order $\widetilde{q}_\perp^{-2}$ and $(\widetilde{q}_\perp)^0$ cancels, this is a pending task. Secondly, one can check that limits 1 and 4 commute in the sense that the leading behaviour of the eikonal and of the soft gluon cuts is the same if we take limit 1 and then limit 4 or if these limits are taken in the opposite order.

5.7 Summary

We have shown that the imaginary part of the one-loop, two-emission corrections to a Drell-Yan hard process can be separated, gauge-invariantly, into distinct physical

mechanisms for double gluon emission. The sum of these contributions in limits 1-3 can be written in terms of the building blocks that we found in the one-emission case: Coulomb exchange operators, soft-gluon currents and dipole emissions. A cancellation of many graphs imposes precise ordering conditions. The Coulomb gluons exchanged between the incoming partons are always ordered with respect to the transverse momentum of the real emissions. More precisely, the transverse momentum components defined by the direction of the incoming partons. The Coulomb exchanges between the emitted gluons have the same structure as the re-scattering cuts in Section 3.2.3. In the next Chapter we shall discuss their contributions in more detail.

In the calculation of observables like 'gaps between jets', where the rapidity logarithms are subleading, see Eq. (5.41) and the comment below this equation, the leading contribution to the amplitude in limit 1 yields:

$$\begin{aligned}\mathrm{Im}\left|2^{(1)}_{+2}\right\rangle = \Bigg[&\left(\mathbf{C}^{ij}_{(0,q_{2T})} + \mathbf{C}^{q_1q_2}_{(0,q_{2T})}\right)\mathbf{J}_{2+2}(q_2)\mathbf{J}_1(q_1) + \mathbf{J}_{2+2}(q_2)\mathbf{C}^{ij}_{(q_{2T},q_{1T})}\mathbf{J}_{2+1}(q_1) \\ &+ \mathbf{J}_{2+2}(q_2)\mathbf{J}_{2+1}(q_1)\mathbf{C}^{ij}_{(q_{1T},Q)}\Bigg]\left|2^{(0)}\right\rangle . \end{aligned} \tag{5.73}$$

Furthermore, the expression for the amplitude in limits 2 and 3 can be directly derived from this expression. These results constitute substantial progress in confirming the assumption that k_T ordering is the correct ordering variable in the computation of 'gaps between jets'; this expression is in accord with the k_T-ordered colour evolution picture, Eq. (2.73). Although to solve the ordering problem discussed in Section 2.6 one needs to consider the matrix elements that appear at N^{4}LO we think that the results of this chapter suggest that k_T is the correct ordering variable.

Chapter 6

General hard processes

In this chapter, we investigate the imaginary part of the one-loop amplitude for a general hard scattering process accompanied by the emission of two gluons. We will bring together results from previous chapters to express the strongly ordered limit of the amplitude in terms of: soft-gluon currents, dipole emissions and Coulomb operators. We will see that cancellations between many graphs imposes a precise ordering condition on the Coulomb gluon operators.

The main conclusion of this chapter is a generalisation of previous chapters: the Coulomb gluon exchanged by a pair $\{i, j\}$, either incoming or outgoing and either hard parton or soft emissions, should be ordered with respect to the transverse momentum (to $\{p_i, p_j\}$) of adjacent gluon emissions. In a schematic notation, this ordering condition can be summarised as follows

$$\left(\mathbf{T}_i \frac{p_i \cdot \varepsilon_2}{p_i \cdot q_2}\right) \left(-i\pi \mathbf{T}_i \cdot \mathbf{T}_j \int_{q^2_{2T(ij)}}^{q^2_{1T(ij)}} \frac{\mathrm{d}k_T}{k_T}\right) \left(\mathbf{T}_i \frac{p_i \cdot \varepsilon_1}{p_i \cdot q_1}\right) \ . \tag{6.1}$$

In Section 6.1, the different contributions to the amplitude are organised in terms of the physical mechanisms for double-gluon emission. Exact results for the amplitude are presented in Section 6.2. In order to avoid cluttered notation, we shall restate our notation in Section 6.3. Further sections will discuss the structure of the different physical mechanisms. Firstly, we address the cuts over eikonal lines in Section 6.4 and the soft gluon cuts in Section 6.5. We will find that their expressions are straightforward generalisations of the previous chapter. Then, in Section 6.6, we study re-scattering cuts which contain physics that we have not yet encountered in previous chapters. We conclude this chapter in Section 6.7 where, based upon the assumption that the ordering structure that we found in this and previous chapters continues to higher orders, we conjecture an expression for the one-loop amplitude with any number of strongly ordered real emissions.

6.1 Physical mechanisms for double emission

The imaginary part of the two emission amplitude for a general hard process can be organised into the sum of the different mechanisms for double gluon emission, each of which is separately gauge invariant. This time, there are eleven different possibilities; these are illustrated in Fig. 3.3. As in the equivalent figure for the one emission case, Fig. 6.1, we have abbreviated graphs by only showing the lines that are cut and the emitted gluons. Furthermore, the gluons radiated from black shaded circular blobs should be understood to be radiated in all possible ways. The derivation of the cutting rules that gives rise to these graphs can be done following analogous steps to those in Appendix D.

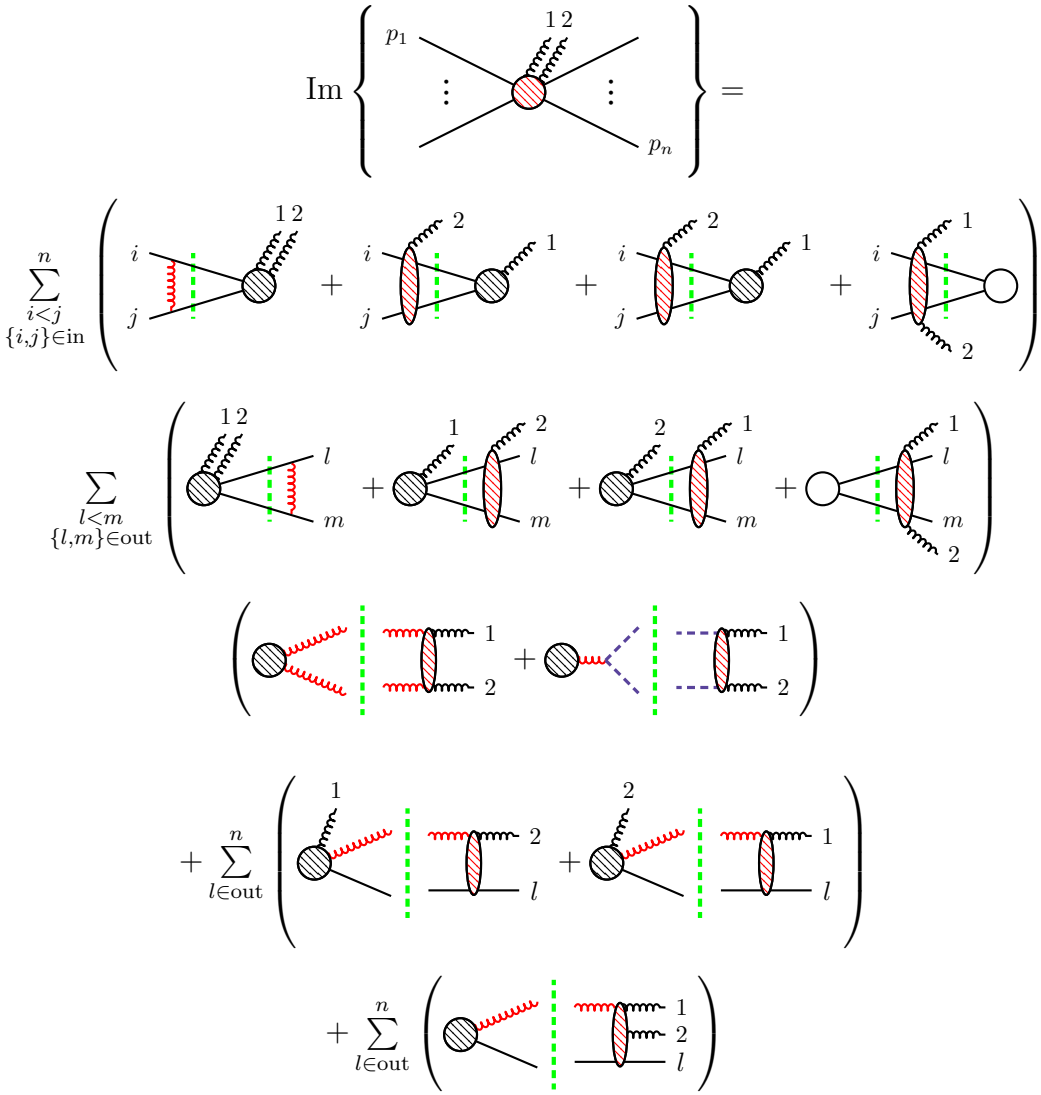

Figure 6.1: Imaginary part of the one-loop corrections to a general hard process organised in terms of the different physical mechanisms for double gluon emission. These graphs are the generalisation of Fig. 3.3. The second graph in the fourth row stands for the production of two ghosts that scatter into two gluons.

6.2 Exact results and cross-checks

We have calculated the exact[1] infrared poles and logarithmic enhancements of each graph in Fig. 6.1. The necessary integration methods can be found in [98, 99, 100, 101, 102], these are discussed in Appendix H and were implemented using `Wolfram Mathematica` with `Feyncalc`. As far as we are aware, such corrections for a completely general hard scattering have not been studied previously in the literature except for particular processes, see [43, 46] and references therein. Remarkably, although the exact amplitude is a complicated expression with involved logarithmic corrections[2], see for instance the scalar integral in Eq. (H.19), the dependence on the hard scale (Q) and the sum of the infrared poles have simple expressions. We recall that the tree-level amplitude with two soft gluon emissions (with colour c_1 and c_2) $\left|2^{(0)}_{+2}\right\rangle$ can be expressed in terms of an operator $\mathbf{K}_{n+2}(q_1,q_2)$ that acts on the hard process to insert two real emissions:

$$\left\langle c_1 c_2 \middle| n^{(0)}_{+2}\right\rangle \equiv g_2^2\mu^{2\epsilon}\,\mathbf{K}^{c_1c_2}_{n+2}(q_1,q_2)\middle|n^{(0)}_{+2}\right\rangle\,, \tag{6.2}$$

its explicit form is given in Eq. (4.3). The sum over all of the infrared $1/\epsilon$ poles of the cut graphs in Fig. 6.1 can be written as

$$\begin{aligned}\mathrm{Im}\left\{\left\langle c_2c_1\middle|n^{(1)}_{+2}\right\rangle\right\} = \frac{-i\pi\alpha_s c_\epsilon}{2\pi}\frac{1}{\epsilon}\times\Bigg[&\sum_{i<j}^{n}\widetilde{\delta}_{ij}\mathbf{T}_i\cdot\mathbf{T}_j\delta^{c_1a_1}\delta^{c_2a_2}\\ &+\widetilde{\delta}_{q_1q_2}(\mathbf{T}^d_{q_2})_{c_2a_2}(\mathbf{T}^d_{q_1})_{c_1a_1}\\ &+\sum_i^n\widetilde{\delta}_{iq_1}(\mathbf{T}^d_{q_1})^{c_2a_2}\mathbf{T}^d_i\delta^{c_1a_1}+\sum_i^n\widetilde{\delta}_{iq_2}(\mathbf{T}^d_{q_2})^{c_1a_1}\mathbf{T}^d_i\delta^{c_2a_2}\Bigg]\mathbf{K}^{a_1a_2}_{n+2}\middle|n^{(0)}\right\rangle,\end{aligned} \tag{6.3}$$

where $\widetilde{\delta}_{km}=1$ if $\{k,m\}$ are both incoming or outgoing and $\widetilde{\delta}_{km}=0$ otherwise. The terms in the first, second and third line in Eq. (6.3) correspond to Coulomb exchanges between: hard partons (second and third rows in Fig. 6.1), the emitted gluons (fourth row in Fig. 6.1) and an emitted gluon and a hard parton (fifth and sixth row in Fig. 6.1). Eq. (6.3) is not a new result but a cross-check. Indeed, one could derive it from the universality of the singular infrared behaviour of the one-loop corrections to a general scattering, i.e. setting $\mathcal{N}\to n_{+2}$ in Eq. (2.39). Nevertheless, this is a strong cross-check of our `Mathematica` calculation as it involves proving the cancellation between many graphs, e.g. the cancellation of collinear poles illustrated in Fig. 5.8 that includes a four-gluon vertex!

[1] Without specialising to any particular phase space region for the two emissions.

[2] We will not present the complete expression for the amplitude as it is too lengthily to include. We have the contributions in `Wolfram Mathematica` notebooks.

In general, the sum over all of the contributions in Fig. 6.1 can be written as

$$\mathrm{Im}\left\{\left|n^{(1)}_{+2}\right\rangle\right\} = \left[\mathbf{K}_{n+2}\mathrm{Im}\left\{\mathbf{I}^{(1)}_{n}\right\} + \mathrm{Im}\left\{\mathbf{K}^{(1)}_{n+2}\right\}\right]\left|n^{(0)}\right\rangle \tag{6.4}$$

where $\mathrm{Im}\{\mathbf{I}^{(1)}_n\}$ is the Coulomb gluon operator (see Eqs. (2.23) and (2.25)), i.e. Eq. (2.25), and all the other contribution, $\mathrm{Im}\{\mathbf{K}^{(1)}_{n+2}\}$, are power suppressed in the uv region. Some of them are infrared divergent but this is not relevant for the rest of this section. We recall that the contributions in $\mathrm{Im}\{\mathbf{I}^{(1)}_n\}$ are logarithmically divergent when the momentum of the (Coulomb) exchanges becomes arbitrarily large, see Appendix A for more details. Such uv divergences are fictitious in the sense that they have been introduced by the eikonal approximation in the propagators. In chapters 3 and 5 we introduced cut-off scales to regularise these uv divergences. However, Eq. (6.4), and the same applies to Eq. (3.29), shows that we could have presented our results without imposing a cut-off and expressing the uv divergences only in terms of $\mathbf{I}^{(1)}_n$. The conclusions in this and previous chapters would be the same.

6.3 Notation

From now on, we will focus on the leading behaviour of the amplitude in the strongly ordered limit $q_2 \gg q_1$, i.e. limit 1 from before. Specifically, we take $q_2 \to \lambda q_2$ and keep the leading term for small λ. For the sake of readability, we will present our results without explicitly projecting over the colour states of the emitted gluons and in this section we outline simple rules to project over the colour states of the gluons $\{c_1, c_2\}$.

Let us start by considering the double emission tree-level amplitude, $\left|n^{(0)}_{+2}\right\rangle$. In the strongly ordered limit this yields

$$\mathbf{J}_{n+2}(q_2)\mathbf{J}_{n+1}(q_1)\left|n^{(0)}\right\rangle \tag{6.5}$$

where

$$\mathbf{J}_{n+a}(q_a) = g_s\mu^{\epsilon}\sum_{i=1}^{n+a}\mathbf{T}_i\frac{p_i\cdot\varepsilon_a}{p_i\cdot q_a}, \qquad (a=0,1), \tag{6.6}$$

and it should be understood that $\mathbf{T}_{n+1} \equiv \mathbf{T}_{q_1}$ and $p_{n+1} \equiv q_1$. We recall that the action of $\mathbf{T}_{q_1}$ over the space spanned by the vectors $\{\mathbf{T}_i\left|n^0\right\rangle \,|\, i = \{1,\dots n\}\}$ and similarly, the action of $\mathbf{T}_{n+2} \equiv \mathbf{T}_{q_2}$ over the vectors $\{\mathbf{T}_j\mathbf{T}_i\left|n^0\right\rangle \,|\, j = \{1,\dots n+1\}, i = \{1,\dots n\}\}$ is defined as in the eikonal rules[3]. Also, we will find it convenient to denote

[3]See Fig. 2.1 and Eq. 2.8

$p_{n+2} \equiv q_2$.

We can project Eq. (6.6) over the colour state $\{c_1, c_2\}$ of the emitted gluons using the following simple steps

$$\begin{aligned}\left\langle c_1 c_2 \middle| \mathbf{J}_{n+2}(q_2)\mathbf{J}_{n+1}(q_1) \middle| n^{(0)} \right\rangle &= \left[\left\langle c_1 c_2 \middle| \mathbf{J}_{n+2}(q_2) \middle| a_1 \right\rangle\right] \left\langle a_1 \middle| \mathbf{J}_{n+1}(q_1) \middle| n^{(0)} \right\rangle \\ &= \left[\sum_{j=1}^{n} g_s \mathbf{T}_j^{c_2} \frac{p_j\cdot\epsilon_2}{p_j\cdot q_2}\delta^{c_1 a_1} + g_s i f^{c_1 c_2 a_1}\frac{q_1\cdot\varepsilon_2}{q_1\cdot q_2}\right] \mathbf{J}_{n+1}^{a_1}(q_1)\middle| n^{(0)} \right\rangle .\end{aligned} \tag{6.7}$$

At one-loop order we will often express our results in terms of two emission operators $\mathbf{T}_j$ and $\mathbf{T}_i$ and a single virtual exchange $(\mathbf{T}_l\cdot\mathbf{T}_k)$. The different combinations that we will encounter are

$$\begin{aligned}&(\mathbf{T}_l\cdot\mathbf{T}_k)\,\mathbf{T}_j\,\mathbf{T}_i\middle| n^{(0)} \right\rangle, \\ &\mathbf{T}_j\,(\mathbf{T}_l\cdot\mathbf{T}_k)\,\mathbf{T}_i\middle| n^{(0)} \right\rangle, \\ &\mathbf{T}_j\,\mathbf{T}_i(\mathbf{T}_l\cdot\mathbf{T}_k)\middle| n^{(0)} \right\rangle .\end{aligned} \tag{6.8}$$

These vectors can be projected following the simple rules:

$$\begin{aligned}\left\langle c_1 c_2 \middle| \mathbf{T}_j\,\mathbf{T}_i(\mathbf{T}_l\cdot\mathbf{T}_k)\middle| n^{(0)} \right\rangle &= \left\langle c_1 c_2 \middle| \mathbf{T}_j \middle| a_1 \right\rangle \left\langle a_1 \middle| \mathbf{T}_i(\mathbf{T}_l\cdot\mathbf{T}_k)\middle| n^{(0)} \right\rangle \\ \left\langle c_1 c_2 \middle| \mathbf{T}_j \middle| a_1 \right\rangle &= \begin{cases} \mathbf{T}_j^{c_2}\delta^{c_1 a_1} & \text{if } j = \{1,\ldots,n\} \\ i f^{c_1 c_2 a_1} & \text{if } j = q_1 \end{cases}\end{aligned} \tag{6.9}$$

$$\begin{aligned}&\left\langle c_1 c_2 \middle| \mathbf{T}_j\,(\mathbf{T}_l\cdot\mathbf{T}_k)\,\mathbf{T}_i\middle| n^{(0)} \right\rangle = \left\langle c_1 c_2 \middle| \mathbf{T}_j \middle| b_1 \right\rangle \left\langle b_1 \middle| \mathbf{T}_l\cdot\mathbf{T}_k \middle| a_1 \right\rangle \left\langle a_1 \middle| \mathbf{T}_i \middle| n^{(0)} \right\rangle, \\ &\left\langle c_1 c_2 \middle| \mathbf{T}_j \middle| b_1 \right\rangle = \begin{cases} \delta^{c_1 b_1}\mathbf{T}_j^{c_2} & \text{if } j \in \{1,\ldots n\}, \\ i f^{c_1 c_2 b_1} & \text{if } j = q_1 \,. \end{cases} \\ &\left\langle b_1 \middle| \mathbf{T}_l\cdot\mathbf{T}_k \middle| a_1 \right\rangle = \begin{cases} \delta^{b_1 a_1}\mathbf{T}_l\cdot\mathbf{T}_k & \text{if } \{l,k\} \in \{1,\ldots n\}, \\ i f^{b_1 d a_1}\mathbf{T}_k^d & \text{if } l = q_1 \text{ and } k \in \{1,\ldots n\}, \end{cases}\end{aligned} \tag{6.10}$$

$$
\begin{aligned}
&\Big\langle c_1c_2\Big|(\mathbf{T}_l\cdot\mathbf{T}_k)\,\mathbf{T}_j\,\mathbf{T}_i\Big|n^{(0)}\Big\rangle = \Big\langle c_1c_2\Big|\mathbf{T}_l\cdot\mathbf{T}_k\Big|b_1b_2\Big\rangle\Big\langle b_1b_2\Big|\mathbf{T}_j\Big|a_1\Big\rangle\Big\langle a_1\Big|\mathbf{T}_i\Big|n^{(0)}\Big\rangle,\\
&\Big\langle a_1\Big|\mathbf{T}_i\Big|n^{(0)}\Big\rangle = \mathbf{T}_i^{a_1}\Big|n^{(0)}\Big\rangle.\\
&\Big\langle b_1b_2\Big|\mathbf{T}_j\Big|a_1\Big\rangle = \begin{cases}\delta^{b_1a_1}\mathbf{T}_j^{b_2} & \text{if } j\in\{1,\dots n\},\\ if^{b_1b_2a_1} & \text{if } j\in\{1,\dots n\}\ .\end{cases}\\
&\Big\langle c_1c_2\Big|\mathbf{T}_l\cdot\mathbf{T}_k\Big|b_1b_2\Big\rangle = \begin{cases}\delta^{c_1b_1}\delta^{c_2b_2}\mathbf{T}_l\cdot\mathbf{T}_k & \text{if } \{k,l\}\in\{1,\dots n\},\\ if^{c_1db_1}\mathbf{T}_k^d\delta^{c_2b_2} & \text{if } l=q_1 \text{ and } k\in\{1,\dots n\},\\ if^{c_2db_2}\mathbf{T}_k^d\delta^{c_1b_1} & \text{if } l=q_2 \text{ and } k\in\{1,\dots n\},\\ if^{c_2db_2}if^{c_1db_1} & \text{if } l=q_2 \text{ and } k=q_1\ .\end{cases}
\end{aligned}
\tag{6.11}
$$

The rules for amplitudes with many more strongly ordered emissions would be defined in an analogous way.

6.4 Initial- and final-state eikonal cuts

The sum over the eikonal cuts through a pair of incoming partons $\{i,j\}$ can be organised into four physical mechanisms illustrated on the second row of Fig. 6.1. These mechanisms correspond to an on-shell scattering of two eikonal lines $\{i,j\}$ in the initial state before the hard process, and the real emissions can occur either as part of this initial-state scattering or as part of the hard scattering. This graph is the generalisation of Fig. 5.3 for the Drell-Yan case. In fact, the red ovals in both figures abbreviate exactly the same graphs.

The first physical mechanism in the second row of Fig 6.1, where both emissions occur as part of the hard scattering, yields

$$
\mathbf{C}^{ij}(0,Q)\times\mathbf{K}_{n+2}^{c_1c_2}(q_1,q_2)\Big|n^{(0)}\Big\rangle\ . \tag{6.12}
$$

The limits of integration of the Coulomb exchange are independent of the kinematics of the emissions.

The expression for the second physical mechanism (the third one is obtained swapping $(1\leftrightarrow 2)$) in the second row of Fig 6.1, where emission q_2 occurs as part of the on-shell scattering and q_1 as part of the on-shell scattering, adds up to:

$$
\left[\frac{-i\pi\alpha_s g_s}{2\pi}\mathbf{T}_i^d if^{dc_2e}\mathbf{T}_j^e\left(\frac{p_i\cdot\varepsilon_2}{p_i\cdot q_2}-\frac{p_j\cdot\varepsilon_2}{p_j\cdot q_2}\right)\int_{q_{2Tij}^2}^{Q^2}\frac{\mathrm{d}k_T^2}{k_T^2}\right]\times\mathbf{J}_{n+1}^{c_1}(q_1)\Big|n^{(0)}\Big\rangle\ . \tag{6.13}
$$

Notably, the part of this expression corresponding to the $2\to 3$ on-shell scattering (inside the brackets) is independent of the emission q_1. The fourth mechanism in

the second row of Fig 6.1 does not have a simple expression in general but in the strongly ordered limit ($q_1 \gg q_2$) it becomes

$$\frac{-i\pi\alpha_s g_s^2}{2\pi}\left[\frac{p_j\cdot\varepsilon_1}{p_j\cdot q_1}-\frac{p_a\cdot\varepsilon_1}{p_a\cdot q_1}\right]\Bigg\{\left[\frac{p_j\cdot\varepsilon_2}{p_j\cdot q_2}-\frac{q_1\cdot\varepsilon_2}{q_1\cdot q_2}\right]\left[\mathbf{T}_j^d i f^{dc_2b} i f^{bc_1a}\mathbf{T}_i^a\right] + \left[\frac{q_1\cdot\varepsilon_2}{q_1\cdot q_2}-\frac{p_i\cdot\varepsilon_2}{p_i\cdot q_2}\right]\left[\mathbf{T}_j^d i f^{dc_1b} i f^{bc_2a}\mathbf{T}_i^a\right]\Bigg\}\int_{q_{1T(ij)}^2}^{2p_i\cdot p_j}\frac{\mathrm{d}k_T^2}{k_T^2}\Big|n^{(0)}\Big\rangle\ . \tag{6.14}$$

It is worth pointing out that these are exactly the same expressions that we found in the Drell-Yan case ($n = 2$). Note that Eq. (6.14) can be obtained directly by considering the coherent emission of q_2 off the $2 \to 3$ scattering process described by Eq. (3.16).

In addition to the physical picture that we have just described, the sum of these four physical mechanims can be written in terms of emission currents and Coulomb exchanges. Crucially, the k_T of the Coulomb gluon is ordered with respect to the transverse momentum, defined by the direction of partons $\{i, j\}$ involved in the exchange, of the real emissions:

$$\begin{aligned}&\Big[\mathbf{C}^{ij}\big(0, q_{2T(ij)}\big)\ \mathbf{J}_{n+2}(q_2)\mathbf{J}_{n+1}(q_1) + \mathbf{J}_{n+2}(q_2)\,\mathbf{C}^{ij}\big(q_{2T(ij)}, q_{1T(ij)}\big)\ \mathbf{J}_{n+1}(q_1)\ ,\\ &+\mathbf{J}_{n+2}(q_2)\,\mathbf{J}_{n+1}(q_1)\,\mathbf{C}^{ij}\big(q_{1T(ij)}, Q\big)\Big]\Big|n^{(0)}\Big\rangle\ ,\end{aligned} \tag{6.15}$$

where the Coulomb gluon operator is defined in Eq. (3.37).

We do not need to compute separately the expressions for the final-state eikonal cuts depicted in the third row of Fig. 6.1. Instead, we can infer them from the identity illustrated in Fig. 3.4. As this identity holds on a graph-by-graph basis, we can obtain the expression for the final-state eikonal cuts by simply replacing $i \to l$ and $j \to m$ in Eqs. (6.12)–(6.15).

Based upon the observation that the structure of the eikonal cuts (of a general hard process) in the one- and two-emission cases is exactly the same, we conjecture that the sum of eikonal cuts (both in the initial and final state) in the presence of $q_1 \gg q_2 \gg \cdots \gg q_b$ strongly ordered emissions should add up to

$$\begin{aligned}\sum_{i<j}^{n}\tilde{\delta}_{ij}\Bigg[&\mathbf{C}^{ij}(0,\tilde{q}_b)\,\mathbf{J}_{n+b}(q_b)\cdots\mathbf{J}_{n+1}(q_1)\\ &+\mathbf{J}_{n+b}(q_b)\mathbf{C}^{ij}(\tilde{q}_{b-1},\tilde{q}_b)\,\mathbf{J}_{n+b-1}(q_{b-1})\cdots\mathbf{J}_{n+1}(q_1)\\ &+\cdots+\mathbf{J}_{n+b}(q_b)\cdots\mathbf{J}_{n+1}(q_1)\mathbf{C}^{ij}(\tilde{q}_1,Q)\Bigg]\Big|n^{(0)}\Big\rangle\ ,\end{aligned} \tag{6.16}$$

where, here and subsequently, $\tilde{q} = q_{T(ij)}$ when used in the argument of an $\mathbf{C}^{ij}$ operator. We used this notation to emphasise the simplicity of the ordering condition.

6.5 Soft gluon cuts

We will now focus on the physical mechanism in the fourth row of Fig. 6.1. As we discussed in Section 5.5.1, this mechanism corresponds to the on-shell scattering between the emitted soft gluons whilst the ghost graphs only serve to remove the unphysical degrees of freedom. Up to terms that cancel due to colour conservation, the structure of cuts over soft gluon lines for a Drell-Yan process is the same for a general scattering. In particular, in the strongly ordered limit the sum over the soft gluon cuts has the same dipole structure that we found in the Drell-Yan case, see Eq. (5.39):

$$\sum_{\substack{j=1\\ j\neq\{q_1\}}}^{n+1} \frac{-i\alpha_s}{2\pi}\left\{\mathbf{T}_{q_1}\cdot\mathbf{T}_{q_2}\int_0^{q^2_{2T(jq_1)}}\frac{\mathrm{d}k_T^2}{k_T^2}\right\} g_s\mathbf{T}_j\left[\frac{p_j\cdot\varepsilon_2}{p_j\cdot q_2}-\frac{q_1\cdot\varepsilon_2}{q_1\cdot q_2}\right]\mathbf{J}_{n+1}(q_1)\Big|n^{(0)}\Big\rangle, \quad (6.17)$$

if the amplitude $\mathbf{J}_{n+1}(q_1)\left|n^{(0)}\right\rangle$ is thought of as an effective hard process for the virtual gluon and the softer gluon q_2, this expression has the remarkable property of being equal to the re-scattering cuts that we found in one-emission case, i.e. Eq. (3.22). Exactly as in the one emission case, the softer emission, q_2, that will subsequently exchange a Coulomb gluon is emitted from the dipole formed by the harder gluon q_1, with which it will exchange a Coulomb gluon, and hard parton j. In addition, the k_T of the Coulomb exchange is limited by the dipole momentum, i.e. $k_T < q_{2T(lq_1)}$.

Observe that each term in Eq. (6.17) is gauge invariant with respect to the softer gluon, i.e. it vanishes under the replacement $\varepsilon_2 \to q_2$. In general, we will find that gluons that subsequently exchange Coulomb gluons are always emitted via a dipole structure. Anticipating this observation, let us introduce the dipole operator for the emission of gluon q_2 from a dipole formed by l, the parton with which it will exchange a Coulomb gluon, and each of the partons $j \neq \{l\}$:

$$\mathbf{d}_{n+2(jl)}(q_2) = g_s\mu^\epsilon\mathbf{T}_j\left[\frac{p_j\cdot\varepsilon_2}{p_j\cdot q_2}-\frac{p_l\cdot\varepsilon_2}{p_l\cdot q_2}\right]. \quad (6.18)$$

The sum over the different dipoles adds up to a tree-level soft-gluon current:

$$\sum_{\substack{j=1\\ j\neq\{l\}}}^{n+2}\mathbf{d}_{n+1(jl)}(q_2)\Big|n^0_{+1}\Big\rangle = \mathbf{J}_{n+2}(q_2)\Big|n^{(0)}_{+1}\Big\rangle\,, \quad (6.19)$$

and it should be understood that $\mathbf{T}_{n+1} = \mathbf{T}_{q_1}$ and $p_{n+1} = q_1$. However, observe that the sum symbol in Eq. (6.17) cannot be commuted to the right of the Coulomb operators as these exchanges have a "memory" of where q_2 was emitted from. It is this memory and the requirement of gauge invariance (with respect to softer emission

q_2) that forces the softer gluon to be emitted from a dipole operator. Written in terms of dipoles, the total expression for the soft gluon cuts, Eq. (6.17), reads

$$\sum_{\substack{j=1\\ j\neq\{q_1\}}}^{n+1} \mathbf{C}^{q_1 q_2}\left(0, q_{2T(jq_1)}\right) \mathbf{d}_{n+2(jq_1)}(q_2)\mathbf{J}_{n+1}(q_1)\Big|n^{(0)}\Big\rangle \ . \tag{6.20}$$

In this equation and throughout this chapter we shall show the sum indices very explicitly to avoid any confusion.

6.6 Re-scattering cuts

We shall now study the physical mechanisms corresponding to an on-shell re-scattering between an outgoing hard parton and a previously emitted gluon. There exist three different physical mechanisms; these are illustrated in the fourth and fifth row of Fig. 6.1. The red hatched ovals represent the $2 \to 2$ and $2 \to 3$ on-shell scatterings between the gluons and the hard parton l. To be precise about the definition of these ovals, we point out that the first graph in the fourth row of Fig. 6.1 can be also represented as in Fig. 6.2.

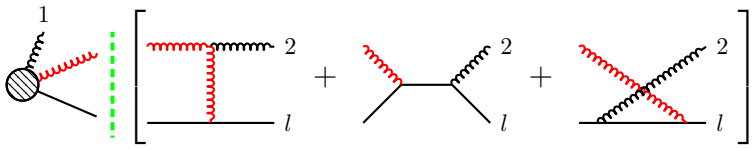

Figure 6.2: Explicit representation of the red oval of first graph in the fourth row of Fig. 6.1.

In the strongly ordered region, $q_1 \gg q_2$, the total expression of the contributions in Fig. 6.3 is

$$\begin{aligned}&\frac{-i\pi\alpha_s g_s}{2\pi}\mathbf{T}_l^d i f^{c_2 d b_2}\left\{\sum_{j\neq l}^{n}\mathbf{T}_j^{b_2}\delta^{c_1 a_1}\left[\frac{p_j\cdot\varepsilon_2}{p_j\cdot q_2}-\frac{p_l\cdot\varepsilon_2}{p_l\cdot q_2}\right]\int_0^{q^2_{2T(lj)}}\frac{\mathrm{d}k_T^2}{k_T^2}\right.\\ &\left.+if^{c_1 b_2 a_1}\left[\frac{q_1\cdot\varepsilon_2}{q_1\cdot q_2}-\frac{p_l\cdot\varepsilon_2}{p_l\cdot q_2}\right]\int_0^{q^2_{2T(lq_1)}}\frac{\mathrm{d}k_T^2}{k_T^2}\right\}\mathbf{J}_1^{a_1}(q_1)\Big|n^{(0)}\Big\rangle \ .\end{aligned} \tag{6.21}$$

As in case of the soft gluon cuts, if the amplitude $\mathbf{J}_1(q_1)\left|n^{(0)}\right\rangle$ is thought of as the hard subprocess, Eq. (6.21) is equal to the expression for the re-scattering cuts in the one-emission case; compare Eq. (6.21) with Eq. (3.22) and Fig. 6.3 with the fourth row of Fig. 3.3. Motivated by this observation, let us write this expression,

Eq. (6.21), in terms of the dipole operator, $\mathbf{d}_{n+2(jl)}(q_2)$, defined in Eq. (6.18), i.e.

$$\sum_{\substack{j=1\\ j\neq\{l\}}}^{n+1} \mathbf{C}^{lq_2}\left(0, q_{2T(jl)}\right) \mathbf{d}_{n+2(jl)}(q_2)\, \mathbf{J}_{n+1}(q_1) \Big| n^{(0)} \Big\rangle. \tag{6.22}$$

It is worth noting that this formula has the same structure as the expression that we found for the cuts over soft gluon lines, Eq. (6.20), and that their common feature is they can be written in terms of Coulomb exchanges between q_1 and the outogoing partons.

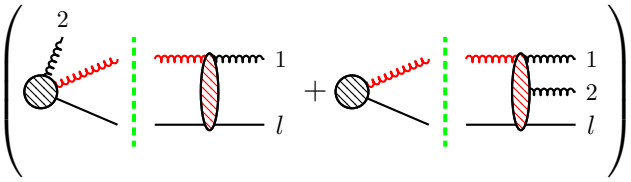

Figure 6.3: In the strongly ordered regime $q_1 \gg q_2$ the sum of these two gauge invariant physical mechanisms adds up to the simple transverse momentum expression given by Eq. (6.23).

There are only two more distinct physical mechanisms left to study, these are illustrated in Fig. 6.3. Up to this point, we found that the individual expression for each physical mechanisms has a simple structure in the strongly ordered region, $q_1 \gg q_2$. This is not the case for these two mechanisms[4]. Nevertheless, their expressions in the strongly ordered limit greatly simplifies when these are combined together, for each outgoing parton l they sum up to

$$\sum_{\substack{j=1\\ j\neq\{l\}}}^{n} \Big\{ \mathbf{C}^{lq_1}(0, \tilde{q}_2)\, \mathbf{J}_{n+2}(q_2) + \mathbf{J}_{n+2}(q_2) \mathbf{C}^{lq_1}\left(\tilde{q}_2, q_{1T(jl)}\right) \Big\} \mathbf{d}_{n+1(jl)}(q_1) \Big| n^{(0)} \Big\rangle \tag{6.23}$$

where $\mathbf{d}_{n+1(jl)}(q_1)$ is defined identically to the dipole operator that we introduced for the re-scattering cuts of the one-emission amplitude (see Eq. (3.39)) and, as in Eq. (6.16), where $\tilde{q}_2 = q_{2T(lq_1)}$ when used in the argument of an $\mathbf{C}^{lq_1}$.

As in the case of one-emission, in Eq. (6.23) the emission of a gluon q_1 that may subsequently exchange Coulomb gluons is emitted from dipoles, $\mathbf{d}_{n+1(jl)}(q_1)$, and each dipole sets an effective hard scale for the k_T of the subsequent Coulomb exchange, i.e. $k_T < q_{1T(jl)}$. Crucially, Eq. (6.23) shows that when there is a real emission and a Coulomb exchange after the dipole, the Coulomb exchanges are ordered exactly as the eikonal cuts. More precisely, the softer of the emissions appears emitted through a current, $\mathbf{J}_{n+2}(q_2)$, and the k_T of the Coulomb gluon is ordered with respect to the

[4]Of course, the first mechanism would simplify in the opposite strongly ordered region $q_2 \gg q_1$ as the the contributions in Fig. 6.2 do when $q_1 \gg q_2$, i.e. Eq. (6.22).

transverse momentum of this emission: when the emission acts closer to the hard process the Coulomb gluon has $k_T < q_{2T(q_1 l)}$ and when the Coulomb gluon acts closer to the hard process it has $q_{2T(q_1 l)} < k_T$. Expression (6.23) is a crucial result of this chapter as it highlights a remarkably simple structure that cannot be inferred from previous chapters.

6.6.1 Physical picture

As we already mentioned, the $2 \to 2$ and the $2 \to 3$ on-shell scattering illustrated in Fig. 6.3 have complicate expressions. Nevertheless, in this section we will show that when their expression are combined in a different way than above to render physics analogous to the eikonal cuts of the one-emission case. To be precise about how to combined these scatterings, it is convenient to point out that contributions of the $2 \to 3$ scattering Fig. 6.3 can be written in terms of the following colour tensors:

$$\mathbf{M}^{c_1,c_2}_{2\to 3,l}(q_2,q_1)\Big|n^{(0)}\Big\rangle = \\ g_s^2 \sum_{\substack{j=1 \\ j\neq\{l\}}}^{n} \left[\mathbf{T}_l^d \; i f^{dc_2 g} i f^{gc_1 e} \; \mathbf{T}_j^e \; \mathcal{F}^{lj}(q_1,q_2) + \mathbf{T}_l^d \; i f^{dc_1 g} i f^{gc_2 e} \; \mathbf{T}_j^e \; \mathcal{F}^{lj}(q_2,q_1)\right] \Big|n^{(0)}\Big\rangle \; . \tag{6.24}$$

The function $\mathcal{F}^{lj}(q_1,q_2)$ has a very simple behaviour in the strongly ordered regime, $q_1 \gg q_2$,

$$\mathcal{F}^{lj}(q_1,q_2) = \frac{i\pi\alpha_s}{2\pi}\left[\frac{p_l\cdot\varepsilon_2}{p_l\cdot q_2} - \frac{q_1\cdot\varepsilon_2}{q_1\cdot q_2}\right]\left[\frac{p_j\cdot\varepsilon_1}{p_j\cdot q_1} - \frac{p_l\cdot\varepsilon_1}{p_l\cdot q_1}\right]\int_{q^2_{2T(lq_1)}}^{q^2_{1T(lj)}}\frac{\mathrm{d}k_T^2}{k_T^2} \; . \tag{6.25}$$

Then, by using the colour algebra and colour conservation, the sum of these contributions can be written as

$$\sum_{\substack{j=1 \\ j\neq\{l\}}}^{n} \mathbf{T}_l^d \; i f^{dc_2 g} i f^{gc_1 e} \; \mathbf{T}_j^e \; \mathcal{F}^{lj}(q_1,q_2)\Big|n^{(0)}\Big\rangle = \tag{6.26}$$
$$\sum_{\substack{j=1 \\ j\neq\{l\}}}^{n} \left\{\frac{-i\pi\alpha_s}{2\pi}\mathbf{T}_l^a \; i f^{ac_2 d}(\mathbf{T}^d_{q_1})_{c_1 b_1} \int_{q^2_{2T(q_1 l)}}^{q^2_{1T(jl)}}\frac{\mathrm{d}k_T^2}{k_T^2}\left[\frac{p_l\cdot\varepsilon_2}{p_l\cdot q_2} - \frac{q_1\cdot\varepsilon_2}{q_1\cdot q_2}\right]\right\} \mathbf{d}^{b_1}_{n+1(jl)}(q_1)\Big|n^{(0)}\Big\rangle \; .$$

Each term inside braces has the same structure as the physical mechanism that we denoted by $(\mathrm{A}^{\mathrm{out}}_{lm})$ in the one-emission case, i.e. Eq. (3.19). In this comparison, we are identifying parton m with the harder emission q_1 and the dipole momentum $q_{1T(jl)}$ with hard scale Q.

The coefficient functions $\mathcal{F}^{lj}(q_2,q_1)$ that gives rise to the remaining contributions

in Eq. (6.24) do not have a simple behaviour in the strongly ordered limit, $q_2 \ll q_1$. The total expression for the $2 \to 2$ scattering in Fig. 6.3, $\mathbf{M}^{c_1,c_2}_{2\to 2,l}(q_2,q_1)\left|n^{(0)}\right\rangle$ is also complicated in this limit. However, they sum up to a simple expression:

$$\left[\mathbf{M}^{c_1,c_2}_{2\to 2,l}(q_2,q_1) + \sum_{\substack{j=1\\ j\neq\{l\}}}^{n} \mathbf{T}^d_j \; if^{dc_1g} if^{gc_2e}\; \mathbf{T}^e_l \; \mathcal{F}^{lj}(q_2,q_1)\right]\left|n^{(0)}\right\rangle = \\ \left\langle c_1c_2\right| \sum_{\substack{j=1\\ j\neq\{l\}}}^{n} \mathbf{C}^{lq_1}\left(0, q_{1T(jl)}\right)\mathbf{J}_{n+2}(q_2)\,\mathbf{d}_{n+1(jl)}(q_1)\left|n^{(0)}\right\rangle \,. \tag{6.27}$$

Observe that the Coulomb gluon is completely independent of the softer emission q_2. This is exactly the physical picture that we encountered for the cuts of type (B^{out}_{lm}) in the one-emission case, see the second line in Eq. (3.19). In this comparison $\mathbf{d}^{b_1}_{n+1(jl)}(q_1)\left|n^{(0)}\right\rangle$ is thought of as the effective hard subprocess and we are identifying parton m with q_1 and the dipole momentum $q_{1T(jl)}$ with the hard scale Q.

To show that the sum of Eqs. (6.26) and (6.27) is equal to Eq. (6.23) we point out that (6.26) can also be written as

$$\sum_{\substack{j=1\\ j\neq\{l\}}}^{n} \mathbf{T}^d_l \; if^{dc_2g} if^{gc_1e}\; \mathbf{T}^e_j \; \mathcal{F}^{lj}(q_1,q_2)\left|n^{(0)}\right\rangle = \\ \left\langle c_1c_2\right| \sum_{\substack{j=1\\ j\neq\{l\}}}^{n} \left[\mathbf{T}_l \frac{p_l\cdot\varepsilon_2}{p_l\cdot q_2} + \mathbf{T}_{q_1}\frac{q_1\cdot\varepsilon_2}{q_1\cdot q_2}\,,\, \mathbf{C}^{lq_1}\left(\tilde{q}_2, q_{1T(lj)}\right)\right]\mathbf{d}_{n+1(jl)}(q_1)\left|n^{(0)}\right\rangle \,. \tag{6.28}$$

6.7 Conjecture for the case of many emissions

In the case of the one-loop amplitude with more than two real emissions we expect that the amplitude can still be organised into the different mechanisms for multi-gluon emission as we did in Fig. 6.1. To be precise, we expect that the amplitude will be equal to the sum of eikonal cuts in the initial and final state, cuts over soft gluons and re-scattering cuts. We recall that we already conjectured the expression for the eikonal cuts, see Eq. (6.16). In this section, we present a conjecture for the sum of all of the re-scattering and soft gluon cuts.

Let us start by recalling that, in the strongly ordered region ($q_1 \gg q_2$), the total expression for the soft gluon cuts, Eq. (6.20), and the re-scattering cuts, Eqs. (6.23)

and (6.22), can be written as

$$\left\{\sum_{l=1}^{n+1}\tilde{\delta}_{lq_2}\sum_{j\neq\{l\}}^{n+1}\mathbf{C}^{lq_2}\big(0,q_{2T(jl)}\big)\,\mathbf{d}_{n+2(jl)}(q_2)\right\}\mathbf{J}_{n+1}(q_1)\Big|n^{(0)}\Big\rangle \tag{6.29}$$
$$+\sum_{l=1}^{n}\tilde{\delta}_{lq_1}\sum_{j\neq\{l\}}^{n}\left[\mathbf{C}^{lq_1}(0,\tilde{q}_2)\,\mathbf{J}_{n+2}(q_2)+\mathbf{J}_{n+2}(q_2)\mathbf{C}^{lq_1}\left(\tilde{q}_2,q_{1T(jl)}\right)\right]\mathbf{d}_{n+1(jl)}(q_1)\Big|n^{(0)}\Big\rangle\,.$$

The complete imaginary part of the double emission amplitude is given by adding the eikonal cuts in Eq. (6.15) to this expression. Observe that the first sum symbol (to the left) runs over the Coulomb exchanges between each of the gluon emissions and harder partons.

In the case of a general hard scattering process accompanied with b strongly ordered gluon emissions $\{p_1,\dots p_n\}\gg q_1\gg\cdots\gg q_a\gg\cdots\gg q_b$ we conjecture that the total expression for the sum of re-scattering and soft gluon cuts can be written as the sum over the Coulomb exchanges between each gluon emission q_a and harder outgoing partons. More precisely, the sum of Coulomb exchanges between q_a and each of the outgoing hard partons and between q_a and each of the harder gluon emissions, $\{q_{a+1},\dots,q_1\}$. In addition, based upon the structure exhibited by Eq. (6.29), we expect that the sum of the Coulomb gluon exchanges between q_a and each of the harder outgoing partons l yields:

$$\tilde{\delta}_{lq_a}\sum_{\substack{j=1\\ j\neq\{l\}}}^{n+a-1}\big[\mathbf{C}^{lq_a}(0,\tilde{q}_b)\,\mathbf{J}(q_b)\cdots\mathbf{J}(q_{a+1})+\mathbf{J}(q_b)\,\mathbf{C}^{lq_a}(\tilde{q}_{b-1},\tilde{q}_b)\,\mathbf{J}(q_{b-1})\cdots\mathbf{J}(q_{a+1})$$
$$+\ldots+\mathbf{J}_{n+b}(q_b)\cdots\mathbf{J}(q_{a+2})\,\mathbf{C}^{lq_a}(\tilde{q}_{a+2},\tilde{q}_{a+1})\,\mathbf{J}_{n+a+1}(q_{a+1}) \tag{6.30}$$
$$\left\{\mathbf{J}(q_b)\cdots\mathbf{J}(q_{a+1})\,\mathbf{C}^{lq_a}\big(\tilde{q}_{a+1},\tilde{q}_{aT(jl)}\big)\right\}\Big]\,\mathbf{d}_{(jl)}(q_a)\Big|n^{(0)}_{+a-1}\Big\rangle\,,$$

where the dipole operator is defined as before:

$$\mathbf{d}_{n+a(jl)}(q_a)\equiv g_s\mu^{\epsilon}\mathbf{T}_j\left[\frac{p_j\cdot q_a}{p_j\cdot q_a}-\frac{p_l\cdot q_a}{p_l\cdot q_a}\right], \tag{6.31}$$

and it should be understood the momentum and colour charge of the $(n+d)$th parton are denoted by $p_{n+d}=q_d$ and $\mathbf{T}_{n+d}=\mathbf{T}_{q_d}$.

Each of the terms in Eq. (6.30) has the same structure as those in (6.29). Precisely speaking, this structure is defined as follows:

- Before q_a is emitted, the gluons harder than q_a are radiated via soft-gluon

currents, i.e.

$$\left|n^{(0)}_{+a-1}\right\rangle = \mathbf{J}_{n+a-1}(q_{a-1})\mathbf{J}_{n+a-2}(q_{a-2})\dots\mathbf{J}_{n+1}(q_1)\left|n^{(0)}\right\rangle \ . \tag{6.32}$$

Observe that this is in agreement with the first line on the right-hand side of (6.29).

- Since q_a will subsequently exchange a Coulomb gluon, with parton l, it is emitted via a dipole operator $\mathbf{d}_{n+a,(jl)}(q_a)$ formed by parton l and each of the harder partons $j \leq n+a$ different from parton l:

$$\sum_{\substack{j=1\\ j\neq\{l\}}}^{n+a} [\dots]\mathbf{d}_{n+a(lj)}(q_a)\left|n^{(0)}_{+a-1}\right\rangle, \tag{6.33}$$

  where the ellipsis denote emissions or exchanges to the left of the dipole in Eq. (6.30). Indeed, the sum over all possible dipoles adds up to a soft-gluon current:

$$\sum_{\substack{j=1\\ j\neq\{l\}}}^{n+a} \mathbf{d}_{n+a,(lj)}(q_a)\left|n^{(0)}_{+a-1}\right\rangle = \mathbf{J}_{n+a}(q_2)\left|n^{(0)}_{+a-1}\right\rangle \ . \tag{6.34}$$

- Each dipole sets an effective hard scale that limits the transverse momentum, k_T, of the subsequent Coulomb exchanges, i.e $k_T < q_{aT(lj)}$.

- Finally, the term enclosed in squared brackets in Eq. (6.30) accounts for the softer emissions, $q_b \ll q_{b-1} \ll \dots q_{a+1}$, emitted via soft-gluon currents and Coulomb gluon operators that appear ordered with respect transverse momentum of these emissions. More precisely, the transverse momentum components defined by the direction of the partons that exchange the Coulomb gluon, i.e. $\{q_a, l\}$. Observe that this is in accord with the second line in Eq. (6.29).

The total expression for the cuts over soft gluons and the re-scattering cuts is obtained by adding the Coulomb gluons exchanged (given by Eq. (6.30)) between each

gluon emission and other gluons or hard partons, i.e.

$$\begin{aligned}
&\sum_{a=1}^{b}\sum_{l=1}^{n+a-1}\tilde{\delta}_{q_a l}\sum_{\substack{j=1\\ j\neq\{l\}}}^{n+a-1}\Bigg[\Big\{\mathbf{C}^{lq_a}(0,\tilde{q}_b)\,\mathbf{J}_{n+b}(q_b)\cdots\mathbf{J}_{n+a+1}(q_{a+1})\Big\}\\
&+\Big\{\mathbf{J}_{n+b}(q_b)\,\mathbf{C}^{lq_a}(\tilde{q}_{b-1,},\tilde{q}_b)\,\mathbf{J}_{n+b-1}(q_{b-1})\cdots\mathbf{J}_{n+a+1}(q_{a+1})\Big\}\\
&+\ldots+\Big\{\mathbf{J}_{n+b}(q_b)\cdots\mathbf{J}_{n+a+2}(q_{a+2})\,\mathbf{C}^{lq_a}(\tilde{q}_{a+2},\tilde{q}_{a+1})\,\mathbf{J}_{n+a+1}(q_{a+1})\Big\}\\
&+\Big\{\mathbf{J}_{n+b}(q_b)\cdots\mathbf{J}_{n+a+1}(q_{a+1})\,\mathbf{C}^{lq_a}\big(\tilde{q}_{a+1}\,,q_{aT(lj)}\big)\Big\}\Bigg]\,\mathbf{d}_{n+a(jl)}(q_a)\Big|n^{(0)}_{+a-1}\Big\rangle\;.
\end{aligned}\tag{6.35}$$

It is straightforward to check that for $b=1$ this expression is identical to the rescattering cuts in the one-emission case, Eq. (3.40), and that for $b=2$ this expression is equal to Eq. (6.29). Then, the total imaginary part of the double emission amplitude amplitude, Fig. 6.1, is obtained by adding the eikonal cuts in Eq. (6.16) to this expression.

Let us recall that when studied the one-emission and one-loop corrections in Section 3.4, it was found that the eikonal and Coulomb parts of the loop integrals had the same colour and kinematic pre-factors, see Eq. (3.36) and the discussion above this. If we assume that, in the presence of many gluon emissions, the eikonal and Coulomb contributions still have the same kinematical and colour pre-factors we can conjecture that the expression for the complete amplitude is given simply by replacing each of the Coulomb gluons in Eqs. (6.16) and (6.35) with

$$\begin{aligned}
\tilde{\delta}_{ij}\mathbf{C}^{ij}(\alpha,\beta) &= i\pi\tilde{\delta}_{ij}\epsilon\mathbf{T}_i\cdot\mathbf{T}_j\frac{\alpha_s c_\epsilon}{\epsilon^2}\left[\left(\frac{\beta^2}{\mu^2}\right)^{-\epsilon}-\left(\frac{\alpha^2}{\mu^2}\right)^{-\epsilon}\right]\\
&\to[1+i\pi\tilde{\delta}_{ij}\epsilon]\mathbf{T}_i\cdot\mathbf{T}_j\frac{\alpha_s c_\epsilon^2}{\epsilon^2}\left[\left(\frac{\beta^2}{\mu^2}\right)^{-\epsilon}-\left(\frac{\alpha^2}{\mu^2}\right)^{-\epsilon}\right],
\end{aligned}\tag{6.36}$$

To highlight the simplicity of this conjecture we rewrite it using a more compact notation. After making the substitution in Eq. (6.36), the complete amplitude with b strongly ordered emissions reads[5]

$$\begin{aligned}
\Big|n^{(1)}_{+b}\Big\rangle &= \sum_{m=0}^{b}\sum_{i=2}^{p}\sum_{j=1}^{i-1}\mathbf{J}(q_b)\cdots\mathbf{J}(q_{m+1})\,\mathbf{I}_{ij}(\tilde{q}_{m+1},\tilde{q}_m)\,\Big|n^{(0)}_{+m}\Big\rangle\\
&+\sum_{m=1}^{b}\sum_{j,k=1}^{n+m-1}\mathbf{J}(q_b)\cdots\mathbf{J}(q_{m+1})\,\mathbf{I}_{n+m,j}(\tilde{q}_{m+1},q_{mT(jk)})\,\mathbf{d}_{jk}(q_m)\Big|n^{(0)}_{+m-1}\Big\rangle,
\end{aligned}\tag{6.37}$$

[5]Omitting the dimension of the current and dipole operators, i.e. $\mathbf{J}_{n+a}(a)\to\mathbf{J}(q_a)$ and $\mathbf{d}_{n+a(ij)}(a)\to\mathbf{d}_{(ij)}(q_a)$.

where $p = n$ if $m = 0$ or $p = n + m - 1$ if $m \geq 1$ and where the one-loop insertion operator is given by

$$\mathbf{I}_{ij}(\alpha, \beta) \;=\; \frac{\alpha_s}{2\pi}\frac{c_\epsilon}{\epsilon^2}\mathbf{T}_i \cdot \mathbf{T}_j \left(1 + i\tilde{\delta}_{ij}\pi\epsilon\right)\left\{\left(\frac{\beta^2}{\mu^2}\right)^{-\epsilon} - \left(\frac{\alpha^2}{\mu^2}\right)^{-\epsilon}\right\}\,, \qquad (6.38)$$

where $\tilde{q} = q_{Tij}$ when used in the argument of an $\mathbf{I}_{ij}$ operator. This expression summarises many of the results of this thesis. In particular, it reproduces our fixed order calculations for the one- and two- emission case. As in the one-emission case, see Eq. (3.36), we expect that Eq. (6.37) be accurate up to non-logarithmic terms of order ϵ^0 in the real part and order ϵ^1 in the imaginary part.

It is worth noting that the universality of the infrared singular behaviour of the one-loop QCD corrections, i.e. Eq. (2.39), places a strong constraint on our conjecture for the real part of the amplitude. The consistency with this constraint can be proven by induction over the number of emissions. In addition, the complete amplitude, Eq. (6.37), has two remarkable properties. Firstly, we point out that our conjecture for the complete amplitude is gauge invariant with respect to each of the soft emissions. The proof of gauge invariance follows directly from colour conservation, see Appendix B.1 for more details. Secondly, in an idealised wide-angle region[6] colour conservation can be used to write the complete amplitude (Eq. (6.37) as

$$\left|n^{(1)}_{+b}\right\rangle \;\approx\; \sum_{m=0}^{b}\sum_{i=2}^{n+m}\sum_{j=1}^{i-1}\mathbf{J}(q_b)\cdots\mathbf{J}(q_{m+1})\,\mathbf{I}_{ij}(q^0_{m+1}, q^0_m)\left|n^{(0)}_{+m}\right\rangle\,. \qquad (6.39)$$

This expression is equal to the one-loop matrix elements of the energy-ordered colour evolution picture, i.e. first line of Eq. (2.71) with the Sudakov operators expanded at one-loop order. A naïve use of quantum uncertainty suggests to associate a time scale to the radiation as the inverse of the magnitude of its momentum components. With this interpretation, the above expression exhibits a time-ordered structure. The importance of this property is that it suggests that, in the same idealised wide-angle region, the amplitude with many loops may also reduce to this energy-ordered picture. We close this chapter by mentioning that future studies should address the generalisation of the results presented in this chapter beyond one-loop order.

[6] $\hat{q}_c \cdot \hat{p}_i \approx 0$ for $i = \{1, \ldots n\}$ and $c = \{1, \ldots b\}$ and also $\hat{q}_a \cdot \hat{q}_c \approx 0$ for all $c \neq a$ with $a = 1, \ldots, b$.

Chapter 7

Conclusions

There has been a growing interest in ascertaining the contributions of Coulomb gluons to non-inclusive observables, in part spurred on by the discovery of the super-leading logarithms in 'gaps between jets', and also motivated by the fact that Coulomb gluons introduce violations of coherence and violations of strict collinear factorisation in partonic scatterings. Previous analyses have been based on the colour evolution picture, a framework devised to account for the soft gluon corrections to non-inclusive observables, including Coulomb gluons and their colour interference. In this thesis we have made substantial progress in determining the correct ordering variable that should be used.

We did this by making a full Feynman diagrammatic calculation of the one-loop correction to a general hard process accompanied by the emission of up to two gluons. Although different graphs have different and intricate ordering conditions, the result for the physical process, i.e. the sum of all contributions, can be written in terms of soft-gluon currents, dipole emissions and Coulomb gluon exchanges that satisfy very simple ordering conditions: the k_T of the Coulomb gluons should be always ordered with respect to the transverse momentum (defined by the direction of the two partons that exchange the Coulomb gluon) of the real emissions and, in addition, each soft gluon that may subsequently exchange a Coulomb gluon is emitted via a dipole that limits the k_T of the subsequent exchanges.

Based upon the assumption that this simple structure continues for the one-loop corrections to a general hard scattering accompanied by many more strongly ordered real emissions, we conjectured that the same ordering variable should be used to dress the imaginary part of the amplitude with many more real emissions, Eqs. (6.16) and (6.35). When we studied the one-loop, one-emission amplitude we also showed that the eikonal, or real, part of the loop corrections obeys the same simple ordering condition that the Coulomb exchange does. More precisely, the eikonal exchanges have the same colour and kinematic pre-factors; the only difference is that Coulomb gluons are only exchanged between incoming and between outgoing partons while

eikonal gluons are also exchanged between incoming and outgoing partons, Eq. (3.47). Based upon the assumption that, in the presence of many more emissions, eikonal and Coulomb gluons still satisfy the same ordering condition, we also conjectured an expression for the complete one-loop amplitude accompanied of any number of strongly ordered emissions, Eq. (6.37).

These studies constitute a formal step towards the inclusion of colour interference into parton shower event generators. Note that Coulomb gluon effects are currently neglected even in the recent framework [34] that incorporates some of the subleading colour interference. Furthermore, even in the large N_c approximation, our studies propose a particular parton shower in the sense that they suggest a specific variable that should be used to order the successive emissions. Hopefully, these studies will help to improve the accuracy of parton showers by using an ordering variable that correctly describes the leading behaviour of the matrix elements, as we did in this thesis.

Our analytical calculations have also shed light into the structure of Coulomb gluon corrections. Specifically, we have seen that the full emission and exchange process can be separated, gauge-invariantly, into distinct physical processes (Figs. 3.3 and 6.1). Each process corresponds to on-shell scattering between the incoming or between outgoing partons, with gluon emission being part of the hard process or any of exchange processes. Perhaps this offers hope of a deeper understanding of the role of Coulomb gluons and a generalisation of our calculation to an arbitrary number of loops.

Appendix A

Regularisation of one loop corrections

The integration of Eq. (2.15) is carried out in dimensional regularisation. The integration for each pair $\{i,j\}$ in the sum of Eq. (2.15) is more easily performed expressing the loop momentum k in light-cone variables $(k^-,k^+,k_\perp)$ defined as:

$$k^\mu = \frac{k^+}{\sqrt{2p_i\cdot p_j}}p_i^\mu + \frac{k^-}{\sqrt{2p_i\cdot p_j}}p_j^\mu + k_T^\mu \ , \tag{A.1}$$

where k_T is a $d-2$ dimensional vector that satisfies $p_i\cdot k_T = p_j\cdot k_T = 0$. In terms of these variables we have $\mathrm{d}^d k = \mathrm{d}k^+\mathrm{d}k^-\mathrm{d}^{d-2}k_T$ and $\delta^+(k) = \theta(k^+k^-)\delta(k^2)$. For the real part of the integrals, i.e. Eq. (2.16), the transverse components can be integrated out using the delta function[1]:

$$\int \frac{\mathrm{d}^d k}{(2\pi)^{d-1}} \frac{\delta^+(k) g_s^2 \mu^{2\epsilon} p_i\cdot p_j}{(p_j\cdot k)(p_i\cdot k)} = \frac{g_s^2\mu^{2\epsilon}c_\epsilon 2^{-\epsilon}}{8\pi^2}\int \mathrm{d}k^+ (k^+)^{-1-\epsilon}\int \mathrm{d}k^- (k^-)^{-1-\epsilon}. \tag{A.2}$$

The infrared divergences are regularised by performing the integration in $d = 4-2\epsilon > 4$ dimensions. In accordance with our usage of the eikonal rules, we cut-off momentum components above the hard scale $Q \sim \sqrt{2p_i\cdot p_j}$. To do this, we cut-off the integration over the light cone variables[2] $\{k^+,k^-\}$ respectively at the scales $\{p_i^+, p_j^-\}$. This can be done in a Lorentz invariant manner by constraining the integration domain using the step function $\theta_{ij}(k) = \theta(p_i\cdot(p_j-k))\theta(p_j\cdot(p_i-k))$

$$\begin{aligned} &\int \frac{\mathrm{d}^d k}{(2\pi)^{d-1}} \frac{\delta^+(k)\mu^{2\epsilon} p_i\cdot p_j}{(p_j\cdot k)(p_i\cdot k)} \to \int \frac{\mathrm{d}^d k}{(2\pi)^{d-1}} \frac{\delta^+(k)\mu^{2\epsilon}\theta_{ij}(k) p_i\cdot p_j}{(p_j\cdot k)(p_i\cdot k)} \ , \\ &= \frac{\alpha_s}{2\pi} c_\epsilon \left(\frac{2p_i\cdot p_j}{\mu^2}\right)^{-\epsilon} \frac{1}{(-\epsilon)^2}. \end{aligned} \tag{A.3}$$

[1] For an introductory reference to the integration of d dimensional solid angles see [9]

[2] Observe that by doing this the on-shell condition requires us to cut-off the transverse momentum l_T at $l_T^2 = 2p_i\cdot p_j$.

We now study the Coulomb part, i.e. Eq. (2.17). The delta functions fix $l^{\pm}$ equal to zero and one is left with an integral over the transverse momentum:

$$\frac{-ig^2\pi c_\epsilon \mu^{2\epsilon}}{8\pi^2}\int \frac{\mathrm{d}k_T^2}{k_T^{6-d}}. \tag{A.4}$$

In accordance with our previous approximation, we cut-off the integration of the transverse components at $l_T^2 = 2p_i\cdot p_j$. By doing this, integration in $d = 4-2\epsilon > 0$ dimensions yields

$$\frac{-i\pi\alpha_s c_\epsilon}{2\pi}\frac{1}{-\epsilon}\left(\frac{2p_i\cdot p_j}{\mu^2}\right)^{-\epsilon}. \tag{A.5}$$

Finally, we put together the eikonal (real) and Coulomb (imaginary) contributions

$$\int^Q \frac{\mathrm{d}^d l}{(2\pi)^d}\frac{g_s^2\mu^{2\epsilon}p_i\cdot p_j}{[p_i\cdot k+\delta_i\frac{i0}{2}][-p_j\cdot k+\delta_j\frac{i0}{2}][k^2+i0]} = \frac{\alpha_s c_\epsilon}{2\pi}\left[\frac{2p_i\cdot p_j}{\mu^2}\right]^{-\epsilon}\frac{[1+i\pi\epsilon]}{(-\epsilon)^2} \tag{A.6}$$

Clearly, this integral would be *uv* divergent without the upper cut-off. It is worth noting that this divergence is fictitious in the sense that it is introduced by the linearisation of propagators in the eikonal approximation. The exact integral would instead yield

$$\begin{aligned}
&\int \frac{\mathrm{d}^d k}{(2\pi)^d}\frac{-ip_i\cdot p_j}{[-p_j\cdot k+\delta_j\frac{i0}{2}][p_i\cdot k+\delta_i\frac{i0}{2}][l^2+i0]} \to \\
&\int \frac{\mathrm{d}^d k}{(2\pi)^d}\frac{-i4p_i\cdot p_j\delta_i\delta_j}{[(k-\delta_j p_j)^2+i0][(k+\delta_i p_i)^2+i0][k^2+i0]} \\
&= \frac{1}{8\pi^2}c_{\widetilde{\Gamma}}\left(\frac{2p_i\cdot p_j e^{-i\widetilde{\delta}_{ij}\pi}}{\mu^2}\right)^{-\epsilon}\frac{1}{\epsilon^2},
\end{aligned} \tag{A.7}$$

where $c_{\widetilde{\Gamma}} = \frac{(4\pi)^\epsilon\Gamma^2[1-\epsilon]\Gamma[1+\epsilon]}{\Gamma[1-2\epsilon]} = c_\epsilon + \mathcal{O}(\epsilon^3)$. Comparing expressions (A.6) and (A.7), we see that our naïve regularisation procedure gives us the correct expression up to constant terms of order ϵ^0.

Appendix B

Gauge invariance and consistency with the Bloch-Nordsieck theorem

In Section 2.5.1 we introduced the energy-ordered colour evolution picture. Its corresponding matrix elements are given in Eq. (2.71). In this appendix, we demonstrate that they are gauge invariant with respect to each gluon emission and that their inclusive integration is consistent with the Bloch-Nordsieck theorem.

B.1 Gauge invariance

The first show that the multi-emission tree-level matrix elements are gauge invariant. This can be done recursively. Let $|\mathcal{N}\rangle$ be any amplitude with n external partons that satisfies colour conservation $\sum_{k=1}^{n} \mathbf{T}_k^a |\mathcal{N}\rangle = 0$, then the amplitude $\mathbf{T}_i |\mathcal{N}\rangle$ with $i \in \{1, \ldots, n\}$ satisfies the identity

$$\left(\sum_{k=1}^{n} \mathbf{T}_k^a \delta^{bd} + i f^{bad} \right) \mathbf{T}_i^d \Big| \mathcal{N} \Big\rangle = 0 \; . \tag{B.1}$$

This can be shown using the colour algebra to commute $\mathbf{T}_k^a$ to the right of $\mathbf{T}_i^d$ in Eq. (B.1), then by colour conservation of $|\mathcal{N}\rangle$ the resulting expression vanishes. Observe that the term $if^{bad}\mathbf{T}_i^d$ is exactly the colour tensor corresponding to a gluon with colour a emitted off a gluon with colour b emitted off parton i. Thus, in a colour index free notation, Eq. (B.1) reads

$$\left(\sum_{k=1}^{n+1} \mathbf{T}_k \right) \mathbf{T}_i \Big| \mathcal{N} \Big\rangle = 0. \tag{B.2}$$

These observations show that the following tree level matrix element

$$\mathbf{J}_{n+2}(q_2)\mathbf{J}_{n+1}(q_1) \Big| n^{(0)} \Big\rangle, \tag{B.3}$$

is gauge invariant with respect to each of the two emissions. A recursive use of the above argument shows that the tree-level amplitude with any number of emissions, Eq. (2.62), is gauge invariant.

Now we move to consider the complete matrix elements dressed with their virtual corrections, i.e. Eq. (2.71). Let us first show $\mathbf{T}_i{\cdot}\mathbf{T}_j\,|\mathcal{N}\rangle$ with $i,j\in\{1,\ldots,n\}$ satisfies $\sum_i^n \mathbf{T}_k^a(\mathbf{T}_i{\cdot}\mathbf{T}_j)\,|\mathcal{N}\rangle = 0$ if $\sum_i^m \mathbf{T}_k^a\,|\mathcal{N}\rangle = 0$ does. Again, thanks to colour conservation, the following identity holds

$$\left(\sum_{k=1}^{m}\mathbf{T}_k^a\right)\,\mathbf{T}_i{\cdot}\mathbf{T}_j\Big|\mathcal{N}\Big\rangle = \left[\mathbf{T}_i{\cdot}\mathbf{T}_j,\sum_{k}^{m}\mathbf{T}_k^a\right]\Big|\mathcal{N}\Big\rangle. \tag{B.4}$$

Using the colour algebra, it is straightforward to show that this commutator vanishes. This observation together with the proof of gauge invariance at tree-level shows that the matrix elements in Eq. (2.71) expanded at one-loop order is also gauge invariant. Finally, it is easy to generalise this argument for an arbitrary number of virtual emissions. To see this, observe that same argument applied recursively shows that $(\mathbf{T}_{i_1}\cdot\mathbf{T}_{j_1})\ldots(\mathbf{T}_{i_m}\cdot\mathbf{T}_{j_m})\,|\mathcal{N}\rangle$ with $\{i_e,j_e\}\in\{1,\ldots,n\}$ satisfies the same colour conservation equation that $|\mathcal{N}\rangle$ does. Hence, we have shown that the all orders matrix elements Eq. (2.65), with or without Coulomb interactions, are gauge invariant with respect to each gluon emission.

B.2 Bloch-Nordsieck cancellation of soft gluons

We will show that the inclusive integration of the matrix elements in Eq. (2.67) is consistent with the Bloch-Nordsieck theorem, i.e. soft gluon corrections exactly cancel. To do this, it is convenient to define an additional piece of notation for the argument of the Sudakov operators, Eq. (2.71),

$$\mathbf{I}_{n+r}^{(\beta,\alpha)} \equiv \left[\frac{1}{2}\int \mathrm{d}[k]\mathbf{J}_{r+1}(k){\cdot}\mathbf{J}_{r+1}(k)\Theta(\alpha<k_0<\beta)+\sum_{i<j}^{n}\delta_{ij}\mathbf{C}_{ij}^{(\beta,\alpha)}\right], \tag{B.5}$$

where k_0 denotes the energy component of the virtual emission. Also, to avoid cluttered algebra we modify our notation for the current operators as: $\mathbf{J}_{n+r}\to\mathbf{J}_r$.

Expectation value of a squared current

We first prove the identity:

$$\mathbf{V}_n^{(0,Q)\dagger}\mathbf{V}_n^{(0,Q)}-1=\int \mathrm{d}[q_1]\mathbf{V}_n^{(q_1^0,Q)\dagger}\mathbf{J}_1^2(q_1)\mathbf{V}_n^{(q_1^0,Q)}\,\Theta(0<q_1^0<Q), \tag{B.6}$$

where we used the shorthand $\mathbf{J}_1^2(q_1) \equiv \mathbf{J}_1^\mu(q_1)\cdot\mathbf{J}_{1\mu}(q_1)$ and the Sudakov operator, ordered in energy, is given in Eq. (2.71). This identity can be proven by expanding the right hand side as

$$\begin{aligned}
&\int \mathrm{d}[q_1] \sum_{m,r=0}^{\infty} \frac{(\mathbf{I}_n^{(q_1^0,Q)\dagger})^m}{m!}\mathbf{J}_1^2(q)\frac{(\mathbf{I}_n^{(q_1^0,Q)})^r}{r!}\,\Theta(0<q_1^0<Q)\\
&= \sum_{m,r=0} \frac{1}{m+r+1}\left[\frac{(\mathbf{I}_n^{(0,Q)\dagger})^m}{m!}\left(\int \mathrm{d}[q]\mathbf{J}_1^2(q_1)\Theta(0<q_1^0<Q)\right)\frac{(\mathbf{I}_n^{(0,Q)})^r}{r!}\right] \qquad \text{(B.7)}\\
&= \sum_{m,r=0}^{\infty} \frac{1}{m+r+1}\left[\frac{(\mathbf{I}_n^{(0,Q)\dagger})^{m+1}}{m!}\frac{(\mathbf{I}_n^{(0,Q)})^r}{r!}+\frac{(\mathbf{I}_n^{(0,Q)\dagger})^m}{m!}\frac{(\mathbf{I}_n^{(0,Q)})^{r+1}}{r!}\right]\\
&= \left[\mathbf{V}_n^{(0,Q)\dagger}\mathbf{V}_n^{(0,Q)}-1\right].
\end{aligned}$$

In the second line we used the following identity

$$\left[\int_a^b \mathrm{d}l_0 f(l_0)\right]\left[\int_a^{l_0}\mathrm{d}k_0 f(k_0)\right]^{m+r} = \frac{1}{(m+r+1)}\left[\int_a^b \mathrm{d}l_0 f(l_0)\right]^{m+r+1}, \qquad \text{(B.8)}$$

and, to deduce the third line from the second, we replaced the integral inside parenthesis by $\mathbf{I}_n^{(0,Q)}+\mathbf{I}_n^{(0,Q)\dagger}$. Eq. (B.6) is just the simplest case of the following series of identities for $r=\{0,1,\dots\}$:

$$\mathbf{V}_{n+r}^{(0,q_r^0)\dagger}\mathbf{V}_{n+r}^{(0,q_r^0)}-1 = \int \mathrm{d}[q_{r+1}]\mathbf{V}_{n+r}^{(q_{r+1}^0,q_r^0)\dagger}\mathbf{J}_{r+1}^2(q_{r+1})\mathbf{V}_{n+r}^{(q_{r+1}^0,q_r^0)}\,\theta(0<q_{r+1}^0<q_r^0), \quad \text{(B.9)}$$

that can be shown along the same lines as Eq. (B.6). Each of these identities relates the virtual corrections to a hard process with n partons and r soft gluon emissions to the matrix element obtained by inserting an additional softer emission.

All orders soft corrections

Let us calculate the contributions to an observable ϕ using the matrix elements of the colour evolution picture ordered in energy, i.e. Eq. (2.71). The contribution due to purely virtual corrections is

$$\sigma_0 \equiv \langle n|n\rangle = \left\langle n^{(0)}\right|\left[\left(\mathbf{V}_n^{(0,Q)\dagger}\mathbf{V}_n^{(0,Q)}-1\right)+\{1\}\right]\left|n^{(0)}\right\rangle, \qquad \text{(B.10)}$$

while the contribution due to the amplitude with m soft emissions is

$$\sigma_m \equiv \frac{m!}{m!}\int_{0<q_m^0<\dots q_1^0<Q}\langle n_{+m}|n_{+m}\rangle\,\phi_{\{m\}} \qquad \text{(B.11)}$$

where we used the following short-hand notation

$$\int_{0<q_m^0<\ldots q_1^0<Q} \equiv \int \mathrm{d}[q_m]\ldots\mathrm{d}[q_1]\,\Theta(0<q_m^0<\ldots q_1^0<Q)\ . \tag{B.12}$$

The $m!$ in the denominator (numerator) is the symmetry factor for m identical gluon emissions (different energy-ordered configurations). Finally, $\phi_{\{m\}}$ is the function that defines the observable for m gluon emissions. It is convenient to re-write the $m\geq 1$ emissions amplitude as

$$\begin{aligned}\sigma_m = \int_{0<q_m^0<\ldots q_1^0<Q} \Bigg\{ &\left\langle n'_{+m}\right| \left(\mathbf{V}_{n+m}^{(0,q_m^0)\dagger}\mathbf{V}_{n+m}^{(0,q_m^0)} - 1\right)\left|n'_{+m}\right\rangle \\ &- \left\langle n'_{+m-1}\right|\mathbf{V}_{n+m-1}^{(q_m^0,q_{m-1}^0)\dagger}\mathbf{J}_m^2(q_m)\mathbf{V}_{n+m-1}^{(q_m^0,q_{m-1}^0)}\left|n'_{+m-1}\right\rangle\Bigg\}\phi_{\{m\}},\end{aligned} \tag{B.13}$$

where we have used the definition

$$\left|n'_{+m}\right\rangle \equiv \mathbf{J}_m(q_m)\mathbf{V}_{n+m-1}^{(q_m^0,q_{m-1}^0)}\mathbf{J}_{m-1}(q_{m-1})\ldots\mathbf{V}_{n+1}^{(q_2^0,q_1^0)}\mathbf{J}_1(q_1)\mathbf{V}_n^{(q_1^0,Q)}\left|n^{(0)}\right\rangle. \tag{B.14}$$

Observe that $\left|n'_{+m}\right\rangle$ is almost identical to $|n_{+m}\rangle$, but in the former, the softest (leftmost) emission is not dressed with virtual corrections with energies in the interval $(0,q_m^0)$. Finally, using the above definitions, the corrections to an observable ϕ to all orders reads

$$\begin{aligned}&\sum_{m=0}^{\infty}\sigma_m = \left\langle n^{(0)}\right|\left.n^{(0)}\right\rangle + \sum_{m=0}^{\infty}\int_{0<q_m^0<\ldots q_1^0<Q}\left\langle n'_{+m}\right|\Bigg[\left(\mathbf{V}_{n+m}^{(0,q_m^0)\dagger}\mathbf{V}_{n+m}^{(0,q_m^0)} - 1\right)\phi_{\{m\}} \\ &- \int \mathrm{d}[q_{m+1}]\Theta(0<q_{m+1}^0<q_m^0)\mathbf{V}_{n+m}^{(q_{m+1}^0,q_m^0)\dagger}\mathbf{J}_{m+1}^2(q_{m+1})\mathbf{V}_{n+m}^{(q_{m+1}^0,q_m^0)}\phi_{\{m+1\}}\Bigg]\left|n'_{+m}\right\rangle \\ &= \left\langle n^{(0)}\right|\left.n^{(0)}\right\rangle + \sum_{m=0}^{\infty}\int_{0<q_m^0<\ldots q_1^0<Q}\left\langle n'_{+m}\right|\Bigg[\int \mathrm{d}[q_{m+1}]\left[\phi_{\{m+1\}}-\phi_{\{m\}}\right] \\ &\Theta(0<q_{m+1}^0<q_m^0)\mathbf{V}_{n+m}^{(q_{m+1}^0,q_m^0)\dagger}\mathbf{J}_{m+1}^2(q_{m+1})\mathbf{V}_{n+m}^{(q_{m+1}^0,q_m^0)}\Bigg]\left|n'_{+m}\right\rangle\ .\end{aligned} \tag{B.15}$$

Here it should be understood that $\left|n'_{+0}\right\rangle = \left|n^{(0)}\right\rangle$ and to deduce the second equality we made use of the identities in Eq. (B.9). Observe that for a total cross section, i.e. $\phi_{\{m\}}=1$, all soft corrections identically vanish and one is left only with the Born level amplitude. A discussion of the general conditions that a general observable must satisfy in order to be collinear safe is beyond the scope of this appendix. Nevertheless, we can point out an important feature of the last expression. Suppose that the observable is fully inclusive below a scale Q_0. In this case, Eq. (B.15) shows that one can set Q_0 as the lower integration limit of real and virtual corrections.

Appendix C

Choice of polarisation vectors

A choice of polarisation vectors in the Feynman gauge is presented that enables us to consider collinear limits at amplitude level [85]. The kinematic configuration in which a physical light-like vector q becomes collinear with another light-like vector p_k can be parametrised as the limit $q^\mu_{T,kr} \to 0$ of the following Sudakov decomposition:

$$q^\mu = \frac{r\cdot q}{r\cdot p_k} p_k^\mu + \frac{q^2_{T,kr}}{2r\cdot q} r^\mu + q^\mu_{T,kr} \ , \tag{C.1}$$

where r^μ is a light-like reference vector that parametrises how the collinear limit is approached. In order to compute collinear limits at amplitude level it is convenient work with the following choice of polarisation vectors:

$$\begin{aligned} \varepsilon^\mu(q,\perp) &\equiv \frac{i\epsilon^{\mu\nu\alpha\beta} q_\nu p_{k_\alpha} r_\beta}{\sqrt{2p_k\cdot r p_k\cdot q r\cdot q}} \ , \\ \varepsilon^\mu(q,\parallel) &\equiv \frac{q\cdot r p_k^\mu - q\cdot p_k r^\mu - p_k\cdot r q^\mu}{\sqrt{2p_k\cdot r p_k\cdot q r\cdot q}} \ . \end{aligned} \tag{C.2}$$

One can show by direct substitution that they have the correct normalisation

$$\varepsilon^*(q,\sigma)\cdot\varepsilon(q,\sigma') = -\delta_{\sigma\sigma'}, \tag{C.3}$$

and that the sum over polarisations yields

$$\sum_{\sigma=\perp,\parallel} \varepsilon^{*\mu}(q,\sigma)\varepsilon^{*\nu}(q,\sigma) = -g^{\mu\nu} + \frac{q^\mu r^\nu + q^\nu r^\mu}{q\cdot r} \ . \tag{C.4}$$

Polarisation vectors can be also Sudakov decomposed as

$$\varepsilon(q,\sigma) = \frac{\varepsilon^+(q,\sigma)}{\sqrt{p_k\cdot r}} p_k^\mu + \frac{\varepsilon^-(q,\sigma)}{\sqrt{p_k\cdot r}} r^\mu + \varepsilon_T^\mu(q,\sigma). \tag{C.5}$$

In the collinear limit $q_{T,rk} \to 0$, all the (non-vanishing) components of polarisation vectors behave like $(q_{T,rk})^0$ except the minus component of the parallel polarisation $\varepsilon^-(q,\|) = -|q_{T,rk}|\sqrt{p_k\cdot r}/r\cdot q$, which vanishes linearly in this limit.

Proof: Introducing the decomposition of q into the above polarisation vectors we get

$$\varepsilon(q,\perp) = \frac{\epsilon_{\mu\nu\alpha\beta}q_T^\nu p_k^\alpha r^\beta}{p_k\cdot r|q_{T,kr}|}, \tag{C.6}$$

$$\varepsilon(q,\|) = -\frac{|q_{T,kr}|}{r\cdot q}r^\mu - \frac{1}{|q_{T,kr}|}q_{T,kr}^\mu. \tag{C.7}$$

We can rewrite these polarisation vectors as follows

$$\varepsilon(q,\sigma) = \frac{\varepsilon^+(q,\sigma)}{\sqrt{p_k\cdot n}}p_k^\mu + \frac{\varepsilon^-(q,\sigma)}{\sqrt{p_k\cdot r}}r^\mu + \varepsilon_T^\mu(q,\sigma), \tag{C.8}$$

because of Eq. (C.6) we have $p_k\cdot\varepsilon(q,\perp) = r\cdot\varepsilon(q,\perp) = 0$ and hence $\varepsilon^+(q,\perp) = \varepsilon^-(q,\perp) = 0$. Also, since $q\cdot\varepsilon(q,\perp) = 0$ one has $q_{T,kr}\cdot\varepsilon(q,\perp) = 0$ and therefore the vector $\varepsilon(q,\perp) = \varepsilon_T(q,T)$ lies in the transverse plane (to the colliding axis) and is perpendicular to $q_{T,kr}^\mu$. Similarly, for the polarisation in Eq. (C.7), one can show that $\varepsilon^+(q,\|) = 0$, $\varepsilon^-(q,\|) = -|q_{T,kr}|\sqrt{p_k\cdot r}/r\cdot q$ and $\varepsilon_T^\mu(q,\|) = -q_{T,kr}^\mu/|q_{T,kr}|$.

An entirely analogous proof shows that if we rescale $r\cdot q \to r\cdot q/\lambda$ in Eq. (C.1) and take the limit $\lambda \to 0$, all the (non-vanishing) components of polarisation vectors behave like λ^0 except for the minus component of the parallel polarisation $\varepsilon^-(q,\|) \sim \lambda$, which linearly vanishes in this limit. This is the case relevant for limit 3 in Section 5.1.

C.1 Collinear limit of the tree-level single emission amplitude

To illustrate the use of the above vectors, we will now compute the collinear limit of the single emission amplitude at tree-level, i.e. $\left|n_{+1}^{(0)}\right\rangle$. In this limit:

$$\lim_{q_{T,kr}\to 0}\mathbf{J}_{n+1}^\mu(q)\left|n^{(0)}\right\rangle = \left(g\mu^\epsilon\mathbf{T}_k\frac{p_k^\mu}{p_k\cdot q} + \mathcal{O}(q_{T,kr}^0)\right)\left|n^{(0)}\right\rangle, \tag{C.9}$$

where $p_k\cdot q = \mathcal{O}(q_{T,rk}^2)$. We have not yet included the contribution of the polarisation vector of the soft emission. To do this one needs to contract the leading term on the right-hand side of this expression with the different polarisations. Because $p_k\cdot\varepsilon(q,\perp) = 0$, the contraction of $\varepsilon(q,\perp)$ is subleading and, thus, the contraction

with $\varepsilon(q, \|)$ gives the leading contribution:

$$\widetilde{\mathbf{Sp}}^{(0)}(q, p_k) \equiv \lim_{q\|p_k} \mathbf{J}_{n+1}(q)\cdot\varepsilon(\|) = \mathbf{T}_k \frac{-2g\mu^\epsilon}{|q_{T,rk}|}. \tag{C.10}$$

One can check that the leading behaviour of the squared amplitude is equal to the leading behaviour of the amplitude squared.

Appendix D

Cutting rules

In this appendix we derive cutting rules to isolate the real and imaginary parts of one-loop graphs in the eikonal approximation. For simplicity, we consider graphs with only incoming hard partons[1] with momenta $\{p_i, p_j\}$ and any number of gluon emissions. However, by the end of the appendix it will be clear that these derivations can be extended to a more general process.

In principle, instead of the rules derived in this appendix we could have used Cutkosky rules [103] or the Feynman tree theorem [104]. Instead, we found it useful to derive cutting rules to isolate the imaginary parts of the loop integrals by studying the contour integration of individual graphs; in the eikonal approximation there is a cancellation between many contributions that enter in intermediate steps. Incidentally, our derivation of the cutting rules to isolate the imaginary contribution will give us, as a by-product, rules to calculate also the real part of the loop integrals.

As the derivation of these rules is technical, we first present the cutting rules that are relevant in the rest of this thesis for the imaginary contributions in Section D.1 and for the real parts in Section D.2 . Then, we shall discuss the mechanism responsible for the cancellation of many imaginary contributions in Section D.3 and for many real contributions in Section D.4. Finally, in Section D.5 we work out the complete derivation of the cutting rules to isolate the imaginary and real parts for a particular graph, but the derivation for other graphs can be done along the same lines.

D.1 Cutting rules to calculate the imaginary part

It is convenient to organise the one-loop amplitude according to whether the loop involves both of the incoming hard partons, one hard parton or no hard partons,

[1] As in a Drell-Yan process.

e.g. as in Figure D.1. Here we derive the cutting rules that we use to determine the imaginary part of the first two of these three types of graph. The third type of graph is an exact loop integral because it does not have any virtual propagator in the eikonal approximation. For this topology class more conventional methods can be applied[2].

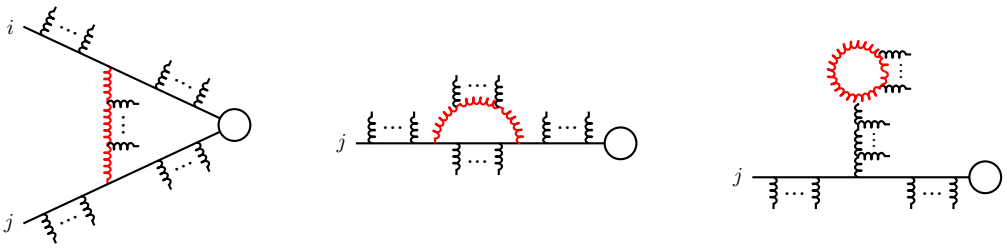

Figure D.1: The three types of one loop contribution. Only those hard parton legs that couple to the virtual exchange are drawn.

Let us consider a general one-loop integral involving both incoming hard partons (e.g. the left-most graph in Figure D.1). Real emissions occuring before the virtual exchange lead to propagators that do not depend upon the loop momentum. We therefore bundle these emissions into a single four-momentum: r_0 for emissions off incoming parton i and q_0 off the incoming parton j. We then suppose there are k subsequent emissions off i and m emissions off j, as illustrated in Figure D.2. We also allow for n emissions off the virtual exchange. The resulting integral can be written as

$$\mathcal{I}_{ij} = \int_l i\mathcal{V} \left[\prod_{a=0}^{k} \frac{1}{p_i \cdot (l + \tilde{r}_a + \tilde{h}_n) - i\frac{0}{2}}\right] \left[\prod_{c=0}^{m} \frac{1}{p_j \cdot (\tilde{q}_c - l) - i\frac{0}{2}}\right] \left[\prod_{d=0}^{n} \frac{1}{(l + \tilde{h}_d)^2 + i0}\right], \tag{D.1}$$

where

$$\tilde{r}_e \equiv \sum_{f=0}^{e} r_f, \quad \tilde{q}_e \equiv \sum_{f=0}^{e} q_f, \quad \tilde{h}_e \equiv \sum_{f=0}^{e} h_f, \quad h_0 \equiv 0\ . \tag{D.2}$$

In what follows the momenta $\{r_0, ...r_k\}, \{q_0, ..., q_m\}, \{h_1, ..., h_n\}$ could represent either on-shell emissions or off-shell emissions that branch into many more emissions (not drawn in the figure). The momenta of the two hard partons i and j are denoted by p_i and p_j. All external partons are assumed to be non-collinear and to have positive energy. We omit colour factors and we only invoke the form of the numerator $\mathcal{V}$

[2]For instance, graphs with this topology can be thought of as the decay of a virtual gluon into many real emissions and one can apply the Cutkosky rules.

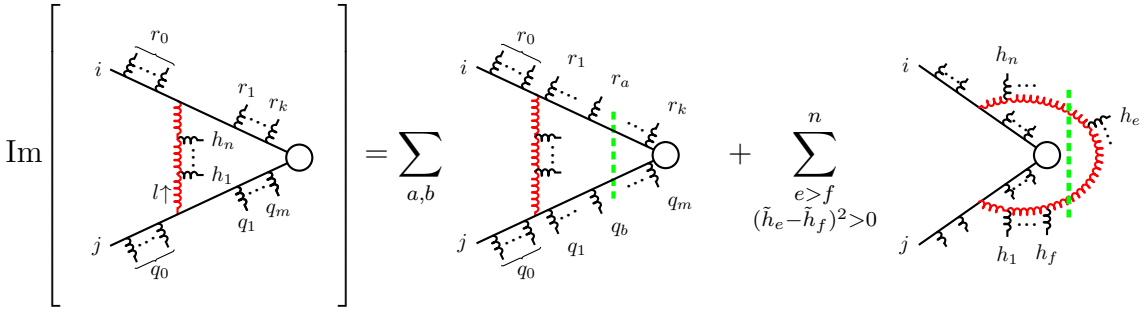

Figure D.2: The two types of cut that contribute to the imaginary part of graphs with a virtual exchange between the incoming partons.

when is relevant. Finally, we will use the following compact notation

$$\int_l \equiv \int \frac{\mathrm{d}^d l}{2\pi^d}. \tag{D.3}$$

In Section D.5, we will show that the imaginary part of Eq. (D.1) can be written as the sum of two contributions $\mathrm{Im}(\mathcal{I}_{ij}) = \mathcal{I}^G_{ij} + \mathcal{I}^E_{ij}$. The term $\mathcal{I}^G_{ij}$ consists of kinematically allowed cuts through soft lines $\mathcal{I}^G_{ij}$, and $\mathcal{I}^E_{ij}$ contains only cuts through a pair of incoming hard lines. The application of these cutting rules to Eq. (D.1) gives

$$\mathcal{I}^E_{ij} \equiv \frac{1}{2}\int_l \mathcal{V}\left[\prod_{e=0}^{n}\frac{1}{(l+\tilde{h}_e)^2}\right]\left[\sum_{c=0}^{m}(-2\pi i)\delta(p_j\cdot(\tilde{q}_c-l))\prod_{d=0,d\neq c}^{m}\frac{1}{p_j\cdot(\tilde{q}_d-l)}\right]\times \left[\sum_{a=0}^{k}(-2\pi i)\delta(p_i\cdot(l+\tilde{r}_a+\tilde{h}_n))\prod_{b=0,b\neq a}^{k}\frac{1}{p_i\cdot(l+\tilde{r}_b+\tilde{h}_n)}\right], \tag{D.4a}$$

and

$$\mathcal{I}^G_{ij} \equiv \int_l \mathcal{V}\left[\prod_{a=0}^{k}\frac{1}{p_i\cdot(l+\tilde{r}_a+\tilde{h}_n)}\right]\left[\prod_{c=0}^{m}\frac{1}{p_j\cdot(\tilde{q}_c-l)}\right]\times \tag{D.4b}$$
$$\sum_{\substack{e>f \\ (\tilde{h}^0_e-\tilde{h}_f)^2>0}}^{n}\frac{(-2\pi i)\delta^+((l+\tilde{h}_e)^2)(-2\pi i)\delta^+((-\tilde{h}_f-l)^2)}{2}\prod_{\substack{g=0 \\ g\neq e,f}}^{n}\frac{1}{(l+\tilde{h}_g)^2}+(4-\text{G.C.})\,.$$

The term $(4-\text{G.C.})$ denotes possible terms with 4 soft gluon propagators set on-shell that also appear in our derivation below. They only exist for $n \geq 3$, i.e. for cases in which there are at least three real emissions. In the calculations of chapters 3, 5 and 6 we only consider graphs $n \leq 2$. Also, we point out that such graphs with four cut propagators cannot give rise to poles or logarithmic enhancements as the respective delta functions would constrain the four momentum components. We

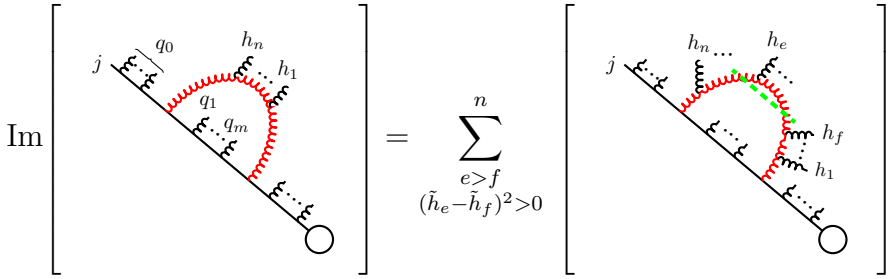

Figure D.3: The two types of cut that contribute to the imaginary part of graphs with a virtual between an incoming parton.

think that these contributions vanish but we have not shown this yet. The cutting rules expressed by Eq. (D.4a) and (D.4b) are illustrated in Fig. D.2, where four gluon cuts are omitted.

Similarly, the loop integral corresponding to graphs like the second graph in Figure D.3 can be written

$$\mathcal{I}_i = \int_l i\mathcal{V} \left[\prod_{c=0}^{m} \frac{1}{p_j\cdot(\tilde{q}_c - l) - i0/2}\right] \left[\prod_{d=0}^{n} \frac{1}{(l+\tilde{h}_d)^2 + i0}\right], \tag{D.5}$$

and its imaginary part is

$$\begin{aligned}\mathrm{Im}(\mathcal{I}_i) \;=\; & \frac{1}{2}\int_l \mathcal{V}\left[\prod_{c=0}^{m} \frac{1}{p_j\cdot(\tilde{q}_c - l) - i0/2}\right] \sum_{\substack{e>f \\ (\tilde{h}_e^0-\tilde{h}_f)^2>0}}^{n} (-2\pi i)\delta^+((l+\tilde{h}_e)^2) \\ & \times(-2\pi i)\delta^+((-\tilde{h}_f - l)^2) \prod_{\substack{g=0 \\ g\neq e,f}}^{n} \frac{1}{(l+\tilde{h}_g)^2} + (\text{4-G.C.}).\end{aligned} \tag{D.6}$$

Again, for $n \geq 3$, the term 4-G.C. denotes possible contributions with 4 gluon propagators set on-shell. The cutting rules expressed by Eq. (D.6) are illustrated in Fig. D.3 where four gluon cuts are omitted.

The key point of the above cutting rules, Eq. (D.4a), (D.4b) and (D.6), is that there are no "mixed cut" contributions, i.e. cuts that set both soft and eikonal lines on-shell. The general mechanism responsible for the cancellation of such contributions is discussed in Section D.2. The application of the cutting rules in Figs. D.2 and D.3 to the one-emission amplitude, $\left|2^{(1)}_{+1}\right\rangle$, gives directly the cut graphs in Fig. 3.1. The application of these cutting rules to the two-emission amplitude, $\left|2^{(1)}_{+2}\right\rangle$, gives rise to the eikonal cuts depicted in Fig. 5.3 (due to Fig D.2) and the cuts over soft gluon lines in Fig. D.3 (due to Fig. (D.3)).

We close this section with a remark concerning the physical significance of these

rules. When we applied the above cutting rules to the calculation of the imaginary part of $\left|2^{(1)}_{+1}\right\rangle$ and $\left|2^{(1)}_{+2}\right\rangle$, we realised that the different cut graphs can be organised, gauge invariantly, into physical mechanisms for gluon emission. Each of which can be written as the product of two on-shell scattering amplitudes integrated over allowed on-shell states, see Eqs. (3.13) and (5.65). Indeed, this strongly suggests that the cutting rules in this section can be derived using using the unitarity of the S-matrix, see for instance [32].

D.2 Cutting rules to calculate the real part

In Section D.5, we will show that the real part of Eqs. (D.1) and (D.5) is given by

$$\begin{aligned}\mathrm{Re}\{\mathcal{I}_{ij}\} = \mathrm{Pv}\int_l \mathcal{V}\left[\prod_{a=0}^{k}\frac{1}{p_i\cdot(l+\tilde{r}_a+\tilde{h}_n)}\right]\left[\prod_{c=0}^{m}\frac{1}{p_j\cdot(\tilde{q}_c-l)}\right]\times \\ \sum_{e=0}^{n}(-2\pi i)\delta^+((l+\tilde{h}_e)^2)\prod_{\substack{g=0\\ g\neq e}}^{n}\frac{1}{(l+\tilde{h}_g)^2}+\text{3-G.C.}\,,\end{aligned} \tag{D.7a}$$

$$\begin{aligned}\mathrm{Re}\{\mathcal{I}_{j}\} = \mathrm{Pv}\int_l \mathcal{V}\left[\prod_{c=0}^{m}\frac{1}{p_j\cdot(\tilde{q}_c-l)}\right]\sum_{e=0}^{n}(-2\pi i)\delta^+((l+\tilde{h}_e)^2)\prod_{\substack{g=0\\ g\neq e}}^{n}\frac{1}{(l+\tilde{h}_g)^2} \\ +\text{3-G.C.}\,,\end{aligned} \tag{D.7b}$$

where the symbol Pv indicates that the principal value prescription is applied for all the propagators that are not cut, we shall precisely define this prescription below. The terms denoted by 3-G.C. are cuts over three soft gluon propagators. In Appendix F, we apply Eq. (D.7a) to a non-trivial case to calculate the real (eikonal) part of the loop integrals of the one-emission amplitude ($n \leq 1$) obtaining the correct expression for this amplitude previously reported [41].

Expressions (D.7a) and (D.7b) resemble the Feynman tree theorem but they are not the same. As presented in [104], the Feynman's tree theorem can be used to write a general one-loop integral as a sum of single cuts over each of the virtual propagators. In contrast, the sum over single cuts in Eqs. (D.7a) and (D.7b) only runs over the soft gluon propagators but not over the propagators of the eikonal lines. In Section D.4, the mechanism responsible for the cancellation of the single cuts over the eikonal lines is discussed.

D.3 On the cancellation of "mixed cuts"

The loop integrals corresponding to the first two types of graph in Fig. D.1, i.e. Eqs. (D.1) and (D.5), can be written as

$$\int_l \frac{if(l)}{[p_j\cdot l - p_j\cdot q + i0/2][l^2+i0]}\ , \tag{D.8}$$

where $f(l)$ is a function that represents the contribution of the rest of the graph and q is a light-like or time-like vector, with positive energy, that represents the momentum of some of the emitted gluons. To illustrate the cancellation of "mixed cuts" we only need to consider the contributions written in this form. In this section, we show that Eq. (D.8) gives rise to two "mixed cuts" contributions in which the eikonal and a soft gluon propagator go on-shell, and that they identically cancel. When we consider the complete derivation of the cutting rules for a particular graph in Section D.5, it will become clear that the cancellation of other "mixed cuts", due to propagators not shown in $f(l)$, occurs due to this same mechanism.

For simplicity, we work in the frame in which $p_j = p_j^0(1,-1,0_\perp)$. The two propagators shown in Eq. (D.8) have poles in the lower half of the l^0 complex plane located at (e.g. see [104])

$$l_1^0 = -l_z + q_0 + q_z - i0/2p_j^0, \tag{D.9}$$

$$\text{and}\quad l_2^0 = \sqrt{|\vec{l}|^2 - i0}\ . \tag{D.10}$$

The residue of these two poles sums up to

$$\int \frac{\mathrm{d}^{d-1}l}{(2\pi)^d} if(l)\left[\frac{-2\pi i}{p_j^0[l^2+i0]}\bigg|_{l_0=l_1^0} + \frac{-2\pi i}{[p_j\cdot l - p_j\cdot q + \frac{i0}{2}]2\sqrt{|\vec{l}|-i0}}\bigg|_{l_0=l_2^0}\right]\ .$$

The important point to note here is that the evaluation of the residues fixes the prescription of the poles as follows:

$$\left[l^2+i0\right]\big|_{l_0=l_1^0} = \left[l^2 + i0\left[1-\frac{l^0}{p_j^0}\right] + \mathcal{O}\left((i0)^2\right)\right]\Big|_{l_0=-l_z+q_0+q_z}, \tag{D.11}$$

$$\left[p_j\cdot l - p_j\cdot q + \frac{i0}{2}\right]\Big|_{l_0=l_2^0} = \left[p_j\cdot(l-q) + i0\frac{p_j^0}{2l^0}\left[\frac{l^0}{p_j^0}-1\right] + \mathcal{O}\left((i0)^2\right)\right]\Big|_{l_0=|\vec{l}|}\ .$$

Taking into account these shifts, the integral can be written as

$$\int_l if(l)\left[\frac{(-2\pi i)\delta(p_j\cdot(l-q))}{l^2+i0\left(1-\frac{l^0}{p_j^0}\right)} + \frac{(-2\pi i)\delta(l^2)\theta(l^0)}{\left[p_j\cdot l - p_j\cdot q + i0\frac{p_j^0}{2l^0}\left(\frac{l^0}{p_j^0}-1\right)\right]}\right]\ . \tag{D.12}$$

Note that we have neglected any possible shifts in the imaginary prescriptions of any propagators in $f(l)$: when we consider the complete derivation of the cutting rules for a particular graph in Sec. D.5 we will justify this subtlety. In the derivations in this appendix we make use of the Sokhotski-Plemelj (SP) identity:

$$\begin{aligned}
&\lim_{\epsilon\to 0^+}\frac{1}{x+i\epsilon} = \mathrm{Pv}\left(\frac{1}{x}\right) - i\mathrm{sign}(\epsilon)\pi\delta(x),\\
&\mathrm{Pv}\left(\frac{1}{x+i\epsilon}\right) \equiv \lim_{\epsilon\to 0}\frac{x}{x^2+\epsilon^2},\\
&\delta(x) \equiv \lim_{\epsilon\to 0^+}\frac{\epsilon}{\pi(x^2+\epsilon^2)},
\end{aligned} \tag{D.13}$$

where $\mathrm{sign}(\epsilon)$ denotes the sign of ϵ and the second line is the definition of the principal value prescription applied to a propagator $1/(x+i\epsilon)$. In what follows, we are only interested in the imaginary part that results after applying this identity to each of the propagators within the squared bracket in Eq. (D.12). After doing this, the imaginary parts of the two terms add up to

$$\int_l if(l)\,(-2i\pi)(i\pi)\delta(p_j\cdot(l-q))\delta(l^2)\,\mathrm{sgn}\left(\frac{l^0}{p_j^0}-1\right)\theta(-l^0). \tag{D.14}$$

Since both delta functions cannot simultaneously be satisfied, this integral vanishes. It is interesting to note that the cancellation occurs for all l^0/p_j^0. This would have not been the case if we had not originally included the factor of one half in the pole prescriptions of eikonal propagators. Also notice that the cancellation no longer occurs if the imaginary prescription in the eikonal propagator in Eq. (D.8) had the opposite sign[3]. To summarise, we have illustrated that the imaginary part of Eq. (D.8) due to the "mixed cuts" cancels.

D.4 On the cancellation of single cuts over eikonal lines

We will now illustrate how the single cuts over eikonal propagators vanish. For simplicity, we focus on the particular case of the second graph in Fig. D.4 when there is only one virtual propagator associated to the eikonal line. It is convenient to consider the expression for this graph without contracting the vectors associated to emissions radiated off the virtual exchange (red line), the corresponding loop integral

[3]When it has the opposite sign, this propagator corresponds to an outgoing, instead of an incoming, parton. In this case, these cuts do not cancel and, in fact, give rise to the re-scattering cuts illustrated in Fig. 3.5. This emphasises the relevance of the imaginary prescriptions in the eikonal propagators. In this appendix we only consider a DY process.

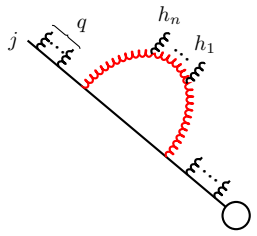

Figure D.4: A particular graph that we consider to illustrate the cancellation of single cuts over the eikonal lines.

can be written as

$$\int_l \frac{i\mathcal{V}^{\mu_1\cdots\mu_n}}{p_j\cdot(q-l)-i0/2}\prod_{d=0}^{n}\frac{1}{(l+\tilde{h}_d)^2+i0}, \tag{D.15}$$

where $\mathcal{V}^{\mu_1\cdots\mu_n}$ is the tensor associated with the triple gluon vertices in the numerator. We work again in the frame where $p_j = p_j^0(1,-1,0_\perp)$. Closing the l^0 contour below we get residues from from the soft gluon and eikonal propagators. Up to a constant factor, the residue corresponding the eikonal pole is of the form

$$\int \mathrm{d}l_z \mathcal{V}^{\mu_1\cdots\mu_n}\prod_{e=0}^{n}\frac{1}{l_z-a_e-i0g_e}, \tag{D.16}$$

where $a_e = a_e(l_T)$ and $g_e = g_e(\vec{l}\,)$ are functions of the loop momentum[4] whose explicit forms are not relevant here. Suppose we apply the SP relation (D.13) to each of the denominators in this expression. Because every denominator is linear in l^1, terms with more than one propagator set on-shell vanish. The terms with one more soft gluon propagator cut are purely imaginary and we are not interested in them for the rest of this section[5]; we are only interested in the real part, i.e. the term with the principal value prescription applied to each denominator. This contribution would correspond to a single cut over an eikonal line and below we show it vanishes. To do this we point out that this single cut contribution is equal to

$$\mathrm{Pv}\int \mathrm{d}l_z \mathcal{V}^{\mu_1\cdots\mu_n}\prod_{e=0}^{n}\frac{1}{l_z-a_e-i0g_e} = \mathrm{Pv}\int \mathrm{d}l_z \mathcal{V}^{\mu_1\cdots\mu_n}\prod_{e=0}^{n}\frac{1}{l_z-a_e-i0|g_e|}\ , \tag{D.17}$$

[4]These are also functions of the external momenta but this is not relevant in what follows.

[5]In fact, theses imaginary contributions are mixed cuts that identically cancel by virtue of the mechanism of cancellation illustrated in the previous section, compare Eq. (D.8) with Eq. (D.15). But this is not relevant in what follows.

Furthermore, by using the SP identity on the right-hand side of (D.17) one can show that this integral vanishes if the following integral does

$$\int \mathrm{d}l_z \mathcal{V}^{\mu_1\cdots\mu_n} \prod_{e=0}^{n} \frac{1}{l_z - a_e - i0|g_e|} \ . \tag{D.18}$$

From now on we focus on showing that this integral vanishes as this proves that the left hand side of (D.17), i.e. the expression corresponding to the single cut over the eikonal propagator in Fig. D.4, also does. This would be the case if we could close the contour in the lower half of the l_z complex plane. The tensor $\mathcal{V}^{\mu_1\cdots\mu_n}$ has at most n triple particle vertices and thus, in principle, could have terms of the form $l^{\mu_1}\dots l^{\mu_n}$ that contain n powers of l_z. At first glance, this indicates that one cannot close the contour. However, one can show that such terms were reduced $l^{\mu_1}\dots l^{\mu_n} \to l^{\mu_1}\dots l^{\mu_{n-1}} q^{\mu_n}$ when we picked the residue of the eikonal propagator in (D.15), i.e. $p_j \cdot l = p_j \cdot q$. Hence, the highest power possible of l_z in the numerator is $n-1$ and then, the contour can be closed and the integral in Eq. (D.17) vanishes[6].

We close this section by commenting on the extensions of this result for more general graphs. The generalisation for a graph with many virtual eikonal propagator (due to multiple emissions off parton j) is direct as exactly the same steps apply to the residue of each propagator associated to the eikonal line. The case of a graph that involves both hard partons is very similar. In fact it is easier as the denominators contain more powers of l_z. Finally, we comment that the cancellation of the single eikonal cuts occurs in a similar way if the hard parton in j in Fig. D.4 is outgoing.

D.5 Deduction of cutting rules for a particular graph

In this section, we will work out the derivation of the cutting rules to isolate the real and imaginary contributions of a particular graph. In order to avoid cluttered notation, we consider a graph represented by Eq. (D.1) that has only two eikonal propagators:

$$I_{ij} \equiv \int_l \frac{i\mathcal{V}}{[p_i \cdot (l + r + \tilde{h}_n) - i0/2][p_j \cdot (q - l) - i0/2]} \left[\prod_{e=0}^{n} \frac{1}{(l + \tilde{h}_e)^2 + i0}\right] \ . \tag{D.19}$$

[6] Due to the radiation and absorption of the virtual gluon (red gluon in Fig. D.4), the tensor $\mathcal{V}^{\mu_1\cdots\mu_n}$ is contracted twice with p_j. It follows that terms with n powers of the loop momentum $l^{\mu_1}\dots l^{\mu_n}$ either vanish (because they are proportional to $p_j^2 = 0$) or the number of powers are reduced $l^{\mu_1}\dots l^{\mu_n} \to l^{\mu_1}\dots l^{\mu_{n-1}} q^{\mu_n}$ (because they are contracted at least once with the vector p_j and, then, can be evaluated at $p_j \cdot l = p_j \cdot q$. Hence, we have shown that the highest power possible of l_z in the numerator is $n-1$.

We will show that the real and imaginary parts of this expression are respectively given by Eq. (D.4a) and (D.7b). The derivation of these rules for more general graphs can be carried out along similar lines. In the frame in which $p_j = p_j^0(1,-1,0_\perp)$, the poles of Eq. (D.19) in the lower-half l_0 plane are located at

$$-l_z + q_0 + q_z - i0/(2p_j^0)\ , \tag{D.20}$$

$$\text{and} \qquad -(\tilde{h}_e)_0 + \sqrt{|\vec{l} + \vec{\tilde{h}}_e|^2 - i0}, \quad e = \{0,1,...,n\}\ . \tag{D.21}$$

We will denote by I_1 the contribution due to the pole in the eikonal propagator in Eq. (D.20) and by I_2 that due to the poles of the gluon propagators, i.e. $I_{ij} = I_1 + I_2$. Following the same steps we took to deduce Eq. (D.12), the residue of the pole in Eq. (D.20) gives

$$I_1 \equiv \int_l \frac{(2\pi i) i\mathcal{V}\delta(p_j\cdot(l-q))}{[p_i\cdot(l+r+\tilde{h}_n) - i0(1+\frac{p_i^0}{p_j^0})/2]} \left[\prod_{f=0}^{n} \frac{1}{(l+\tilde{h}_f)^2 + i0\left(1 - \frac{l^0+\tilde{h}_f^0}{p_j^0}\right)}\right]. \tag{D.22}$$

The integration over the energy component of the loop momentum, l_0, renders an integrand with a denominator that is the product of propagators that are linear in the integration variable l_z:

$$\int dl^1 \mathcal{V} \prod_{e=0}^{n+1} \frac{1}{l_z - a_e - i0 g_e}, \tag{D.23}$$

where $a_e = a_e(l_T)$ and $g_e = g_e(l)$ are functions of the loop momentum[7] whose explicit forms are not relevant here. Suppose we apply the SP relation (D.13) to each of the denominators in this expression. According to the results of Section D.4, the only terms that survive this expansion are those with one of the propagators in (D.23) set on-shell, i.e. the contributions with a single cut over the eikonal propagator vanish. It follows that Eq. (D.22) is purely imaginary and its value is obtained by summing over the $n+1$ contributions obtained by setting one more propagators on-shell in Eq. (D.22). The sum contains two terms, one with mixed cuts and one with an eikonal cut:

$$\begin{aligned} I_1 = &\int_l \frac{(2\pi i)\mathcal{V}\delta(p_j\cdot(l-q))}{p_i\cdot(l+r+\tilde{h}_n)} \sum_{e=0}^{n} i\pi\delta((l+\tilde{h}_e)^2)\ \mathrm{sgn}\left(\frac{l^0+\tilde{h}_e^0}{p_j^0} - 1\right) \prod_{\substack{f=0\\ f\neq e}}^{n} \frac{1}{(l+\tilde{h}_f)^2} \\ &+ \int_l \mathcal{V} \frac{(-2\pi i)\delta(p_j\cdot(l-q))(-2\pi i)\delta(p_i\cdot(l+r+\tilde{h}_n))}{2} \prod_{f=0}^{n} \frac{1}{(l+\tilde{h}_f)^2}\ . \end{aligned} \tag{D.24}$$

[7] These are also functions of the external momenta but this is not relevant in what follows.

Now we turn to the residues in (D.21), these add up to

$$I_2 = \int_l \frac{i\mathcal{V}}{\left[p_i\cdot(l+r+\tilde{h}_n)\right]\left[p_j\cdot(l-q)+i0\frac{p_j^0}{2\left(l^0+\tilde{h}_e^0\right)}\left(\frac{l^0+\tilde{h}_e^0}{p_j^0}-1\right)\right]}\times \sum_{e=0}^{n} 2\pi i\delta^+(l+\tilde{h}_e)\prod_{\substack{f=0\\f\neq e}}^{n}\frac{1}{(l+\tilde{h}_f)^2-i0\frac{\tilde{h}_f^0-\tilde{h}_e^0}{l^0+\tilde{h}_e^0}}\,. \tag{D.25}$$

We have ignored the pole prescription in the first eikonal propagator because this never vanishes now that one of the soft gluon propagators is on-shell. By using the SP identity for the eikonal propagator of hard parton j, the above expression yields:

$$I_2 = \sum_{e=0}^{n}\int_l \frac{i\mathcal{V}(2\pi i\delta^+(l+\tilde{h}_e))}{[p_i\cdot(l+r+\tilde{h}_n)]}\prod_{\substack{f=0\\f\neq e}}^{n}\frac{1}{(l+\tilde{h}_f)^2-i0\frac{\tilde{h}_f^0-\tilde{h}_e^0}{l^0+\tilde{h}_e^0}}\times \left[\frac{\mathrm{Pv}}{p_j\cdot(l-q)}-i\pi\mathrm{sgn}\left(\frac{l^0+h_e^0}{p_j^0}-1\right)\delta(p_j\cdot(l-q))\right]\,. \tag{D.26}$$

We will now show that the contributions with one on-shell eikonal propagator cancel all of the contributions in (D.24), except for the term in which the two eikonal propagators are cut. To see this, we use the SP identity on the gluon propagators. One can be shown that the term in which the eikonal propagators are on-shell exactly vanishes when three or more propagators are set on-shell[8]. Then, the above expression reduces to

$$\begin{aligned} I_2 = &\int_l \frac{i\mathcal{V}(2\pi i\delta^+(l+\tilde{h}_e))}{[p_i\cdot(l+r+\tilde{h}_n)]}\sum_{e=0}^{n}\prod_{\substack{f=0\\f\neq e}}^{n}\frac{1}{(l+\tilde{h}_f)^2-i0\frac{\tilde{h}_f^0-\tilde{h}_e^0}{l^0+\tilde{h}_e^0}}\times\left[\frac{\mathrm{Pv}}{p_j\cdot(l-q)}\right]\\ &+\int_l \frac{i\mathcal{V}(2\pi i\delta^+(l+\tilde{h}_e))}{[p_i\cdot(l+r+\tilde{h}_n)]}\sum_{e=0}^{n}\prod_{\substack{f=0\\f\neq e}}^{n}\frac{1}{(l+\tilde{h}_f)^2}\times \\ &\left[-i\pi\mathrm{sgn}\left(\frac{l^0+h_e^0}{p_j^0}-1\right)\delta(p_j\cdot(l-q))\right]\,. \end{aligned} \tag{D.27}$$

When this expression is added to Eq. (D.24), there is a pairwise cancellation of the mixed cuts. This cancellation is entirely analogous to the cancellation encountered for Eq. (D.14).

[8] As the different delta functions that appear cannot be simultaneously satisfied.

Hence,

$$I_{ij} = \int_l \mathcal{V} \frac{(-2\pi i)\delta(p_j \cdot (l-q))(-2\pi i)\delta(p_i \cdot (l+r+\tilde{h}_n))}{2} \prod_{f=0}^{n} \frac{1}{(l+\tilde{h}_f)^2}$$
$$+ \int_l \sum_{e=0}^{n} \frac{(-2\pi i \delta^+(l+\tilde{h}_e))i\mathcal{V}}{[p_i \cdot (l+r+\tilde{h}_n)]} \frac{\mathrm{Pv}}{[p_j \cdot (q-l)]} \prod_{\substack{f=0 \\ f\neq e}}^{n} \frac{1}{(l+\tilde{h}_f)^2 - i0\mathrm{sgn}(\tilde{h}_f^0 - \tilde{h}_e^0)} \,. \quad \text{(D.28)}$$

The integral on the first line is purely imaginary. To separate the real and imaginary contributions in the second line we apply the SP relation on each of the uncut gluon propagators. In order to spot terms that vanish because their respective delta functions cannot be simultaneously satisfied, it is convenient to make the shift $l \to l - \tilde{h}_e$, after which, the integral (D.28) becomes

$$\int_l (-2\pi i \delta^+(l)) \prod_{\substack{f=0 \\ f\neq e}}^{n} \frac{1}{\left[2l \cdot (\tilde{h}_f - \tilde{h}_e) + (\tilde{h}_f - \tilde{h}_e)^2 - i0\mathrm{sgn}(\tilde{h}_f^0 - \tilde{h}_e^0)\right]} (...), \quad \text{(D.29)}$$

where (...) denotes the rest of integrand not explicitly shown. We recall that $h_1, \ldots h_n$ represent the momenta of on-shell emissions or off-shell emissions that branch into many more emissions and

$$\tilde{h}_e \equiv \sum_{f=0}^{e} h_f. \quad \text{(D.30)}$$

Now, suppose that one of the denominators in Eq. (D.29) is set on-shell, i.e.

$$\delta^+(l)\delta\left(2l \cdot (\tilde{h}_f - \tilde{h}_e) + (\tilde{h}_f - \tilde{h}_e)^2\right). \quad \text{(D.31)}$$

If the vector $\tilde{h}_f - \tilde{h}_e$ is light-like, $(\tilde{h}_f - \tilde{h}_e)^2 = 0$, both delta functions cannot be satisfied simultaneously. Indeed, this case corresponds to a two-to-one on-shell process which is not kinematically possible. If $f > e$, $(\tilde{h}_f - \tilde{h}_e)$ can be either light-like or time-like with positive energy. Since we already ruled out the light-like case, we focus on the time-like case. Clearly, both delta functions (D.31) cannot be simultaneously satisfied if $(\tilde{h}_f - \tilde{h}_e)$ is time-like with positive energy. On the other hand if $f < e$, then $(\tilde{h}_e - \tilde{h}_f)$ is either light-like or time-like with positive energy. Since the light-like possibility is ruled out, the only case in which both delta functions can be satisfied is when $f < e$ and $(\tilde{h}_e - \tilde{h}_f)^2 > 0$ is time-like. Kinematical considerations show that in this case[9]: $\delta^+(l)\delta\left(2l \cdot (\tilde{h}_f - \tilde{h}_e) + (\tilde{h}_f - \tilde{h}_e)^2\right) = \delta^+(l)\delta^+\left(l + \tilde{h}_f - \tilde{h}_e\right)$, and then

[9] To see this, go to the reference frame in which $\tilde{h}_e - \tilde{h}_f$ is at rest.

finally we can write

$$I_{ij} = \int_l i\mathcal{V}\,\frac{(-2\pi i)\delta(p_j\cdot(l-q))(-2\pi i)\delta(p_i\cdot(l+r+\tilde{h}_n))}{2}\prod_{f=0}^{n}\frac{1}{(l+\tilde{h}_f)^2}+$$
$$\int_l \frac{i\mathcal{V}}{[p_i\cdot(l+r+\tilde{h}_n)][p_j\cdot(q-l)]}\sum_{\substack{e>f\\(\tilde{h}_e^0-\tilde{h}_f)^2>0}}^{n}\frac{(-2\pi i\delta^+(l+\tilde{h}_e))(-2\pi i\delta^+(-l-\tilde{h}_f))}{2}$$
$$\times\prod_{\substack{g=0\\g\neq\{e,f\}}}^{n}\frac{1}{(l+\tilde{h}_g)^2}+\mathrm{Pv}\int_l\sum_{e=0}^{n}\frac{(-2\pi i\delta^+(l+\tilde{h}_e))i\mathcal{V}}{[p_i\cdot(l+r+\tilde{h}_n)][p_j\cdot(q-l)]}\prod_{\substack{f=0\\f\neq e}}^{n}\frac{1}{(l+\tilde{h}_f)^2} \qquad \text{(D.32)}$$
$$+(3,4\text{-G.C.})$$

where the symbol $3,4$-G.C. denotes terms with three or four cuts over soft gluon propagators. These are respectively real and imaginary. This proves the particular case Eqs. (D.4b) and (D.4a), that we are considering. The general case is a straightforward extension because no two eikonal propagators from the same hard line can vanish simultaneously and, thus, we can consider separately the residues of every pair of eikonal propagators as we did in this section. The cutting rules for one-loop integrals which involve only one hard line, i.e. Eq. (D.6), can be deduced along similar lines.

D.5.1 Final remarks

Identical rules to isolate the real and imaginary parts of loop integrals apply to graphs where the virtual exchange radiates gluons through four-gluon vertices and to cases in which some of the lines in the virtual exchange correspond to ghosts. Repeating the above proof taking into account these possibilities is straightforward. We close this appendix by remarking that more mathematical rigour would be desirable in our proofs. In particular, we have not proved that the principal value prescription applied over the uncut propagators, Eq. (D.13), can be commuted with the loop integration as we often assumed. Nevertheless, the fact that these rules render the correct real and imaginary parts of the one-emission amplitude, $\left|n_{+1}^{(1)}\right\rangle$, and that, more generally, the imaginary parts can be related to a product of physical amplitudes (physical mechanisms for gluon emission) validate the derivations of this appendix to a good extent.

Appendix E

Reductions of $\left|n^{(1)}_{+1}\right\rangle$

In this appendix, we show how to reduce the one-loop, one-emission amplitude $\left|n^{(1)}_{+1}\right\rangle$ to the scalar integral shown in Eq. (3.29). This amplitude receives contribution from the different topologies illustrated in Fig. 3.6. After straightforward tensorial reductions, the graphs illustrated in Fig. 3.6 yield:

$$\mathbf{G}^c_{(a),ij}\left|n^{(0)}\right\rangle = (g_s\mu^\epsilon)^3\mathbf{T}^c_i\mathbf{T}_j\cdot\mathbf{T}_i\left\{\frac{p_i\cdot p_j p_i\cdot\varepsilon}{p_i\cdot q}\mathrm{C}^1_{ij}(q)\right\}\left|n^{(0)}\right\rangle, \tag{E.1a}$$

$$\mathbf{G}^c_{(b),ij}\left|n^{(0)}\right\rangle = (g_s\mu^\epsilon)^3\mathbf{T}_j\cdot\mathbf{T}_i\mathbf{T}^c_i\left\{p_i\cdot p_j p_i\cdot\varepsilon\mathrm{D}^2_{ij}(q)\right\}\left|n^{(0)}\right\rangle, \tag{E.1b}$$

$$\mathbf{G}^c_{(c),ijk}\left|n^{(0)}\right\rangle = (g_s\mu^\epsilon)^3\mathbf{T}_j\cdot\mathbf{T}_i\mathbf{T}_k\left\{p_i\cdot p_j\frac{p_k\cdot\varepsilon}{p_k\cdot q}\mathrm{C}^2_{ij}\right\}\left|n^{(0)}\right\rangle, \tag{E.1c}$$

$$\begin{aligned}\mathbf{G}^c_{(d),ij}\left|n^{(0)}\right\rangle =& (g_s\mu^\epsilon)^3\mathbf{T}^b_j if^{bca}\mathbf{T}^a_i\Bigg\{-p_i\cdot\varepsilon p_j\cdot q\mathrm{D}^1_{ij}(q)+\frac{p_i\cdot q p_j\cdot\varepsilon}{p_j\cdot q}\mathrm{C}^3_i(q)\\ &+\frac{1}{2}\mathrm{C}^1_{ij}(q)p_i\cdot p_j\left(\frac{p_i\cdot\varepsilon}{p_i\cdot q}+\frac{p_j\cdot\varepsilon}{p_j\cdot q}\right)+(i\leftrightarrow j)\Bigg\}\left|n^{(0)}\right\rangle,\end{aligned} \tag{E.1d}$$

$$\mathbf{G}^c_{(e),i}\left|n^{(0)}\right\rangle = (g_s\mu^\epsilon)^3\mathbf{T}^a_i if^{acb}\mathbf{T}^b_i\left\{\frac{2p_i\cdot\varepsilon}{p_i\cdot q}\mathrm{B}(q)-p_i\cdot\varepsilon\mathrm{C}^3_i(q)\right\}\left|n^{(0)}\right\rangle, \tag{E.1e}$$

$$\mathbf{G}^c_{(f),i}\left|n^{(0)}\right\rangle = (g_s\mu^\epsilon)^3\mathbf{T}^d_i\frac{p^\mu_i}{p_i\cdot q}\pi(q^2)\left(g_{\mu\nu}-\frac{q_\mu q_\nu}{q^2}\right)\varepsilon^\nu\left|n^{(0)}\right\rangle, \tag{E.1f}$$

$$\mathbf{G}^c_{(g),i}\left|n^{(0)}\right\rangle = (g_s\mu^\epsilon)^2\mathbf{J}^c_{n+1}(q)\Sigma_i(p_i^2)\left|n^{(0)}\right\rangle, \tag{E.1g}$$

where $\pi(q^2)$ denotes the soft gluon self energy correction, $\Sigma_i(p_i^2)$ denotes the self energy correction of external parton i and $\mathrm{B}_0(q), \mathrm{C}^1_{ij}(q), \mathrm{C}^2_{ij}, \mathrm{C}^3_i(q), \mathrm{D}^1_{ij}(q), \mathrm{D}^2_{ij}(q)$ are

two, three and four point scalar functions:

$$\begin{aligned}
\mathrm{B}_0(q) &\equiv \int_l \frac{-i}{[l^2+i0]\,[(l+q)^2+i0]}\ , \\
\mathrm{C}^1_{ij}(q) &\equiv \int_l \frac{-i}{[l^2+i0]\left[p_i\cdot(l+q)+\delta_i\frac{i0}{2}\right]\left[p_j\cdot(-l)+\delta_j\frac{i0}{2}\right]}\ , \\
\mathrm{C}^2_{ij} &\equiv \int_l \frac{-i}{[l^2+i0]\left[p_i\cdot l+\delta_i\frac{i0}{2}\right]\left[p_j\cdot(-l)+\delta_j\frac{i0}{2}\right]}\ , \\
\mathrm{C}^3_{i} &\equiv \int_l \frac{-i}{[l^2+i0]\,[(l+q)^2+i0]\left[p_i\cdot(l+q)+\delta_i\frac{i0}{2}\right]}\ , \\
\mathrm{D}^1_{ij} &\equiv \int_l \frac{-i}{[l^2+i0]\,[(l+q)^2+i0]\left[p_i\cdot(l+q)+\delta_i\frac{i0}{2}\right]\left[p_j\cdot(-l)+\delta_j\frac{i0}{2}\right]}\ , \\
\mathrm{D}^2_{ij} &\equiv \int_l \frac{-i}{[l^2+i0]\left[p_i\cdot l+\delta_i\frac{i0}{2}\right]\left[p_i\cdot(l+q)+\delta_i\frac{i0}{2}\right]\left[p_j\cdot(-l)+\delta_j\frac{i0}{2}\right]}\ ,
\end{aligned} \tag{E.2}$$

and we have used the shorthand $\int_l \equiv \mathrm{d}^d l/(2\pi)^d$. In Fig. 3.6 we have drawn all the topologies as if partons $\{i,j,k\}$ were all in the final state, but Eqs. (E.1) are valid in general, i.e. each of these partons can be either incoming or outgoing. The number of independent scalar integrals can be further reduced noticing that, in d dimensions,

$$\begin{aligned}
\mathrm{D}^1_{ij}(q) &= \mathrm{D}^1_{ji}(q), \\
\mathrm{D}^2_{ij}(q) &= \frac{2}{p_i\cdot p_j}\mathrm{C}^3_i(q), \\
\mathrm{C}^1_{ij}(q) &= \mathrm{C}^2_{ij} - p_i\cdot q\,\mathrm{D}^2_{ij}(q).
\end{aligned} \tag{E.3}$$

The first line can be verified by direct substitution, the second line follows from comparing the integrated expressions (F.21) and (F.22) and the third line is a consequence of the identity:

$$\frac{1}{xy} = \frac{1}{x(x+y)} + \frac{1}{y(x+y)}\ . \tag{E.4}$$

It is convenient to separate out the contributions in $\mathbf{G}^c_{(e),i}$ as follows: $\mathbf{G}^c_{(e),i} = \tilde{\mathbf{G}}^c_{(e),i} + \mathbf{G}^c_{(uv),i}$ with

$$\widetilde{\mathbf{G}}^c_{(e),i} \equiv (g_s\mu^\epsilon)^3 \mathbf{T}^a_i i f^{acb}\mathbf{T}^b_i p_i\cdot\varepsilon \mathrm{C}^3_i(q), \qquad \mathbf{G}^c_{(uv)i} \equiv (g_s\mu^\epsilon)^3 C_A \frac{\mathbf{T}^c_i\, p_i\cdot\varepsilon}{p_i\cdot q}\mathrm{B}(q). \tag{E.5}$$

In order to spot cancellations between different graphs we need to use the colour algebra and the colour conservation of the hard scattering. In particular, by using

Eq. (E.4) and the colour algebra to combine graphs (a) and (b) one gets

$$\begin{aligned}
&\mathbf{G}^c_{(a),ij} + \mathbf{G}^c_{(b),ij} = \mathbf{G}^c_{(I),ij} + \mathbf{G}^c_{(II),ij},\\
&\mathbf{G}^c_{(I),ij} \equiv (g_s\mu^\epsilon)^3 \frac{\mathbf{T}^c_i p_i\cdot\varepsilon}{p_i\cdot q}\mathbf{T}_j\cdot\mathbf{T}_i p_i\cdot p_j \mathrm{C}^2_{ij},\\
&\mathbf{G}^c_{(II),ij} \equiv (g_s\mu^\epsilon)^3 \mathbf{T}^b_j i f^{bca}\mathbf{T}^a_i p_i\cdot p_j p_i\cdot\varepsilon \mathrm{D}^2_{ij}(q).
\end{aligned} \tag{E.6}$$

Observe that $\mathbf{G}^c_{(II),ij}$ has the same colour factor as $\mathbf{G}^c_{(e),i}$. Due to colour conservation, the colour part of graph $\mathbf{G}_{(e),i}$ can be expressed as a linear combination of the colour tensors appearing in $\mathbf{G}^c_{d,ij}$, i.e.

$$\mathbf{T}^a_i i f^{acb}\mathbf{T}^b_i\left|n^{(0)}\right\rangle = \sum_{j\neq\{i\}}^{n} \mathbf{T}^b_j i f^{bca}\mathbf{T}^a_i\left|n^{(0)}\right\rangle. \tag{E.7}$$

By using this colour identity and Eqs. (E.3) the sum over all graphs for a general hard wide-angle scattering with n external hard partons can be written as

$$\left[\sum_{i=1}^{n}\sum_{j\neq\{i\}}^{n}\mathbf{G}^c_{(I),ij} + \sum_{i<j}^{n}\sum_{k\neq\{i,j\}}^{n}\mathbf{G}^c_{(c),ijk}\right]\left|n^{(0)}\right\rangle = \mathbf{J}^c_{n+1}(q)\mathbf{I}^{(1)}_n\left|n^{(0)}\right\rangle, \tag{E.8a}$$

$$\begin{aligned}
&\sum_{i=1}^{n}\sum_{j\neq\{i\}}^{n}\mathbf{G}^c_{(II),ij} + \sum_{i<j}^{n}\mathbf{G}^c_{(d),ij} + \sum_{i=1}^{n}\widetilde{\mathbf{G}}^c_{(e),i}\\
&= (g_s\mu^\epsilon)^3\sum_{i<j}^{n}\mathbf{T}^b_j i f^{bca}\mathbf{T}^a_i\big[p_j\cdot\varepsilon p_i\cdot q - p_i\cdot\varepsilon p_j\cdot q\big]\mathrm{D}^1_{ij}(q) \equiv \mathbf{J}^{(1)\,c}(q),
\end{aligned} \tag{E.8b}$$

where $\mathbf{I}^{(1)}_n$ denotes the one loop insertion operator, Eq. (2.15), and the contributions on the second line depend only on the four point scalar $\mathrm{D}^1_{ij}(q)$. Finally, using colour conservation, one can write

$$\begin{aligned}
&\sum_{i=1}^{n}\left[\mathbf{G}^c_{(f),i} + \mathbf{G}^c_{(g),i} + \mathbf{G}^c_{(uv)i}\right] = \mathbf{J}_{n+1}(q)\widetilde{K}_{uv}\\
&= \mathbf{J}_{n+1}(q)\left[(g_s\mu)^2 C_A \mathrm{B}(q) + \pi(q^2) + \sum_i^n \Sigma_i(p_i^2)\right] .
\end{aligned} \tag{E.9}$$

Appendix F

Virtual and phase space integrals at order α_s^2

In this appendix, we present the master scalar integrals that appear in the calculation of the real and imaginary parts of the one-loop, one-emission amplitude $\left|n_{+1}^{(1)}\right\rangle$, i.e. the scalar integrals in Appendix E, and the phase space integrals that appear in the calculation of the total cross-section at order α_s^2 in Chapter 4:

$$\int \mathrm{d}[q] \left\langle n_{+1}^{(0)} \middle| n_{+1}^{(1)} \right\rangle \ , \int \mathrm{d}[q_1]\mathrm{d}[q_2] \left\langle n_{+2}^{(0)} \middle| n_{+2}^{(0)} \right\rangle . \tag{F.1}$$

F.1 Imaginary parts of the one emission amplitude $\left|n_{+1}^{(1)}\right\rangle$

In this section, we show the master scalar integrals that appear in the calculation of the imaginary part of $\left|n_{+1}^{(1)}\right\rangle$. These integrals are obtained performing the tensorial reductions of the cut graphs in Fig. 3.1 and 3.5. By integrating out the delta functions associated to a cut in one of these integrals, see below, these reduce to integrals over k_T components. There are contributions that diverges as $k_T \to 0$ (IR divergent) and contributions that are power suppressed as $k_T \to \infty$ (uv finite).

F.1.1 Eikonal cuts

We shall now present the integrated expressions of the master scalar integrals that appear in the calculation of the graphs in Fig. 3.1.

uv **divergent**

The scalar integral corresponding to graph (a) of Fig. 3.1 is

$$\frac{1}{2}\int \frac{\mathrm{d}\!\!\!^{\,d}k}{(2\pi)^d}\frac{(-2\pi i)^2\delta(p_i\cdot(k+q))\delta(p_j\cdot k)}{k^2} = \frac{c_\epsilon}{8\pi p_i\cdot p_j}\int \frac{\mathrm{d}k^2_{T(ij)}}{k^{2+2\epsilon}_{T(ij)}} \qquad \text{(F.2)}$$
$$\to \frac{c_\epsilon}{8\pi p_i\cdot p_j}\int^{Q^2} \frac{\mathrm{d}k^2_{T(ij)}}{k^{2+2\epsilon}_{T(ij)}},$$

where we introduced a cut-off scale Q^2 to regularise the *uv* divergence. The contribution of cuts (b) and (c) in Fig. 3.1 is similar. It is worth mentioning that if we set the cut-off scale equal to $2p_i\cdot p_j$, this expression is equal to the imaginary part of the corresponding exact (without using the eikonal approximation) integral up to terms of order ϵ.

uv **finite**

After tensorial reductions, the calculation of graph (d) of Fig. 3.1 reduces to the following scalar integral

$$\begin{aligned}
&\frac{1}{2}\int \frac{\mathrm{d}^d k}{(2\pi)^d}\frac{(-2\pi i)^2\delta(p_i(q+k))\delta(p_j\cdot k)}{k^2(k+q)^2}\\
&= \frac{1}{2p_i\cdot p_j}\int \frac{\mathrm{d}^{d-2}k_{T(ij)}}{(2\pi)^{d-2}}\frac{1}{\left(k_{T(ij)}\right)^2\left(k_{T(ij)}+q_{T(ij)}\right)^2} \qquad \text{(F.3)}\\
&= \frac{1}{8\pi p_i\cdot q p_j\cdot q}\left(\frac{q^2_{T(ij)}}{\mu^2}\right)^{-\epsilon}\frac{c_\Gamma}{\epsilon},
\end{aligned}$$

This is the integral that was represented as a "switch" in Eq. (3.5), i.e

$$\int \frac{\mathrm{d}^{d-2}k_{T(ij)}}{(2\pi)^{d-2}}\frac{q^2_{T(ij)}}{\left(k_{T(ij)}\right)^2\left(k_{T(ij)}+q_{T(ij)}\right)^2} \approx 2\int \frac{\mathrm{d}^{d-2}k_{T(ij)}}{(2\pi)^{d-2}}\frac{q^2_{T(ij)}}{k^2_{T(ij)}(k^2_{T(ij)}+q^2_{T(ij)})}. \qquad \text{(F.4)}$$

F.1.2 Re-scattering cuts

We now discuss the scalar integrals that appear in the calculation of the cuts in Fig. 3.5.

uv **divergent**

The calculation of graphs (a)–(f) of Fig. 3.5 involves *uv* divergent integrals of the form:

$$\begin{aligned}&\frac{1}{2}\int\frac{\mathrm{d}^dk}{(2\pi)^d}\frac{(-2\pi i)^2\delta^+(k)\delta(p_l\cdot(q-k))}{p_j\cdot k}\frac{-c_\epsilon}{8\pi p_l\cdot p_j}\int\mathrm{d}k^2_{T(lj)}k^{-2-2\epsilon}_{T(lj)},\\&\to\frac{-c_\epsilon}{8\pi p_i\cdot p_j}\int^{2p_l\cdot q}\mathrm{d}k^2_{T(lj)}k^{-2-2\epsilon}_{T(lj)},\end{aligned}\tag{F.5}$$

where in the second line we introduced a cut-off scale $2p_i\cdot q$ to regularise the *uv* divergences. This is the cut-off that matches the respective exact integral up to terms of order ϵ. However, this choice of cut-off scale is irrelevant because, as we showed in Section 3.2.4, the sum of all the contributions that are *uv* divergent cancel in this case.

uv **finite**

Graphs (a) and (d) of Fig. 3.5 involve the following scalar integral:

$$\frac{1}{2}\int\frac{\mathrm{d}^dk}{(2\pi)^d}\frac{(-2\pi i)^2\delta^+(k)\delta(p_l\cdot(q_1-k))}{p_j\cdot k(q-k)^2}=\frac{1}{8\pi p_l\cdot qp_j\cdot q}\frac{(q^2_{Tlj})^{-\epsilon}c_\Gamma}{-\epsilon}\tag{F.6}$$

Clearly, this integral can again be written as a "switch".

F.2 Real parts of the integrals of $\left|n^{(1)}_{+1}\right\rangle$

In Appendix E we reduced the computation of the one-loop, one-emission amplitude, $\left|n^{(1)}_{+1}\right\rangle$, to scalar integrals. Apart from the one-loop integral contributions in $\mathbf{I}_n$, that were already considered in Appendix A, the relevant scalar integrals are $\{\mathrm{D}^1_{ij}(q),\mathrm{D}^2_{ij}(q),\mathrm{C}^3_{ij}(q)\}$, see Eqs. (E.2). Their imaginary parts can be calculated by cutting the propagators of these scalar integrals, as in Figs. 3.1 and Fig. 3.5, and are equal to the integral that we considered in Section F.1. In this section, we focus on their real parts. We do this by using the cutting rules derived in Section D.2.

F.3 $\mathbf{D}^1_{ij}(q)$

The general expression for this master scalar integral is

$$\mathrm{D}^1_{ij}(q)\equiv\int_l\frac{-i}{[p_i(l+q)+\delta_i\frac{i0}{2}][p_j(-l)+\delta_j\frac{i0}{2}][l^2+i0][(l+q)^2+i0]}\ .\tag{F.7}$$

According to the cutting rules[1] in Eq. D.7a the real part of this integral can be obtained by adding the residues of the soft gluon propagators and applying the principal value prescription on each of the propagators that are not cut:

$$\begin{aligned}\mathrm{Re}\{\mathrm{D}^1_{ij}(q)\} \equiv \mathrm{Pv}\int_l \frac{-2\pi\delta^+(l)}{\left[p_i\cdot(l+q)+\frac{i0}{2}\left[\delta_i-\frac{|\vec{p}_i|}{|\vec{l}|}\right]\right]\left[-p_j\cdot l+\frac{i0}{2}\left[\delta_j+\frac{|\vec{p}_j|}{|\vec{l}|}\right]\right]\left[(l+q)^2-i0\frac{|\vec{q}|}{|\vec{l}|}\right]} \\ + \mathrm{Pv}\int_l \frac{-2\pi\delta^+(l+q)}{\left[p_i\cdot(l+q)+\frac{i0}{2}\left[\delta_i-\frac{|\vec{p}_i|}{|\vec{l}+\vec{q}|}\right]\right]\left[-p_j\cdot l+\frac{i0}{2}\left[\delta_j+\frac{|\vec{p}_j|}{|\vec{l}+\vec{q}|}\right]\right]\left[l^2+i0\frac{|\vec{q}|}{|\vec{l}+\vec{q}|}\right]}. \quad \text{(F.8)}\end{aligned}$$

After making the change of variables $l+q\to l$ in the second integral, we can write this expression as

$$\begin{aligned}\mathrm{Re}\{\mathrm{D}^1_{ij}(q)\} = &\int_l \frac{-2\pi\delta^+(l)}{[p_i\cdot(l+q)]\,[p_j\cdot(-l)]\,[2l\cdot q]} \\ &+\int_l \frac{-2\pi\delta^+(l)}{[p_i\cdot l]\,[-2l\cdot q]}\frac{\mathrm{Pv}}{[p_j\cdot(q-l)+i\epsilon]}.\end{aligned} \quad \text{(F.9)}$$

where $\epsilon=\frac{0}{2}\left[\frac{|\vec{p}_j|}{|\vec{l}|}+\delta_j\right]$. Observe that we only retained the principal value prescription on the rightmost eikonal propagator. To justify this simplification we point out that by keeping the dimension $d=4-2\epsilon>0$ the infrared divergences of the other propagators are regularised.

By using Eq. (D.13) in Eq. (F.9) we can write

$$\begin{aligned}\mathrm{Re}\left\{\mathrm{D}^1_{ij}(q)\right\} = &\int_l \frac{-2\pi\delta^+(l)}{[p_i\cdot(l+q)]\,[p_j\cdot(-l)]\,[2l\cdot q]} \\ &+\int_l \frac{-2\pi\delta^+(l)}{[p_i\cdot l]\,[-2l\cdot q]}\left[\frac{1}{p_j\cdot(q-l)\pm i|\epsilon|}\pm i\pi\delta(p_j\cdot(q-l))\right].\end{aligned} \quad \text{(F.10)}$$

Although the integrals in the second line render separately complex numbers, their sum is a real number. The first two integrals, with a single delta function, are particular cases of (F.12) and the integral with two delta functions is given by Eq. (F.6). After inserting these integrals one gets

$$\begin{aligned}\mathrm{Re}\left\{\mathrm{D}^1_{ij}(q)\right\} &= \frac{1}{8\pi^2 p_i\cdot q p_j\cdot q}\frac{\Gamma^2[1+\epsilon]\Gamma^3[1-\epsilon]}{\Gamma[1-2\epsilon]}\frac{1}{\epsilon^2}\left(\frac{2p_i\cdot q p_j\cdot q}{4\pi p_i\cdot p_j}\right)^{-\epsilon}\cos(\epsilon\pi) \\ &= \cos^2(\epsilon\pi)\int \mathrm{d}[l]\frac{1}{[p_i\cdot(l+q)]\,[p_j\cdot l]\,[2l\cdot q]},\end{aligned} \quad \text{(F.11)}$$

where the second identity follows from comparing the first line with Eq. (F.16).

[1] In fact, in Section D.2 we derived the cutting rules for the specific case in which the hard partons i and j are both incoming. However, one can show that the same rules also still apply when one or both of these partons are in the final state. The proof in those such cases can be carried out along the lines of those of Section D.2. The key point is that as we remarked in Section D.4, the cancellation of single eikonal cuts also occurs also in such cases.

F.3.1 Catani and Grazzini's Integral

The calculation of the real part of the scalar integral $\{\mathrm{D}_{ij}^1\}$ in Section F.10 was reduced to Eq. (F.10). The two phase-space integrals that appear in this expression are particular cases of:

$$I_{CG}(p_i, q, p_j, s) = \int \frac{\mathrm{d}^d l}{(2\pi)^{d-1}} \frac{\delta^+(l)}{(p_i \cdot l)(q \cdot l)} \frac{1}{p_j \cdot l + s}, \tag{F.12}$$

where and s is a complex number. This phase-space integral also appears in the integration of the double emission contributions below, in Section F.5. Although it can be found in [41, 105], we integrate it here to illustrate how the other phase space integrals in this appendix can be carried out.

Case $s > 0$

It is convenient to use the standard method of Feynman parametrisation to combine two of the propagators as

$$I_{CG} = \int_0^1 dx \int \frac{\mathrm{d}^d l}{(2\pi)^{d-1}} \frac{\delta^+(l)}{p_i \cdot l} \left(l \cdot (qx + p_j(1-x)) + s(1-x)\right)^{-2} \ . \tag{F.13}$$

For every $x \in (0,1)$ the vector $h^\mu \equiv q^\mu x + p_j^\mu (1-x)$ is light-like with positive energy. Thus, there is always a frame in which this vector is at rest, i.e. $h^\mu = \sqrt{2q \cdot p_j x(1-x)}(1, \vec{0})$, and in this frame we have

$$I_{CG} = \int_0^1 \mathrm{d}x \int \frac{\mathrm{d}^d l}{(2\pi)^{d-1}} \frac{\delta^+(l)}{(1 - \hat{p}_i \cdot \hat{l}) p_i^0 l^0} \left(l^0 h^0 + s(1-x)\right)^{-2}. \tag{F.14}$$

One can use the delta function to integrate out the energy component. Integration over the remaining components can be done by the standard method of separating angular and radial integrals [9], $\mathrm{d}^{d-1} l = \mathrm{d}\Omega_{d-2} \mathrm{d}|\vec{l}||\vec{l}|^{d-2}$, i.e

$$I_{CG} = \left\{ \int \frac{\mathrm{d}\Omega_{d-2}}{(2\pi)^{d-1}} \frac{1}{2(1 - \hat{p}_i \cdot \hat{l})} \right\} \int_0^1 \mathrm{d}x \frac{1}{p_i \cdot h \sqrt{h^2}} \int \mathrm{d}|\vec{l}||\vec{l}|^{d-4} \left(|\vec{l}| + s(1-x)/\sqrt{h^2} \right)^{-2}. \tag{F.15}$$

The integral inside the braces evaluates to a number that depends only on ϵ. The integration over $|\vec{l}|$ is straightforward and, after this, the integration over x is also elementary. Observe that we have expressed the latter in terms of only Lorentz invariants. After integration one gets

$$I_{CG} = \frac{1}{8\pi^2 s(p_i \cdot q)} \left[\Gamma(1+2\epsilon)\Gamma(1+\epsilon)\Gamma^2[1-\epsilon]\right] \frac{1}{\epsilon^2} \left(\frac{2\pi (p_j \cdot q)(p_i \cdot p_j)}{(p_i \cdot q) s^2} \right)^\epsilon \ . \tag{F.16}$$

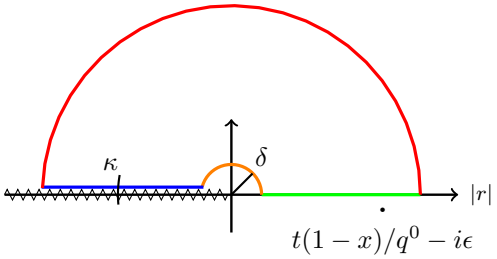

Figure F.1: Contour integration for the case $s = -t + i0$. The zig-zag line indicates the branch cut of the complex function (F.18) and the black dot denotes the only (simple) pole of the integrand. The blue contour is located at a infinitesimal distance κ from the negative real axis, and δ is a small radius of the orange semicircular contour.

Case $s = -t \mp i\epsilon, t, \epsilon > 0$

Following the same steps as in the previous case we can write

$$I_{CG} = \{...\} \int_0^1 dx \frac{1}{p_i \cdot h\sqrt{h^2}} \int_0^\infty d|\vec{l}||\vec{l}|^{d-4} \left(|\vec{l}| - (t \pm i0)(1-x)/h^0\right)^{-2} . \quad \text{(F.17)}$$

Observe that the integration over $|\vec{l}|$ passes closes to the complex pole $|\vec{l}| = t(1-x)/h^0 \pm i\epsilon$, with $\epsilon \equiv 0(1-x)/h^0 > 0$. In what follows, we focus on the lower sign case but the other case is similar. Below, we use contour integration over the radial component of the virtual momentum $r = |\vec{l}|$. In order to identify a convenient contour deformation, we need to identify the branch cuts of the integrand. Clearly, this is single valued in $d = 4 - 2\epsilon > 4$ if we define:

$$r^{-2\epsilon} = |r|^{-2\epsilon} e^{-i2\epsilon \text{Arg}(r)} , \quad \text{(F.18)}$$

and identify $\mathbb{R}^-$, including the origin, as a branch cut. The contour depicted in Fig. F.1 avoids this branch cut and deforms the green contour away from the pole of the integrand $r = t(1-x)/h^0 - i\epsilon$. In the limit $\delta \to 0$ the green contour reduces to the original integration domain. Since the integrand does not enclose any pole, the clockwise oriented contour integral over the green, blue, and orange contour vanishes. Clearly the integral over the red contour vanishes as we increase the radius whilst the integral over the orange contour behaves as $\delta^{-2\epsilon}$ and vanishes in the limit $\delta \to 0$. Then, we are left with the blue contour, this yields

$$I_{CG} = \{...\} \int_0^1 \mathrm{d}x \frac{(-1)}{p_i \cdot h\sqrt{h^2}} \int_0^\infty \mathrm{d}|\vec{l}| \left(|\vec{l}|e^{i\pi}\right)^{-2\epsilon} \left(-|\vec{l}| - t(1-x)/q^0\right)^{-2} . \quad \text{(F.19)}$$

Observe that, up to the phase factor $-(e^{i\pi})^{-2\epsilon}$, this is the same integral as in Eq. (F.16). More generally, this integral can be written as

$$I_{CG} = \frac{[\Gamma(1+2\epsilon)\Gamma(1+\epsilon)\Gamma^2[1-\epsilon]]}{8\pi^2(-t\pm i0)(p_i\cdot q)}\frac{1}{\epsilon^2}\left(\frac{2\pi(p_j\cdot q)(p_1\cdot p_j)}{(p_i\cdot p_2)t^2}\right)^{\epsilon} e^{\pm i2\pi\epsilon}. \tag{F.20}$$

F.4 $\mathrm{D}^2_{ij}(q)$ and $\mathrm{C}^3_{ij}(q)$

These yield:

$$\begin{aligned}\mathrm{D}^2_{ij}(q) &= \int \frac{\mathrm{d}^d k}{(2\pi)^d}\frac{-i}{[k^2+i0]\left[p_i\cdot k+\delta_i\frac{i0}{2}\right]\left[p_i\cdot(k+q)+\delta_i\frac{i0}{2}\right]\left[p_j\cdot(-k)+\delta_j\frac{i0}{2}\right]}\\ &= \frac{(4\pi)^{-\epsilon}\Gamma[1+\epsilon]}{8\pi^2 p_i\cdot p_j p_i\cdot q}\frac{(2p_i\cdot q e^{-i\pi\delta_{iq}})^{-\epsilon}}{\epsilon^2},\end{aligned} \tag{F.21}$$

$$\begin{aligned}\mathrm{C}^3_{ij}(q) &= \int \frac{\mathrm{d}^d k}{(2\pi)^d}\frac{-i}{[k^2+i0]\left[(k+q)^2+i0\right]\left[p_i\cdot(k+q)+\delta_i\frac{i0}{2}\right]}\\ &= \frac{(4\pi)^{-\epsilon}\Gamma[1+\epsilon]}{16\pi^2 p_i\cdot q}\frac{(2p_i\cdot q e^{-i\pi\delta_{iq}})^{-\epsilon}}{\epsilon^2}\ .\end{aligned} \tag{F.22}$$

Observe that these two integrals are equal. The calculation of the real part reduces to phase space integral, see in Section F.5.1, while the imaginary contribution reduces to one of the integrals in (F.1). It is worth noting that these two integrals are equal even without imposing cut-off scales. It is important to point out that even without introducing cut-off scales these two integrals can be shown to be equal. As a consequence, in the computation of the one-emission amplitude, $\left|n^{(1)}_{+1}\right\rangle$ the contribution that involves these two integrals cancels.

F.5 Phase space integrals for double emission

In this section we present the details for the scalar integral necessary for the inclusive integration of the double gluon emission $\left\langle n^{(0)}_{+2}\middle| n^{(0)}_{+2}\right\rangle$ in Section 4.1 . Our integration methods neglect the recoil effect against gluon emissions. In principle, in accordance with our deduction of the eikonal approximation, we should cut-off the integration for momentum components greater than the characteristic scale of the hard process. In practice, it is easier to only cut-off the integration along the directions in which the integrals are uv divergent. We shall now explain this in more detail.

F.5.1 Integrals for $\mathbf{K^2_{s.o.2}}$

Let us consider the following integral

$$\int \mathrm{d}[q_1] \frac{1}{[p_i \cdot q_1][p_i \cdot (q_1+q_2)][p_j \cdot q_1]} \ . \tag{F.23}$$

It is convenient to consider the integration expressing q_1 in terms of the following light-cone coordinates

$$q_1^\mu = \frac{q_1^+}{\sqrt{2p_i \cdot q_2}} p_i^\mu + \frac{q_1^-}{\sqrt{2p_i \cdot q_j}} q_j^\mu + q_{1T}^\mu \ . \tag{F.24}$$

One can integrate out the transverse components using the on-shell condition. After this, one is left with an integral over q_1^+ and over q_1^-. The integration over q_1^- is power suppressed as $q_1^- \to \infty$ and hence we do not need to impose a cut-off for the integration of this variable. In contrast, the integration over q_1^+ diverges logarithmically as $q_1^+ \to \infty$. To regularise this integral, we cut off the integration over q_1^+ at p_i^+. This cut-off regularisation can be written in a Lorentz invariant way:

$$\begin{aligned} &\int \mathrm{d}[q_1] \frac{1}{[p_i \cdot q_1][p_i \cdot (q_1+q_2)][p_j \cdot q_1]} \to \int \mathrm{d}[q_1] \frac{\theta(p_j \cdot (p_i - q_1))}{[p_i \cdot q_1][p_i \cdot (q_1+q_2)][p_j \cdot q_1]}, \\ &= \frac{(4\pi)^\epsilon \Gamma[1+\epsilon]}{8\pi^2} \frac{1}{p_i \cdot p_j p_i \cdot q_2} \frac{(2p_i \cdot q)^{-\epsilon}}{\epsilon^2} \ . \end{aligned} \tag{F.25}$$

We applied the same procedure to regularise the uv divergent integrals that appear in the inclusive integration of the other phase space integrals that appear in Chapter 4 and in the calculation of the real part of the one loop integrals in Section F.5.1. Below, we present the complete list of scalar integrals, indicating explicitly their cut-off regularisation:

$$\begin{aligned} &\int \mathrm{d}[q_1] \frac{1}{[q_1 \cdot q_2][p_i \cdot (q_1+q_2)][p_i \cdot q_1]} \to \int \mathrm{d}[q_1] \frac{\theta(q_2 \cdot (p_i - q_1))}{[q_1 \cdot q_2][p_i \cdot (q_1+q_2)][p_i \cdot q_1]} \\ &= \frac{(4\pi)^\epsilon \Gamma[1+\epsilon]}{8\pi^2} \frac{1}{(p_i \cdot q_2)^2} \frac{(2p_i \cdot q)^{-\epsilon}}{\epsilon^2}, \end{aligned} \tag{F.26}$$

$$\begin{aligned} &\int \mathrm{d}[q_1]\mathrm{d}[q_2] \frac{p_i \cdot p_j^2}{p_i \cdot (q_1+q_2) p_j \cdot (q_1+q_2) p_i \cdot q_1 p_j \cdot q_1} \\ &\to \int \mathrm{d}[q_1]\mathrm{d}[q_2] \frac{p_i \cdot p_j^2 \theta_{ij}(q_1)\theta_{ij}(q_2)}{p_i \cdot (q_1+q_2) p_j \cdot (q_1+q_2) p_i \cdot q_1 p_j \cdot q_1}, \\ &= \frac{1}{4} \left(\frac{c_\epsilon}{8\pi^2} \frac{(2p_i \cdot p_j)^{-\epsilon}}{\epsilon^2} \right)^2 \ , \end{aligned} \tag{F.27}$$

where $\theta_{ij}(q) = \theta(p_i(p_j - q))\theta(p_j(p_i - q))$. There is one more phase space integral that appears in the integration of the double emission cross section:

$$\int \mathrm{d}[q_1] \frac{p_i \cdot p_j}{q_1 \cdot q_2 p_i \cdot q_1 p_j \cdot (q_1 + q_2)}, \tag{F.28}$$

this is uv finite and is given by Eq. (F.12).

In all the above cases we have performed the integration over one of the two real emissions. The integration over the second variable is always reduced to the following uv divergent integral

$$\begin{aligned} &\int \mathrm{d}[q_1] \left(\frac{p_i \cdot p_j}{p_i \cdot q_1 p_j \cdot q_1} \right)^{1+\epsilon} \to \int \mathrm{d}[q_1] \left(\frac{p_i \cdot p_j}{p_i \cdot q_1 p_j \cdot q_1} \right)^{1+\epsilon} \theta_{ij}(q_1) \\ &= \frac{1}{(-2\epsilon)^2} \frac{2^\epsilon c_\epsilon}{8\pi^2} (2 p_i \cdot p_j)^{-2\epsilon} \, . \end{aligned} \tag{F.29}$$

F.5.2 Integral for $\mathbf{K^2_{sub}}$

The integration over the phase space of one of the gluon emissions is uv finite. It can be performed with the same methods of Section F.3.1. It yields

$$\begin{aligned} &\int \mathrm{d}[q_2] \frac{1}{q_1 \cdot q_2} \frac{1}{p_i \cdot (q_2 + q_1)} \frac{1}{p_j \cdot (q_2 + q_1)} = \\ &\frac{1}{8\pi^2} \frac{\Gamma[1+\epsilon]^2 \Gamma[1-\epsilon]}{(1+2\epsilon)} \frac{1}{-\epsilon} \frac{(4\pi)^\epsilon}{q_1 \cdot p_i q_1 \cdot p_j} \left(\frac{p_i \cdot p_j}{2 q_1 \cdot p_i q_1 \cdot p_j} \right)^\epsilon . \end{aligned} \tag{F.30}$$

Appendix G

On the breaking of strict collinear factorisation

By inspecting the eikonal rules[1] corresponding to the graphs in Fig. 3.6, one can deduce that the one-loop corrections to a hard process that absorbs an incoming gluon with momentum q is

$$\left|n^{(1)}(-q)\right\rangle = \mathbf{J}_{n+1}(-q)\left(\mathbf{I}_n^{(1)} + \tilde{K}_{uv}\right)\left|n^{(0)}\right\rangle + \mathbf{J}_{n+1}^{(1)}(-q)\left|n^{(0)}\right\rangle\left|n^{(0)}\right\rangle \ .$$

In this case, the symbol δ_{iq} in $\mathbf{J}_{n+1}^{(1)}(-q)$ is equal to one when i is incoming and zero otherwise. We can now derive all of the conclusions drawn in Section 2.4.4 for the breaking of strict factorisation in the two particle collinear limit. This time, however, one can derive not only the collinear behaviour of the pole part but for the finite part of one-loop splitting operators $\widetilde{\mathbf{Sp}}^{(1)}$:

$$\begin{aligned}\lim_{p_l\|q}\left|n_{+1}^{(1)}\right\rangle &= \mathbf{Sp}^{(0)}(q)\left(\mathbf{I}_n^{(0,Q)} + K_{uv}\right)\left|n^{(0)}\right\rangle + \mathbf{S}^{(1)}\left|n^{(0)}\right\rangle, \\ \widetilde{\mathbf{Sp}}^{(0)} &\equiv \lim_{p_l\|q}\mathbf{J}_{n+1}(q)\ , \qquad \widetilde{\mathbf{Sp}}^{(1)} \equiv \lim_{p_l\|q}\mathbf{J}_{n+1}^{(1)}(q)\ .\end{aligned} \tag{G.1}$$

We remind the reader that strict factorisation holds whenever $\widetilde{\mathbf{Sp}}^{(1)}$ can be expressed in terms of the collinear partons only (see Section 2.4.4). In the particular case where q is an emission which becomes collinear with an outgoing hard parton l, we have

$$\widetilde{\mathbf{Sp}}^{(1)\,c}\left|n^{(0)}\right\rangle = \frac{\alpha_s}{2\pi}\mathbf{T}_q\cdot\mathbf{T}_l\frac{c_\Gamma}{\epsilon^2}\left[\frac{q_{T(lr)}^2 e^{-i\pi\delta_{lq}}}{\mu^2}\right]^{-\epsilon}\widetilde{\mathbf{Sp}}^{(0)}\left|n^{(0)}\right\rangle\ , \tag{G.2}$$

[1] From Fig. 2.1 we can infer that the eikonal rule for momentum q flowing in the initial (final) state is the same as minus the eikonal rule for momentum $-q$ flowing in the final (initial) state.

and thus, in this case, strict factorisation holds. In striking contrast, when q is collinear with an incoming parton l we have

$$\begin{aligned}\widetilde{\mathbf{Sp}}^{(1),c}\Big|n^{(0)}\Big\rangle &= \frac{\alpha}{2\pi}\frac{c_\Gamma}{\epsilon^2}\mathbf{T}_q\cdot\mathbf{T}_l\left[\frac{q^2_{T(lr)}e^{-i\pi}}{\mu^2}\right]^{-\epsilon}\widetilde{\mathbf{Sp}}^{(0)}\Big|n^{(0)}\Big\rangle \\ &+ (i\sin(\pi\epsilon))\frac{\alpha_s}{4\pi}\frac{c_\Gamma}{\epsilon^2}4\mathbf{T}_{\mathrm{NC}\cap\mathrm{in}}\cdot(\mathbf{T}_l-\mathbf{T}_P)\left[\frac{q^2_{T(lr)}}{\mu^2}\right]^{-\epsilon}\widetilde{\mathbf{Sp}}^{(0)}\Big|n^{(0)}\Big\rangle,\end{aligned} \tag{G.3}$$

where $\mathbf{T}_P=\mathbf{T}_l+\mathbf{T}_q$, is the colour charge of the parent parton. Again the first line depends only on collinear partons, whereas the second is purely imaginary and in general, depends on $\mathbf{T}_{\mathrm{NC}\cap\mathrm{in}}$, the total charge of the non-collinear incoming partons. Indeed, this expression has the same violations of strict factorisation as Eq. (2.47). Hence, the violations of collinear factorisation of the finite part of the one-loop splitting operator has the same structure that the pole part does.

Appendix H

Reductions: from cut pentagons into boxes

In this appendix we discuss the methods of integration required to calculate the tensor integrals that appear in the calculation double emission case. These were implemented in `Wolfram Mathematica` notebooks using the `Feyncalc` package. For reasons explained below, we adopted the dimensional reduction scheme [106, 107] in chapters 5 and 6, i.e. we imposed the condition that the momenta of all the external partons are four dimensional vectors and their respective polarisation vectors and spinors have exactly 2 helicities. The virtual momentum is a vector in $d = 4-2\epsilon > 0$ dimensions.

Schematically, the tensor integrals that appear in the calculation are:

$$\int_k \frac{(\text{double cut})}{d_0} \,, \tag{H.1}$$

$$\int_k \frac{(\text{double cut})\{1, k^\mu\}}{d_0 d_1} \,, \tag{H.2}$$

$$\int_k \frac{(\text{double cut})\{1, k^\mu, k^\mu k^\nu\}}{d_0 d_1 d_2} \,, \tag{H.3}$$

where $\{d_0, d_1, d_2\}$ denote propagators, and the explicit form of the double cuts depends on whether we are considering eikonal, soft gluon or re-scattering cuts. It is customary to refer to these integrals as three, four and five point integrals and to the number of powers of the loop momenta in the denominator as the integral rank. In what follows, we will show that, up to non-logarithmic corrections, these integrals can be reduced to scalar three and four point functions.

The reduction of rank 1 tensor integrals can be carried out using the standard technique of Passarino-Veltman (PaVe) reductions [98]. The reduction of the second rank and scalar five-point integrals into boxes are more subtle and we discuss them in detail. For simplicity, we specialise to the particular case of the eikonal cuts. But

the reduction in the cases of soft gluon cuts and re-scattering cuts is similar. Eikonal cuts can be expressed as transverse momentum integrals after integrating out the delta function associated to the cuts. After this, the double cut five-point integrals become three point functions:

$$\begin{aligned}
&\int \mathrm{d}^{d-2}k_T \frac{\{1, k_T^\mu, k_T^\mu k_T^\nu\}}{d_0 d_1 d_2}, \\
&d_0 \to k_T^2 + m_0^2, \\
&d_1 \to (k+q_1)_T^2 + m_1^2, \\
&d_2 \to (k+q_2)_T^2 + m_2^2 \ ,
\end{aligned}$$

where $\{q_{1T}, q_{2T}\}$ denote the transverse components, and the masses $\{m_0, m_1, m_2\}$ are positive constants[1]. Observe that the double cut pentagons in $d = 4-2\epsilon$ dimensions becomes three point functions in $d = 2-2\epsilon$. In what follows, we will show these three point integrals can be reduced to scalar two point integrals.

To carry out reductions for five-point functions, it convenient to introduce the so-called Van Neerven (VN) basis [99]. Our presentation of this method closely follows [108]. The first step of this method is the construction of a basis that spans the same space as the vectors $\{q_{1T}, q_{2T}\}$ such that

$$q_{aT} \cdot v_b = \begin{cases} 1 \text{ if } a = b \ , \\ 0 \text{ if } a = b \ . \end{cases} \tag{H.4}$$

The explicit form of these vectors can be easily written in terms of the two-dimensional, completely anti-symmetric, tensor $\epsilon^{\mu\nu} = 1$. In terms of this tensor, such a basis is given by

$$\left\{ v_1^\mu \equiv \frac{q_{2\nu_1}\epsilon^{\mu\nu_1}}{q^{\mu_2}q^{\nu_2}\epsilon_{\mu_2\nu_2}} \ , v_2^\mu \equiv \frac{q_{1\mu_1}\epsilon^{\mu_1\mu}}{q^{\mu_2}q^{\nu_2}\epsilon_{\mu_2\nu_2}} \right\} \ . \tag{H.5}$$

Here and in what follows, we omit the subscript T in the transverse vectors. In terms of the Van-Neerven basis vectors, the $d-2 = 2-2\epsilon > 2$ transverse components of the loop momentum can be written as

$$k^\mu = \alpha_1 v_1^\mu + \alpha_2 v_2^\mu + k_\epsilon^\mu, \tag{H.6}$$

where $\alpha_{1,2}$ are coefficients of the linear decomposition and k_ϵ is a vector that parametrises the $d-4 = -2\epsilon$ dimension. Since we are working in the dimensional reduction scheme, the vectors $\{q_1, q_2\}$ live in exactly 2 dimensions and hence $q_a \cdot k_\epsilon = 0$ for

[1] They can depend on the non-transverse components of the real emissions, but this is irrelevant for what follows.

$a = \{1, 2\}$. By construction, see Eq. (H.4), $q_a \cdot k = \alpha_a$ and from this it follows that

$$\begin{aligned} \alpha_a &= \frac{1}{2}\left[d_a - d_0 + r_a\right] \ , \\ r_a &\equiv m_0^2 - m_a^2 - q_a^2 \ . \end{aligned} \tag{H.7}$$

By contracting (H.6) with the loop momentum k and after some algebra one has, (additional details can be found in Ref. [108])

$$k^2 = \frac{1}{2}\left[\sum_{a=\{1,2\}} \left([2k \cdot v_a - \omega \cdot v_a]d_a + (\omega - 2k) \cdot v_a d_0\right) + \omega^2\right] \ , \tag{H.8}$$

where $\omega^\mu \equiv r_1 v_1^\mu + r_2 v_2^\mu$ is a vector independent of the loop momentum. This expression can be rearranged into the following form

$$1 = \frac{1}{4m_0^2 + \omega^2}\left[\sum_{a=1}^{2} \left[\omega \cdot v_i - 2k \cdot v_i\right] d_i + [4 - (2k - \omega) \cdot (v_1 + v_2)]d_0 - 4k_\epsilon^2\right] \ . \tag{H.9}$$

We can now use this expression to reduce the three point function:

$$\begin{aligned} \int \mathrm{d}^{d-2}k \frac{1}{d_0 d_1 d_2} = \frac{1}{4m_0^2 + \omega^2} \int \mathrm{d}^{d-2}k \left[\frac{\omega \cdot v_1 - 2k \cdot v_1}{d_0 d_2} + \frac{\omega \cdot v_2 - 2k \cdot v_2}{d_0 d_1}\right] \\ \frac{1}{4m_0^2 + \omega^2} \int \mathrm{d}^{d-2}k \left[\frac{4 + (2k - \omega) \cdot (v_1 + v_2)}{d_1 d_2} - \frac{4k_\epsilon^2}{d_0 d_1 d_2}\right] \ . \end{aligned} \tag{H.10}$$

Observe that the first three integrals are now two-point functions with denominators that depend on the loop momentum. Due to the euclidean invariance in $d - 2$ dimension, the terms linear in the first two integrals vanish. Indeed, they have to be respectively proportional to q_2 and q_1 but because $v_1 \cdot q_2 = v_2 \cdot q_1 = 0$ these terms disappear. The same occurs in the third integral, after a change of variables $k \to k - q_1$. After this, the three-point function reduces to

$$\begin{aligned} \int \mathrm{d}^{d-2}k \frac{1}{d_0 d_1 d_2} = \frac{1}{4m_0^2 + \omega^2} \int \mathrm{d}^{d-2}k \left[\frac{\omega \cdot v_1}{d_0 d_2} + \frac{\omega \cdot v_2}{d_0 d_1}\right] \\ \frac{1}{4m_0^2 + \omega^2} \int \mathrm{d}^{d-2}k \left[\frac{2 - \omega \cdot (v_1 + v_2)}{d_1 d_2} - \frac{4k_\epsilon^2}{d_0 d_1 d_2}\right] \ . \end{aligned} \tag{H.11}$$

Hence, the first three integrals have been reduced to scalar integrals. Observe that the fourth integral is still a three-point integral. In general, these remainders that arise from the decompositions of (cut) pentagons into (cut) boxes are known as rational terms. They can contribute to the loop integrals with finite (as $d \to 4$) rational polynomials of the kinematical invariants [108, 100]. In chapters 5 and 6, we neglected these contributions as they do not contain logarithmic and pole corrections.

The latter arise from the integration of the two point functions.

We shall now study the reductions of the tensor three-point integrals. These integrals can be straightforwardly reduced by inserting the parametrisation of the loop momentum in terms of the VN basis, see Eq. (H.6). For instance, in the case of the scalar three-point function one gets

$$\int \mathrm{d}^{d-2}k_T \frac{k^\mu}{d_0 d_1 d_2} = \int \mathrm{d}^{d-2}k_T \frac{\alpha_1 v_1^\mu + \alpha_2 v_2^\mu + k_\epsilon^\mu}{d_0 d_1 d_2}. \tag{H.12}$$

Since, see Eq. (H.7), the coefficients, $\alpha_{1,2}$, are linear combinations of the propagators the terms proportional to the VN vectors can be now reduced to two-point functions. Finally, within the context of dimensional reduction, the terms proportional to the vector k_ϵ^μ, that parametrises the $d-4$ dimensions, exactly cancel at the amplitude level. Indeed, they always appear contracted with two-dimensional vectors and hence vanish, e.g. $\varepsilon_T \cdot k_\epsilon = 0$.

The reduction of the second rank, three point function in terms of the VN vectors is analogous. In principle, we could use more conventional reduction methods, such as the PaVe reductions. A naïve use of the PaVe reductions suggests that the right hand side of the second rank tensor is a linear combination of all possible tensor structures:

$$\int \mathrm{d}^{d-2}k_T \frac{k^\mu k^\nu}{d_0 d_1 d_2} = \left[I_1 q_1^\mu q_1^\nu + I_2 q_2^\mu q_2^\nu + I_3 \left[q_1^\mu q_2^\nu + q_2^\mu q_1^\nu \right] + \eta_{d-2}^{\mu\nu} I_4 \right], \tag{H.13}$$

where $\eta_{d-2}^{\mu\nu}$ denotes the metric tensor in $d-2$ euclidean dimensions and $I_{1,2,3,4}$ denote scalar functions. This naïve parametrisation of the possible tensor structures on the right-hand side is wrong. The reason is that the space spanned by the first three tensors, i.e. $\{q_1^\mu q_1^\nu, q_2^\mu q_2^\nu, q_1^\mu q_2^\nu + q_2^\mu q_2^\nu\}$, already contains the two-dimensional metric tensor $\eta_2^{\mu\nu}$. It follows that the introduction of the tensor $\eta_{d-2}^{\mu\nu}$ on the right hand side over-parametrises the space of possible tensor structures. The reduction in terms of the VN vectors solves this problem as, by construction, it parametrises exactly the $d-2$ dimensions of the loop momentum.

To summarise, we have discussed how, up to rational (non-logarithmic) contributions, the calculation of the eikonal cuts can be reduced to scalar two-point functions. Exactly the same methods can be applied to the re-scattering cuts. In the case of soft gluon cuts, it is easier to reduce the integrals to scalar boxes before integrating out the delta functions corresponding to the double cut. In an analogous manner, one can introduce VN vectors to reduce the (double cut) pentagons into (double cut) boxes. In the rest of this appendix we present the relevant master scalar integrals. The epsilon expansion of this expression can be carried out using the mathematical package in [109].

H.0.3 Master integrals for eikonal and re-scattering cuts

The eikonal and re-scattering cuts can always be reduced to transverse momentum integrals. In addition to the integrals encountered in the one-emission case, the required integrals for the case of two-emission (Figs. 5.5, 6.2 and 6.3) are:

$$\int \frac{\mathrm{d}^{d-2}k}{(2\pi)^{d-2}} \frac{\mu^{2\epsilon}}{k^2[k^2+a]} = \frac{(4\pi\mu^2)^\epsilon \Gamma[1+\epsilon]}{4\pi} \frac{a^{-1-\epsilon}}{-\epsilon}. \tag{H.14}$$

$$\begin{aligned} &\int \frac{\mathrm{d}^{d-2}k}{(2\pi)^{d-2}} \frac{1}{k^2[(k+q)^2+a]} \\ &= \frac{(4\pi\mu^2)^\epsilon \Gamma[1+\epsilon]}{4\pi} \frac{(a+h^2)^{-1-\epsilon}}{-\epsilon} \, {}_2F_1[-\epsilon, 1+\epsilon, 1-\epsilon, \frac{h^2}{a+h^2}] \\ &= \frac{(4\pi)^\epsilon \Gamma[1+\epsilon]}{4\pi} \frac{1}{(a+h^2)} \left(\frac{1}{-\epsilon} + \ln \frac{(h^2+a)^2}{a\mu^2} \right) + \mathcal{O}(\epsilon), \end{aligned} \tag{H.15}$$

where in these two expressions $a > 0$.

H.0.4 Master integrals for soft gluon cuts

We shall now present the four point scalar functions that appear in the calculation of the cuts over soft gluon lines (Fig. 5.10). It is convenient to introduce the following notation:

$$\Delta(k) \equiv [-2\pi i \delta^+(l^2)][-2\pi i \delta^+((\widetilde{q}-k)^2)]/2, \tag{H.16}$$

where here and throughout this section $\widetilde{q} \equiv q_1 + q_2$. Exactly as we did with Eq.(5.33), the soft gluon cuts can be reduced to an integration over the solid angle in $d-2$ dimension, see (5.34). The exact expressions of the resulting integrals in dimensional regularisation can be found in Ref. [101, 102]. In particular, the cut box integrals yield:

$$\begin{aligned} &\int_k \frac{\Delta(k)}{p_j \cdot (\widetilde{q}-k)(q_1+k)^2} = \frac{c_\epsilon}{8\pi p_j \cdot q_2 \widetilde{q}^2} \left[\frac{\widetilde{q}^2 p_j \cdot q_2}{p_j \cdot \widetilde{q}} \right]^{-\epsilon} \frac{1}{-\epsilon} \times \\ &\left[\frac{\Gamma^2[1-\epsilon]}{\Gamma[1-2\epsilon]} \left[\frac{p_j \cdot q_2}{p_j \cdot \widetilde{q}} \right]^{1+\epsilon} {}_1F_2[1, 1, 1-\epsilon; \frac{p_j \cdot q_2}{p_j \cdot \widetilde{q}} \right] \\ &= \frac{c_\epsilon}{8\pi p_j \cdot q_2 \widetilde{q}^2} \left[\frac{\widetilde{q}^2 p_j \cdot q_2}{p_j \cdot \widetilde{q}} \right]^{-\epsilon} \frac{1}{-\epsilon} \times \left[1 + \mathcal{O}(\epsilon^2) \right], \end{aligned} \tag{H.17}$$

$$\int_k \frac{\Delta(k)}{p_i\cdot k(k-q_1)^2} = \frac{c_\epsilon}{8\pi p_i\cdot q_1 \widetilde{q}^2}\left[\frac{\widetilde{q}^2 p_i\cdot q_1}{p_i\cdot\widetilde{q}}\right]^{-\epsilon}\frac{1}{-\epsilon}\times$$
$$\left[\frac{\Gamma^2[1-\epsilon]}{\Gamma[1-2\epsilon]}\left[\frac{p_i\cdot q_1}{p_i\cdot\widetilde{q}}\,{}_1F_2[1,1,1-\epsilon;\frac{p_i\cdot q_1}{p_i\cdot\widetilde{q}}]\right]\right] \tag{H.18}$$
$$= \frac{c_\epsilon}{8\pi p_i\cdot q_q\widetilde{q}^2}\left[\frac{2q_1\cdot q_2 p_i\cdot q_1}{p_i\cdot\widetilde{q}}\right]^{-\epsilon}\frac{1}{-\epsilon}\times\left[1+\mathcal{O}(\epsilon^2)\right],$$

$$\int_k \frac{\Delta(k)}{[p_i\cdot k][p_j\cdot(\widetilde{q}-k)]} = \frac{-c_\epsilon}{8\pi[2p_i\cdot\widetilde{q}p_j\cdot(\widetilde{q})-p_i\cdot p_j\widetilde{q}^2]}\left[\widetilde{q}^2\left[1-\frac{p_i\cdot p_j\widetilde{q}^2}{2p_i\cdot\widetilde{q}p_j\cdot\widetilde{q}}\right]\right]^{-\epsilon}\frac{1}{-\epsilon}\times$$
$$\left[\frac{\Gamma^2[1-\epsilon]}{\Gamma[1-2\epsilon]}\left[1-\frac{p_i\cdot p_j\widetilde{q}^2}{2p_i\cdot\widetilde{q}p_j\cdot\widetilde{q}}\right]^{1+\epsilon}{}_1F_2[1,1,1-\epsilon;1-\frac{p_i\cdot p_j\widetilde{q}^2}{2p_i\cdot\widetilde{q}p_j\cdot\widetilde{q}}\right] \tag{H.19}$$
$$= \frac{-c_\epsilon}{8\pi[2p_i\cdot\widetilde{q}p_j\cdot(\widetilde{q})-p_i\cdot p_j\widetilde{q}^2]}\left[\widetilde{q}^2\left[1-\frac{p_i\cdot p_j\widetilde{q}^2}{2p_i\cdot\widetilde{q}p_j\cdot\widetilde{q}}\right]\right]^{-\epsilon}\frac{1}{-\epsilon}\times\left[1+\mathcal{O}(\epsilon^2)\right].$$

Bibliography

[1] G. F. Sterman, *An Introduction to quantum field theory*. Cambridge University Press, 1993.

[2] L. D. Faddeev and V. N. Popov, "Feynman Diagrams for the Yang-Mills Field," *Phys. Lett.* **B25** (1967) 29–30.

[3] R. K. Ellis, W. J. Stirling, and B. R. Webber, "QCD and collider physics," *Camb. Monogr. Part. Phys. Nucl. Phys. Cosmol.* **8** (1996) 1–435.

[4] T. Muta, "Foundations of quantum chromodynamics: An Introduction to perturbative methods in gauge theories," *World Sci. Lect. Notes Phys.* **5** (1987) 1–409.

[5] G. 't Hooft, "Renormalization of Massless Yang-Mills Fields," *Nucl. Phys.* **B33** (1971) 173–199.

[6] H. D. Politzer, "Reliable Perturbative Results for Strong Interactions?," *Phys. Rev. Lett.* **30** (1973) 1346–1349.

[7] D. J. Gross and F. Wilczek, "Asymptotically Free Gauge Theories. 1," *Phys. Rev.* **D8** (1973) 3633–3652.

[8] D. J. Gross and F. Wilczek, "Ultraviolet Behavior of Nonabelian Gauge Theories," *Phys. Rev. Lett.* **30** (1973) 1343–1346.

[9] M. H. Seymour, "Quantum chromodynamics," in *2004 European School of High-Energy Physics, Sant Feliu de Guixols, Spain, 30 May - 12 June 2004*, pp. 49–94. 2005. `arXiv:hep-ph/0505192 [hep-ph]`. `http://doc.cern.ch/yellowrep/CERN-PH-TH-2005-083`.

[10] G. F. Sterman, "Partons, factorization and resummation, TASI 95," in *QCD and beyond. Proceedings, Theoretical Advanced Study Institute in Elementary Particle Physics, TASI-95, Boulder, USA, June 4-30, 1995*. 1995. `arXiv:hep-ph/9606312 [hep-ph]`.

[11] L. D. Landau, "On analytic properties of vertex parts in quantum field theory," *Nucl. Phys.* **13** (1959) 181–192.

[12] S. Coleman and R. E. Norton, "Singularities in the physical region," *Nuovo Cim.* **38** (1965) 438–442.

[13] G. F. Sterman, "Mass Divergences in Annihilation Processes. 1. Origin and Nature of Divergences in Cut Vacuum Polarization Diagrams," *Phys. Rev.* **D17** (1978) 2773.

[14] S. B. Libby and G. F. Sterman, "Mass Divergences in Two Particle Inelastic Scattering," *Phys. Rev.* **D18** (1978) 4737.

[15] J. Collins, *Foundations of perturbative QCD*. Cambridge University Press, 2013. `http://www.cambridge.org/de/knowledge/isbn/item5756723`.

[16] R. Gastmans and R. Meuldermans, "Dimensional regularization of the infrared problem," *Nucl. Phys.* **B63** (1973) 277–284.

[17] T. Kinoshita, "Mass singularities of Feynman amplitudes," *J. Math. Phys.* **3** (1962) 650–677.

[18] T. D. Lee and M. Nauenberg, "Degenerate systems and mass singularities," *Phys. Rev.* **133** (1964) B1549–B1562.

[19] M. A. Shifman, A. I. Vainshtein, and V. I. Zakharov, "QCD and Resonance Physics. Theoretical Foundations," *Nucl. Phys.* **B147** (1979) 385–447.

[20] R. P. Feynman, *Photon-hadron interactions*. Addison-Wesley, 1972. `http://www-library.desy.de/cgi-bin/spiface/find/hep/www?key=6634834&FORMAT=WWWBRIEFBIBTEX`. Reading 1972, 282p.

[21] J. C. Collins, D. E. Soper, and G. F. Sterman, "Factorization of hard processes in QCD," *Adv. Ser. Direct. High Energy Phys.* **5** (1989) 1–91, `arXiv:hep-ph/0409313 [hep-ph]`.

[22] J. C. Collins, D. E. Soper, and G. F. Sterman, "Factorization for Short Distance Hadron - Hadron Scattering," *Nucl. Phys.* **B261** (1985) 104.

[23] S. M. Aybat and G. F. Sterman, "Soft-Gluon Cancellation, Phases and Factorization with Initial-State Partons," *Phys. Lett.* **B671** (2009) 46–50, `arXiv:0811.0246 [hep-ph]`.

[24] M. Diehl, J. R. Gaunt, D. Ostermeier, P. Ploessl, and A. Schafer, "Cancellation of Glauber gluon exchange in the double Drell-Yan process," `arXiv:1510.08696 [hep-ph]`.

[25] G. T. Bodwin, "Factorization of the Drell-Yan Cross-Section in Perturbation Theory," *Phys. Rev.* **D31** (1985) 2616. [Erratum: Phys. Rev.D34,3932(1986)].

[26] J. C. Collins, D. E. Soper, and G. F. Sterman, "Soft Gluons and Factorization," *Nucl. Phys.* **B308** (1988) 833.

[27] G. Altarelli and G. Parisi, "Asymptotic Freedom in Parton Language," *Nucl. Phys.* **B126** (1977) 298.

[28] S. Catani and M. Seymour, "A General algorithm for calculating jet cross-sections in NLO QCD," *Nucl.Phys.* **B485** (1997) 291–419, arXiv:hep-ph/9605323 [hep-ph].

[29] S. Catani, D. de Florian, and G. Rodrigo, "Space-like (versus time-like) collinear limits in QCD: Is factorization violated?," *JHEP* **07** (2012) 026, arXiv:1112.4405 [hep-ph].

[30] J. R. Forshaw, M. H. Seymour, and A. Siodmok, "On the Breaking of Collinear Factorization in QCD," *JHEP* **11** (2012) 066, arXiv:1206.6363 [hep-ph].

[31] J. R. Forshaw, A. Kyrieleis, and M. Seymour, "Super-leading logarithms in non-global observables in QCD," *JHEP* **0608** (2006) 059, arXiv:hep-ph/0604094 [hep-ph].

[32] J. R. Gaunt, "Glauber Gluons and Multiple Parton Interactions," *JHEP* **1407** (2014) 110, arXiv:1405.2080 [hep-ph].

[33] M. Zeng, "Drell-Yan process with jet vetoes: breaking of generalized factorization," *JHEP* **10** (2015) 189, arXiv:1507.01652 [hep-ph].

[34] Z. Nagy and D. E. Soper, "Parton shower evolution with subleading color," *JHEP* **06** (2012) 044, arXiv:1202.4496 [hep-ph].

[35] Z. Nagy and D. E. Soper, "Ordering variable for parton showers," *JHEP* **06** (2014) 178, arXiv:1401.6366 [hep-ph].

[36] J. R. Forshaw, A. Kyrieleis, and M. H. Seymour, "Super-leading logarithms in non-global observables in QCD: colour basis independent calculation, arXiv:1206.6363v1," *Journal of High Energy Physics* **9** (Sept., 2008) 128, arXiv:0808.1269 [hep-ph].

[37] O. Almelid, C. Duhr, and E. Gardi, "Three-loop corrections to the soft anomalous dimension in multi-leg scattering," arXiv:1507.00047 [hep-ph].

[38] A. Banfi, G. P. Salam, and G. Zanderighi, "Phenomenology of event shapes at hadron colliders," *JHEP* **1006** (2010) 038, arXiv:1001.4082 [hep-ph].

[39] A. Buckley *et al.*, "General-purpose event generators for LHC physics," *Phys. Rept.* **504** (2011) 145–233, arXiv:1101.2599 [hep-ph].

[40] A. Banfi, G. P. Salam, and G. Zanderighi, "Principles of general final-state resummation and automated implementation," *JHEP* **03** (2005) 073, arXiv:hep-ph/0407286 [hep-ph].

[41] S. Catani and M. Grazzini, "The soft gluon current at one loop order," *Nucl.Phys.* **B591** (2000) 435–454, arXiv:hep-ph/0007142 [hep-ph].

[42] C. Anastasiou, S. Buehler, C. Duhr, and F. Herzog, "NNLO phase space master integrals for two-to-one inclusive cross sections in dimensional regularization," *JHEP* **11** (2012) 062, arXiv:1208.3130 [hep-ph].

[43] A. Gehrmann-De Ridder, T. Gehrmann, and E. W. N. Glover, "Infrared structure of e+ e- - 2 jets at NNLO," *Nucl. Phys.* **B691** (2004) 195–222, arXiv:hep-ph/0403057 [hep-ph].

[44] C. Anastasiou, C. Duhr, F. Dulat, F. Herzog, and B. Mistlberger, "Higgs Boson Gluon-Fusion Production in QCD at Three Loops," *Phys. Rev. Lett.* **114** (2015) 212001, arXiv:1503.06056 [hep-ph].

[45] S. Caron-Huot, "Resummation of non-global logarithms and the BFKL equation," arXiv:1501.03754 [hep-ph].

[46] C. Anastasiou, C. Duhr, F. Dulat, E. Furlan, F. Herzog, and B. Mistlberger, "Soft expansion of double-real-virtual corrections to Higgs production at N^3LO," *JHEP* **08** (2015) 051, arXiv:1505.04110 [hep-ph].

[47] S. Catani and M. Ciafaloni, "Many Gluon Correlations and the Quark Form-factor in QCD," *Nucl. Phys.* **B236** (1984) 61.

[48] S. Catani and M. Ciafaloni, "Gauge covariance of QCD coherent states," *Nucl. Phys.* **B289** (1987) 535.

[49] A. Bassetto, M. Ciafaloni, G. Marchesini, and A. H. Mueller, "Jet Multiplicity and Soft Gluon Factorization," *Nucl.Phys.* **B207** (1982) 189.

[50] Z. Nagy, G. Somogyi, and Z. Trocsanyi, "Separation of soft and collinear infrared limits of QCD squared matrix elements," arXiv:hep-ph/0702273 [HEP-PH].

[51] J. Keates and M. H. Seymour, "Super-leading logarithms in non-global observables in QCD: Fixed order calculation," *JHEP* **0904** (2009) 040, arXiv:0902.0477 [hep-ph].

[52] S. Catani, "The Singular behavior of QCD amplitudes at two loop order," *Phys. Lett.* **B427** (1998) 161–171, arXiv:hep-ph/9802439 [hep-ph].

[53] M. H. Seymour and M. Sjodahl, "Symmetry of anomalous dimension matrices explained," *JHEP* **12** (2008) 066, arXiv:0810.5756 [hep-ph].

[54] S. Catani and M. Grazzini, "Infrared factorization of tree level QCD amplitudes at the next-to-next-to-leading order and beyond," *Nucl.Phys.* **B570** (2000) 287–325, arXiv:hep-ph/9908523 [hep-ph].

[55] G. F. Sterman and M. E. Tejeda-Yeomans, "Multiloop amplitudes and resummation," *Phys. Lett.* **B552** (2003) 48–56, arXiv:hep-ph/0210130 [hep-ph].

[56] S. M. Aybat, L. J. Dixon, and G. F. Sterman, "The Two-loop soft anomalous dimension matrix and resummation at next-to-next-to leading pole," *Phys. Rev.* **D74** (2006) 074004, arXiv:hep-ph/0607309 [hep-ph].

[57] L. J. Dixon, L. Magnea, and G. F. Sterman, "Universal structure of subleading infrared poles in gauge theory amplitudes," *JHEP* **08** (2008) 022, arXiv:0805.3515 [hep-ph].

[58] L. J. Dixon, E. Gardi, and L. Magnea, "On soft singularities at three loops and beyond," *JHEP* **02** (2010) 081, arXiv:0910.3653 [hep-ph].

[59] T. Becher and M. Neubert, "On the Structure of Infrared Singularities of Gauge-Theory Amplitudes," *JHEP* **06** (2009) 081, arXiv:0903.1126 [hep-ph]. [Erratum: JHEP11,024(2013)].

[60] L. Magnea, V. Del Duca, C. Duhr, E. Gardi, and C. D. White, "Infrared singularities in the high-energy limit," *PoS* **LL2012** (2012) 008, arXiv:1210.6786 [hep-ph].

[61] C. D. White, "An Introduction to Webs," *J. Phys.* **G43** no. 3, (2016) 033002, arXiv:1507.02167 [hep-ph].

[62] L. Magnea, "Progress on the infrared structure of multi-particle gauge theory amplitudes," *PoS* **LL2014** (2014) 073, arXiv:1408.0682 [hep-ph].

[63] E. Gardi, "Infrared singularities in multi-leg scattering amplitudes," *PoS* **LL2014** (2014) 069, arXiv:1407.5164 [hep-ph].

[64] E. Laenen, K. J. Larsen, and R. Rietkerk, "Imaginary parts and discontinuities of Wilson line correlators," *Phys. Rev. Lett.* **114** no. 18, (2015) 181602, arXiv:1410.5681 [hep-th].

[65] D. Amati, A. Bassetto, M. Ciafaloni, G. Marchesini, and G. Veneziano, "A Treatment of Hard Processes Sensitive to the Infrared Structure of QCD," *Nucl. Phys.* **B173** (1980) 429.

[66] F. Fiorani, G. Marchesini, and L. Reina, "Soft gluon factorisation and multi-gluon amplitude," *Nucl.Phys.* **B309** (1988) 439.

[67] S. Catani and M. Ciafaloni, "Generalized Coherent State for Soft Gluon Emission," *Nucl.Phys.* **B249** (1985) 301.

[68] G. Marchesini, "Soft radiation in QCD jets," *Acta Phys. Polon.* **B15** (1984) 277. [,337(1983)].

[69] F. Bloch and A. Nordsieck, "Note on the Radiation Field of the electron," *Phys. Rev.* **52** (1937) 54–59.

[70] G. F. Sterman, "Infrared Divergences in Perturbative QCD.," *AIP Conf. Proc.* **74** (1981) 22–40.

[71] J. G. M. Gatheral, "Exponentiation of Eikonal Cross-sections in Nonabelian Gauge Theories," *Phys. Lett.* **B133** (1983) 90.

[72] J. Frenkel and J. C. Taylor, "Nonabelian eikonal exponentiation," *Nucl. Phys.* **B246** (1984) 231.

[73] E. Laenen, G. Stavenga, and C. D. White, "Path integral approach to eikonal and next-to-eikonal exponentiation," *JHEP* **03** (2009) 054, arXiv:0811.2067 [hep-ph].

[74] E. Gardi, E. Laenen, G. Stavenga, and C. D. White, "Webs in multiparton scattering using the replica trick," *JHEP* **11** (2010) 155, arXiv:1008.0098 [hep-ph].

[75] A. Mitov, G. Sterman, and I. Sung, "Diagrammatic Exponentiation for Products of Wilson Lines," *Phys. Rev.* **D82** (2010) 096010, arXiv:1008.0099 [hep-ph].

[76] E. Gardi, J. M. Smillie, and C. D. White, "The Non-Abelian Exponentiation theorem for multiple Wilson lines," *JHEP* **06** (2013) 088, arXiv:1304.7040 [hep-ph].

[77] A. A. Vladimirov, "Exponentiation for products of Wilson lines within the generating function approach," *JHEP* **06** (2015) 120, arXiv:1501.03316 [hep-th].

[78] J. R. Forshaw and D. A. Ross, "Quantum chromodynamics and the pomeron," *Cambridge Lect. Notes Phys.* **9** (1997) 1–248.

[79] A. Kyrieleis and M. H. Seymour, "The Colour evolution of the process q q - q q g," *JHEP* **01** (2006) 085, arXiv:hep-ph/0510089 [hep-ph].

[80] M. Dasgupta and G. P. Salam, "Resummation of nonglobal QCD observables," *Phys. Lett.* **B512** (2001) 323–330, arXiv:hep-ph/0104277 [hep-ph].

[81] M. Dasgupta and G. P. Salam, "Accounting for coherence in interjet E(t) flow: A Case study," *JHEP* **03** (2002) 017, arXiv:hep-ph/0203009 [hep-ph].

[82] J. C. Collins and D. E. Soper, "Back-To-Back Jets in QCD," *Nucl. Phys.* **B193** (1981) 381. [Erratum: Nucl. Phys.B213,545(1983)].

[83] J. Frenkel, P. Sorensen, and J. C. Taylor, "An Eikonal Line Integral Model and Factorization in QCD," *Z. Phys.* **C35** (1987) 361.

[84] S. Catani, M. Ciafaloni, and G. Marchesini, "Noncancelling infrared divergences in QCD coherent state STATE," *Nucl. Phys.* **B264** (1986) 588–620.

[85] R. Angeles-Martinez, J. R. Forshaw, and M. H. Seymour, "Coulomb gluons and the ordering variable," *JHEP* **12** (2015) 091, arXiv:1510.07998 [hep-ph]. http://dx.doi.org/10.1007/JHEP12%282015%29091.

[86] R. Gastmans, J. Verwaest, and R. Meuldermans, "Dimensional Regularization in Massless QED," *Nucl. Phys.* **B105** (1976) 454.

[87] G. Gustafson, "Dual Description of a Confined Color Field," *Phys. Lett.* **B175** (1986) 453. [,193(1986)].

[88] G. Gustafson and U. Pettersson, "Dipole Formulation of QCD Cascades," *Nucl. Phys.* **B306** (1988) 746.

[89] B. Andersson, G. Gustafson, and L. Lonnblad, "Gluon Splitting in the Color Dipole Cascades," *Nucl. Phys.* **B339** (1990) 393–406.

[90] L. Lonnblad, "ARIADNE version 4: A Program for simulation of QCD cascades implementing the color dipole model," *Comput. Phys. Commun.* **71** (1992) 15–31.

[91] S. Schumann and F. Krauss, "A Parton shower algorithm based on Catani-Seymour dipole factorisation," *JHEP* **03** (2008) 038, arXiv:0709.1027 [hep-ph].

[92] S. Schumann and F. Krauss, "A Parton shower algorithm based on Catani-Seymour dipole factorisation," *JHEP* **03** (2008) 038, arXiv:0709.1027 [hep-ph].

[93] S. Hoche and S. Prestel, "The midpoint between dipole and parton showers," *Eur. Phys. J.* **C75** no. 9, (2015) 461, arXiv:1506.05057 [hep-ph].

[94] S. M. Aybat, L. J. Dixon, and G. F. Sterman, "The Two-loop anomalous dimension matrix for soft gluon exchange," *Phys. Rev. Lett.* **97** (2006) 072001, arXiv:hep-ph/0606254 [hep-ph].

[95] S. Catani, B. R. Webber, and G. Marchesini, "QCD coherent branching and semiinclusive processes at large x," *Nucl. Phys.* **B349** (1991) 635–654.

[96] Y. L. Dokshitzer, V. A. Khoze, and S. I. Troian, "Specific features of heavy quark production. LPHD approach to heavy particle spectra," *Phys. Rev.* **D53** (1996) 89–119, arXiv:hep-ph/9506425 [hep-ph].

[97] S. Pltzer, "Summing Large-N Towers in Colour Flow Evolution," *Eur. Phys. J.* **C74** no. 6, (2014) 2907, arXiv:1312.2448 [hep-ph].

[98] G. Passarino and M. J. G. Veltman, "One Loop Corrections for e+ e- Annihilation Into mu+ mu- in the Weinberg Model," *Nucl. Phys.* **B160** (1979) 151.

[99] W. L. van Neerven and J. A. M. Vermaseren, "Large loop integrals," *Phys. Lett.* **B137** (1984) 241.

[100] T. Binoth, J. P. Guillet, and G. Heinrich, "Algebraic evaluation of rational polynomials in one-loop amplitudes," *JHEP* **02** (2007) 013, arXiv:hep-ph/0609054 [hep-ph].

[101] W. van Neerven, "Dimensional Regularization of Mass and Infrared Singularities in Two Loop On-shell Vertex Functions," *Nucl.Phys.* **B268** (1986) 453.

[102] W. Beenakker, H. Kuijf, W. L. van Neerven, and J. Smith, "QCD Corrections to Heavy Quark Production in p anti-p Collisions," *Phys. Rev.* **D40** (1989) 54–82.

[103] R. E. Cutkosky, "Singularities and discontinuities of Feynman amplitudes," *J. Math. Phys.* **1** (1960) 429–433.

[104] S. Catani, T. Gleisberg, F. Krauss, G. Rodrigo, and J.-C. Winter, "From loops to trees by-passing Feynman's theorem," *JHEP* **09** (2008) 065, arXiv:0804.3170 [hep-ph].

[105] T. Gleisberg, *Automating methods to improve precision in Monte-Carlo event generation for particle colliders*. PhD thesis, Dresden, Tech. U., 2007. http://iktp.tu-dresden.de/IKTP/pub/07/diss_gleisberg.pdf.

[106] J. Smith and W. L. van Neerven, "The Difference between n-dimensional regularization and n-dimensional reduction in QCD," *Eur. Phys. J.* **C40** (2005) 199–203, arXiv:hep-ph/0411357 [hep-ph].

[107] D. M. Capper, D. R. T. Jones, and P. van Nieuwenhuizen, "Regularization by Dimensional Reduction of Supersymmetric and Nonsupersymmetric Gauge Theories," *Nucl. Phys.* **B167** (1980) 479.

[108] R. K. Ellis, Z. Kunszt, K. Melnikov, and G. Zanderighi, "One-loop calculations in quantum field theory: from Feynman diagrams to unitarity cuts," *Phys.Rept.* **518** (2012) 141–250, arXiv:1105.4319 [hep-ph].

[109] T. Huber and D. Maitre, "HypExp 2, Expanding Hypergeometric Functions about Half-Integer Parameters," *Comput. Phys. Commun.* **178** (2008) 755–776, arXiv:0708.2443 [hep-ph].